# PERFORMANCE OF GABION FACED REINFORCED EARTH RETAINING WALLS

*A Thesis*

*submitted to*
*Cochin University of Science and Technology*

**JAYASREE P. K.**

*for the award of the degree*

*of*

**DOCTOR OF PHILOSOPHY**

**DIVISION OF CIVIL ENGINEERING**
SCHOOL OF ENGINEERING
COCHIN UNIVERSITY OF SCIENCE AND TECHNOLOGY
KOCHI, 682 022
APRIL 2008

# CERTIFICATE

*This is to certify that the thesis entitled* ***"PERFORMANCE OF GABION FACED REINFORCED EARTH RETAINING WALLS"*** *is a report of the original work done by Smt. Jayasree P. K., under my supervision and guidance in School of Engineering, Cochin University of Science and Technology, Kochi 682 022. No part of this thesis has been presented for any other degree from any other institution.*

**Place: Kochi**
**Date:** 21-4-2008

**Guide: Dr. K. S. Beena**
**Reader in Civil Engineering**
**School of Engineering**
**Cochin University of Science and Technology**
**Kochi**
**Pin – 682 022**

SCHOOL OF ENGINEERING
UNIVERSITY OF SCIENCE AND TECHNOLOGY
KOCHI-682 022

# DECLARATION

*I hereby declare that the work presented in the thesis entitled* ***"PERFORMANCE OF GABION FACED REINFORCED EARTH RETAINING WALLS"*** *is based on the original work done by me, under the supervision and guidance of Dr. K. S. Beena, Reader in Civil Engineering, School of Engineering, Cochin University of Science and Technology, Kochi 682 022. No part of this thesis has been presented for any other degree from any other institution.*

**Place: Kochi .**
**Date:** 21/04/08

**Jayasree P. K.**

# ACKNOWLEDGEMENTS

*A journey is easier when you travel together. Interdependence is certainly more valuable than independence. This thesis is the result of seven years of part time work whereby I have been accompanied and supported by many people. It is a pleasant aspect that I have now the opportunity to express my gratitude to all of them.*

*The first person I would like to thank is my supervisor Dr. K. S. Beena, Reader in Civil Engineering, School of Engineering, CUSAT. I have been associating with her since 1995 when I started my M. Tech. thesis work. During these years I have recognised Dr. Beena as a sympathetic and supporting person. Her real enthusiasm and integral outlook on research have made an indelible impression on me. I owe her lots of gratitude for having shown me this way of research. She could not even realize how much I have learned from her. Besides being an excellent supervisor, Dr. Beena was as close as a relative and a good friend to me. Consequently, research life became smooth and rewarding for me.*

*I would like to thank Prof. (Dr.) T S. Ramanatha Ayyar, Former Director of Technical Education, Government of Kerala who kept a constant vigil on the progress of my work and was always accessible whenever I was in need of an advice. Especially the extensive discussions and interactions with Dr. Ayyar had a direct impact on the final form and quality of this thesis. I am equally indebted to Prof. (Dr.) Kuncheria P. Isaac, Principal, Government Engineering College, Wayanad for his valuable advices and help in getting financial aid for this work. The expert advices from Prof. (Dr.) K. Rajagopal, Professor of Civil Engineering, IIT Madras had become a turning point during my thesis work which is gratefully acknowledged.*

*I also wish to express my profound sense of gratitude to the Kerala State Council for Science, Technology and Environment (KSCSTE), Trivandrum for the financial assistance given to the experimental investigation of this work. I also express my sincere thanks to Mrs. Sheeja George, Former Principal Scientific Officer, KSCSTE, Trivandrum, and Dr. K. R. S. Krishnan, Former Director, KSCSTE for sanctioning the project.*

*My warm thanks are due to Dr. Vinod J. S., Post Doctoral Research Fellow, School of Civil, Mining & Environmental Engineering, University of Wollongong, NSW, Australia for assisting me in literature collection. I also thank Mr. Jayakrishnan P. V. and*

*Mr. Anwar Mohammed of M/s Maccaferri Pvt. Ltd., Mumbai for supplying the materials required for the experiments in time.*

*I recollect with gratitude the support and encouragement extended to me by Prof. (Dr.) P. S. Sreejith (Principal) and Prof. (Dr). Benny Mathews Abraham (Professor and Head of Civil Engineering Division), School of Engineering, CUSAT, Kochi. I also wish to express my sincere thanks to Prof. (Dr.) J. Letha (Principal) and Prof. (Dr.) R. Sathikumar (Professor and Head of Civil Engineering Department), College of Engineering, Trivandrum.*

*Thanks are also due to all the faculty members of Departments of Civil Engineering at SoE, CUSAT, Kochi and CET. A special mention to Dr. Sreekumar S., Assistant Professor, CET who provided me with the required computing facilities for my thesis work. The encouragement and support rendered by Dr. K. K. Babu, Selection Grade Lecturer in Civil Engg., N. S. S. College of Engineering, Palakkad needs a special mention at this moment. Special thanks are also due to my friends and colleagues at CET – Bindu, Binu, Leema, Manju, Salini, Priyadarsini, Girija, Latheswary, Ajitha, Ajitha Bhaskar, Mariamma Joseph, Sheela Evangeline, the list goes on unending, for providing me a friendly, pleasant and cooperative atmosphere during my working hours at CET. I would like to express my heartfelt gratitude to the laboratory technical staff Smt. E. J. Saramma, Sri. K. T. Purushothaman, Sri. K. Pradeep, Sri. Babu Varghese, Sri. A. Aboobacker, Sri. Kunjumon and Ms. Preethi, C. D. of School of Engineering, CUSAT, for the technical assistance and co-operation during the experimental work.*

*My sincere thanks are also due to Mrs. Leena G, Mrs. Indu B., Ms. Meera Vasudevan and Ms. Ann George, Former P. G. students, Department of Civil Engineering, College of Engineering, Trivandrum and Ms. Nia Mathew, Ms. Dhanya and Ms. Chinchu former U. G. students, School of Engineering, CUSAT, Kochi for the continuous enthusiasm shown in helping me to carry out the experimental works.*

*I am extremely grateful to my husband Hari R. Chandran, for his support, patience and advices extended to me during the Ph.D. period. One of the best experiences that we lived through in this period was the birth of our daughter Harinandana J., who added a joyful dimension to our life. Without their encouragement and understanding it would have been impossible for me to finish this work.*

*In my opinion, doing a Ph.D. is a sacred task and this was definitely one of the best decisions of my life which was inspired by my father N. Parameswaran Pillai. Additional energy and vitality for this research was rendered by my mother D. Kamala Devi Amma who in spite of her ill health supported me through out the work, especially nurturing my daughter, giving her a mother's care and comfort during my absence. My sister Dhanyasree P. K. helped me throughout the earlier stages of the work by assisting me in developing the finite element code as well as managing my house hold duties including taking care of my parents during the period of their illness and admission in hospital. Her services and support during the period of work can never be forgotten. It would be a flaw on my part, if I forget to mention the services and encouragement provided by my in - laws Mr. Ramachandran Nair and Mrs. Lalitha Bai Amma during the experimental part of my work The continuous enthusiasm shown by my father - in - law in urging me to hasten up the long - winded work is deeply acknowledged. The supplementary supports provided by Mrs. Rani and Mr. Gopakumar (My sister-in-law and her husband) are also noteworthy which are deeply remembered with gratitude. The generous support from Mr. Venugopal, Kannan and Mrs. Sarojini Amma (Dr. Beena's family) is gratefully appreciated. Within this period of research work, I have become a member of their family and I owe deep obligations to them for making me feel at home whenever I stayed with them and also for sparing Dr. Beena for me even at times they needed her most.*

*The chain of my gratitude would be definitely incomplete if I would forget to thank the first cause of this chain, using Aristotle's words, The Prime Mover. My deepest and sincere gratitude for inspiring and guiding this humble being are due to Almighty GOD.*

**Jayasree P. K.**

# ABSTRACT

**Key words:** Gabions, reinforced soil, finite element analysis, cohesionless backfill, parametric studies, material properties, geometric properties, design charts, cost effectiveness

Gabion faced retaining walls are essentially semi rigid structures that can generally accommodate large lateral and vertical movements without excessive structural distress. Because of this inherent feature, they offer technical and economical advantage over the conventional concrete gravity retaining walls. Although they can be constructed either as gravity type or reinforced soil type, this work mainly deals with gabion faced reinforced earth walls as they are more suitable to larger heights.

The main focus of the present investigation was the development of a viable plane strain two dimensional non linear finite element analysis code which can predict the stress - strain behaviour of gabion faced retaining walls - both gravity type and reinforced soil type. The gabion facing, backfill soil, in - situ soil and foundation soil were modelled using 2D four noded isoparametric quadrilateral elements. The confinement provided by the gabion boxes was converted into an induced apparent cohesion as per the membrane correction theory proposed by Henkel and Gilbert (1952). The mesh reinforcement was modelled using 2D two noded linear truss elements. The interactions between the soil and the mesh reinforcement as well as the facing and backfill were modelled using 2D four noded zero thickness line interface elements (Desai et al., 1974) by incorporating the nonlinear hyperbolic formulation for the tangential shear stiffness. The well known hyperbolic formulation by Duncan and Chang (1970) was used for modelling the non - linearity of the soil matrix. The failure of soil matrix, gabion facing and the interfaces were modelled using Mohr – Coulomb failure criterion. The construction stages were also modelled.

Experimental investigations were conducted on small scale model walls (both in field as well as in laboratory) to suggest an alternative fill material for

the gabion faced retaining walls. The same were also used to validate the finite element programme developed as a part of the study. The studies were conducted using different types of gabion fill materials. The variation was achieved by placing coarse aggregate and quarry dust in different proportions as layers one above the other or they were mixed together in the required proportions. The deformation of the wall face was measured and the behaviour of the walls with the variation of fill materials was analysed. It was seen that 25% of the fill material in gabions can be replaced by a soft material (any locally available material) without affecting the deformation behaviour to large extents. In circumstances where deformation can be allowed to some extents, even up to 50% replacement with soft material can be possible.

The developed finite element code was validated using experimental test results and other published results. Encouraged by the close comparison between the theory and experiments, an extensive and systematic parametric study was conducted, in order to gain a closer understanding of the behaviour of the system. Geometric parameters as well as material parameters were varied to understand their effect on the behaviour of the walls.

The final phase of the study consisted of developing a simplified method for the design of gabion faced retaining walls. The design was based on the limit state method considering both the stability and deformation criteria. The design parameters were selected for the system and converted to dimensionless parameters. Thus the procedure for fixing the dimensions of the wall was simplified by eliminating the conventional trial and error procedure. Handy design charts were developed which would prove as a hands – on – tool to the design engineers at site. Economic studies were also conducted to prove the cost effectiveness of the structures with respect to the conventional RCC gravity walls and cost prediction models and cost breakdown ratios were proposed.

The studies as a whole are expected to contribute substantially to understand the actual behaviour of gabion faced retaining wall systems with particular reference to the lateral deformations.

# CONTENTS

**Certificate**

**Declaration** **Page No.**

**Acknowledgements** i

**Abstract** iv

**Contents** vi

**Abbreviations** xii

**List of figures** xiii

**List of notations** xvii

**List of tables** xxiii

**CHAPTER 1 INTRODUCTION**

1.1 General 1

1.2 Scope of the present study 4

1.3 Objectives 5

1.4 Organisation of the thesis 5

**CHAPTER 2 LITERATURE REVIEW**

2.1 General 7

2.2 Experimental investigations 8

2.2.1 Gravity walls 8

2.2.2 Reinforced earth walls 10

2.2.3 Segmental retaining walls 15

2.2.4 Gabion faced retaining walls 17

2.3 Analytical studies 19

2.3.1 Gravity walls 19

2.3.2 Reinforced earth walls 21

2.3.3 Segmental retaining walls 26

2.4 Numerical modelling 26

2.4.1 Gravity walls 26
2.4.2 Reinforced earth walls 28
2.4.3 Segmental retaining walls 36
2.4.4 Gabion faced retaining walls 39
2.5 Economic studies 41
2.6 Need for the present study 43

**CHAPTER 3 GABION FACED RETAINING WALLS**
3.1 General 44
3.2 Construction 44
3.2.1 Wire mesh 44
3.2.2 Gabions 46
3.2.3 Construction procedure 47
3.3 Advantages 50
3.4 Analysis of gabion faced reinforced earth retaining walls 53
3.4.1 Limit state method 54
3.4.2 Partial factors 54
3.4.3 Partial material factors for reinforcements 56
3.4.4 Design loads and design strengths 58
3.4.5 Design procedure 59
3.4.5.1 Fixing the dimensions 59
3.4.5.2 External stability analysis 59
3.4.5.3 Internal stability analysis 62
3.4.5.4 Serviceability limit considerations 64
3.5 Summary 65

**CHAPTER 4 FINITE ELEMENT MODELLING**
4.1 General 66
4.2 Modelling 67
4.3 Non linear analysis of soil media 68
4.3.1 Incremental method 69
4.3.2 Constitutive laws 70
4.3.2.1 Non linear elastic hyperbolic model 70
4.4 Elements used in the present analysis 76

4.4.1 Two-dimensional four noded quadrilateral element 76
4.4.2 Two-dimensional two noded truss element 79
4.4.3 Zero thickness four noded line interface element 80
4.4.3.1 Hyperbolic relation for the interface 83
4.5 Composite model for gabion encased material 86
4.6 Modelling of construction phases 87
4.7 Numerical implementation 88
4.8 Finite element modelling 89
4.9 Summary 92

**CHAPTER 5 EXPERIMENTAL INVESTIGATIONS**
5.1 General 93
5.2 Model studies 93
5.2.1 Field model studies – Set I 95
5.2.1.1 Construction of model gabion wall 95
5.2.1.2 Loading set up 97
5.2.2 Laboratory model studies – Set II 99
5.2.2.1 Experimental set up 99
5.2.2.2 Loading set up 101
5.3 Results and discussions 102
5.3.1 Load deformation characteristics 103
5.3.2 Bulging patterns 104
5.4 Summary 107

**CHAPTER 6 VALIDATION STUDIES**
6.1 General 109
6.2 Four noded quadrilateral element 109
6.3 Two noded truss element 111
6.4 Modelling of non linear behaviour of soil 112
6.5 Modelling of interface behaviour 114
6.6 Modelling of reinforced soil behaviour 116
6.7 Modelling of reinforced soil wall 118
6.8 Modelling of gabion faced reinforced soil wall 120
6.8.1 Hyperbolic constants for soil 123

6.8.2 Elastic constants for gabion fill materials 124
6.8.3 Hyperbolic constants for interface 126
6.8.4 Finite element modelling 128
6.9 Summary 133

**CHAPTER 7 GEOMETRIC PARAMETRIC STUDIES**
7.1 General 134
7.2 System analysed 135
7.3 Effect of reinforcement spacing (h) 138
7.4 Effect of reinforcement length (L) 144
7.5 Effect of facing width (b) 146
7.6 Selection of geometric parameters 147
7.7 Effect of position of strip loading 150
7.8 Summary 153

**CHAPTER 8 MATERIAL PARAMETRIC STUDIES**
8.1 General 154
8.2 Effect of gabion fill material 155
8.3 Effect of gabion fill – backfill combination 159
8.4 Effect of reinforcement on backfill 168
8.5 Summary 180

**CHAPTER 9 DESIGN OF GABION FACED REINFORCED EARTH RETAINING WALLS**
9.1 General 181
9.2 Design procedure 182
9.2.1 Forces acting on the wall 183
9.2.2 External stability analysis 185
9.2.2.1 Bearing and tilt failure 185
9.2.2.2 Sliding along the base 185
9.2.3 Internal stability analysis 186
9.2.3.1 Rupture of reinforcement 186
9.2.3.2 Loss of adherence of reinforcement 188
9.2.4 Serviceability limit state 189
9.3 Design example 190

9.3.1 Data available from site 190
9.3.2 Initial dimensions 190
9.3.3 Forces acting on the wall 190
9.3.4 External stability analysis 191
9.3.4.1 Bearing and tilt failure 191
9.3.4.2 Sliding along the base 191
9.3.5 Internal stability analysis 192
9.3.6 Serviceability limit considerations 193
9.4 Development of design charts 194
9.4.1 Assumptions 194
9.4.2 Selection of variables 195
9.4.3 External stability analysis 195
9.4.3.1 Bearing and tilt failure 195
9.4.3.2 Sliding failure 199
9.4.4 Internal stability analysis 200
9.4.4.1 Failure due to mesh breakage 200
9.4.4.2 Failure due to mesh pullout 202
9.4.5 Serviceability limit state 207
9.5 Design charts based on deformation criteria 209
9.6 Design steps using design charts 216
9.7 Design example using design charts 217
9.8 Summary 225

**CHAPTER 10 ECONOMIC STUDIES**

10.1 General 226
10.2 Data collection 227
10.3 Cost prediction models 237
10.4 Cost breakdown studies 241
10.5 Summary 243

**CHAPTER 11 SUMMARY AND CONCLUSIONS**

11.1 Summary 244
11.2 Conclusions 247
11.2.1 General 247

11.2.2 Based on geometric parametric studies 247
11.2.3 Based on material parametric studies 248
11.2.4 Based on economic studies 249
11.3 Scope for future work 250

**REFERENCES** **251**

**BIBLIOGRAPHY** **264**

**PUBLICATIONS BASED ON THE RESEARCH WORK** **268**

# ABBREVIATIONS

| Notation | Description |
|---|---|
| ASF | Average safety factor |
| BCF | Bearing capacity factor |
| DF | Depth factor |
| FE | Finite element |
| FEA | Finite element analysis |
| FEM | Finite element method |
| FWF | Facing width factor |
| LF | Length factor |
| MSE | Mechanically stabilised earth |
| PVC | Poly vinyl chloride |
| RCC | Reinforced cement concrete |
| RF | Rock factor |
| RLF | Reinforcement load factor |
| RPR | Response parameter ratio |
| RSF | Reinforcement stiffness factor |
| SF | Surcharge factor |
| VSF | Vertical spacing factor |

# LIST OF FIGURES


| Figure no. | Title | Page no. |
|---|---|---|
| 1.1 | A gravity retaining wall | 2 |
| 1.2 | A reinforced soil retaining wall | 2 |
| 3.1 | Hexagonal wire mesh | 45 |
| 3.2 | Double twisted wire | 45 |
| 3.3 | Cross section of gabion wire | 45 |
| 3.4 | A typical gabion | 46 |
| 3.5 | Gabion with extension | 46 |
| 3.6 | Typical configurations of gabion faced walls | 48 |
| 3.7 | Gravity type gabion wall – construction procedure | 49 |
| 3.8 | MSE type gabion faced wall – construction sequence | 50 |
| 3.9 | Monolithic wall | 52 |
| 3.10 | Flexible wall | 52 |
| 3.11 | Permeable ecofriendly wall | 52 |
| 4.1 | Incremental method of non linear analysis | 69 |
| 4.2 | Determination of hyperbolic constants | 73 |
| 4.3 | Elements used in the analysis | 78 |
| 4.4 | Determination of hyperbolic constants for the interfaces | 84 |
| 4.5 | Discretisation of gabion faced reinforced soil wall | 89 |
| 4.6 | Nodal connectivity at the reinforcing junction | 90 |
| 5.1 | Dimensions of model gabion box | 96 |
| 5.2 | Model gabion box with geotextile lining | 96 |
| 5.3 | Cross section of the model wall (Set I) | 96 |
| 5.4 | Elevation of the model wall (Set I) | 96 |
| 5.5 | Schematic sketch of the loading set up | 98 |
| 5.6 | Deformation measurements (Set I) | 98 |
| 5.7 | Experimental set up for the model gabion wall | 100 |
| 5.8 | Schematic diagram of the test tank | 102 |
| 5.9 | Load deformation behaviour after seating load (Set I) | 104 |
| 5.10 | Load deformation behaviour (Set II) | 104 |

| | | |
|---|---|---|
| 5.11 | Bulging of front face of walls | 106 |
| 5.12 | Increase in top sway | 106 |
| 5.13 | Variation of top lateral deformation with quantity of quarry dust | 107 |
| 6.1 | Cantilever beam loaded with couple | 110 |
| 6.2 | Plane truss structure | 111 |
| 6.3 | Discretisation of soil medium | 113 |
| 6.4 | Validation of non linear analysis of soil medium | 114 |
| 6.5 | Sliding block problem | 115 |
| 6.6 | Discretisation of reinforced soil medium | 117 |
| 6.7 | Validation of reinforced soil behaviour | 118 |
| 6.8 | Discretisation used for validation of reinforced soil wall | 119 |
| 6.9 | Validation of reinforced soil wall – Facing deformation | 121 |
| 6.10 | Validation of reinforced soil wall – Strain in geotextile | 121 |
| 6.11 | Determination of non linear elastic properties for sand | 123 |
| 6.12 | Determination of linear elastic properties for coarse aggregate | 125 |
| 6.13 | Determination of linear elastic properties for quarry dust | 125 |
| 6.14 | Determination of non linear elastic properties for steel mesh – sand interface | 127 |
| 6.15 | Discretisation of gabion faced reinforced earth wall | 128 |
| 6.16 | Validation curves for gabion faced reinforced earth wall with different facings – load deflection curves | 129 |
| 6.17 | Validation curves for gabion faced reinforced earth wall with different facings – bulging patterns at 60kN/m load | 130 |
| 6.18 | Load – deflection data: Comparison between theory and experiment | 132 |
| 6.19 | Facing deflection data: Comparison between theory and experiment | 132 |
| 7.1 | Finite element mesh used for the parametric studies | 136 |
| 7.2 | Reinforcement spacing configurations used in the study | 139 |
| 7.3 | Facing deflection patterns for different reinforcement spacing configurations | 140 |
| 7.4 | Variation of earth pressure with spacing | 141 |
| 7.5 | Effect of reinforcement spacing | 143 |

| | | |
|---|---|---|
| 7.6 | Effect of reinforcement length | 145 |
| 7.7 | Effect of facing width | 147 |
| 7.8 | Design chart for selecting geometric parameters (H = 6m) | 149 |
| 7.9 | Interpolation chart for selecting geometric parameters for any height | 149 |
| 7.10 | Schematic representation of parameters of strip loading studies | 151 |
| 7.11 | Effect of strip position on deformation | 151 |
| 7.12 | Design chart for fixing strip loading position | 152 |
| 8.1 | Load vs. top lateral deformation plots for different gabion fill materials | 157 |
| 8.2 | Facing deformation plots for walls with different gabion fills at 150 kPa surcharge | 157 |
| 8.3 | Variation of maximum wall deflection for different backfills | 165 |
| 8.4 | Variation of maximum strain in reinforcement for different backfills | 166 |
| 8.5 | Variation of average safety factor for different backfills | 167 |
| 8.6 | Variation of the response parameter ratio with wall height | 168 |
| 8.7 | Load deformation plots | 171 |
| 8.8 | Lateral displacement of facing at end of construction | 171 |
| 8.9 | Vertical stress contours | 172 |
| 8.10 | Stress distributions at the back face of wall | 174 |
| 8.11 | Horizontal stress contours | 174 |
| 8.12 | Shear stress contours | 175 |
| 8.13 | Plot of plastic points | 176 |
| 8.14 | Axial force in reinforcement at different levels | 178 |
| 8.15 | Axial force in reinforcement on various vertical planes | 178 |
| 8.16 | Contours of axial force in reinforcement | 179 |
| 8.17 | Contours of FoS against breakage in reinforcement | 179 |
| 9.1 | Initial dimensions of the wall | 183 |
| 9.2 | Material properties and principal forces | 184 |
| 9.3 | Pressure distribution along base of wall | 184 |
| 9.4 | Design chart from bearing and tilt considerations for BCF = 5 | 197 |

| | | |
|---|---|---|
| 9.5 | Design chart from bearing and tilt considerations - Interpolation chart | 198 |
| 9.6 | Design chart from sliding considerations | 201 |
| 9.7 | Design chart from mesh breakage considerations | 203 |
| 9.8 | Interpolation chart from mesh breakage considerations | 204 |
| 9.9 | Design chart from mesh pullout considerations | 206 |
| 9.10 | Design chart from serviceability limit state considerations | 208 |
| 9.11 | Interpolation chart from serviceability limit state considerations | 208 |
| 9.12 | Design chart for fixing geometric parameters (H = 6m) | 209 |
| 9.13 | Design chart for fixing backfill – gabion fill combination (Gravel and sand backfill, H = 6m) | 211 |
| 9.14 | Design chart for fixing backfill – gabion fill combination (Silty sand backfill, H = 6m) | 212 |
| 9.15 | Design chart for fixing backfill – gabion fill combination (Clayey sand backfill, H = 6m) | 213 |
| 9.16 | Design chart for fixing backfill – gabion fill combination (Clay with low plasticity backfill, H = 6m) | 214 |
| 9.17 | Interpolation chart for selection of geometric and material parameters for any wall height | 215 |
| 9.18 | Design chart for fixing strip loading position | 215 |
| 9.19 | Illustration of design example: Step 2 | 219 |
| 9.20 | Illustration of design example: Step 3 | 219 |
| 9.21 | Illustration of design example: Step 4 | 220 |
| 9.22 | Illustration of design example: Step 5 | 222 |
| 9.23 | Illustration of design example: Step 7 | 222 |
| 9.24 | Illustration of design example: Step 8 | 223, 224 |
| 10.1 | Variation of cost of retaining walls with height | 239 |
| 10.2 | Cost variation of retaining walls | 239 |
| 10.3 | Percentage savings in gabion faced walls compared to RCC walls | 240 |
| 10.4 | Space requirements of retaining walls | 242 |

# LIST OF NOTATIONS

The notations listed below are for general reference. Symbols which do not appear here are explained in the text where they first occur.

| Notation | Description | Unit |
|---|---|---|
| a | Friction interaction factor | - |
| $a_s$ | Distance of starting end of strip load from back face of wall | m |
| $a^1$, $b^1$ | Kondner's constants for soil | - |
| $a_i^1$, $b_i^1$ | Kondner's constants for interfaces | - |
| $A_j$ | Cross sectional area of the jth layer of reinforcement | $m^2$ |
| $A_t$ | Cross sectional area of truss element | $m^2$ |
| b | Facing width of gabion wall | m |
| [B] | Strain displacement matrix | m |
| $B_{soil}$ | Bulk modulus of soil | kPa |
| $B_{min}$ | Minimum value of bulk modulus of soil | kpa |
| c | Cohesion | kPa |
| $c_a$ | Adhesion of soil to reinforcement | kPa |
| $c_g$ | Cohesion of gabion facing | kPa |
| $c_i$ | Cohesion induced by gabion mesh | kPa |
| $c_s$ | Cohesion of soil | kPa |
| $c_u$ | Undrained cohesion | kPa |
| $c_x$, $c_y$ | Direction cosines | - |
| [C] | Constitutive matrix | kPa |
| $C_u$ | Uniformity coefficient | - |
| {d} | Nodal displacement vector | m |
| D | Least lateral dimension of rock pieces inside gabions | m |
| $D_m$ | Depth of embedment | m |
| $D_o$ | Initial least lateral dimension of gabion box | m |
| $D_{10}$ | Effective size | mm |
| e | Eccentricity | m |
| $e_{max}$ | Maximum voids ratio | - |

| | | |
|---|---|---|
| $e_{min}$ | Minimum voids ratio | - |
| E | Modulus of elasticity of the reinforcement | kPa |
| $E_i$ | Initial tangent modulus of elasticity | kPa |
| $E_t$ | Tangent modulus of elasticity | kPa |
| $E_{tr}$ | Modulus of elasticity of material of truss element | kPa |
| $f_f$ | Partial factor applied to external dead loads | - |
| $f_{fs}$ | Partial factor applied to soil mass | - |
| $f_m$ | Partial factor values applied to reinforcement parameters | - |
| $f_{ms}$ | Partial factor values applied to soil parameters | - |
| $f_{m1}$ | Partial factor values applied to intrinsic properties of reinforcement material | - |
| $f_{m11}$ | Partial factor values applied to consistency of manufacture of reinforcement | - |
| $f_{m111}$ | Partial factor values applied to reinforcement manufactured according to standards | - |
| $f_{m112}$ | Partial factor values applied to reinforcement manufactured not according to standards | - |
| $f_{m12}$ | Partial material factor related extrapolation of test data dealing with base strength | - |
| $f_{m121}$ | Partial factor values applied to assessment of available data on base strength of reinforcement to derive a statistical envelope | - |
| $f_{m122}$ | Partial material factor related to the extrapolation of the statistical envelope over the expected service life of the reinforcement | - |
| $f_{m2}$ | Partial factor values applied to reinforcement concerned with construction and environmental effects | - |
| $f_{m21}$ | Partial material factor related to the susceptibility of the reinforcement to damage during installation | - |
| $f_{m22}$ | Partial material factor related to the environment in which the reinforcement is installed | - |
| $f_n$ | Partial factor applied to economic ramifications of failure | - |
| $f_p$ | Partial factor for reinforcement pullout resistance | - |

| | | |
|---|---|---|
| $f_q$ | Partial factor applied to external live loads | - |
| $f_s$ | Partial factor applied to sliding | - |
| G | Specific gravity | - |
| h | Spacing of reinforcement | m |
| $h_j$ | Depth of the jth layer of reinforcement from the top | m |
| H | Height of wall | m |
| j | Layer number of the reinforcement | - |
| $k_s$, $k_n$ | Interface unit stiffness along tangential and normal directions | $kN/m^3$ |
| $k_{si}$ | Initial shear modulus of interface | $kN/m^3$ |
| $k_{st}$ | Tangent shear modulus of interface | $kN/m^3$ |
| [k] | Element stiffness matrix | kN/m |
| $[k_m]$ | Element stiffness matrix along member axis | kN/m |
| K, n | Hyperbolic constants for soil for determination of elastic modulus of soil | - |
| $K^1$, $n^1$ | Hyperbolic constants for interface | - |
| $K_a$ | Coefficient of active earth pressure | - |
| $K_{a1}$ | Coefficient of active earth pressure of backfill soil | - |
| $K_{a2}$ | Coefficient of active earth pressure of retained soil | - |
| $K_{mu}$, m | Hyperbolic constants for determination of bulk modulus | - |
| $K_o$ | Coefficient of earth pressure in at – rest condition | - |
| $K_p$ | Coefficient of passive earth pressure | - |
| [K] | Global stiffness matrix | kN/m |
| L | Length of reinforcement | m |
| $L_{aj}$ | Length of reinforcement in the active zone | m |
| $L_{ej}$ | Embedded length of reinforcement | m |
| $L_i$ | Length of interface element | m |
| $L_{min}$ | Minimum length of reinforcement | m |
| $L_t$ | Length of truss element | m |
| M | Net factored moments acting about the toe of the system | kNm |
| $M_g$ | Secant modulus of gabion mesh | kN/m |
| $M_o$ | Total factored overturning moments about toe | kNm |
| $M_r$ | Total factored resisting moments about toe | kNm |

| | | |
|---|---|---|
| $N_i$ | Shape functions | - |
| [N] | Shape function matrix | - |
| $P_{atm}$ | Atmospheric pressure | kPa |
| $P_l$ | Perimeter of reinforcement | M |
| $P_q$ | Lateral force due to surcharge | kN/m |
| $P_r$ | Lateral force in reinforced case | kN/m |
| $P_s$ | Lateral force due to retaining soil | kN/m |
| $P_u$ | Lateral force in unreinforced case | kN/m |
| q | Surcharge over backfill | kN/m |
| { q } | Element load vector | kN |
| $q_{all}$ | Allowable bearing capacity of soil | kPa |
| $q_r$ | Factored bearing pressure at the base of wall | kPa |
| $q_{ult}$ | Ultimate bearing capacity of soil | kPa |
| r, s | Local coordinates of any point | m |
| $r_i$, $s_i$ | Local coordinates of ith node | m |
| $R_f$ | Failure ratio for soil elements | - |
| $R_f^I$ | Failure ratio for interface elements | - |
| $R_h$ | Resultant of all factored horizontal loads | kN/m |
| $R_v$ | Resultant of all factored vertical loads | kN/m |
| S | Stress level expressed as a fraction of strength | - |
| SD | Standard deviation of the reinforcement base strength | kN/m |
| $S_{vj}$ | Vertical spacing of reinforcements at the jth level | m |
| $t_d$ | Design life of reinforcement | - |
| $t_t$ | Duration over which real time creep tests have been performed for reinforcement | - |
| $T_{avj}$ | Average tensile load along the length of the jth layer of reinforcements | kN/m |
| $T_{cj}$ | Tensile force per metre run developed in the jth layer of reinforcement due to cohesion of the reinforced soil fill | kN/m |
| $T_D$ | Design strength of reinforcement | kN/m |
| $T_{fj}$ | Tensile force per metre run developed in the jth layer of reinforcement due to a vertical strip load | kN/m |
| $T_j$ | Maximum ultimate limit state tensile force to be resisted | kN/m |

| | | |
|---|---|---|
| | by the jth layer of reinforcement | |
| $T_{pj}$ | Tensile force per metre run developed in the jth layer of reinforcement due to self weight of fill plus any surcharge on the reinforced fill | kN/m |
| $T_{sj}$ | Tensile force per metre run developed in the jth layer of reinforcement due to a horizontal shear load | kN/m |
| $T_{ult}$ | Unfactored ultimate tensile strength of reinforcement | kN/m |
| [T] | Transformation matrix | - |
| u, v | Nodal displacements | m |
| $u_i$, $v_i$ | Nodal displacements at any point | m |
| $u_r$ | Maximum lateral deformation in the reinforced case | m |
| $u_u$ | Maximum lateral deformation in the unreinforced case | m |
| {u} | Nodal displacement vector at any point | m |
| $\{u_n\}$, $\{v_n\}$ | u and v vectors of an element | m |
| $W_g$ | Weight of gabion facing | kN/m |
| $W_s$ | Weight of reinforced soil block | kN/m |
| $W_q$ | Weight of surcharge | kN/m |
| x, y | X and Y (global) coordinates | m |
| $x_i$, $y_i$ | X and Y (global) coordinates of ith node | m |
| $x_j$, $y_j$ | X and Y (global) coordinates of jth node | m |
| $\{x_n\}$, $\{y_n\}$ | X and Y coordinate vectors of an element | m |
| $x_s$ | Width of strip loading | m |
| $\alpha$ | Adhesion coefficient relating soil cohesion to soil / reinforcement bond | - |
| $\delta$ | Angle of interfacial friction | degrees |
| $\delta_s$ | Sway factor | - |
| $\Delta d$ | Increment in displacement | M |
| $\Delta P$ | Change in lateral force | kN/m |
| $\Delta q$ | Increment in load | kN |
| $\Delta u$ | Percentage reduction in lateral deformation | % |
| $\Delta\sigma_3$ | Confining pressure | kPa |
| $\varepsilon_a$ | Axial strain | - |
| $\varepsilon_{all}$ | Allowable strain in the reinforcement | % |

| | | |
|---|---|---|
| $\varepsilon_j$ | Strain in the jth layer of reinforcement | % |
| $\varepsilon_s$ | Strain in soil | - |
| $\varepsilon_x$, $\varepsilon_y$ | Strains along x and y directions | - |
| $\{\varepsilon\}$ | Element strain vector | - |
| $\phi$ | Angle of internal friction | degrees |
| $\phi^c$ | Angle of internal friction | radians |
| $\phi_s$ | Angle of internal friction of soil | degrees |
| $\phi_{s1}$ | Angle of internal friction of backfill soil | degrees |
| $\phi_{s2}$ | Angle of internal friction of retained soil | degrees |
| $\gamma$ | Unit weight of any material | $kN/m^3$ |
| $\gamma_m$ | Unit weight of material under consideration | $kN/m^3$ |
| $\gamma_g$ | Unit weight of materials in gabion facing | $kN/m^3$ |
| $\gamma_s$ | Unit weight of soil | $kN/m^3$ |
| $\gamma_{s1}$ | Unit weight of backfill soil | $kN/m^3$ |
| $\gamma_{s2}$ | Unit weight of retained soil | $kN/m^3$ |
| $\gamma_w$ | Unit weight of water | $kN/m^3$ |
| $\gamma_{xy}$ | Shear strain on the xy plane | - |
| $\Gamma$ | Mean reinforcement base strength | kN/m |
| $\mu$ | Poisson's ratio | - |
| $\{\sigma\}$ | Stress vector | kPa |
| $\sigma_d$ | Deviator stress | kPa |
| $\sigma_n$ | Normal stress | kPa |
| $\sigma_x$, $\sigma_y$ | Stresses along x and y directions | kPa |
| $\sigma_1$ | Major principal stress | kPa |
| $\sigma_3$ | Minor principal stress | kPa |
| $\bar{\sigma}$ | Mean stress | kPa |
| $\tau$ | Shear stress | kPa |
| $\tau_f$ | Shear stress at failure | kPa |
| $\tau_{max}$ | Maximum shear stress developed | kPa |
| $\tau_{xy}$ | Shear stress on the xy plane | kPa |

# LIST OF TABLES


| Table no. | Title | Page no. |
|---|---|---|
| 2.1 | Numerical summary of literature survey | 43 |
| 3.1 | Partial load factors for load combinations | 55 |
| 3.2 | Summary of partial factors | 56 |
| 6.1 | Comparison of deflection for cantilever beam | 110 |
| 6.2 | Comparison of deflection for a plane truss structure | 112 |
| 6.3 | Input data for soil medium | 112 |
| 6.4 | Input data for reinforced soil foundation | 116 |
| 6.5 | Input data for reinforced soil wall | 120 |
| 6.6 | Non linear elastic properties of sand | 124 |
| 6.7 | Elastic properties of coarse aggregate and quarry dust | 126 |
| 6.8 | Non linear elastic properties of interface | 127 |
| 6.9 | Linear elastic properties of steel mesh | 127 |
| 6.10 | Input data for gabion faced reinforced soil wall | 128 |
| 7.1 | Material properties adopted for parametric studies | 137 |
| 7.2 | Deflection values to produce active earth pressure state | 142 |
| 8.1 | Properties of gabion fill materials | 156 |
| 8.2 | Properties chosen for gabion fill | 160 |
| 8.3 | Properties chosen for backfill | 161 |
| 8.4 | Rock factor values for different rock types | 162 |
| 9.1 | Determination of $f_m$ for PVC coated gabion mesh | 188 |
| 9.2 | Internal stability calculations for mesh breakage | 192 |
| 9.3 | Internal stability calculations for mesh pullout | 193 |
| 9.4 | Strain in the reinforcements | 193 |
| 9.5 | Spacing values at salient depths | 218 |
| 10.1 | Data collected for economic studies | 228 |
| 10.2 | Design details of cantilever type RCC walls | 229 |
| 10.3 | Design details of counterfort type RCC walls | 230 |
| 10.4 | Design details of gabion faced retaining walls | 231 |
| 10.5 | Estimation of RCC walls | 233 |
| 10.6 | Estimation of gabion faced gravity walls | 234 |
| 10.7 | Estimation of gabion faced reinforced soil walls | 236 |
| 10.8 | Cost breakdown for gabion faced retaining walls | 243 |

# Chapter 1

# INTRODUCTION

## 1.1 GENERAL

A retaining wall is defined as a structure whose primary purpose is to provide lateral support for soil or rock. In some cases, the retaining wall may support vertical loads also. Examples include basement walls and certain types of bridge abutments. It is also described as a structure that prevents retained soil from assuming its natural slope. More clearly, it is constructed to maintain level difference of the soil on either side of it.

It is quite understandable that retaining wall design and construction has occupied a pivotal position in the historic development of geotechnical engineering. Along with this, came a variety of retaining wall types, design methods and related construction methodologies. Over time, the classical gravity retaining walls transitioned into reinforced concrete types. A paradigm shift occurred in the 1960s with the advent of mechanically stabilized earth (MSE) masses, i.e., reinforced layers of soil allowing for modular construction, which was clearly recognized as being advantageous in most situations. The reinforcement was initially steel strips, and subsequently, welded wire mesh provided an alternative. Wall facings varied from metallic – to – reinforced concrete – to – segmental units of a variety of types and shapes. By the 1980s this MSE technology segued into polymeric reinforcement using geogrids, geotextiles and polymer strips.

Gravity retaining walls (Fig. 1.1) depend upon their weight for stability or in other words, they are walls which are stabilized by their mass. These walls are usually constructed of concrete or masonry. Such walls are not economical for large heights. They usually show a rigid behaviour against the surrounding deformations.

frictional shear on the periphery of the horizontal reinforcing strips induces a uniformly increasing tension in its section, which varies from zero at the free end to a maximum at the point of fixity with the facing skin, in a first order approach. The facing skin itself needs only extremely low structural thickness, which together with the thin reinforcing strips makes it a highly economical proposition in the place of conventional retaining structures of the gravity type. Since the system basically owes its performance to the reinforcements frictionally interacting with the soil medium, highly frictional soils and reinforcements with good frictional surface characteristics are most essential and economical for reinforcing earth systems.

But recently retaining walls are being constructed with thick and stiff facings like modular concrete blocks or gabions in order to reduce the length of reinforcement and thus to minimize the space utilisation of reinforced soil walls. They may be classified as semi rigid walls. Gabions are wire mesh containers filled with stones. They are stacked one above the other as well as one beside the other, and securely tied together to form a monolithic massive structure.

Gabion faced retaining walls are commonly built as gravity type walls for low wall heights and as reinforced soil type for medium and high walls. In the case of gravity type walls gabion boxes are stacked as mentioned above to form the wall facing. The stability is achieved by the self weight of the structures and hence high density rock boulder pieces are used as the common fill material. The gabion boxes are also available with mesh extension at their base. The self weight of the stones inside the gabion boxes and the backfill portion into which the basal mesh extends provides stability to the structure. In addition to this, the basal mesh extending into the backfill acts as reinforcement inside the soil and the frictional interaction between the backfill and the basal mesh provides additional stability to the structure. These types of structures are termed as gabion faced reinforced earth retaining walls. Since these walls acquire additional stability from the frictional interaction between the basal mesh and the backfill, the facing width may be kept to a minimum

value. The advantages of these walls over the gravity type walls are added stability and the reduction in cost of the structure due to the reduction in facing width. The latter feature owes to the lesser amount of stones required compared to the gravity type gabion faced retaining walls. Because of these reasons, the construction of the gabion faced reinforced earth walls is gaining high momentum these days.

## 1.2 SCOPE OF THE PRESENT STUDY

The concept of retaining walls with gabion facing is gathering tremendous growth in the present time. They are gaining considerable attention as retaining structures and providing a valuable alternative to traditional concrete walls. Gabion faced walls present a low environmental impact and a good ratio between cost and effectiveness. This comes about for a number of reasons, among which are: no casting, ease of placement, good tolerance for foundation irregularities and (perhaps most importantly) outstanding aesthetics. Building architects, landscape developers, private property owners etc., have also readily accepted these wall systems in addition to geotechnical consultants. No longer confined to low and medium heights, gabion walls with mesh reinforcement now compete with other wall types in all height categories. (The highest wall located in Taiwan is approximately 38m high.) In the author's opinion, the profession finds itself in the midst of a massive transition from a flock of wall types to a predominance of gabion walls with basal mesh reinforcement.

The studies on gravity type rigid retaining walls commenced along with the birth of the geotechnical engineering subject and those on MSE type flexible walls since 1960s after the evolution of the principle of reinforced earth. Numerous studies have been conducted on these types till date and hence the behaviour is quite familiar to any practising geotechnical engineer. The gabion faced retaining walls being semi rigid in nature (due to the partial rigidity offered by the facing and flexibility offered by the reinforced portion), their behaviour is quite unknown to the engineering community. But the popularity of these walls is gaining high impetus because of their other advantages listed in

Chapter 3. Hence there arises an urgent need to study the force – deformation characteristics of gabion faced retaining walls which forms the main objective of the present study.

## 1.3 OBJECTIVES

The following specific objectives are considered:

1. Study the existing literature on retaining walls, its analysis and economics along with the performance of gabion faced reinforced earth walls in order to ascertain the need for the study.

2. Develop a finite element prediction tool which can simulate the behaviour of gabion faced retaining walls.

3. Validate the finite element code developed through experimental programme.

4. Explore the possibility of the use of any locally available material instead of the costly rock pieces inside gabion boxes to bring down the cost of construction.

5. Conduct parametric studies to examine the effect of variation of geometric and material properties on the load – deformation behaviour of gabion faced retaining walls using the finite element code.

6. Develop design charts based on the limit state method of design.

7. Conduct economic studies to prove the cost effectiveness of gabion faced retaining walls over conventional gravity type concrete walls.

## 1.4 ORGANISATION OF THE THESIS

Chapter I gives an introductory outline to the purpose and behaviour of retaining walls in general. The scope of the present study and the exact objectives are also pointed out in this chapter. Chapter II deals with an

extensive literature review on the different topics of the research work. Since the concept of gabion retaining walls, its construction, analysis and design are not well documented, a separate chapter is devoted to gabion faced retaining walls presenting all possible information collected from various sources. Hence, Chapter III contains a general introduction to the gabion faced retaining walls, the prevailing construction techniques and advantages of using these walls over conventional walls. The chapter concludes with a brief discussion on the design and analysis of these walls.

In Chapter IV, a general description of the finite element code developed is given clearly outlining the features of the elements used in the study and the simulation techniques adopted to predict the behaviour of gabion faced retaining walls. Chapter V deals with the experimental studies conducted in the field as well as in the laboratory, to validate the developed FE code and also to investigate the use of a locally available cheap material as an alternative to the costly stone pieces which are commonly used as gabion fill materials. Chapter VI briefs out the validation studies conducted to prove the effectiveness of the developed finite element code in predicting the behaviour of reinforced soil structures.

Chapter VII and VIII describe the geometric and material parametric studies conducted respectively on gabion faced reinforced soil retaining walls which clearly reflects the effect of the variation of these properties on the behaviour of these walls. Chapter IX portraits the development of handy design charts for the design of gabion faced retaining walls using the limit state method. Chapter X outlines the economic studies conducted to establish the cost reduction features of gabion faced walls along with suggesting cost prediction models and cost breakdown aspects. Finally, Chapter XI summarises the research work, clearly pointing out the conclusions drawn from the experimental and numerical investigations and bringing out the scope for future research in this area. A list of References cited follows this chapter.

Thus the thesis is organised in a methodical way.

# Chapter 2

# LITERATURE REVIEW

## 2.1 GENERAL

It has been a long time since boxes made of hexagonal mesh fabric, known as gabions, have become an effective technical solution in the design, construction and maintenance of a variety of protective flexible structures. Gabions, by virtue of their matchless strength, excellent engineering adaptability and reliability, have become the chosen building material for a tremendous variety of construction works. These include road construction, river training, weirs, control and training of natural and flood waters, earth retaining structures, water recharge dams, rock slide protection, soil erosion protection and bridge protection.

An extensive literature survey was conducted to identify the research works conducted on gabion faced retaining walls. But it was truly disheartening to note that, even though the construction of these walls is booming up in every nook and corner of the world, the research works conducted to understand the behaviour of these walls are very much limited in number, which is clearly proved at the end of this chapter. This obviously means that the present situation may have disastrous outcomes if the prevailing practice continues. Hence the author shifted her attention to collection of literature based on behaviour of retaining walls in general which may be categorised as gravity walls, reinforced soil walls, segmental retaining walls and gabion faced walls. The studies in this chapter are divided mainly into four groups as follows:

i. Literature on experimental investigations
ii. Analytical studies
iii. Studies on numerical modelling
iv. Economic studies

Literatures on experimental works were collected to understand how the retaining wall can be modelled physically and how the deformations can be measured. Works on finite element modelling of different types of retaining walls were collected to understand how a FE prediction model could be developed to simulate the behaviour of gabion faced retaining walls by modelling the different components individually. Analytical works on retaining walls were collected to understand how the design charts could be developed from the results of the present study.

## 2.2 EXPERIMENTAL INVESTIGATIONS

### 2.2.1 Gravity walls

Tweedie et al. (1998) constructed a 4.88m high retaining wall test facility to test tire shreds as retaining wall backfill. The front wall of the facility could be rotated outward away from the fill and was instrumented to measure the horizontal stress. Measurement of movement within the backfill and settlement of the backfill surface during wall rotation allowed estimation of the pattern of movement within the fill. Huang et al. (1999) developed a 2D model retaining wall system to investigate the effect of the bending rigidity of a wall, supported at the top and bottom, on the lateral pressure distribution at completion of backfilling condition.

Briaud et al. (2000) proposed the use of a vertically reinforced wall, a new type of top-down retaining wall. Typically, three to four rows of 1m diameter cemented soil columns were constructed to the depth of soil to be retained. After one year, the horizontal movements and vertical settlements of the wall were very close to the movements of the similar size tieback wall built at the same site. The authors claim this performance as an indication of the viability of this new wall type.

Lee et al. (2001) presented experimental data concerning the lateral earth pressures acting against a small-scale retaining wall, with a backfill consisting of waste foundry sand (WFS) mixtures. It was seen that the lateral earth

pressures on the wall depend on the backfilling sequence, the type and drainage characteristics of the WFS mixture, and the shear strength of the mixtures. Judging from the retaining wall model tests, the authors recommend that the backfilling of a 6-m high retaining wall can be completed in two days with two backfilling stages.

Chen and Fang (2002) investigated the effect of stress - history on the earth pressure at rest, using an instrumented stiff model retaining wall of 1.6m high using dry Ottawa sand. Calculations based on the experimental data indicated that the resultant forces were located at 0.34 H to 0.35 H above the base of the wall. For the backfill, the measured coefficient of earth pressure at - rest, $K_o$ was found to be independent of the thickness of the fill.

Fang et al. (2002) conducted experiments on a vertical rigid wall which moved towards a mass of dry sand and the earth pressure was measured. As the wall movement exceeded 12% of the wall height, the authors concluded that the passive earth thrust would reach a constant value, regardless of the initial density of backfill.

Hanna and Khoury (2005) conducted an experimental investigation on the passive earth pressure of overconsolidated cohesionless soil on retaining walls, using a prototype model of a vertical rough wall, retaining horizontal backfill. It was seen that the over consolidation ratio and the soil condition below the founding level significantly affect the value of the coefficient of passive earth pressure on these walls. Design charts and formulae were also developed for practical use.

Bentler and Labuz (2006) used earth pressure cells, tilt meters, strain gauges, inclinometer casings, and survey reflectors during the construction of a 7.9m high reinforced concrete cantilever retaining wall. The passive earth pressure in front of the shear key was found to be less than 10% of the design value and the vertical stress below the heel was greater than that at the toe.

Compaction-induced lateral stresses on the stem were sometimes twice the vertical stress.

Villemus et al. (2007) conducted experimental investigations in the laboratory and in - situ on dry stone gravity retaining walls to seek the knowledge necessary to ensure the stability of these structures. From the results of the experiments, a mathematical model was developed for calculating the stability of dry stone retaining walls. These tests also determined the limits of monolithic behaviour of the masonry, thus defining failure and enabling the fulfillment of practical engineering requirements.

### 2.2.2 Reinforced earth walls

Fukuoka et al. (1986) experimented on a 5 m high experimental fabric faced retaining wall reinforced with columns and steel rod anchors. It was observed that the fabric faced multiple anchored retaining wall is economical, easy to construct and very stable and the steel anchor rods can be used for a long time if they are coated with paint or asphalt.

Fabian and Fourie (1988) built large geotextile reinforced clay wall models to investigate the mechanism of clay-geotextile interaction and the effects of a low-cost, non-woven, needle-punched geotextile reinforcement on the load-bearing capacity of a silty clay. No face panels were used. The wrapped back geotextile reinforcement provided the face of the wall. The results of the testing programme were promising and encourage further research into the applicability of cohesive soils in geotextile-reinforced soil structures which might have great economic significance in areas where good quality granular backfill is not readily available.

Horiya et al. (1988) described an experimental study on a reinforced earth retaining wall constructed using the Hi – Tex wall method. The method of construction was using plate anchors (anchors with bearing plate) and a geotextile acting as a membrane. Pullout tests were conducted on the anchors

with bearing plates to understand the sliding behaviour of this new system. After that, execution of the full scale wall was carried out.

In order to evaluate the behaviour and stability of the embankment during and after execution, the deformations in the horizontal and vertical directions of the wall slope, the tensile forces developed in the anchor rods and the stresses developed in the steel pipes were measured.

Rao et al. (1988) presented three dimensional model studies on reinforced earth walls built and tested using "built to failure" technique. The models were prepared using aluminum foil reinforcement and aluminum sheet facing. The model tests revealed that the failure height by Rankine's theory gives conservative height of failure and that the tension at the joint of reinforcement with the facing is not zero, corroborating the findings of other researchers.

Fannin and Hermann (1990) built and monitored a sloped reinforced soil wall comprising of two sections with a different arrangement and spacing of geogrid reinforcement. The loading conditions used for the study were self weight, a cycle of surcharge load and permanent surcharge loading of the wall crest. Instrumentation was used to measure the force and strain in the reinforcement as well as pressure, strain and temperature in the soil mass. The performance data were collected for 20 months after the completion of construction. The authors found that the mechanisms of behaviour were according to expectations.

Fishman et al. (1993) instrumented an earth reinforced retaining wall to measure the movements of wall faces, lateral earth pressure, vertical stress in the soil mass, strains in the soil and strains along the reinforcement in the field. The wall was reinforced with geogrids and had a full height precast concrete wall facing. They observed that the computation of maximum tension in the reinforcement using the conventional design procedure is satisfactory.

Palmeira and Lanz (1994) presented a study of geotextile reinforced model walls subjected to vertical surcharge. Different reinforcement layouts were tested. Vertical stress distributions were measured at the base of the walls as well as internal displacements and horizontal displacements at the face of the wall. Comparisons between predictions and measurements were also made. The results showed that the reinforcement arrangement used in the wall can significantly affect its face displacements and the stresses at its base.

Wiseman and Shani (1994) described the construction of retaining walls in which the soil is reinforced by panels of welded wire mesh sandwiched between two geotextile layers heat bonded to each other, with precast concrete elements used as facing. Ten separate walls retaining backfill for the city streets with 35° surcharge slopes were constructed in heights varying from 3m to 15m. Pullout tests were conducted on welded wire mesh and geomesh. The authors, from their experience, are of the opinion that geomesh reinforced soil retaining walls have performed very satisfactorily during Israel's wettest winter in 200 years.

Isabel et al. (1996) described a new method of retaining wall construction that combined the reinforced earth technique with a conventional brick wall. The results showed that even short lengths of reinforcement significantly increased the load carrying capacity of a brick retaining wall. Although brick faced retaining walls do not obey the original principles of flexibility, the inclusion of the geotextile as reinforcement, allowed the construction as a whole to endure considerable movement before collapse, showing a high degree of ductility.

Ochiai and Fukuda (1996) conducted full scale failure experiments to study the behavioural characteristics of geotextile reinforced soil walls with different facings like discrete concrete panels, concrete blocks and expanded polystyrol blocks. With the help of the experiments and FEA, the reinforcing performance and mechanism were studied. From the results, it was found that

the deformation of a wall during the construction can be restrained by the gravity resistance of its facing.

Porbaha and Goodings (1996) built twenty four reduced scale models of vertical and steeply sloping (1 H : 6 V) reinforced soil walls using kaolin as the backfill, reinforced with a nonwoven geotextile simulant, and loaded to failure under increasing self weight in the geotechnical centrifuge. Models were constructed on either firm or rigid foundations, and different lengths of reinforcement were tested. A stability analysis using the two - dimensional limit - equilibrium simplified Bishop method incorporating reinforcement, was found to be a good predictor of the behaviour of the models based on calculated factors of safety at failure.

Iyer et al. (2001) studied the effect of bamboo strips as reinforcing elements with and without braided coir rope interface in model retaining walls. Ferro cement panels were used as facing elements tied to the reinforcing elements and backfill used was sea sand. They concluded that the high modulus of bamboo and the frictional characteristics of braided rope can be best made of in retaining walls up to 2m height.

Garga and O' Shaughnessy (2002) constructed a 57m high x 17m wide instrumented test fill, comprising both retaining wall and tire - reinforced slope sections to study the performance of tire reinforced earth fills. Approximately 10,000 tires were used in both cohesionless and cohesive backfills. The testing program included plate load tests, field pull out tests on tire mats, water quality assessment in the field and lab and other complementary lab testing. The authors demonstrated the practical feasibility of constructing reinforced earth fills using scrap tires. The results from the tests showed that the negative wall friction increases the active thrust when the retaining wall becomes more compressible than the backfill. The authors also gave recommendations for the design of retaining walls using scrap tires.

Hegazy (2002) performed laboratory tests to design the connections for a geosynthetic mechanically stabilised earth retaining wall. The connection strength was determined where the connection fails due to rupture of geosynthetic reinforcement (rupture criterion) or pullout of geosynthetic (serviceability criterion), whichever occurs first. A database of laboratory geosynthetic connection tests using different types of geogrid and facing blocks was collected and the design trends of these two parameters were recommended as a function of the confining stress.

Ma and Wu (2004) described the independent full facing reinforced soil wall system and the Fox wall project, with the measured data, and discussed the wall performance. Design implications concerning the initial setback of facing panels, reinforcement strength requirement, and lateral forces on facing panels were also addressed in the paper.

Frankowska (2005) presented the results of the 33-months monitoring of a reinforced wall with geosynthetic wrap-around facing. The wall was exposed to natural weather conditions and the following variables were measured: horizontal and vertical displacements at the surface of the wall faces, the wall settlement and the reduction of basic mechanical properties of geosynthetic after using it as the reinforcement. The observed strength losses of geosynthetic ranged from 83% to 97% over a period of 33 months.

Chen et al. (2007) simulated a clayey vertical geotextile - reinforced earth wall in a wet state due to poor drainage conditions, after several consecutive days of heavy rainfall, by a series of centrifuge models. The models were constructed using clayey soil very close to its liquid limit. Through centrifugal tests on these models, the effectiveness of various reinforcement arrangements was examined. It was seen that for any reinforcement length, there exists a critical value beyond which no further improvement can be attained. Also, smaller vertical reinforcement spacing leads to shorter critical reinforcement length. Four failure modes were observed in this study and their evolution for each reinforcement arrangement was also demonstrated.

Won and Kim (2007) measured the local deformation of geosynthetics, such as geogrids, and nonwoven and woven geotextiles to examine the stability of geosynthetic - reinforced soil (GRS) structures. They proposed a new, more convenient method, to measure the deformation behaviour of non woven geotextiles using a strain gauge and examined its suitability via laboratory tests and field trials on two GRS walls.

Shinde and Mandal (2007) carried out several experiments to understand the deformation behaviour of reinforced soil retaining wall with limited fill zones under vertical surcharge strip loading. Panel displacements and strain distribution along geogrid layers were observed. Effectiveness of the reinforced soil wall was also evaluated using a geogrid material. Finite element analysis was also carried out using commercial software PLAXIS version 8 for the above problem without and with anchoring of reinforced soil retaining wall in the limited fill zone. The results were compared and showed good agreement.

Chen and Chiu (2008) performed model tests on nine model geocell retaining walls to examine the effect of the geocells as a major material in retaining structures and also to study the failure mechanism of the said structures under surcharge. Results showed that the deformation on the wall face and the backfill settlement both increased with increasing facing angle and surcharge.

### 2.2.3 Segmental retaining walls

Segmental retaining walls (SRWs) form a new generation of reinforced earth retaining walls where flexible facing units are replaced with modular block facing units. The facing units may be of reinforced concrete, precast concrete or brick units. The reinforcement may be geogrids or geotextiles. An important criterion in the design of these walls is the connection strength between the facing units and the reinforcement. The overall strength of the structure is thus imparted by the rigidity of the facing units and the friction between soil and reinforcement.

A hybrid segmental retaining wall system using both steel and geosynthetic reinforcement failed in 1998. Collin (2001) analysed this segmental retaining wall failure with respect to the design, and construction to determine the cause/causes of the failure. The results of the forensic analysis were presented along with the remedial measures necessary to correct the problem. The analysis identified that the poor connection between the soil reinforcement and the segmental concrete units was the primary cause of the failure. The design of the wall used a proprietary software program that did not consider the connection strength of the hybrid system used. The remediation included the removal of the wall face and reconstruction increasing the connection capacity between the segmental concrete units and the reinforcement by a factor of three.

Yoo and Lee (2003) presented the measured behaviour of an anchored segmental retaining wall. To understand the overall mechanical behaviour of the anchored segmental retaining wall and to confirm the applicability of the design assumptions, an extensive monitoring program was implemented for a 7-m-high anchored segmental retaining wall.

The results showed that the maximum lateral wall displacement was comparable to or less than that of a typical geosynthetic - reinforced wall. The measured and the inferred horizontal earth pressures showed that the horizontal earth pressures exerting on the wall facing were greater than those inferred from the Rankine active state of stress and the Coulomb wedge analysis, approaching the at-rest state.

Yoo and Jung (2004) presented the observed behaviour of a geosynthetic reinforced segmental retaining wall. A 5.6 m high full scale wall in a tiered configuration was constructed and instrumented, in an attempt to examine the mechanical behaviour and to collect relevant data that will help improve the current design approaches. It was shown that for walls on a less competent foundation, significant post construction wall movements may occur.

### 2.2.4 Gabion faced retaining walls

Garg (1997) highlighted two innovative technologies for stabilisation of slopes. One was a reinforced gabion wall and the other was an anchored drum diaphragm wall implemented successfully in the Garhwal Himalaya during eighties to improve stability of slopes at comparatively lesser cost and time than conventional retaining walls.

Ferriolo et al. (1997) presented the details regarding the use of flexible gabion structures for landslide, road protection and river training works. The authors explained the phenomena of landslide and erosion as modification of equilibrium condition of soil at specific surfaces due to a natural configuration or due to a human activity. Gabion mattresses being flexible structures have added advantages in their use in these areas. It is also mentioned that the internal structure details of the gabions such as opening size, double twist mesh, hexagonal shape, wire diameter, extent of galvanisation, diaphragms and joint details play an important role in the functioning of the structure as a whole.

Simac et al. (1997 A and B) described the design and construction of the MSE walls on the Tellico plains to Robbinsville highway. The walls were built with hybrid wall system components, consisting of geogrid reinforcement and PVC coated gabion baskets. The selection of these materials was based primarily on the presence of a chemically active environment, availability of an economical fill source, aesthetic appearance and overall cost. The paper summarised the design procedure utilised to ensure wall stability along a mountainous highway alignment. The paper also examined how the general MSE design guidelines presented in the project specifications can be augmented with currently accepted methods of analysis to provide a safe but economical wall design.

The authors concluded that hybrid MSE systems like the one mentioned above can be successfully designed by implementing currently accepted methods of analysis for geosynthetic reinforced soil walls. But appropriate

facing connection tests should be done before implementation of this system. The latter paper also describes the specialised laboratory testing that was carried out to ensure that the connection formed between gabion baskets and reinforcement was adequate.

Bergado et al. (2000 B) studied the horizontal deformations of gabion walls on a fully instrumented test embankment reinforced with hexagonal wire, constructed on a soft Bangkok clay foundation in Thailand. The reinforced wall consisted of an inclined gabion facing on one side and a sloping unreinforced sand wall on the opposite side, with a total height of 6 m. Two different types of hexagonal wire meshes were utilized for the study. The wall system was extensively instrumented both in the foundation subsoil and the embankment, in order to monitor the behaviour of the wall both during and after the construction phase. A maximum settlement of 0.35 m was observed 200 days after construction. It was found that there is a direct correlation between displacement and stress in hexagonal wire mesh reinforcement. For both types of meshes, the maximum deformation was observed in the top most layers.

Bergado et al. (2001) conducted pullout tests on hexagonal wire mesh of gabions embedded in silty sand locally known as Ayuttaya sand to investigate the soil reinforcement interaction. Two types of hexagonal wire mesh were tested, namely: (a) galvanised (zinc-coated) which had smaller aperture (cell) dimension of 60 mm x 80 mm and (b) PVC coated which had larger aperture (cell) dimension of 80 mm x 100 mm. The tests were conducted under normal pressures ranging from 35 to 91 kPa and the specimens were pulled at a rate of 1 mm/min. The total pullout resistance of hexagonal wire mesh reinforcement consists of two components, namely: friction and bearing resistance. It was seen that the bearing resistance is higher than the friction resistance for both types of reinforcement. Higher friction and bearing resistances were obtained with increasing normal pressures. The friction and bearing resistances mobilised on the galvanised wire mesh were greater than the PVC-coated wire mesh, due to higher friction coefficient as well as greater number of transverse and longitudinal members (elements) per unit width in the former than the

latter. The authors proposed an analytical method for predicting the pullout resistance and displacement relation using the basic soil and reinforcement properties which agreed reasonably well with the test results.

## 2.3 ANALYTICAL STUDIES

### 2.3.1 Gravity walls

Bang and Hwang (1986) developed an approximate analytical solution to estimate the developed lateral earth pressures behind rigid retaining walls experiencing various types of outward movements with horizontal cohesionless backfill soil. Various stages of wall movement, starting from an at - rest condition to a full active condition were included.

Day (1994) examined the effect, which the stiffness of the lateral support system has on the movement of ground and adjacent buildings. The properties of both the supported material and the support system which influence the movement of the retaining structures were identified with the illustrations of the performance of a variety of retaining structures. It was stated that the movement of the ground behind a retaining structure is dependent on the consistency of the ground, the in - situ stress condition and the stiffness of the support system.

Hazarika and Matsuzawa (1996) developed a new numerical method, based on a smeared shear band technique for the analysis of earth pressure that incorporates two shear bands for a localised element. The method, which is valid for plane strain condition, was applied to explain the generation of the active earth pressure against a rigid retaining wall for different modes of the displacement that the wall is likely to undergo.

Chang (1997) presented a simple analysis method for predicting the lateral earth pressure at any wall displacement behind a rotating wall using a modified Coulomb's solution of active earth pressure. The deformation pattern and the associated mobilisation of shearing resistance in the soil as affected by

the wall movement are considered in a simplified manner. The method was validated with solutions from FEM and observations from model tests.

Filz and Duncan (1997) developed a simple theory for calculating the magnitude of vertical shear loads on nonmoving walls. Retaining walls that do not move are customarily designed based on the assumption of at - rest conditions, with no consideration of vertical shear loads applied by the backfill. However, field and laboratory measurements have shown that vertical shear loads do act on nonmoving walls. Typical results from the theory incorporating vertical shear loads were also discussed.

Jalla (1999) presented details of the design methodology of multiple level retaining walls as used in residential construction. Each tier of multiple retaining walls should be safe against sliding, overturning, and bearing capacity failure. In addition, the global slope stability behaviour should also be checked.

Greco (2001) showed that the wall stability against overturning can, however, be assessed using the position of the resultant force on the base, which is unaffected by the assumed thrust surface and contrary to overturning, safety factors against sliding and bearing capacity are unaffected by the assumed thrust surface.

Long (2001) prepared a database of some 300 case histories of wall and ground movements due to deep excavations worldwide. It was analysed that for still soil sites, movements were generally less than those suggested in the published well - known relationships. He suggested that, in the case of cantilever walls and for all walls in stiff soils worldwide, design practice is conservative and the inclusion of a cantilever stage at the beginning of a construction sequence seems to be the main cause of unusually large movements.

Kim and Barker (2002) generated values of equivalent height of soil $h_{eq}$ for the live load model in the AASHTO specifications acting on a gravity retaining wall based on the elastic theory for determining soil pressures within

a soil mass due to loads on the surface. The paper discusses the theoretical background, an analytical approach to estimation of actual earth pressure, a number of innovative approaches to obtain a simplified pressure distribution, an extensive parametric study, calibration procedures for the traditional method and recommendations.

Wang (2007) presented approximate but analytical - based solutions for computing the lateral force and centroid location induced by horizontal and vertical surcharge surface loads resting on a cross-anisotropic backfill. The surcharge loading types include: point load, finite line load, and uniform rectangular area load. The planes of cross-anisotropy were assumed to be parallel to the ground surface of the backfill. The results showed that both the lateral force and centroid location in a cross-anisotropic backfill were quite different from those in an isotropic one.

### 2.3.2 Reinforced earth walls

Saran and Talwar (1983) investigated a form of soil reinforcing for retaining walls where the lateral pressure on conventional retaining walls is sought to be reduced by reinforcing the backfill by unattached horizontal bamboo strips. The expressions for intensity of lateral pressure, resultant earth pressure and its point of application were derived in terms of strength parameters of soil as well as the characteristics and distribution of reinforcement.

Sawicki and Lesniewska (1987) dealt with the theoretical analyses of the bearing capacity of reinforced soil retaining walls on the basis of a rigid-plastic model of reinforced soil and limit theorems. The results obtained could be useful in engineering calculations and design of geotextile reinforced retaining walls.

Bauer (1988) analysed earth reinforced structures, reinforced with plastic geogrids, using limit equilibrium and finite element methods. The analyses included surcharge effects and various soil materials. The results

were presented as normalized graphs which can be used as design guides to estimate the critical geometry of a reinforced earth structure for various reinforcing configurations.

Leshchinsky and Perry (1988) evolved a design procedure for geotextile - reinforced walls subjected to uniform surcharge loads. Design charts were included for the evaluation of internal stability of the wall, which were developed from a limit equilibrium analysis.

Bathurst and Simac (1993) described and compared the features of two computer programs GEOWALL and GRSWALL which were written by the first author to allow the geotechnical engineer to design a geosynthetic reinforced soil wall quickly. The authors conclude that GRSWALL allows the user more flexibility with respect to the number of reinforcement types and reinforcement layout. On the other hand, GEOWALL is more advanced as a design aid that will guide the user through the analysis and design of a geosynthetic reinforced soil wall.

Singh and Basudhar (1993) successfully demonstrated the application of a generalized approach to the estimation of the lower bound bearing capacity of reinforced soil retaining walls by using the finite element technique in conjunction with non linear programming to isolate the optimal solution. The analysis was based on a rigid plastic model for reinforced soil, treating it as a macroscopically homogeneous anisotropic material. The results obtained were found to be in good agreement with the theoretical and experimental data reported in the literature.

Fantini and Roberti (1996) described the study, design and execution of a vegetated geogrid reinforced slope used to recover a degraded area due to the construction of a viaduct in a highway in Italy. Reinforced slopes of height varying from 3 m to 20 m were constructed using different bioengineering techniques, to obtain a well established and permanent vegetation cover.

The authors finally infer that a good use of the geosynthetics can solve extremely difficult problems with due respect to the environment.

Mannsbart and Kropik (1996) reported the construction and analysis of a temporary retaining wall, 2.1m high, in the course of the lifting and widening of a railroad track in Vienna. Due to the limited time and space available, the wall was built using non woven needle punched continuous filament geotextiles as reinforcing elements. In spite of the heavy traffic load, measurements showed that the deformation of the structure was negligible, proving that even low modulus nonwoven geotextiles can fulfill reinforcement functions, especially in low, temporary structures.

Motta (1996) utilised the limit equilibrium analysis applied to a plane failure surface for the evaluation of the active earth pressure on reinforced earth retaining walls under different loading conditions, such as seismic loading, pore water pressures into the fill, vertical and horizontal loads acting on the top at some distance. Pore water pressure effects on the earth pressure were taken into account by means of the pore pressure ratio ($u/\gamma H$). In the design procedure, the analysis also allowed to define the spacing or the number of reinforcement as well as their length according to the failure wedge predicted.

Soong and Koerner (1997) discussed a number of short and long term issues during and after a geosynthetic reinforced soil wall is constructed and its required connection strength.

Garg (1998) dealt with the design, construction and cost economics of a 11m high and 19.5m long random rubble stone masonry wall retaining reinforced earth fill. The cohesionless fill, available at the construction site, was reinforced by geogrids, which were not attached to the wall face. The design philosophy developed by the author for rigid reinforced earth wall was discussed in detail in the paper. It was also reported that the retaining wall with geogrid reinforced earth fill was constructed at 79% of the cost of the retaining wall with conventional earth fill.

Porbaha et al. (2000) applied a kinematic approach based on the framework of limit analysis for the stability analysis of model reinforced vertical and sloping walls with cohesive backfill that were brought to failure under self-weight in a geotechnical centrifuge. A rotational failure mechanism was used to compute critical heights of the unreinforced and reinforced models; and the constrained Simplex method was employed in the optimization scheme. The prototype equivalent heights predicted by the analyses were within the distress range; i.e., development of tension crack and collapse of the retaining walls occurred during centrifuge tests.

Hatami et al. (2001) investigated the structural response of reinforced-soil wall systems with more than one reinforcement type (non uniform reinforcement) using a numerical approach. The selected reinforcement types and mechanical properties represent actual polyester geogrid and woven wire mesh products. The model walls were mainly of wrapped-face type with different reinforcement lengths, arrangements, and stiffness values. Additional wall models with tiered and vertical gabion facings were included for comparison purposes. The numerical simulation of wall models was carried out using a finite difference-based program which included sequential construction of the wall and placement of reinforcement at uniform vertical spacing followed by a sloped surcharge.

Srbulov (2001) analyzed the stabilities of slopes and walls using a method based on limit equilibrium. The results of measurements of axial strains in geogrids of two reinforced steep slopes and two retaining walls were interpreted. However, the results obtained by the method remain only approximate due to necessity to introduce a number of simplifying assumptions.

Horvath (2003) discussed a geosynthetic based earth retention concept. This new concept allows controlled yielding within a retained soil mass by using a compressible inclusion composed of certain types of geofoam geosynthetic that can be used alone or combined with MSE. Two basic ways were outlined,

in which geofoam compressible inclusions are used with earth retaining structures – Reduced - Earth - Pressure and Zero - Earth - Pressure concepts. Typical applications of the same were also discussed.

Leshchinsky et al. (2004) developed a rational design methodology for multitiered MSE walls that accurately predicts wall performance. The study presented the results of parametric studies conducted in parallel using two independent types of analyses based on – limiting equilibrium and continuum mechanics. Parametric studies were carried out to assess the required tensile strength as a function of reinforcement length and stiffness, offset distance, the fill and foundation strength, water, surcharge, and number of tiers. It was concluded that limiting equilibrium analyses may be extended to the analysis of multitiered walls.

Bathurst et al. (2005) developed a new working stress method for the calculation of reinforcement loads in geosynthetic reinforced soil walls. As a precursor to this objective, back-analyses of a database of instrumented and monitored full-scale field and laboratory walls was used to demonstrate that the prevailing AASHTO Simplified Method used in North America results in excessively conservative estimates of the volume of reinforcement required to generate satisfactory long-term wall performance.

Mittal et al. (2006) analysed the case of a rigid wall with inclined back face retaining reinforced cohesive frictional backfill subjected to uniformly distributed surcharge load using limit equilibrium approach. The analysis considered the stability of an element of the failure wedge, which is assumed to develop in the reinforced earth mass adjoining the back face of wall. Non-dimensional charts were developed for computing the lateral earth pressure on wall and the height of its point of application above the base of wall. The theoretical findings were verified by model tests on a rigid wall retaining a dry cohesive-frictional soil reinforced by geogrid strips. Experimental results were in good agreement with the theoretical predictions.

A design example was also added in the paper to illustrate the design procedure.

### 2.3.3 Segmental retaining walls

Rimoldi et al. (1997) discussed the various aspects of design methodology, installation and construction practices of geogrid reinforced retaining walls. It was stated that before the design of a reinforced earth retaining wall, the properties of the reinforcement viz., friction, tensile strength, creep resistance, junction strength, chemical and biological resistance should be carefully evaluated. The walls should be checked for external and internal failure modes, facing failures and global stability. The design criteria include tensile overtension failure analysis, geogrid pullout failure analysis and local stability of segmental retaining wall units.

Koerner and Soong (2001) compared three design methods of geosynthetic reinforced segmental retaining walls to one another with respect to their details and idiosyncrasies. This was followed by a numeric example which illustrated that the modified Rankine method is the most conservative, the FHWA method is intermediate, and the NCMA method is the least conservative. A survey of the literature was included where it can be seen that there have been approximately 26 walls which suffered either excessive deformation or actual collapse. The survey described 12 serviceability problems and 14 wall failures. Of the total, 17 of the cases had low permeability backfill soils in the reinforced zone and 8 had uncontrolled or inadequate quality control in the construction of the walls.

## 2.4 NUMERICAL MODELLING

### 2.4.1 Gravity walls

Bolton et al. (1989) studied the behaviour right up to the collapse of a retaining wall embedded in overconsolidated clay using FE analysis and the results were compared with those of centrifuge modelling. Six noded triangles were used to model the soil and 8 noded quadrilaterals to model the diaphragm

wall. Slip elements of 0.1 mm thickness were used between the retaining wall and the soil to model the interface conditions which may permit relative slip.

Larkin and Williams (1994) developed a simplified computer model of lateral earth pressure and compared its efficiency with some large scale experimental work. The computer model included a linear elastic stress strain relationship with the values of the elastic constants adjusted to be consistent with deformations. The computed force - deformation relationship of the translating wall was compared with that recorded from an experimental set up with a 1m retaining wall backfilled with cohesionless soil. Comparisons between recorded and computed pressure distributions were made for several values of wall translation.

Matsuzwa and Hazarika (1996) carried out a numerical investigation to evaluate the effect of wall movement modes on static active earth pressure. The authors developed new interface elements having bilinear stress – displacement relations and introduced them between the backfill soil and the wall to simulate the frictional behaviour. To avoid the separation between the wall and the backfill soil, during the active movement of the wall, conventional linkage elements were idealized suitably. The active state was defined based on the progressive formation of a failure zone in the backfill. Empirical equations, containing wall movement made as a governing parameter, were derived for calculating the active earth pressure coefficient and the relative height of the resultant active thrust for various angles of internal friction of the backfill.

Filz et al. (1997) constructed massive concrete walls on rock foundations, as well as other nonmoving retaining walls, customarily designed for at - rest earth pressures. In this paper, model test results and case history data were reviewed, the results of finite - element calculations were presented, and a simple design procedure was developed. It was shown that significant economies can result from consideration of vertical shear forces in design of nonmoving retaining walls.

Addenbrooke et al. (2000) used the results from 30 nonlinear finite element analyses of undrained deep excavation in stiff clay to support the use of a new displacement flexibility number in multi propped retaining wall design. The analyses addressed the effects of different initial stress regimes and various values of prop stiffness for the internal supports to the excavation.

### 2.4.2 Reinforced earth walls

Romstad et al. (1976 and 1978) represented the reinforced earth as a composite material with associated composite properties. The composite model was developed by consideration of a small unit of the material as a fundamental building block called the unit cell. The composite properties defining the stress - strain relationships were predicted by successively considering a number of simple composite stress - strain states and approximately determining the response of the unit cell.

Shen et al. (1976) described an analytical study using the FE program of an instrumented complex field prototype constructed in Southern California. The analytical results were then compared with the field performance data to illustrate the overall behaviour of the structure and the strengths and weakness of the analytical model. In addition, implications of the study relative to the existing design procedures were drawn and recommendations were made for simple reinforced earth structure design.

The analysis of the finite element results and field performance indicated that reinforced earth is a relatively rigid supporting unit in which, under normal conditions, the stress state within the wall is approximately $k_0$ condition and the backfill just behind the wall approaches $k_a$ condition. The boundary geometry of the backfill and foundation and compressibility of the foundation material affected the magnitude and direction of the strip forces. Even compressive forces developed in the strip under particular combinations of these parameters.

Naylor (1978) used a special element and formulated a slipping strip analytical model for earth retaining walls using unit cell concept. Soil was assumed to be linear elastic and was represented by six noded rectangular elements. An extra degree of freedom for representing the displacement of a point on the strip relative to the soil matrix in a direction parallel to the strip was given. A parametric study was carried out to investigate the effect of strip slip, fixity at the face, relative longitudinal stiffness of strips and soil as well as stiffness of the foundation.

Ogisako et al. (1988) performed finite element analysis on polymer grid reinforced soil retaining walls. The wall was modelled using the beam element, soil using quadrilateral elements and the polymer grid using truss element whose ends were connected by pin joint. The soil – reinforcement interface and the wall – soil interface were modelled using joint elements. Analyses were performed on various height of the wall and spacings and lengths of the polymer grid. The effect of these parameters on the reduction effect of the earth pressure acting on the wall and the wall deformation was discussed in detail.

Bauer and Halim (1989) reported a composite finite element study on reinforced soil walls constructed with cohesive backfill. Soil was modelled using Duncan and Chang's (1970) hyperbolic stress function. The base was assumed to be rigid. The results showed that the lateral movement of the wall face decreased with a decrease in the wall inclination and the maximum settlement occurred close to the wall face, at the upper part of the wall. The maximum stress in the reinforcing strip depended on the footing location. The direction of load inclination affected the lateral movement and settlement greatly. The introduction of a cohesive backfill was found to reduce the lateral displacement by 25% and settlement by 50% under vertical loads.

Chew and Schmertmann (1990) presented the results of study of the deformation behaviour of reinforced soil walls using a previously validated finite element code. The conventional design procedures for reinforced soil walls consider the overall stability and rupture and pullout capacities of the

reinforcement. But it does not take into account the wall deformations under working stress conditions. The authors attempted to bridge this gap by presenting the summary of a numerical study of the effect of reinforcement length, reinforcement layout and external loadings on the deformation of reinforced soil walls.

The FE code used was capable of modelling the construction sequence and compaction operations. The code could also consider the thrust from the unreinforced soil behind the reinforced soil zone. This modelling method was applied to a range of inextensible reinforcement layouts and external loadings, varying about a reference wall, to predict the end - of - construction wall response.

Karpurapu and Bathurst (1992) described two sets of numerical simulations which were carried out to model the controlled yielding concept. The simulations used finite element method together with a hyperbolic constitutive soil model.

The 1 m high walls were constructed using a continuous stack of 20 articulated platens constrained to move in the horizontal direction by a system of flexible springs and frictionless rollers. Eight-noded quadrilateral elements were used to model both the panels and the soil, and two-noded bar elements were used to simulate the springs. The panels and soil were separated by six-noded isoparametric interface elements. These elements were assumed to have negligible shear stiffness to simulate the teflon surface at the wall that was employed to reduce friction effects in the physical tests. The nodes at the bottom surface of the mesh below the soil were fully constrained. The incremental construction sequence in the physical tests was simulated by building the mesh in 20 rows of elements using several load steps per layer. The material behaviour of the soil was modelled using the hyperbolic constitutive model. Simulations were carried out to generate preliminary design charts for the selection of stiffness and thickness of compressible layers placed

against rigid walls retaining well graded sand backfills compacted to a range of densities.

Bergado et al. (1995) studied the behaviour of a reinforced embankment on soft Bangkok clay by plane strain finite element method. The analysis considered the selection of proper soil / reinforcement properties according to the relative displacement pattern of upper and lower interface elements. A full scale test reinforced embankment with a vertical face wall on Bangkok clay was analysed by this method. The numerical results were compared with the field data and it was concluded that the response of a reinforced embankment on soft ground is principally controlled by the interaction between the reinforced soil mass and the soft ground and the interaction between the grid reinforcement and the backfill soil. The permeability variation of the soft ground was also accounted in the finite element analysis.

Karpurapu and Bathurst (1995) used finite element models to simulate the behaviour of two carefully constructed and monitored large-scale geosynthetic reinforced soil retaining walls. The walls were constructed using a dense sand fill and layers of extensible polymeric (geosynthetic) reinforcement attached to two very different facing treatments. A modified form of hyperbolic constitutive model that includes a dilation parameter was adopted to model the behaviour of the granular soil. The results of analyses show that the finite element model, constitutive models and implementation reported in the study can accurately predict all important features of wall performance.

Ling et al. (1995) discussed the application of the finite element (FE) procedure for simulating the performance of geosynthetic reinforced soil retaining walls. Analyses were performed using a modified version of CANDE code, in which the material properties of the wall (backfill, foundation, geosynthetic and wall face) were expressed using non – linear elastic models. The analytic procedure was validated with the loading test results of a full – scale model comprising silty clay backfill soil and a permeable geotextile. A series of parametric studies was conducted to identify the effects of the

geosynthetic length and the stiffness of the facing and the geosynthetic on the performance of geosynthetic reinforced soil retaining walls. They concluded that the layout of geosynthetic layers affects greatly the performance according to the point of load application and increased wall facing and geosynthetic stiffness improve the performance by restraining the lateral deformations.

Bauer and Brau (1996) proved using back analysis technique that non wovens can be used in earthworks as reinforcement when the material characteristics that describe the stress strain behaviour of the composite system consisting of soil and geotextile are known. The conventional calculations look at soil and geotextile separately and hence these methods do not suit the calculation of the effect of non wovens in soil mass.

Ho and Rowe (1996) examined the effect of geometric parameters such as reinforcement length, number of layers of reinforcement, distribution of reinforcement and wall height on the forces developed in the reinforcement. It was shown that the forces developed are largely independent of reinforcement length for reinforcement to wall height ratios equal to or greater than 0.7. For truncated reinforcement schemes with a ratio of less than 0.7, the forces in the reinforcement increased as the length of the reinforcement decreased. The number of layers of reinforcement was not found to significantly affect the total force required for equilibrium provided the reinforcement stiffness density was the same. The analysis provided theoretical support for the common practice of using truncated reinforcement with equal vertical spacing and length equal to 70% (or greater) of the wall height.

Alfaro et al. (1997) obtained the patterns of deformation of the wall and the soft clay foundation beneath the reinforced soil mass based on the results of full scale field tests and FEA. The performance of two reinforced soil test wall - embankment systems constructed on soft clay foundation with different reinforcement types but having the same backfill were used in the investigation. One test facility used steel grid reinforcement and the other used polymer grid reinforcements. Parametric studies were carried out using FEA to examine the

effects of the stiffness of the reinforced soil system and the foundation on the overall deformation characteristics of reinforced soil wall. Results indicated that increasing the stiffness of the reinforced soil system led to lower lateral spreading of the clay foundation owing to more lateral confinement of the underlying soil.

Kobayashi and Porbaha (1997) presented the numerical modelling of the physical tests on scaled geotextile reinforced retaining walls constructed with cohesive backfill. The aim of the work was to predict the position of critical slip surface which is an important factor in the cost effective design of retaining systems. For this, the effects of maximum shear strain contours and plastic yield zones on the positions and traces of slip surfaces were investigated for unreinforced and reinforced vertical walls.

Rowe and Ho (1997) examined the effects of reinforcement stiffness density, reinforcement – soil friction angle, backfill friction angle and facing rigidity on the behaviour of continuous panel faced reinforced soil walls resting on a rigid foundation. It was shown that the interaction between the components of the reinforced system determines the stress distribution in the soil and the manner in which the required total resisting force is distributed in the reinforcement layers.

Helwany et al. (1999) validated a finite element program by comparing its analytical results with the results of a well instrumented large scale laboratory test conducted on a geosynthetic reinforced soil (GRS) retaining wall under well – controlled test conditions. The validated computer program was used to investigate the effects of backfill type on the behaviour of GRS retaining walls. It was shown that the type of backfill had the most profound effect on the behaviour of the GRS retaining wall. It was also shown that the stiffness of the geosynthetic reinforcement had a considerable effect on the behaviour of the GRS retaining wall when the backfill was of lower stiffness and shear strength.

Lee et al. (1999) studied the use of shredded tires as backfill in reinforced earth structures. Triaxial test results were used in the FE modelling (using commercial FE program ABAQUS) of wall and backfill, both unreinforced and reinforced with geosynthetics. Duncan and Chang's (1970) non linear hyperbolic model was used to model the tire shreds and rubber-sand. Both backfill and wall facing elements were modelled with 8 noded 2D solid elements. Linear elastic model was used to represent the wall elements. The geotextile used as reinforcement in the wall backfill was modelled using zero thickness interface elements following Coulomb's friction mechanism.

The FEA were conducted under at-rest and active conditions. The results were compared with field tests and good estimates of deformations and stresses were obtained for at-rest condition, but showed overestimation for active condition. The analyses indicated that the performance of rubber sand, being both light weight and reasonably strong, compared well with that of a sandy gravel, as a backfill material.

Sreekantiah (2001) used a two dimensional numerical model, based on the finite element method, for investigating the deformation behaviour of a geogrid reinforced soil retaining wall. Relationships between lateral deformation and height of the wall and between vertical settlement and height of the wall were studied numerically and compared with the experimental results on model retaining walls. He concluded that the finite element analysis is capable of the deformation behaviour of a reinforced soil retaining wall with a reasonable degree of accuracy.

Sreekantiah and Sowmya (2001) investigated the behaviour of a geogrid reinforced soil retaining wall using a two dimensional numerical model based on the finite element method. Model retaining walls for different combinations of vertical spacing of reinforcement were investigated for various surcharge loads. Relationships between lateral deformation and height of wall and between vertical settlement and height of wall were studied. The results were verified with experimental data.

Tyagi and Mandal (2001) conducted parametric studies on geosynthetic reinforced retaining walls based on finite element analysis on four different geosynthetic reinforcements and eight different types of backfills to produce 100 combinations. Use of sandwich technique to optimize the cost and strength mobilization of two different backfills was adopted in actual site conditions after validation of FEM results. They concluded that the type of backfill has profound effect on the behaviour of a reinforced soil wall and the stiffness of reinforcement plays a considerable role for soil of lower stiffness and shear strength. The parametric charts developed by the authors will help the geotechnical engineer to choose the appropriate backfill and geosynthetic reinforcement for satisfying the prescribed requirements of maximum displacement, maximum axial strains in reinforcements and safety factors.

Park and Tan (2005) discussed the effects of the inclusion of short fibre in sandy silt (SM) soil on the performance of reinforced walls. The finite element method was used to examine the influence of the reinforced short fibre on reinforced walls. The vertical and horizontal earth pressure, displacement and settlement of the wall face were analyzed. These results were compared to the measured results from two full-scale tests. It was seen that use of short fibre reinforced soil increases the stability of the wall and decreases the earth pressures and displacements of the wall and this effect is more significant when short fibre soil is used in combination with geogrid.

Skinner and Rowe (2005) conducted numerical analysis of a hypothetical 6 m high geosynthetic reinforced soil wall supporting a bridge abutment and approach road constructed on a 10 m thick yielding clayey soil deposit. The soil retaining wall was examined under two-dimensional (plane strain) conditions consistent with normal design assumptions. The finite element mesh used 4335 eight noded isoparametric elements to model the soil, masonry and concrete, 288 linear bar elements (with no significant compressive or bending strength) to model the reinforcement and 1390 interface elements were used between the various materials. The initial geostatic stress conditions in

the foundation were based on the unit weight and effective coefficient of lateral earth pressure at rest ($K_0$) for the soil.

The results of the numerical analysis were compared to current design methodologies to examine the effect of the yielding soil foundation on the behaviour of the wall and abutment. The study included the examination of both the internal and external stability of the wall, and focused on methods of improving the external stability.

### 2.4.3 Segmental retaining walls

Arab et al. (1998) used the finite element method for analysing two full scale experiments on segmental walls (4.35m x 5m) loaded on the top and constructed with extensible reinforcement of non woven and woven geotextiles, using the FE code GOLIATH. Large deformation analyses were conducted simulating the construction process also. The wall was loaded with a concrete slab having surcharge 130kN/m. For the non woven wall, the predicted settlement was found to be more than the experimental values whereas it was lesser for the woven walls. Parametric studies were conducted varying the geometric and material parameters.

It was seen that the influence of reinforcement length is significant only till length equal to half the height of the wall after which nil effect was noticed. With increasing surcharge and stiffness, settlements also increased. In the absence of a facing or using a facing of low stiffness, caused higher deformations. The effect of position of load was also studied and it was seen that when the footing is placed outside the reinforcement space, a shear band is developed from the downstream side of the slab to the bottom of the facing. Also, there was no significant increase in bearing capacity when the reinforcement length exceeded 0.5 times the height. It was concluded that the reinforcements should extend beyond the potential failure surfaces.

Rowe and Skinner (2001) conducted numerical examination of the behaviour of an 8m high geosynthetic reinforced soil wall constructed on a

layered foundation stratum using FEM. The wall was constructed with 16 segmented concrete facing blocks, a sandy backfill and 11 layers of geogrid reinforcement 6m long. Five additional, one metre long layers of reinforcement were used between the 6m long layers within the upper 5m of the wall to improve the local stability of the facing blocks. The analysis examined the effect of uncertainty regarding the drained and undrained strength of the loam foundation material, its stiffness, the thickness of this soft layer and its position with respect to the bottom of the wall on the calculated behaviour and compared the calculated and observed behaviour from the full-scale test wall.

The field case was idealized as two dimensional and a plane-strain analysis was performed. The finite element mesh used 1697 eight noded isoparametric elements to model the soil, concrete and footing blocks and 1117 interface elements were used between the soil and other materials. The reinforcement was modelled using 417 linear bar elements. The concrete and footing block were treated as elastic materials. An elasto-plastic stress–strain model with Mohr–Coulomb failure criterion was adopted for the continuum elements used for the soil. The interface elements were modelled with a stiff spring in each of the shear and normal directions until slip occurred, at which point deformation could occur along the interface and the normal and shear stresses satisfied Mohr–Coulomb failure criterion. The construction analysis of the wall was conducted layer-by-layer.

Yoo (2004) presented the results of an investigation of a geosynthetic reinforced segmental retaining wall, which exhibited signs of distress and unexpected large lateral wall movements 6 years after wall completion. In an attempt to identify possible causes and to provide mitigation measures, a comprehensive investigation was carried out including wall profiling, stability analyses based on the current design approaches, and finite-element analyses.

In the finite element modelling, the wall facing and the backfill soil were discretised using four noded plane strain elements with 4x4 integration, while the reinforcements and the back-slope were modelled using two-noded truss

elements and three noded triangular plane strain elements respectively. The lateral boundary extends to a distance of three times the wall height (H) from the wall face. Considering the competent foundation condition, the wall was assumed to be located on a non-yielding foundation. The interface behaviour between the wall facing and the backfill soil was modelled using the "contact pair", a special type of interface.

In the analysis, the backfill soil was assumed to be an elasto-plastic material with Mohr-Coulomb failure criterion together with the non-associated flow rule. The wall facing block and the reinforcement were assumed to be linear elastic. In the finite-element modelling, the detailed construction sequence was carefully simulated by adding layers of soil and reinforcement at designated steps. Upon completion of the wall, lateral displacements similar in magnitudes to those measured by the wall profiling were then incrementally applied at the wall face in order to create stress–strain fields similar to those of the actual field walls.

Helwany et al. (2007) described the finite element analyses of two full-scale loading tests of GRS bridge abutments. The aim of the study was to study the complex behaviour of GRS structures in general, and the behaviour of GRS bridge abutments with modular block facing in particular. The study also investigated the performance of the GRS bridge abutments with the variation of backfill properties, reinforcement stiffness properties, and reinforcement vertical spacing.

A plane strain finite element model was developed for bridge abutment and analysed. The soil was simulated utilizing an extended two-invariant geologic cap model which is an elastoplastic model, and the geosynthetic reinforcement using an elastoplastic model with failure. The parameters required for this were deduced from the results of the uniaxial tension tests performed on geosynthetics.

Interface elements were used between the modular blocks and reinforcement, and between the blocks and backfill soil. The interface element used allows sliding with friction and separation. A gravity load was applied in the beginning of the analysis to establish the initial stresses within the backfill soil.

### 2.4.4 Gabion faced retaining walls

Helwany et al. (1996) proposed a numerical model incorporating a three - parameter dilatant nonlinear incrementally elastic soil model and used it to analyse three well – controlled full – scale geosynthetic reinforced soil (GRS) retaining wall tests. Three tests were conducted to examine the effects of facing rigidity and reinforcement length on the performance of the walls subject to central loading (far from the facing panel). It was then proved that the numerical model is capable of accurately simulating the behaviour of the three tests under service loads, in particular, their sensitivity to facing rigidity and reinforcement length. The validated numerical model was then used to conduct a comparative analysis on four GRS retaining walls subject to front loading (adjacent to the facing panel). The GRS retaining walls comprised four different types of facings types A, B, C and D having different degrees of rigidity. Type A facing was of a continuous cast - in - place concrete facing panel and type B comprised of discrete precast concrete facing units. Both types had gabions immediately behind the concrete facings to facilitate construction. Type C utilised gabions as the sole facing unit and type D was a wrapped around facing. Reinforcement used in the soil was geogrid attached to the facing. The results of the comparative analysis are considered useful as a guide for selecting the proper facing rigidity of GRS retaining walls subject to front loading.

Sand backfill, foundation soil, concrete facings and gabions were modelled using quadrilateral elements, geosynthetic reinforcement using bar elements and loading plate by beam elements. The gabion was considered to behave as a single block and hence was modelled using a single quadrilateral element. From the plane strain compression tests conducted on gabion stacks,

it was clear that the gabions exhibit a linear but inelastic behaviour. However, in the analyses, the gabions were assumed to behave in a linear elastic manner, since the authors are of the opinion that unloading is unlikely to occur in the full – scale tests of the walls.

Bergado et al. (2000 A) simulated the consolidation behaviour of foundation soil below a full scale test embankment on soft Bangkok clay using hexagonal wire mesh as reinforcement. The embankment was underlain by a layered soft foundation. The elastic, perfectly plastic, Mohr – Coulomb model was adopted to represent the fill embankment and weathered clay layer of the foundation soil. The soft soil model was used for predicting the behaviour of both the soft and medium clay layers. The elastic model was used for the stiff clay layer. Bar elements with linear tension strain were used to model the hexagonal wire mesh reinforcement. The elastic, perfectly plastic model was used to simulate the constitutive relationship of the soil - hexagonal wire mesh interface using PLAXIS.

The gabion boxes were filled with crushed rock. The elastic, perfectly plastic, Mohr – Coulomb model was used to simulate the crushed rock inside the gabions. The hexagonal wire mesh in the gabion system was modelled using beam elements. The embankment was modelled as a plane strain problem. The effects of construction sequences were also considered.

The numerical simulation adopted gave a reasonable representation of the overall behaviour of the reinforced soil wall embankment system on a soft foundation through good agreement between the field measurements and simulated values. The important considerations for simulating the behaviour of the reinforced wall embankment were the method of applying the embankment loading during the construction process, the variation of soil permeability during the construction process, and the selection of the appropriate model and properties at the interface between the soil and the reinforcement.

## 2.5 ECONOMIC STUDIES

Lee et al. (1983) used categories of gravity walls and crib / bin walls and compared them to MSE walls with steel reinforcement. The walls were furthermore subdivided into high ($H \geq 9.0$ m), medium ($4.5 < H < 9.0$ m) and low ($H \leq 4.5$ m) height categories. It was seen that MSE walls with metallic reinforcement are the least expensive wall of the types surveyed at all heights.

Rao and Singh (1988) presented typical results relating to design of reinforced earth walls for varying backfill quality and emphasised the need for full scale field trials in India, for evaluating the techniques as alternative to conventional retaining walls. The global literature was reviewed and proved that the introduction of reinforced earth lowered the cost of structures. It is commented that savings over conventional retaining structures varied between 20% to 50% with an overall average savings in the walls and abutments of 32%.

Durukan and Tezcan (1992) presented a systematic method of determining the possible cost of a reinforced soil-retaining wall and developed an estimate of cost breakdown on the basis of height and length of the retaining wall. Relative economy of reinforced soil retaining walls in comparison with conventional and other types of retaining walls was also determined. For the purpose of illustration, several case studies of cost analyses and a numerical example, were also included.

Koerner et al. (1998) conducted a survey which included four wall categories like gravity walls, crib / bin walls, MSE walls with metal reinforcement and MSE walls with geosynthetic reinforcement. Gravity walls were seen to be the most expensive, with crib/bin walls and MSE (metal) walls significantly less expensive. But the crib/bin walls are rarely above 7m in height. It was also obvious that MSE (geosynthetic) walls are the least expensive of all wall categories and over all wall heights. However, convergence seems to occur within the two different MSE types (metal and geosynthetics) in the high wall height category.

This survey also generated statistical data in providing a mean value, standard deviation and variance. The standard deviation in data is highest with gravity walls, intermediate with crib/bin and MSE (metal) walls, and the least with MSE (geosynthetic) walls. Variance values, however, are similar in all wall categories.

Koerner and Soong (2001) compared the results of survey conducted by various researchers and compared with the results obtained from the survey conducted Koerner et al. (1998). The results showed that MSE walls with geosynthetic reinforcement are the cheapest of all the types considered in the study and MSE walls with metallic reinforcement comes in the second position. The RCC walls were found to be the costliest walls.

Basudhar et al. (2008) dealt with the optimum cost (objective function) design of geosynthetic reinforced earth retaining walls subjected to static and dynamic loading. The design restrictions were imposed as design constraints in the analysis. Choice of the initial designed length and strength of the reinforcement, which are the elements of the design vectors were made in such a way that it forms an initial feasible design vector. The constraints and the objective function being nonlinear in nature, the Sequential Unconstrained Minimization Technique was used in conjunction with conjugate direction and quadratic fit methods for multidimensional and unidirectional minimization to arrive at the optimal (minimum) cost of the reinforced earth wall. Optimal cost tables were presented for different combinations of the loading and the developed procedure was validated by taking up an example problem. It was found from the typical example problem that savings of the order of 7–8% can be made over the conventional design of mechanically stabilised earth (MSE) walls with the aid of design charts presented in the paper.

## 2.6 NEED FOR THE PRESENT STUDY

After a pervasive literature survey conducted on retaining walls it is concluded that research works on gabion faced retaining walls or even segmental retaining walls (both fall under semi rigid walls category) are very much limited in number. But as mentioned in Chapter 1, the construction of these walls is gaining fast momentum all over the world without understanding the exact behaviour of these walls, as evident from the literature survey. Table 2.1 gives a numerical summary of the literature survey conducted as a part of this thesis work. It has also been eventually found from the literature studies that only a numerical tool like the finite element method can yield a complete picture of the behaviour of the retaining wall system and its components.

**Table 2.1 Numerical summary of literature survey**

| No. of literature collected | Gravity walls | MSE walls | Segmental retaining walls | Gabion faced walls |
|---|---|---|---|---|
| Experimental studies | 11 | 22 | 3 | 3 |
| Analytical studies | 17 | 30 | 2 | 0 |
| Numerical studies | 6 | 31 | 3 | 2 |
| **Total** | **34** | **83** | **8** | **5** |

Under these circumstances, a two dimensional finite element study is attempted in this work paying individual attention to soil, facing, reinforcement and the interfaces between soil and reinforcement as well as between soil and facing, considering the soil and interface as non linear, to monitor the behaviour of gabion faced retaining wall systems.

# Chapter 3

# GABION FACED RETAINING WALLS

## 3.1 GENERAL

Gabions are rectangular baskets fabricated from a hexagonal mesh of heavily galvanized steel wire. The baskets are filled with rock and stacked atop one another to form a retaining wall. The functioning of gabion walls depend mainly on the interlocking of the individual stones and rocks within the wire mesh and their mass or weight. Gabions are porous type of structures that can sometimes be vegetated. Gabions are considered to be a "hard" structural solution that has minimal habitat and aesthetic value.

Wire mesh gabions have been used in Civil Engineering projects for many years and their ability to perform well in a variety of applications have earned them the respect of Civil Engineers through out the world. Gabions are highly cost effective construction materials which are easy to install and maintain. With environmental issues now of more concern than in the past, gabions offer a more natural solution to previously designed concrete walls.

In spite of all these, standard literature available on this practice is limited. Hence, in this chapter, a detailed description of the construction method, which is usually adopted by the field practitioners and manufacturers, is given. Along with that, the limit state method of analysis and design for reinforced soil retaining walls (as per BS 8006: 1995) which can be suitably adopted for the design of gabion faced reinforced soil retaining walls is also described herein.

## 3.2 CONSTRUCTION

### 3.2.1 Wire mesh

Double twisted wire meshes made by mechanically twisting continuous pairs of wires (2.5 – 3.5 mm dia.) and interconnecting them with adjacent wires

to form hexagonal shapes (Figs. 3.1 and 3.2) are used to make gabion boxes of various sizes. Materials used for the mesh shall be mild steel having a tensile strength of 350 MPa – 500 MPa and a minimum elongation of 10% at breaking load performed on a gauge length of 250 mm as per BS 1052 : 1980. These wires shall be provided with coating of zinc and an additional coating of PVC (Fig. 3.3).

**Fig. 3.1 Hexagonal wire mesh**

**Fig. 3.2 Double twisted wire**

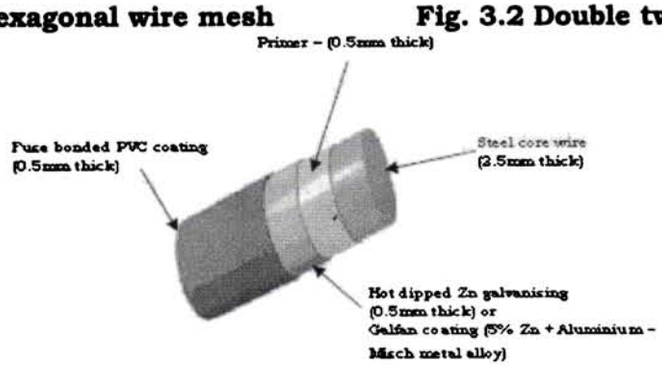


**Fig. 3.3 Cross section of gabion wire**

In the use of gabions the following specifications should be considered as listed in BS 8002: 1994. Hexagonal woven mesh gabions should be made from wire galvanized according to BS 443: 1982. For welded mesh gabions, the panels of mesh which form the cages should be hot dip galvanized after welding according to BS 729 : 1995 (this code has been recently replaced by BS EN ISO 3834 – 3 : 2005). In the case of PVC coated gabion mesh, the PVC coating should conform to BS 4102: 1998. The radial thickness of the coating applied to the galvanized wire core should be a minimum of 0.25 min. The PVC should be sufficiently bonded to the galvanized wire core to prevent a

capillary flow of water between the wire and the PVC coating leading to corrosion.

The filler material shall be naturally occurring hard stones which are weather resistant, insoluble and of minimum size 1 to 2 times the dimension of the mesh. Stones with high specific gravity are preferable since gravity behaviour of the structure is predominant. The mesh dimensions for PVC coated galvanized gabion boxes are 80 x 100 mm and 100 x 120 mm. For galvanized boxes standard mesh sizes are 60 x 80 mm, 80 x 100 mm, 100 x 120 mm. The wire mesh provides an increased strength to the walls due to the friction on the surface of the wire and the mechanical interlocking properties of the backfill (Bergado et al., 2001).

### 3.2.2 Gabions

Gabion boxes are uniformly partitioned into internal cells using diaphragm walls, (Fig. 3.4) interconnected with similar units, and filled with stones at the project site to form flexible, permeable and monolithic structures such as retaining walls, sea walls, channel linings, revetments, facing elements for reinforced soil structures and weirs for erosion control purposes.

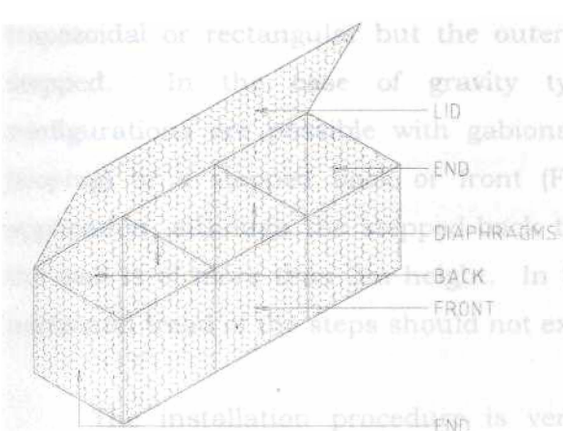


**Fig. 3.4 A typical gabion**

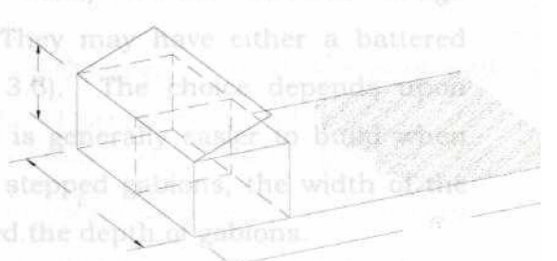

**Fig. 3.5 Gabion with extension**

The gabions are manufactured in factories in sizes of 1.5 m x 1 m x 1m, 2 m x 1 m x 1 m, 4 m x 1 m x 1 m etc.. Individual empty units are connected

The edges are then laced together by single and double twist lacing wires at 100 - 150 mm spacing. The first layer of gabion is seated on levelled flat surface and continuously secured together either by lacing or by tying the edges using fasteners. The end gabion is partly filled with suitable stones to form end anchor and there after bracing wires are fixed at 0.5 m spacing to avoid bulging of front side of gabion.

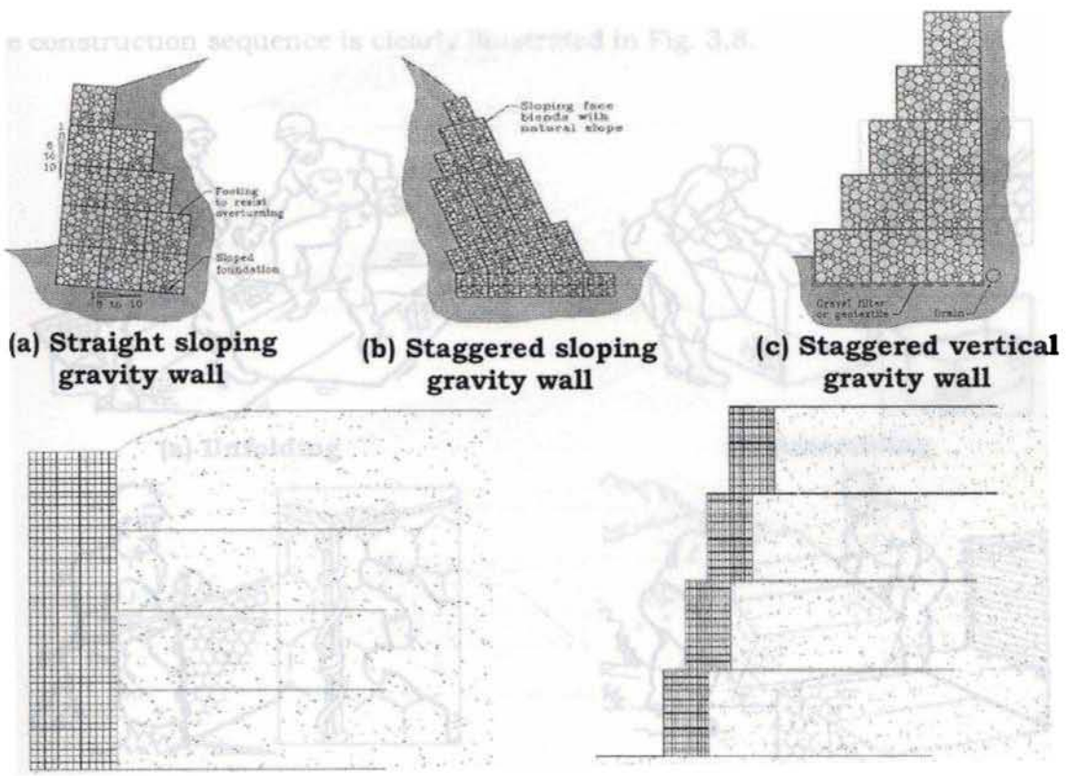


**(a) Straight sloping gravity wall** **(b) Staggered sloping gravity wall** **(c) Staggered vertical gravity wall**

**(d) Straight vertical face MSE wall** **(e) Stepped vertical face MSE wall**

**Fig. 3.6 Typical configurations of gabion faced walls**
(Courtesy: Meccaferri)

Gabions are filled in layers of one-third, ensuring at each stage a good compaction by hand and tensioning of the gabion mesh. Overfilling by 50 - 75 mm is also made to allow for settlement of the infill. The mesh lid is then folded flat, stretched and diaphragms are tied up. The rows of gabions are filled up subsequently in a sequential manner after ensuring that each gabion is properly fixed to adjacent gabions on all sides. A geofilter is positioned at the back of the gabion between the box and backfill to prevent the entry of soil

particles from backfill into void spaces of stones. After this, backfilling is commenced. Backfill is laid in lifts of approximately 200mm and properly compacted up to 95% of proctor density. The top of the backfill is kept in level with the top of the gabion layer. After the completing the full length of a layer, the next unit is placed on top of this and the procedure is continued up to the required level. In the case of reinforced soil type gabion faced retaining walls, gabion boxes with basal extensions are used for the construction. The construction sequence is clearly illustrated in Fig. 3.8.

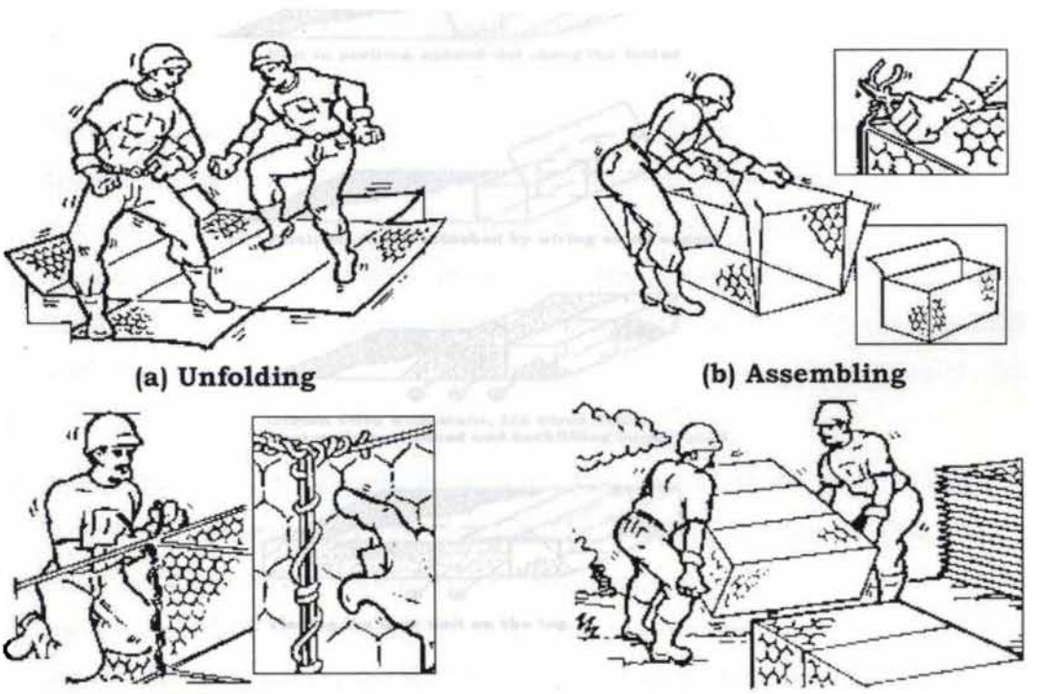


**Fig. 3.7 Gravity type gabion wall – construction procedure**
(Courtesy: Meccaferi)

The first structure of this kind on record is a combination of gabions and mechanically reinforced soil which was built in Sabah, Malaysia in 1979. A vertical skin of gabions was anchored to the backfill using metal strips. The 14 m high structure supports a stretch of the road from Kota Kinabalu to Sinsuran in Malaysia.

Foundation requirements, which must be established by the engineer, will vary with site conditions, height of gabion structure, etc.. Generally, the

top layer of soil is stripped until a layer of the required bearing soil strength is reached. In some cases, the foundation may consist of suitable fill material compacted to a minimum of 95 percent of proctor density.

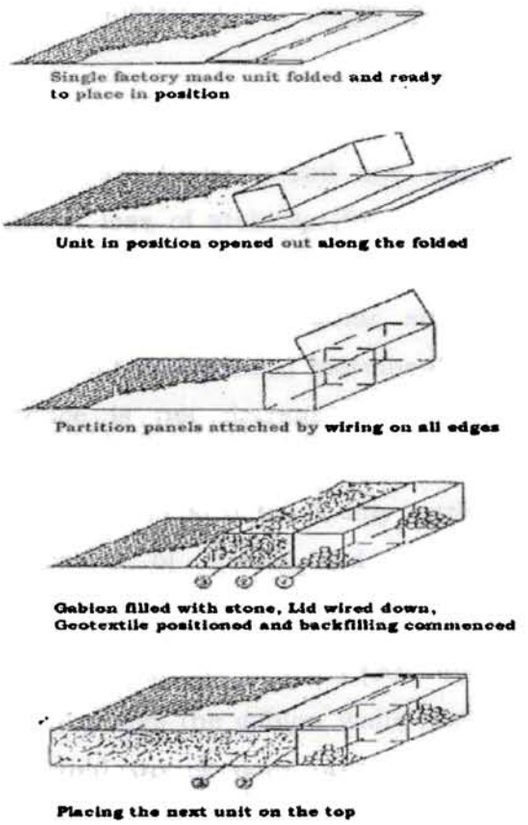


**Fig. 3.8 MSE type gabion faced wall – construction sequence**

(Courtesy: Maccaferri)

## 3.3 ADVANTAGES

The gabion structures stand out as a simple, efficient and economical solution to various civil engineering construction problems due to the following advantages.

- Monolithicity: The various elements in a gabion faced wall are linked through continuous fastening which ensures structural continuity (Fig. 3.9). This allows regular distribution of the imposed forces and ensures that the whole weight of a structure is equal to the sum of the

**Fig. 3.9 Monolithic wall**

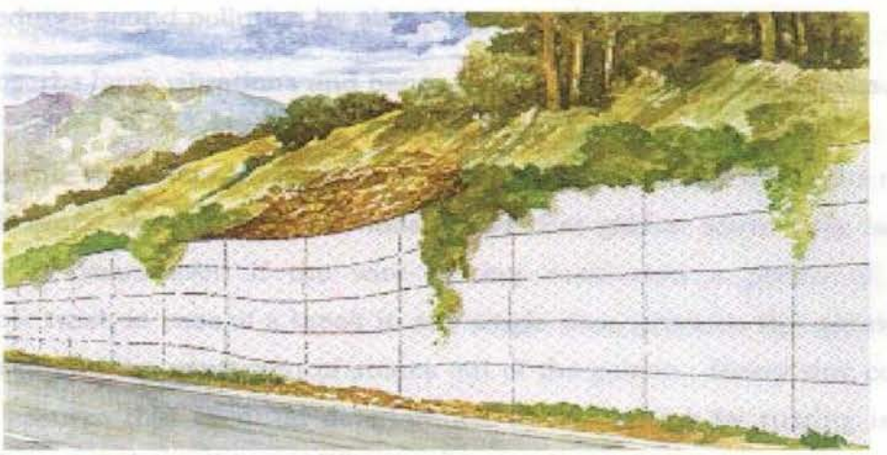

**Fig. 3.10 Flexibile wall**

**Fig. 3.11 Permeable ecofriendly wall**

(Courtesy: Maccaferri)

- Easy to repair any damaged boxes with minimum expense.
- Cost effective and suitable in all types of soil conditions.
- Work is simple and fast to execute.
- No need of shuttering and curing.
- Work is not affected by water shortage and on the other hand it is also not affected due to rains during monsoon.
- Cost savings is of the order ranging from 30% to 50%.
- Ecofriendly (Fig. 3.11).
- Reduces sound pollution by absorbing sounds up to 18-28 db.
- Absorbs large vibrations and hence widely used near railway tracks.

Despite the fallacy that gabion structures are temporary works the reality is far different. Dry walls (stone walls) prove that gabion works may last for hundreds of years even if the wire netting rusts over a period of time. The double twist, in case of a break in any single wire, prevents the unravelling of the mesh and the movement of stones out of the gabion. Heavy zinc coating of wires assures that eventual deterioration of the netting by rusting is very slow under normal conditions. Where corrosion is a more severe problem, it is possible to considerably extend the wire life by making use of PVC coating. With the passage of time, gabion structures provide natural balances with the environment.

## 3.4 ANALYSIS OF GABION FACED REINFORCED EARTH WALLS

Any analysis incorporates the field of mechanics along with the failure theories. To perform an accurate analysis, an engineer must gather information such as structural loads, geometry, support conditions, and material properties of the structure to be analysed after selecting trial dimensions of the structure. The results of the analysis typically include support reactions, stresses and displacements. This information is then compared to criteria that indicate the conditions of failure.

Analysis of gabion faced reinforced earth walls, which is in question for the present study, combines the analysis of reinforced soil walls along with the self weight characteristics of gravity type wall. In the case of reinforced soil walls, the code of practice followed is BS 8006: 1995, the details of which are summarised in this section. The BS code follows the limit state method of design, the principles of which are adopted in the reinforced soil wall design, are explained here.

### 3.4.1 Limit state method

The two limit states considered in the design are ultimate limit state and serviceability limit state. Ultimate limit state is associated with collapse. This state is attained for a specific mode of failure when disturbing forces equal or exceed the restoring forces. Margins of safety against attaining the limit state of collapse, are provided by the use of partial material factors and partial load factors. These partial factors assume prescribed numerical values of unity or greater. Disturbing forces are increased by multiplying by prescribed load factors to produce design loads. Restoring forces are decreased by dividing them by prescribed material factors to produce design strengths. When the design strength equals or exceeds the design load, there deems to be an adequate margin of safety against attaining the ultimate limit state of collapse. Serviceability limit state is attained if the magnitudes of deformation occurring within the design life exceed prescribed limits or if the serviceability of the structure is otherwise impaired.

### 3.4.2 Partial factors

Limit state method for reinforced soil employs partial safety factors namely load factors, material factors and soil – interaction factors. Prescribed ranges of these values are given in BS 8006 : 1995 (Tables 3.1 and 3.2) to take into account the type of structure, the mode of loading and the selected design life. Partial factors are applied in a consistent manner to minimise the risk of attaining a limit state.

**Table 3.1: Partial load factors for load combinations (BS 8006: 1995)**

| Effects | Combinations | | |
|---|---|---|---|
| | A | B | C |
| Mass of the reinforced soil body | $f_{fs} = 1.5$ | $f_{fs} = 1.0$ | $f_{fs} = 1.0$ |
| Mass of the backfill on top of the reinforced soil wall | $f_{fs} = 1.5$ | $f_{fs} = 1.0$ | $f_{fs} = 1.0$ |
| Earth pressure behind the structure | $f_{fs} = 1.5$ | $f_{fs} = 1.5$ | $f_{fs} = 1.0$ |
| Traffic load:<br>On the reinforced soil block<br>Behind the reinforced soil block | <br>$f_q = 1.5$<br>$f_q = 1.5$ | <br>$f_q = 0.0$<br>$f_q = 1.5$ | <br>$f_q = 0.0$<br>$f_q = 0.0$ |

The following descriptions of load cases identify the usual worst combination for the various criteria. All load combinations should be checked for each layer of reinforcement within each structure to ensure that the most critical condition has been found and considered.

Combination A considers the maximum values of all loads and therefore normally generates the maximum reinforcement tension and foundation bearing pressure. It may also determine the reinforcement requirement to satisfy pullout resistance although pullout resistance is usually governed by combination B.

Combination B considers the maximum overturning loads together with minimum self mass of the structure and superimposed traffic load. This combination normally dictates the reinforcement requirement for pullout resistance and is normally the worst case for sliding along the base.

Combination C considers dead loads only without partial load factors. This combination is used to determine foundation settlements as well as generating reinforcement tensions for checking the serviceability limit state.

For reinforced soil applications, the ultimate and serviceability limit states should be considered in terms of both internal and external stability. The assessment of external stability involves consideration of the stability of the reinforced soil mass. This includes assessment of potential failure modes such as bearing and tilt of the wall as well as forward sliding along the base of the wall. For each failure mode considered, prescribed load and material factors are appropriately applied to external disturbing forces and external restoring forces to ensure that the factored restoring force equals or exceeds the factored disturbing force. The internal stability of a reinforced soil mass is governed by the interaction between the soil and the reinforcement. This interaction occurs by friction or adhesion.

**Table 3.2: Summary of partial factors (BS 8006 : 1995)**

| Partial factors | | Ultimate limit state | Serviceability limit state |
|---|---|---|---|
| Load factors | Soil unit mass e.g. Wall fill | $f_{fs}$ to be taken from Table 3.1 | |
| | External dead loads e.g. line or point loads | $f_f$ to be taken from Table 3.1 | |
| | External live loads e.g. traffic loading | $f_q$ to be taken from Table 3.1 | |
| Soil material factors | To be applied to tan $\phi$ | $f_{ms}$ = 1.0 | $f_{ms}$ = 1.0 |
| | To be applied to c | $f_{ms}$ = 1.6 | $f_{ms}$ = 1.0 |
| | To be applied to $c_u$ | $f_{ms}$ = 1.0 | $f_{ms}$ = 1.0 |
| Reinforcement material factor | To be applied to reinforcement base strength | $f_m$ depends on type of reinforcement and its design life (see section 3.4.3) | |
| Soil / reinforcement interaction factors | Sliding across surface of reinforcement | $f_s$ = 1.3 | $f_s$ = 1.0 |
| | Pull out resistance of reinforcement | $f_p$ = 1.3 | $f_p$ = 1.0 |
| Partial factors of safety | Foundation bearing capacity: to be applied to $q_{ult}$ | $f_{ms}$ = 1.35 | NA |
| | Sliding along base of structure or any horizontal surface where there is soil - to - soil contact | $f_s$ = 1.2 | NA |

### 3.4.3 Partial material factors for reinforcements

The unfactored ultimate tensile strength of the reinforcement, $T_{ult}$, is reduced by the reinforcement material factor, $f_m$, to define the reinforcement design strength such that:

$$T_D = \frac{T_{ult}}{f_m} \qquad \text{..... (3.1)}$$

The design strength may be governed by the ultimate limit state of collapse or serviceability limit state. For plain or galvanised steel reinforcements subjected to axial tensile loads only, $f_m$ = 1.5.

For others,

$$f_m = f_{m1} \times f_{m2}$$

$$= \{ (f_{m11}) \times f_{m12}) \} \times \{ f_{m21} \times f_{m22} \}$$

$$= \{ (f_{m111} \times f_{m112}) \times (f_{m121} \times f_{m122}) \} \times \{ f_{m21} \times f_{m22} \} \quad \text{..... (3.2)}$$

where,

$f_{m1}$ = partial material factor related to the intrinsic properties of the material

$f_{m2}$ = partial material factor concerned with construction and environmental effects

$f_{m11}$ = partial material factor related to the consistency of manufacture of the reinforcement

$f_{m12}$ = partial material factor related to the extrapolation of test data dealing with base strength

$f_{m21}$ = partial material factor related to the susceptibility of the reinforcement to damage during installation in the soil. For steel metallic reinforcements, $f_{m21}$ has a value of 1.0 when the minimum steel thickness is greater than or equal to 4 mm. For thinner reinforcements, $f_{m21} > 1.0$.

$f_{m22}$ = partial material factor related to the environment in which the reinforcement is installed. Reinforcements which utilise a protective layer of coating are more resistant to attack, as the load carrying elements are properly protected. In such cases, $f_{m22} = 1.0$.

$f_{m111}$ = partial material factor related to the reinforcement manufactured according to standards. For metallic reinforcement, $f_{m111} = 1.0$ for minimum specification. For polymeric reinforcement, $f_{m111} = 1.0$ for characteristic specification.

$$f_{m111} = 1 + \frac{1.64\,SD}{\Gamma - 1.64\,SD} \quad \text{..... (3.3)}$$

where, $\Gamma$ is the mean reinforcement base strength and SD is the standard deviation of the reinforcement base strength.

$f_{m112}$ = partial material factor related to the reinforcement manufactured not according to standards. For metallic reinforcement, $f_{m112}$ = 1.0 for minimum section size. If the reinforcement base strength for metallic reinforcements is based upon sections other than minimum section size, $f_{m112}$ > 1.0. For polymeric reinforcement $f_{m112}$ = 1.0.

$f_{m121}$ = partial material factor related to assessment of available data on base strength to derive a statistical envelope. $f_{m121}$ = 1.0 if large quantities of data over a long period of time are available or else $f_{m121}$ > 1.0.

$f_{m122}$ = partial material factor related to the extrapolation of the above mentioned statistical envelope over the expected service life of the reinforcement. If extrapolation can be done over one log cycle of time $f_{m122}$ = 1.0. Otherwise,

$$f_{m122} = \log_{10}\left(\frac{t_d}{t_r}\right) \qquad \text{..... (3.4)}$$

where, $t_d$ is the design life of reinforcement and $t_r$ is the duration over which real time creep tests have been performed.

### 3.4.4 Design loads and design strengths

The magnitudes of disturbing loads, such as those which can be developed by lateral earth pressures, are controlled by many factors including soil strength. In calculating disturbing loads and forces, the shear strength parameters of the soil are used unfactored. The numerical value of the calculated raw disturbing load, defined in terms of total stress, is increased by multiplying by a prescribed load factor (Table 3.1) with a value of unity or greater. The end product of this factoring is the design load.

A fundamental principle of limit state design is that the design strength should be greater than or equal to the design load. In the case of external stability, the design load may be resisted by the forces generated in the soil

which will be a function of soil shear strength. Their characteristic values are reduced by a material factor of prescribed value, to produce design strength. In the case of internal stability, the design load may be resisted by forces generated in the soil and reinforcement which is reduced by a material factor to produce design strength.

### 3.4.5 Design procedure

#### *3.4.5.1 Fixing the dimensions*

Prior to considering the external stability, the overall geometry of the wall should be selected. If the external and internal stability conditions are not satisfied, dimensions of the structure should be altered from the initial size. The initial length of reinforcement for medium and high wall should not be less than 0.7H (3m minimum) where H is the height of the wall. The toe of the structure should be embedded below the ground level. Embedment is recommended to avoid local failure due to punching in the vicinity of the facing and to avoid the phenomenon of local soil flow similar to piping. For vertical walls, embedment depth ($D_m$) may be fixed as the maximum value obtained among the Eqns. 3.5 and 3.6 taken from BS 8006: 1995.

$$D_m = H/20 \qquad \text{..... (3.5)}$$

$$D_m / q_{all} = 1.35 \times 10^{-3}\ m^3 / kN \qquad \text{..... (3.6)}$$

where, $q_{all}$ is the allowable bearing capacity of foundation soil.

#### *3.4.5.2 External stability analysis*

This indicates the overall stability of the structure. External stability checks are carried out considering all the external forces. For a safe design, stability checks are made for bearing and tilt failure, forward sliding and slip circle failure as well as for the settlement of the structure.

The lateral earth pressure is usually calculated by the Coulomb equation neglecting cohesion as it adds on to the stability of the structure. Although based on granular material, it is conservative for cohesive material.

If a uniformly distributed surcharge pressure (q) is present on top of the backfill surface, it may be treated as an equivalent layer of soil that creates a uniform pressure over the entire height of the wall.

The wall must be able to withstand the bearing pressure at the bottom. For this, the pressure caused by the vertical component of the resultant at the toe of the wall should not exceed the allowable bearing capacity of the soil. The pressure distribution at the base is assumed based on Meyerhof distribution.

$$q_r = \frac{R_v}{L - 2e} \qquad \text{..... (3.7)}$$

where,

$q_r$ = factored bearing pressure acting at the base of the wall

e = eccentricity of the resultant load $R_v$ about the centre line of base width (L)

$R_v$ = resultant of all factored vertical loads

As per BS 8006: 1995, the imposed bearing pressure, $q_r$, should be compared with the ultimate bearing capacity of the foundation soil as follows:

$$q_r \leq q_{ult} / f_{ms} + \gamma_s D_m \qquad \text{..... (3.8)}$$

where,

$q_{ult}$ = the ultimate bearing capacity of the foundation soil

$\gamma$ = the density of the foundation soil

$f_{ms}$ = partial material factor applied to $q_{ult}$ to be taken from Table 3.2

$D_m$ = embedment depth

The stability against forward sliding of the structure at the interface between the reinforced fill and the subsoil should also be considered. The tendency of the active earth pressure to cause the wall to slide horizontally must be opposed by the frictional resistance at the base of the wall. The resistance to movement should be based upon the properties of either the

subsoil or the reinforced fill, whichever is the weaker, and consideration should be given to sliding on or between any reinforcement layers used at the base of the structure. As per BS 8006: 1995, for long term stability, where there is reinforcement – to – soil contact at the base of the structure,

$$f_s R_h \leq R_v \frac{a \tan\phi}{f_{ms}} + \frac{\alpha c L}{f_{ms}} \qquad \text{..... (3.9)}$$

where,

$f_s$ = the partial factor against base sliding (Table 3.2)

$R_h$ = horizontal factored disturbing force

a = interaction coefficient relating soil / reinforcement interfacial friction angle with tan $\phi$

$\phi$ = internal friction angle of the weaker soil

c = cohesion of the weaker soil

$\alpha$ = adhesion coefficient relating soil cohesion to soil - reinforcement bond

$f_{ms}$ = partial material factor applied to $\phi$ and c (Table 3.2).

To check the overall stability of the structure, all potential slip surfaces should be considered, including those passing through the structure. In the case of a failure plane passing through the structure the resistance to failure provided by the reinforcement crossing the failure plane should be considered. If residual shear surfaces are present, then appropriate soil parameters should be used. The appropriate analysis method and the factors of safety used should conform to BS 8002 : 1994.

The total settlement is the combined effect of the settlement of the foundation soil under the influence of the pressures imposed by the structure and the internal compression of the reinforced backfill. The calculations of foundation settlements supporting reinforced soil structures follow classical soil mechanics theory. The actual pressures imposed on foundations by reinforced soil structures are lower and more evenly distributed than conventional concrete structures and this normally acts to reduce foundation settlements.

The amount of settlement within the reinforced volume will depend mainly upon the nature of the fill, its compaction and the vertical pressures within the fill. The pressure will be a function of the height of structure, fill type, surcharge loading and the type of facing.

### *3.4.5.3 Internal stability analysis*

Stability within a reinforced structure is achieved by the reinforcing elements carrying tensile forces and transferring them by friction, friction and adhesion or friction and bearing. In addition, forces can be transferred through fill trapped by the elements. The fill is then able to support the shear and compressive forces. Internal stability is concerned with the integrity of the reinforced volume. The structure has the potential to fail by rupture or loss of bond of the reinforcements. The arrangement and layout of reinforcing elements should be chosen to provide stability and to suit the size, shape and detail of the facing. For simplicity, a uniform distribution of identical reinforcing elements may be used through out the height of the wall. However, it may be economical to divide the height of the wall into a number of zones and to design appropriate reinforcing elements for each zone (BS 8006: 1995).

The potential failure mechanisms which should be considered are stability of individual elements, resistance to sliding of upper portions of the structure and stability of wedges in the reinforced fill. The factors which influence stability that should be included in the design check are the capacity to transfer shear between the reinforcing elements, the tensile capacity of the reinforcing elements and the capacity of the fill to support compression.

The tie back wedge method is commonly used to determine the internal stability. The coefficient of earth pressure should be taken as the active condition $K_a$ for both the ultimate limit state and serviceability limit state. As per BS 8006: 1995, the maximum ultimate limit state tensile force $T_j$ to be resisted by the jth layer of elements at a depth of $h_j$, below the top of the structure, may be obtained from the summation of the appropriate forces.

$T_j = T_{pj} + T_{sj} + T_{fj} - T_{cj}$ ..... (3.10)

where,

$T_{pj}$ = tensile force per metre run developed in the jth layer of reinforcement due to self weight of fill plus any surcharge on the reinforced fill

$T_{sj}$ = tensile force per metre run developed due to a vertical strip load

$T_{fj}$ = tensile force per metre run developed due to a horizontal shear load

$T_{cj}$ = tensile force per metre run developed in the jth layer of reinforcement due to the cohesive forces in the reinforced soil fill

The effects of vertical strip load and horizontal shear load are not considered in this work and hence they are not discussed further. The other forces are calculated (as per BS 8006: 1995) assuming Meyerhof distribution of stresses as:

$$T_{pj} = \frac{K_{a1}\,(f_{fs}\,\gamma_{s1}\,h_j + f_q\,q)\,S_{vj}}{\left[1 - \dfrac{K_{a2}\,(f_{fs}\,\gamma_{s2}\,h_j + 3\,f_q\,q)\left(\dfrac{h_j}{L}\right)^2}{3\,(f_{fs}\,\gamma_{s1}\,h_j + f_q\,q)}\right]} \qquad \text{..... (3.11)}$$

$$T_{cj} = 2\,S_{vj}\,\frac{c}{f_{ms}}\,\sqrt{K_{a1}} \qquad \text{..... (3.12)}$$

where,

$K_{a1}$ = coefficient of active earth pressure of backfill soil

$K_{a2}$ = coefficient of active earth pressure of retained soil

$S_{vj}$ = vertical spacing of reinforcements at the jth level in the wall

$f_{fs}$ = partial factor applied to dead loads as per Table 3.1

$f_q$ = partial factor applied to traffic loads as per Table 3.1

$f_{ms}$ = partial material factor applied to cohesion as per Table 3.2

The resistance of the jth reinforcing element should be checked against rupture and adherence failure while carrying the factored loads. The tensile

strength of the jth layer of reinforcing elements needed to satisfy local stability considerations is:

$$\frac{T_D}{f_n} \geq T_j \qquad \text{..... (3.13)}$$

in which,

$T_j$ = maximum value obtained from Eqn. 3.10

$T_D$ = design strength of the reinforcement

$f_n$ = partial factor for economic ramifications of failure

Ramification means an usually unintended consequence of an action, decision, or judgment that may complicate a situation or make the desired result more difficult to achieve. $f_n$ = 1 for medium height walls where failure would result in moderate damage and $f_n$ = 1.1 for high walls supporting principal roads or railway embankments. The perimeter, $P_j$, of the jth layer of reinforcing elements needed to satisfy local stability considerations is:

$$P_j \geq \frac{T_j}{a \tan\phi_{s1} \, L_{ej} \, \dfrac{(f_{fs} \, \gamma_{s1} \, h_j + f_q \, q)}{f_p \, f_n} + \dfrac{\alpha \, c \, L_{ej}}{f_{ms} \, f_p \, f_n}} \qquad \text{..... (3.14)}$$

where,

$f_p$ = partial factor for reinforcement pullout resistance taken as 1.3 from Table 3.2

$L_{ej}$ = embedded length of reinforcement in the resistant zone outside the failure wedge

### *3.4.5.4 Serviceability limit considerations*

The serviceability of a structure will usually depend upon the deformations. The deformation will be the sum of the reinforcement strain during construction and loading and the subsequent creep during its service life. For metallic reinforcements, the creep is negligible and consequently, the strain $\varepsilon_j$ in the jth layer of reinforcements may be estimated from Eqn. 3.15.

$$\varepsilon_j = \frac{T_{avj} L}{E A_j} \qquad \text{..... (3.15)}$$

where,

$T_{avj}$ = average tensile load along the length of the jth layer of reinforcements

E = elastic modulus of the reinforcement

$A_j$ = cross sectional area of the jth layer of reinforcement

$T_{avj}$ = average tensile load along the length of the jth layer of reinforcements

## 3.5 SUMMARY

Gabion faced retaining walls are truly revolutionary. The gabion units are strong, flexible and dimensionally stable and can be assembled quickly and easily. These factors contribute to installations which look better, last longer and cost less over the project life than those constructed of competitive products. Due to the endless advantages of the gabion retaining structures, they are now being preferred to the conventional RCC walls. Because of their special functional characteristics and their strength, the use of gabion structures for protective works in residential areas offers the advantage of rapid integration with the surrounding environment. Presently, they are being widely used for a variety of applications like retaining earth and water, highway protection, rock fall protection, river training works, channel lining, soil erosion protection, high security fencing, oil pipeline protection etc.. The construction methods and the design procedure of gabion faced reinforced soil retaining walls have been detailed in this chapter.

# Chapter 4

# FINITE ELEMENT MODELLING

## 4.1 GENERAL

Numerical methods are now widely used in order to have an insight on the stress - strain behaviour of retaining structures, both during construction sequence and working life. Numerical methods can make a very significant contribution to the analysis phase of the design process, when it comes to interpreting measurements of displacements, pressures etc.. Possibly the greatest limitation to application of numerical methods in solving practical problems are, the restrictions posed by difficulties in estimating values for soil properties.

More than 30 years have passed since the finite element method (FEM) was first used for geotechnical engineering applications. In finite element analysis (FEA), the macroscopic behaviour or response of any system can be examined based on the behaviour of microscopic components or elements of the structure. These elements may be one, two or three dimensional depending on the nature of the problems being analysed. By means of incremental and iterative analyses, the finite element method makes it possible to model many complexities of soil and rock behaviour. These complexities include non-linear stress-strain behaviour, dependence of stiffness and strength on confining pressure, irrecoverable plastic deformations, volumetric strains caused by shear stresses etc.. FEA is capable of handling complex geometries and can make use of a realistic constitutive model for soil. Using this, the stress – strain behaviour of any system can be simulated during its entire life. The details of applying FEM in geotechnical engineering are clearly explained in Desai and Abel (1987) and Potts and Zdravkovic (1999 A & B). There are a wide range of books depicting the fundamentals and techniques of FEM, a few of them are: Bathe (1996), Cook et al. (2001), Zienkiewicz and Taylor (1989) and Krishnamoorthy (1987).

Finite element method of analysis has been considered a powerful tool in assessing the deformation of reinforced soil walls having the potential to account virtually the interaction between all components of reinforced soil system as well as the interaction between the reinforced soil mass and the soft foundation. The method of analysis is also appropriate for the problem of a retaining wall because the construction procedure can be modelled reasonably.

In the present study, a plane strain condition, in which the strains are confined to a single plane, is considered. This chapter explains the development of a prediction tool simulating the behaviour of gabion faced reinforced earth walls using the principles of FEM. FE modelling based on 2D plane strain analysis is used. The elements and constitutive models used in the FE model, the composite model for gabion facing and modelling of the construction phases are explained in detail here.

## 4.2 MODELLING

The analysis of geotechnical structures consists of a sequence of modellings which include the geometric modelling of the structure itself, the mechanical modelling of internal forces and behaviour of the constituent materials together with the modelling of the applied loads.

The modelling of a practical problem itself in all its aspects (geometry, loading history, etc.) leads to a properly set mathematical problem to be solved. Solving this problem most often requires numerical methods to be used. This is called as the numerical modelling of a mathematical problem. Together with the very concept of modelling, as far as a geotechnical problem is concerned, validation must also be introduced. This means that the accuracy of a model to represent the structure shall be checked in order to reuse it to study the behaviour of its prototype.

## 4.3 NON LINEAR ANALYSIS OF SOIL MEDIA

Soil being a highly non linear material, for analysing geotechnical problems the ideal method of analysis is non linear analysis. The non linearity in general can be either material non linearity or geometric non linearity. As far as soil mechanics is concerned, it is the material non linearity that comes into the fore front, especially, in the case of reinforced soil structures.

In FEM, the non linearity is solved by one of the three techniques, like, incremental or piecewise linear method, iterative method and mixed method. In the incremental method, the load is increased in a series of steps or increments. The non linear behaviour is approximated in a piecewise linear form, wherein linear laws are used for each load stage. In the iterative method, the maximum load is applied and iterations are performed to satisfy stress and strain equilibrium to give the results pertaining to that load. In the mixed procedure, both the incremental and iterative procedures are combined in a bid to generate more accurate solutions. The description of each method is clearly given in Desai and Abel (1987) and Potts and Zdravkovic (1999 A).

The main advantages of the incremental method are its complete generality and its ability to provide a relatively complete description of the load deformation behaviour. Another advantage is that since the tangent modulus is expressed in terms of stress only, it can be readily employed for analysis of problems involving any arbitrary initial stress conditions. The principal short coming of this method, however, is that it is not possible to simulate a stress – strain relationship in which the stress decreases beyond the peak. To do so one would require the use of a negative value of the modulus, which is not possible with the incremental method.

A geotechnical engineer is primarily concerned with the behaviour of a system before failure. In the present study, in particular, the aim is to study the stresses and displacement histories at different stages of loading as well as due to the self weight of the structure. Due to these reasons, the incremental method has been selected for the analysis reported in this work.

### 4.3.1 Incremental method

The basis of the incremental procedure, also called as stepwise procedure, is the subdivision of the load into many small partial loads or increments. Usually these load increments are of equal magnitude, but in general, they need not be equal. The load is applied at one increment (Fig. 4.1) at a time and during the application of each increment ($\Delta q_i$), the equations are assumed to be linear. In other words, a fixed value of [k] is assumed throughout each increment, but [k] may take different values during different load increments. The solution for each set of loading is obtained as an increment of the displacements ($\Delta d_i$), and is added to the previous value to get the total displacement at any stage of loading. The incremental process is repeated till the total load has been applied. Essentially, the incremental procedure approximates the non linear problems as a series of linear problems, that is, the non linearity is treated as piecewise linear (Desai and Abel, 1987).

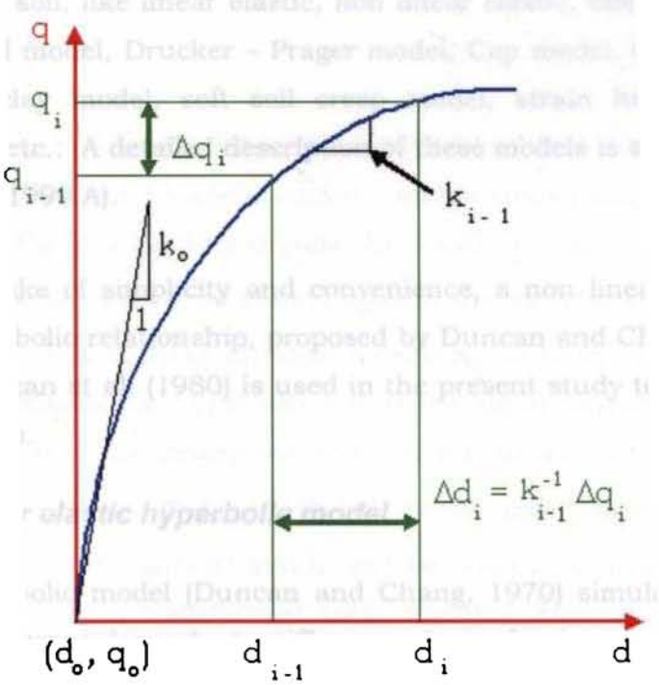


**Fig. 4.1 Incremental method of non linear analysis**

The accuracy of this method improves by applying small load increments, and calculating the modulus value based on the modified Runge – Kutta method, wherein the average value of the stresses during the previous increment is considered in determining the modulus, $E_t$, for the next increment.

## 4.3.2 Constitutive laws

The analytical power available through the finite element method makes it possible to perform analyses of stresses and deformations using constitutive relationships that model many of the complexities of the real soil. The relationship between physical quantities such as stress, strain, time, etc., are called constitutive relations. In the case of soil, the stress – strain relations are dependent on a number of factors like density, water content, drainage conditions, strain or creep conditions, duration of loading, stress histories, confining pressure etc.. A variety of constitutive models are available describing the behaviour of soil, like linear elastic, non linear elastic, bilinear, hyperbolic, Ramberg Osgood model, Drucker – Prager model, Cap model, Cam clay model, modified Cam clay model, soft soil creep model, strain hardening model, hysteritic model etc.. A detailed description of these models is available in Potts and Zdravkovic (1999 A).

For the sake of simplicity and convenience, a non linear elastic model following a hyperbolic relationship, proposed by Duncan and Chang (1970) and modified by Duncan et al. (1980) is used in the present study to model the soil and the interfaces.

### *4.3.2.1 Non linear elastic hyperbolic model*

The hyperbolic model (Duncan and Chang, 1970) simulates non-linear behaviour and stress-dependent stiffness. It is fundamentally an elastic stress-strain relationship because it relates strain increments to stress increments through the extended Hooke's law. In spite of their imperfect simulation of the behaviour of the real soils, simpler models like the hyperbolic model are often adequate under the following conditions:

i. The deformations are not dominated by plastic behaviour.

ii. If local failure occurs, it does not control the behaviour in any region where accurate results are needed.

iii. The conditions analysed are either dry or fully drained (analysed in terms of total stress), so that it is not necessary to calculate undrained changes in pore pressure due to changes in total stress.

These conditions are satisfied for earth-retaining structures in the present study.

The simple and widely used hyperbolic variation of the non linear stress strain relationship is based on the equation proposed by Kondner (1963), in which the stress – strain relation is approximated by a hyperbola with a high degree of accuracy. Fig. 4.2 (a) illustrates such a relation, which can be stated in the equation form, as:

$$(\sigma_1 - \sigma_3) = \frac{\varepsilon}{a^1 + b^1 \varepsilon} \qquad \text{.....(4.1)}$$

in which $\sigma_1$ and $\sigma_3$ are the major and minor principal stresses, $\varepsilon$ is the axial strain, and $a^1$ and $b^1$ are constants whose values may be determined experimentally. Fig. 4.2 (a) thus depicts the result of a triaxial test where the axial strain of the sample ($\varepsilon$) is plotted against the deviator stress $(\sigma_1 - \sigma_3)$ applied. Both $a^1$ and $b^1$ have physical meanings; $a^1$ is the reciprocal of the initial tangent modulus (i.e., $1/E_i$ where $E_i$ is the initial tangent modulus) and $b^1$ is the reciprocal of the asymptotic value of the stress difference (shown in Fig. 4.2 (a)), i.e., $1/(\sigma_1 - \sigma_3)_{ult}$ which the stress-strain curve approaches at infinite strain. The constants $a^1$ and $b^1$ can be readily determined by plotting the stress-strain data on transformed axes. For this, Eqn. 4.1 is transformed as:

$$\frac{\varepsilon}{(\sigma_1 - \sigma_3)} = a^1 + b^1 \varepsilon \qquad \text{.....(4.2)}$$

which plots as a straight line between $\frac{\varepsilon}{(\sigma_1 - \sigma_3)}$ and $\varepsilon$ as seen in Fig. 4.2(b). It may be noted from the figure that $a^1$ and $b^1$ are, respectively, the y-intercept and the slope of the straight line. The theoretical hyperbolic asymptotic value $(\sigma_1 - \sigma_3)_{ult}$ is always higher than the failure (compressive) strength of the specimen obtained in the test $(\sigma_1 - \sigma_3)_f$. The two are related by a factor, $R_f$, called failure ratio (Duncan and Chang, 1970), such that

$$(\sigma_1 - \sigma_3)_f = R_f\,(\sigma_1 - \sigma_3)_{ult} \qquad \text{.....(4.3)}$$

By substituting the value of $a^1$ and $b^1$ in terms of the initial tangent modulus $E_i$ and compressive strength $(\sigma_1 - \sigma_3)_f$ together with the failure ratio $R_f$, Eqn. 4.1 can be written as:

$$(\sigma_1 - \sigma_3) = \frac{\varepsilon}{\left[\dfrac{1}{E_i} + \dfrac{\varepsilon R_f}{(\sigma_1 - \sigma_3)_f}\right]} \qquad \text{.....(4.4)}$$

This hyperbolic representation of the stress-strain curve of the soil has been found to be not only a simple, convenient and useful tool for representing the non-linearity of the stress-strain behaviour of soil, but also one which gives excellent fit with experimental data.

The relation between initial tangent modulus, $E_i$ and confining pressure, $\sigma_3$ is given by Janbu (1963) as:

$$E_i = K\,P_{atm}\left(\frac{\sigma_3}{P_{atm}}\right)^n \qquad \text{.....(4.5)}$$

where $P_{atm}$ is the atmospheric pressure, (which is used to non-dimensionalise n and K), K is a modulus number and n is the exponent determining the rate of variation of $E_i$ with $\sigma_3$.

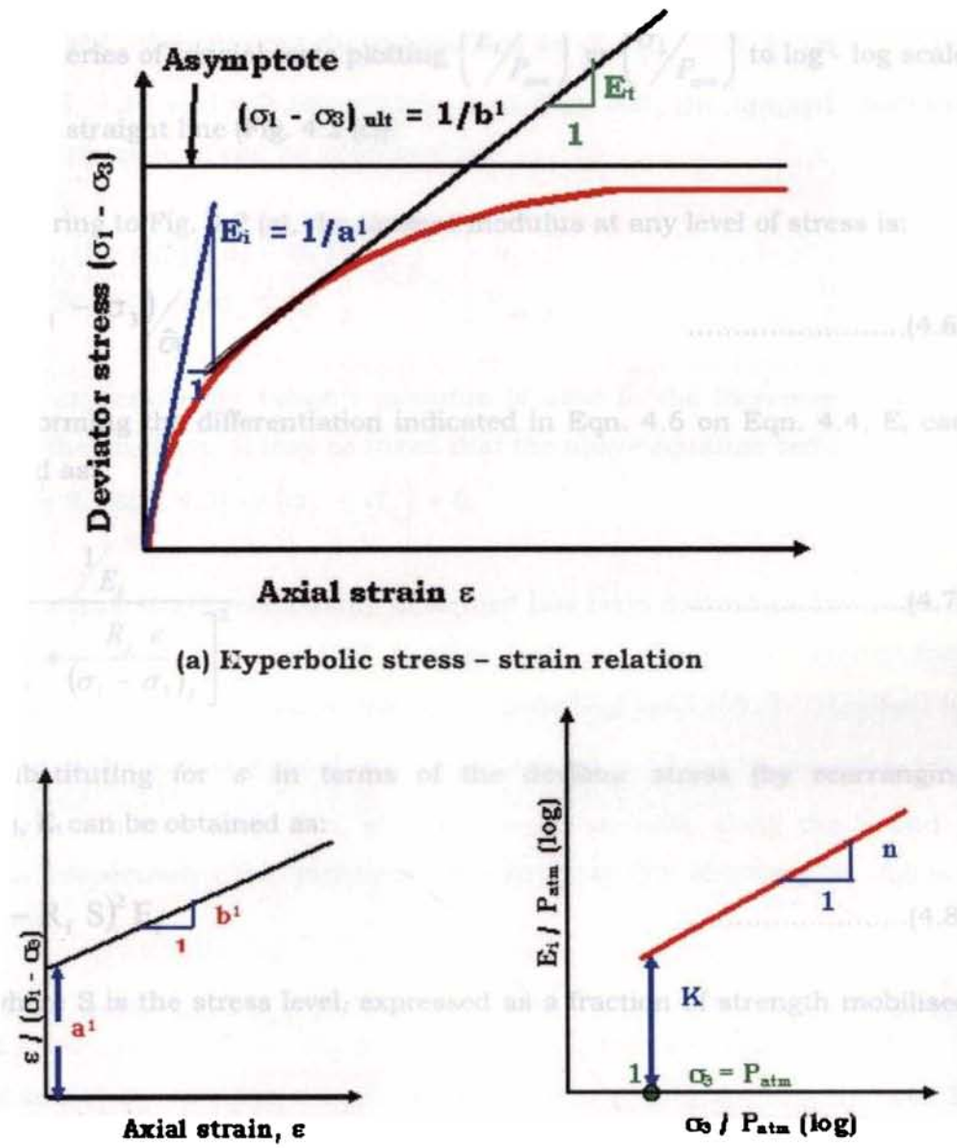


**(b) Transformed plot**

**(c) Variation of $E_i$ with $\sigma_3$ on log – log scale**

**Fig. 4.2 Determination of hyperbolic constants**

Dividing Eqn. 4.5 by $P_{atm}$ and taking logarithm,

$$\log\left(E_i / P_{atm}\right) = \log K + n \log\left(\sigma_3 / P_{atm}\right) \qquad \text{.....(4.5 a)}$$

Both K and n are dimensionless quantities and can be obtained from the results of a series of triaxial tests plotting $\left(E_i/P_{atm}\right)$ *vs* $\left(\sigma_3/P_{atm}\right)$ to log - log scale and fitting a straight line (Fig. 4.2 (c)).

Referring to Fig. 4.2 (a), the tangent modulus at any level of stress is:

$$E_t = \partial(\sigma_1 - \sigma_3)/\partial\varepsilon \qquad \text{.....(4.6)}$$

Performing the differentiation indicated in Eqn. 4.6 on Eqn. 4.4, $E_t$ can be obtained as:

$$E_t = \frac{1/E_i}{\left[1/E_i + \frac{R_f\ \varepsilon}{(\sigma_1 - \sigma_3)_f}\right]^2} \qquad \text{.....(4.7)}$$

Substituting for $\varepsilon$ in terms of the deviator stress (by rearranging Eqn. 4.4), $E_t$ can be obtained as:

$$E_t = (1 - R_f\ S)^2\ E_i \qquad \text{.....(4.8)}$$

where S is the stress level, expressed as a fraction of strength mobilised as:

$$S = \frac{(\sigma_1 - \sigma_3)}{(\sigma_1 - \sigma_3)_f} \qquad \text{.....(4.9)}$$

For a Mohr - Coulomb material at failure,

$$(\sigma_1 - \sigma_3)_f = \frac{2c\ \cos\phi + 2\sigma_3\ \sin\phi}{(1 - \sin\phi)} \qquad \text{.....(4.10)}$$

where, c and $\phi$ are the cohesion and the angle of internal friction of the soil respectively. Substituting the expressions for $E_i$, $(\sigma_1 - \sigma_3)_f$ and S given by Eqns. 4.5, 4.10 and 4.9 respectively, into Eqn. 4.8, the tangent modulus value at any stress level can be expressed as:

$$E_t = \left[1 - \frac{R_f(1-\sin\varphi)(\sigma_1 - \sigma_3)}{2c\cos\varphi + 2\sigma_3 \sin\varphi}\right]^2 K P_{atm} \left[\frac{\sigma_3}{P_{atm}}\right]^n \qquad \text{.....(4.11)}$$

This expression for tangent modulus is used in the incremental stress analysis of the problem. It may be noted that the above equation reduces to the equation for $E_i$ (Eqn. 4.5) at $(\sigma_1 - \sigma_3) = 0$.

The stress-strain relationship described has been derived on the basis of data obtained from the standard triaxial tests in which the intermediate principal stress $(\sigma_2)$ is equal to the minor principal stress $(\sigma_3)$. However in the present case which is a plane strain problem, $\sigma_2$ need not be considered for calculations. In this case, if $\sigma_x$ and $\sigma_y$ are the stresses along the x and y directions respectively, the principal stresses may be obtained as follows (Harr, 1966):

Mean stress, $\sigma = (\sigma_x + \sigma_y)/2$ .....(4.12)

Deviator stress, $\sigma_d = \sqrt{(\sigma_x - \sigma_y)^2 + 4\tau_{xy}^2}$ .....(4.13)

Minor principal stress, $\sigma_3 = (2\bar{\sigma} + \sigma_d)/2$ .....(4.14)

Major principal stress, $\sigma_1 = (\sigma_3 - \sigma_d)$ .....(4.15)

The Poisson's ratio was assumed to vary with the confining stress as per Duncan et al. (1980). According to this, first the bulk modulus of soil may be calculated as:

$B_{soil} = K_{mu} P_{atm} (\sigma_3 / P_{atm})^m$ .....(4.16)

where, $K_{mu}$ and m are hyperbolic constants obtained from a similar procedure as in the determination of $E_t$. But the curve used for transformation is the lateral strain vs. linear strain plot instead of the stress - strain plot. But the minimum value of bulk modulus should not be less than,

$B_{min} = (E_t / 3) (2 - \sin \phi) / \sin \phi$ .....(4.17)

Poisson's ratio may be calculated from the bulk modulus and elastic modulus as:

$$\mu = \frac{1 - \left( \frac{E_t}{3 B_{soil}} \right)}{2} \qquad \text{.....(4.18)}$$

Thus, for the present study, the actual representation of the soil parameters are made by varying them with respect to the confining stresses.

## 4.4 ELEMENTS USED IN THE PRESENT ANALYSIS

### 4.4.1 Two-dimensional four noded quadrilateral element

Two-dimensional four-noded quadrilateral element is used in the analysis to represent the backfill soil and gabion facing. Fig. 4.3 (a) shows the schematic diagram of the 4 noded isoparametric quadrilateral element. It has four nodes with two degrees of freedom per node (u, v) and the stiffness matrix will be of the order 8 x 8. The geometry and the displacements in the element are expressed respectively as (Krishnamoorthy, 1987):

$$\begin{Bmatrix} x \\ y \end{Bmatrix} = \begin{bmatrix} [N] & [0] \\ [0] & [N] \end{bmatrix} \begin{bmatrix} \{x_a\} \\ \{y_a\} \end{bmatrix} \qquad \text{.....(4.19)}$$

and $$\begin{Bmatrix} u \\ v \end{Bmatrix} = \begin{bmatrix} [N] & [0] \\ [0] & [N] \end{bmatrix} \begin{bmatrix} \{u_a\} \\ \{v_a\} \end{bmatrix} \qquad \text{.....(4.20 a)}$$

where,

X coordinate vector = $\{x_n\}^T = \{x_1\ x_2\ x_3\ x_4\}$

Y coordinate vector = $\{y_n\}^T = \{y_1\ y_2\ y_3\ y_4\}$

u displacement vector = $\{u_n\}^T = \{u_1\ u_2\ u_3\ u_4\}$

v displacement vector = $\{v_n\}^T = \{v_1\ v_2\ v_3\ v_4\}$

Shape function matrix = [N]

in which, $x_i$, $y_i$ are the co-ordinates and $u_i$, $v_i$ are the nodal displacements. Eqn. 4.20 (a) can be abridged as:

$$\{u\} = [N]\{d\} \qquad \text{.....(4.20 b)}$$

where, { u } represents the displacement vector at any point and { d } represents the nodal displacement vector.

The shape function matrix [N] contains the interpolation function:

$$N_i = \tfrac{1}{4}(1 + r\,r_i)\ (1 + s\,s_i) \qquad \text{.....(4.21)}$$

where r and s are the local co-ordinates of nodes and $r_i$, $s_i$ represents the local coordinates of points where interpolation is done. The strain-displacement relation is given by:

$$\{\varepsilon\} = [B]\{d\} \qquad \text{.....(4.22)}$$

where [B] represents the strain displacement matrix and { ε } represents the strain vector, given by:

$$\{\varepsilon\}^T = \{\varepsilon_x\ \varepsilon_y\ \gamma_{xy}\} \qquad \text{.....(4.23)}$$

The stress- strain relation is given by:

$$\{\sigma\} = [C]\{\varepsilon\} \qquad \text{.....(4.24)}$$

where stress vector, $\{\sigma\}^T = \{\sigma_x\ \sigma\ \tau_{xy}\}$ .....(4.25)

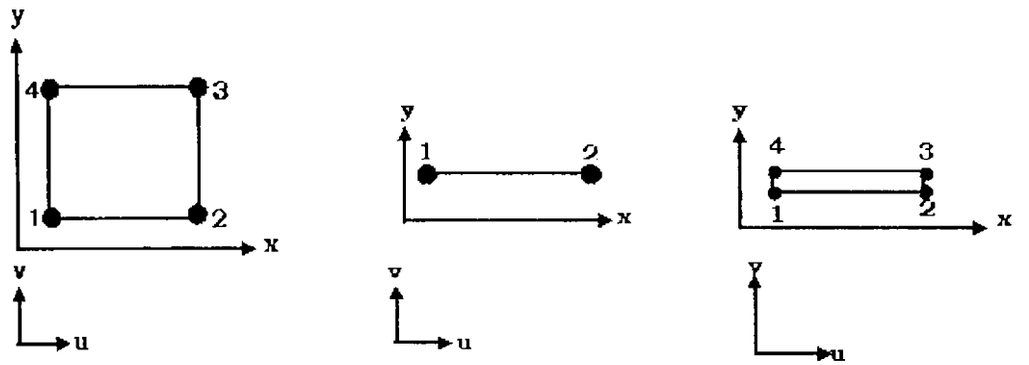


**(a) 2D 4 noded quadrilateral element** **(b) 2D truss element** **(c) 2D line interface element**

**Fig. 4.3 Elements used in the analysis**

$[C]$ is the constitutive matrix given by:

$$[C] = \frac{E}{(1+\mu)(1-2\mu)} \begin{bmatrix} 1-\mu & \mu & 0 \\ \mu & 1-\mu & 0 \\ 0 & 0 & \frac{1-2\mu}{2} \end{bmatrix} \qquad \text{.....(4.26)}$$

Backfill soil is modelled as a non-linear elastic material and for the nonlinear analysis of soil, [C] is updated for each load increment, with the corresponding value of the tangent modulus $E_t$. The gabion facing is modelled as a linear elastic material, for which [C] is kept constant in all load increments but the failure condition is checked as explained later.

Use of the principle of minimum potential energy yields the equilibrium equation for the element as:

$$[k]\{d\} = \{q\} \qquad \text{.....(4.27)}$$

$$[k] = \iiint_V [B]^T [C][\mathbf{B}]\, dV \qquad \text{.....(4.28)}$$

in which, $[k]$ is the element stiffness matrix and $\{q\}$ is the element load vector. A 2 x 2 Guass integration scheme is adopted to evaluate the element stiffness matrix.

### 4.4.2 Two-dimensional two noded truss element

A standard linear two-dimensional truss element is used to represent the reinforcement. A typical truss element with length, $L_t$ is shown in Fig. 4.3 (b). The element has 2 nodes with two degrees of freedom (u, v) per node. The stiffness matrix is of the order 4 x 4 and is given by (Krishnamoorthy, 1987):

$$[k] = \frac{A_t E_{tr}}{L_t} \begin{bmatrix} c_x^2 & c_x c_y & -c_x^2 & -c_y c_x \\ c_x c_y & c_y^2 & -c_x c_y & -c_y^2 \\ -c_x^2 & -c_y c_x & c_x^2 & c_y c_x \\ -c_x c_y & -c_y^2 & c_x c_y & c_y^2 \end{bmatrix} \qquad \text{.....(4.29)}$$

where $E_{tr}$ is the Young's modulus of the material of the truss element, $A_t$ is the cross sectional area of the member, $L_t$ is the length of the member and $c_x$ and $c_y$ are the direction cosines of the element which are given by:

$$\left.\begin{aligned} c_x &= \frac{x_j - x_i}{L_t} \\ c_y &= \frac{y_j - y_i}{L_t} \\ \text{where, } L_t &= \sqrt{(x_j - x_i)^2 + (y_j - y_i)^2} \end{aligned}\right\} \qquad \text{.....(4.30)}$$

in which $x_i$, $y_i$ and $x_j$, $y_j$ are the co-ordinates of the nodes i and j of the truss element respectively. The axial stress in the element is:

$$\{\sigma\} = E\,[B]\,\{d\} \qquad \text{.....(4.31)}$$

$$\text{where, } [B] = \frac{1}{L_t}\begin{bmatrix} -c_x & -c_y & c_x & c_y \end{bmatrix} \qquad \text{.....(4.32)}$$

and $\{d\}^T = \{u_1 \quad v_1 \quad u_2 \quad v_2\}$ .....(4.33)

However the stress strain behaviour of reinforcement was assumed to be linear elastic. This was considered sufficient, as the stress level in the service condition was rather low.

### 4.4.3 Zero thickness four noded line interface element

In reinforced soil structures, with increase in load, the possibility of slip between soil and reinforcement is always expected. To model interface slip between soil and reinforcement and to get an insight into the mechanism of soil – reinforcement interaction, interface elements were used. The use of interface elements can be summarized as follows:

- It allows the properties of joint or interface to be varied independently of the material comprising interface.

- It helps in extracting the information regarding relative movements of the materials along the interface.

Fig. 4.3 (c) shows the four noded interface element which is to be placed between the reinforcement and the soil. This element has length, $L_i$, but zero thickness. This is achieved by providing identical coordinates initially to nodal point pairs (1, 4) and (2, 3). The origin is at the centre as assumed by Goodman et al. (1968).

Linear variation of displacement along the length of the element is assumed. Their relative displacement between top and bottom nodes is taken as the corresponding strain in the element. Accordingly,

$$\{\varepsilon\} = \begin{Bmatrix} \Delta u \\ \Delta v \end{Bmatrix} = \begin{Bmatrix} u_{top} - u_{bottom} \\ v_{top} - v_{bottom} \end{Bmatrix} \qquad \text{.....(4.34)}$$

where,

$$\left.\begin{aligned} u_{top} &= N_4u_4 + N_3u_3 \qquad u_{bottom} = N_1u_1 + N_2u_2 \\ v_{top} &= N_4v_4 + N_3v_3 \qquad v_{bottom} = N_1v_1 + N_2v_2 \end{aligned}\right\} \qquad \text{.....(4.35)}$$

in which, $N_1$, $N_2$,..... are the corresponding shape functions, given by,

$$\left.\begin{aligned} N_1 &= N_4 = 1 - x/L_i \\ N_2 &= N_3 = x/L_i \end{aligned}\right\} \qquad \text{.....(4.36)}$$

From Eqns. 4.34 to 4.36, we get,

$$\{\varepsilon\} = \begin{bmatrix} -N_1 & 0 & -N_2 & 0 & N_3 & 0 & N_4 & 0 \\ 0 & -N_1 & 0 & -N_2 & 0 & N_3 & 0 & N_4 \end{bmatrix} \begin{Bmatrix} u_1 \\ v_1 \\ u_2 \\ v_2 \\ u_3 \\ v_3 \\ u_4 \\ v_4 \end{Bmatrix} \qquad \text{.....(4.37)}$$

from which the strain – displacement matrix is obtained as:

$$[B] = \begin{bmatrix} -N_1 & 0 & -N_2 & 0 & N_3 & 0 & N_4 & 0 \\ 0 & -N_1 & 0 & -N_2 & 0 & N_3 & 0 & N_4 \end{bmatrix} \qquad \text{.....(4.38)}$$

and the displacement vector is:

$$\{d\}^T = \{u_1 \quad v_1 \quad u_2 \quad v_2 \quad u_3 \quad v_3 \quad u_4 \quad v_4\} \qquad \text{.....(4.39)}$$

From the principle of virtual work,

$$\int_A \{\delta\varepsilon\}^T \{\sigma\}\, dv = \{\delta d\}^T \{q\} \qquad \text{.....(4.40)}$$

Substituting for { ε } as [B] { d } and { σ } as [C] { ε }, we get,

$$\int_0^{L_i} \{\delta d\}^T [B]^T [C][B] \{d\}\, dx = \{\delta d\}^T \{q\} \qquad \text{.....(4.41)}$$

Rearranging the terms,

$$\left[\int_0^{L_i}[B]^T\,[C]\,[B]\,dx\right]\{d\} = \{q\} \qquad \text{.....(4.42)}$$

which is of the form [k] {d} = {q}. From this, the element stiffness matrix is obtained as:

$$[k] = \int_0^{L_i}[B]^T\,[C]\,[B]\,dx \qquad \text{.....(4.43)}$$

in which,

$$[C] = \begin{bmatrix} k_s & 0 \\ 0 & k_n \end{bmatrix} \qquad \text{.....(4.44)}$$

where $k_s$ and $k_n$ are the stiffness of interface in the tangential and normal directions respectively. Since the shearing and normal displacements are uncoupled as in a non – dilatant case (Ghaboussi et al., 1973) the [C] matrix is left with no off – diagonal terms. From the above, the stress vector is got as:

$$\begin{Bmatrix} \tau \\ \sigma_n \end{Bmatrix} = \begin{bmatrix} k_s & 0 \\ 0 & k_n \end{bmatrix} \begin{Bmatrix} \Delta u \\ \Delta v \end{Bmatrix} \qquad \text{.....(4.45)}$$

Substituting for [B] from Eqn. 4.38, [C] from Eqn. 4.44 and for the shape functions from Eqn. 4.36, in Eqn. 4.43, and performing the integration, the final element stiffness matrix for the soil – reinforcement interface element is obtained as:

$$[k_m] = \frac{L_i}{2}\begin{bmatrix} 2k_s & 0 & k_s & 0 & -k_s & 0 & -2k_s & 0 \\ 0 & 2k_n & 0 & k_n & 0 & -k_n & 0 & -2k_n \\ k_s & 0 & 2k_s & 0 & -2k_s & 0 & -k_s & 0 \\ 0 & k_n & 0 & 2k_n & 0 & -2k_n & 0 & -k_n \\ -k_s & 0 & -2k_s & 0 & 2k_s & 0 & k_s & 0 \\ 0 & -k_n & 0 & -2k_n & 0 & 2k_n & 0 & k_n \\ -2k_s & 0 & -k_s & 0 & k_s & 0 & 2k_s & 0 \\ 0 & -2k_n & 0 & -k_n & 0 & k_n & 0 & 2k_n \end{bmatrix} \qquad \text{.....(4.46)}$$

The transformation matrix used was:

$$[T] = \begin{bmatrix} c_x & c_y & 0 & 0 & 0 & 0 & 0 & 0 \\ -c_y & c_x & 0 & 0 & 0 & 0 & 0 & 0 \\ 0 & 0 & c_x & c_y & 0 & 0 & 0 & 0 \\ 0 & 0 & -c_y & c_x & 0 & 0 & 0 & 0 \\ 0 & 0 & 0 & 0 & c_x & c_y & 0 & 0 \\ 0 & 0 & 0 & 0 & -c_y & c_x & 0 & 0 \\ 0 & 0 & 0 & 0 & 0 & 0 & c_x & c_y \\ 0 & 0 & 0 & 0 & 0 & 0 & -c_y & c_x \end{bmatrix} \qquad \text{.....(4.47)}$$

The interface element stiffness matrix with respect to the global coordinate axes is then obtained as:

$$[k] = [T]^T [k_m] [T] \qquad \text{.....(4.48)}$$

The shear stress – deformation behaviour of the interface can be expected to be non linear in the general case. The following section describes how the same is accommodated in the analysis.

#### *4.4.3.1 Hyperbolic relation for the interface*

In a similar manner as the soil, the properties of the interface are also assumed to follow the hyperbolic relationship as proved by Desai (1974). Analogous to Eqn. 4.1, the relation between interface shear stress, $\tau$, and the relative tangential displacement, $\Delta$ can be expressed as (see Fig. 4.4 (a)):

$$\tau = \frac{\Delta}{a_i^1 + b_i^1 \Delta} \qquad \text{.....(4.49)}$$

in which $a_i^1$ is the reciprocal of the initial interface shear stiffness, $k_{si}$, and $b_i^1$, the reciprocal of the maximum shear stress, $\tau_{max}$. The constants $a_i^1$ and $b_i^1$ are obtained by fitting a straight line for the shear stress – shear displacement data on transformed axis as in the case of soil (Fig. 4.4 (b)).

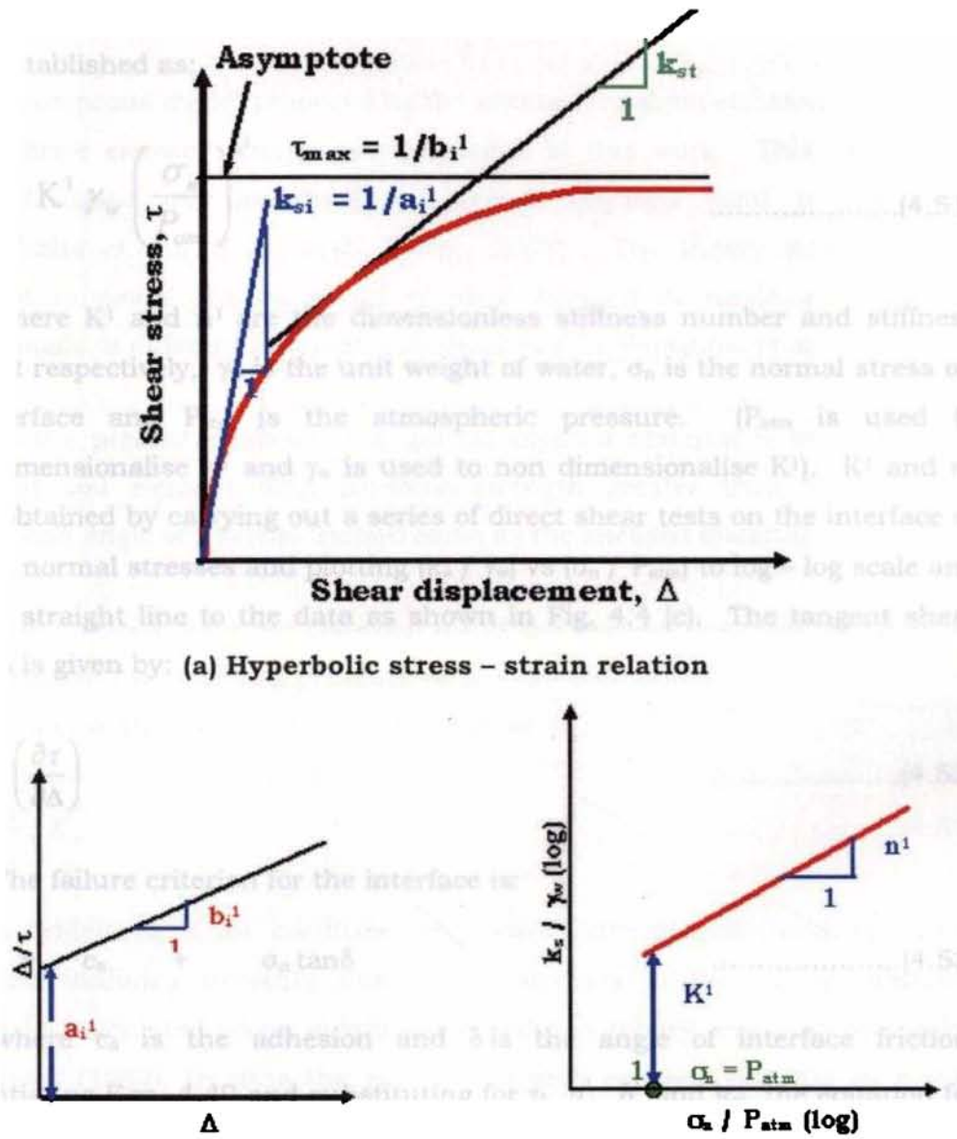


**Fig. 4.4 Determination of hyperbolic constants for the interfaces**

$\tau_{max}$ can be related to $\tau_f$ (shear stress at failure in the direct shear test) by the failure ratio for interface $R_f^1$ as:

$$\tau_f = R_f^1 \, \tau_{max} \qquad \text{.....(4.50)}$$

Similar to Eqn. 4.5, the relation between $k_{si}$ and the normal stress, $\sigma_n$ can be established as:

$$k_{si} = K^1 \gamma_w \left( \frac{\sigma_n}{P_{atm}} \right)^{n^1} \qquad \text{.....(4.51)}$$

where $K^1$ and $n^1$ are the dimensionless stiffness number and stiffness exponent respectively, $\gamma_w$ is the unit weight of water, $\sigma_n$ is the normal stress on the interface and $P_{atm}$ is the atmospheric pressure. ($P_{atm}$ is used to non - dimensionalise $n^1$ and $\gamma_w$ is used to non dimensionalise $K^1$). $K^1$ and $n^1$ can be obtained by carrying out a series of direct shear tests on the interface at different normal stresses and plotting ($k_s$ / $\gamma_w$) vs ($\sigma_n$ / $P_{atm}$) to log – log scale and fitting a straight line to the data as shown in Fig. 4.4 (c). The tangent shear stiffness is given by:

$$k_{st} = \left( \frac{\partial \tau}{\partial \Delta} \right) \qquad \text{.....(4.52)}$$

The failure criterion for the interface is:

$$\tau_f = c_a + \sigma_n \tan\delta \qquad \text{.....(4.53)}$$

where $c_a$ is the adhesion and $\delta$ is the angle of interface friction. Differentiating Eqn. 4.49 and substituting for $\tau_f$, $a_i^1$, $b_i^1$ and $k_{si}$, the equation for $k_{st}$ can be got as:

$$k_{st} = \left[ 1 - \frac{R_f^1 \tau}{c_a + \sigma_n \tan\delta} \right]^2 K^1 \gamma_w \left( \frac{\sigma_n}{P_{atm}} \right)^{n^1} \qquad \text{.....(4.54)}$$

Eqn. 4.54 reduces to Eqn. 4.51 at $\tau = 0$. In the present analysis, $k_n$ is not determined, but it is assigned a high value (such as 1000 units), criterion being the avoidance of interpenetration of nodes (Desai et al., 1982, 1984). The difficulties involved in determining $k_n$ experimentally have been amply highlighted by Sharma and Desai (1992).

## 4.5 COMPOSITE MODEL FOR GABION ENCASED MATERIAL

A composite model proposed by the author for gabion-encased material is used in finite element simulations presented in this work. This model was developed based on the theory of geocell encased sand proposed by Madhavilatha et al. (2000, 2001, 2006, 2007). The theory was originally developed to model the behaviour of sand encased in single and multiple geocells made of different geosynthetics described by Rajagopal et al. (2001).

In the present analyses, the gabion encased material is treated as an equivalent soil element with cohesive strength greater than the encased material and angle of internal friction same as the encased material.

The induced apparent cohesion ($c_i$) in the encased material is related to the increase in the confining pressure on the material due to the confinement of the gabion cage through the following equation:

$$c_i = \frac{\Delta\sigma_3}{2}\sqrt{K_p} \qquad \text{.....(4.55)}$$

in which, $K_p$ is the coefficient of passive earth pressure and $\Delta\sigma_3$ is the additional confining pressure due to the stresses in the gabion material. $\Delta\sigma_3$ can be calculated using membrane correction theory proposed by Henkel and Gilbert (1952), treating the gabion box with encased material as a thin cylinder subjected to internal pressure. Even though the gabion boxes are not cylindrical, for the purpose of modelling, they are treated as a cylindrical unit with initial diameter equivalent to the initial least lateral dimension of the gabion box. Since the encased materials are rock pieces with high strength compared to that of the gabion material, the thin gabion mesh may be treated as a membrane exerting hoop tension on the rock pieces. Hence,

$$\Delta\sigma_3 = \frac{2M_g}{D_o}\left[\frac{1-\sqrt{1-\varepsilon_a}}{1-\varepsilon_a}\right] \qquad \text{.....(4.56)}$$

where, $\varepsilon_a$ is the axial strain of the gabion mesh at failure, $D_o$ is the initial least lateral dimension of the gabion box, M is the secant modulus of the gabion material at axial strain of $\varepsilon_a$.

The cohesive strength ($c_i$) obtained from Eqn. 4.55 should be added to the cohesive strength of the encased material soil (c) to obtain the cohesive strength of the gabion encased soil ($c_g$). The angle of internal friction is taken as the same for the unreinforced and gabion encased materials, as demonstrated by Bathurst and Karpurapu (1993) and Rajagopal et al. (2001) in the case of geocell encased soils. Mohr Coulomb failure criterion was used to model the failure of the gabion encased material as:

$$\tau_f = c_g + \sigma_n \tan \phi \qquad \text{.....(4.57)}$$

where, $\tau_f$ and $\phi$ are the shear strength and the angle of internal friction of the encased material respectively. $\sigma_n$ is the normal stress at failure and $c_g$ is the effective cohesion of the gabion material.

For simplicity in the determination of input parameters, the gabion encased material (which is essentially rock pieces) is considered as a linear elastic material. The determination of non linear hyperbolic parameters using triaxial tests for the large rock pieces is beyond the scope of the present work and hence is not resorted to.

The applicability of the above procedure is verified through finite element simulations of model walls tested in the laboratory as described in Chapter VI.

## 4.6 MODELLING OF CONSTRUCTION PHASES

In the analysis of reinforced soil walls, the simulation of the construction phases is considered an important factor. This is because of the self weight induced stresses which play an important role in the modelling of such walls. Hence the modelling of the construction phases are also included in the

development of the prediction tool for gabion faced reinforced earth walls as per the procedure explained in Potts and Zdravkovic (1999 A). The procedure is as follows.

The analysis is divided into a set of increments at the calculation of initial stresses itself. Nodal forces due to the self weight body forces of the constructed layer are calculated and added to the right hand side load vector. The global stiffness matrix and all other boundary conditions are then assembled for the increment. The equations are solved to obtain the incremental changes in displacements, strains and stresses. For each increment of additional layer, initially, displacements of all nodes are temporarily zeroed irrespective of the nodes which were active in the previous increment. As in the case of incremental method, the displacements are then added to the corresponding nodal displacements in the previous increment.

## 4.7 NUMERICAL IMPLEMENTATION

The software needed for the present investigations has been prepared in C language in the following manner.

A two dimensional plane strain finite element program for the linear analysis of reinforced soil structures coded by the author for her M. Tech. programme (Jayasree, 1996) at College of Engineering, Trivandrum was modified and extended for implementing the present analysis. The programme was originally developed for the linear analysis of reinforced soil systems incorporating the composite element proposed by Romstad et al., (1976 and 1978) considering the unit cell approach. For the present work, this was then modified to a non linear program using discrete element approach incorporating some of the essential features from NOSFIN (a three dimensional non linear FE package called **NO**nlinear **S**oil – **F**oundation **IN**terface **IN**teraction analysis program developed at Indian Institute of Technology, Madras (Beena, 1993)). Within this framework, two dimensional truss element and zero thickness 2D line interface element were incorporated to simulate the discrete element approach. The stiffness of all the elements were calculated and assembled to

obtain the global stiffness equation. Gaussian elimination method was used for the solution of the equilibrium equations.

Additional formulations of the newly developed composite model for gabion representation and modelling of the construction phases were also incorporated in this modified program named as FECAGREW (**F**inite **E**lement **C**ode for the **A**nalysis of **G**abion **RE**taining **W**alls). EXCEL worksheet of Microsoft Office 2003, MATLAB version 7.01 and SURFER Version 7.00 were used as post processors in this research work.

## 4.8 FINITE ELEMENT MODELLING

A full fledged finite element model to simulate the load deformation behaviour of gabion faced reinforced earth walls, was developed as follows using FECAGREW.

The discretisation of soil and gabion facing was done using isoparametric quadrilateral elements, reinforcing mesh using 2D truss elements and the soil – reinforcement interaction as well as the soil – facing interaction using zero thickness line interface elements. A schematic sketch of the discretisation is shown in Fig. 4. 5. The nodal connectivities at the reinforcing junction are clearly illustrated in Fig. 4. 6.

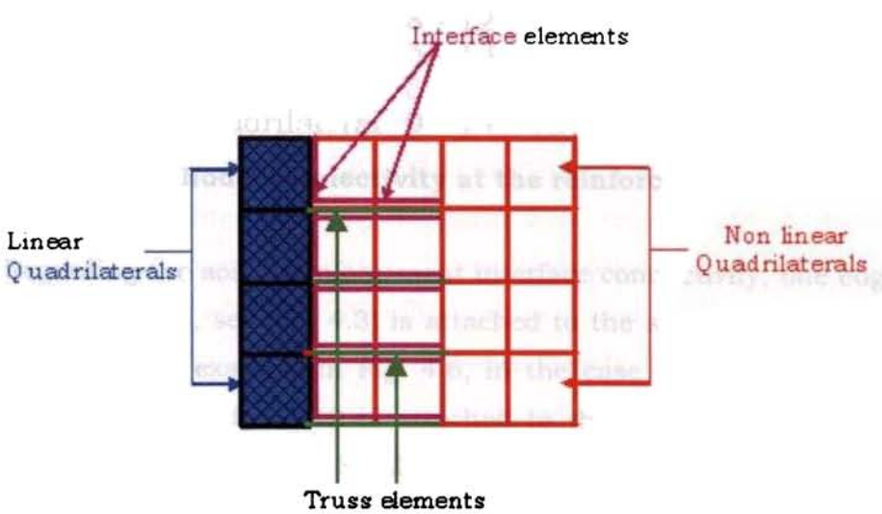


**Fig. 4.5 Discretisation of gabion faced reinforced soil wall**

For the validation and the parametric studies, initially a coarse mesh was used for modelling the wall and it was refined until the results were more or less stabilised with further mesh refinements. The final refined mesh was used for all the analyses. In both the studies, the model was different and the configuration and numbering of the mesh was done in such a way that the same mesh could be adopted for all the analyses in a particular study.

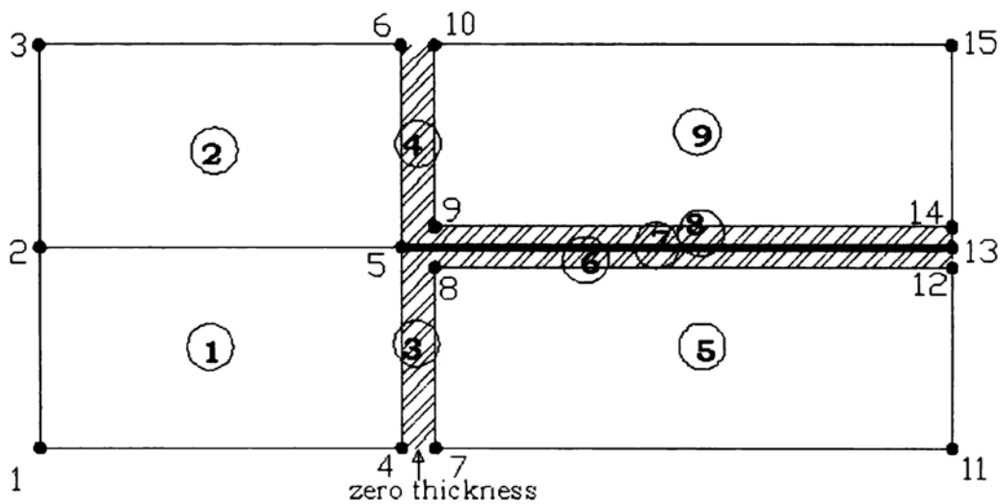


| Element | Type | Nodes |
|---|---|---|
| 1 | Quadrilateral | 1 - 4 - 5 - 2 |
| 2 | Quadrilateral | 2 - 5 - 6 - 3 |
| 3 | Interface | 7 - 8 - 5 - 4 |
| 4 | Interface | 9 - 10 - 6 - 5 |
| 5 | Quadrilateral | 7 - 11 - 12 - 8 |
| 6 | Interface | 8 - 12 - 13 - 5 |
| 7 | Truss | 5 - 13 |
| 8 | Interface | 5 - 13 - 14 - 9 |
| 9 | Quadrilateral | 9 - 14 - 15 - 10 |

**Fig. 4.6 Nodal connectivity at the reinforcing junction**

Regarding the soil – reinforcement interface connectivity, one edge of the interface (1-2 or 3-4, see Fig. 4.3) is attached to the soil and the other to the reinforcement. For example in Fig. 4.6, in the case of the interface element numbered as 6, the edge 8-12 is attached to the soil and the edge 5-13 is attached to the reinforcement. Similarly, for the interface element numbered as 8, the edge 9 -14 is attached to the soil and the edge 5-13 is attached to the

reinforcement. Initially, nodes 5, 8, 9 as well as 12, 13, 14 will have the same coordinates, to represent the zero thickness condition. After the analysis, each node will show different horizontal displacement (u) values, indicating the slip, but they show almost the same vertical displacement (v) values owing to the high normal stiffness ($k_n$) values ($1 \times 10^8$ kN/m) assigned to the interface elements.

The boundary conditions were provided in such a way that, only vertical movement was possible at the extreme end of the backfill zone arresting the horizontal displacements at these nodes. It was assumed that the wall rests on a rigid base for the validation studies and hence complete fixity was provided at the base of the wall. In the case of parametric studies, the wall was assumed to rest on a soft foundation layer and the bottom of the foundation layer was assumed nil movement. Hence in both the studies, the u and v displacements were arrested for the bottom nodes. No restriction should be given to the wall facing and so free movement was allowed at the facing boundary.

During analysis, the failure of the quadrilateral elements (soil and gabion facing) due to shear were checked by verifying the Mohr – Coulomb failure criterion. If an element is found to fail in shear, the same was noted, but no changes were effected and the element was allowed to follow the stress - strain relation as before. However, as regards the elements which fail in tension, the same were assigned very small values of $E_t$ = 0.0005 kPa for further iterations.

If during the analysis, an interface element failed in shear (slip), the value of shear stiffness in the element was reduced to a small value ($3 \times 10^{-7}$ kPa). If tensile condition (debonding) develops across the interface elements, both shear and normal stiffnesses were assigned small values, as per the usual practice found in literature (Beena (1993), Chew and Schmertmann (1990), Miura et al. (1990)). The initial stresses due to gravity in the interface elements were set equal to the stresses in the adjoining soil elements. Initial shear stresses were equal to zero in all the elements.

## 4.9 SUMMARY

The development of a prediction tool with acronym FECAGREW, for simulating the load deformation behaviour of gabion faced reinforced earth walls is described in this chapter. The formulation of the elements used for the two dimensional plane strain analysis as well as the constitutive models used to predict the stress strain behaviour of these elements are also given. The development of a composite model to simulate the confining effect of the gabion facing is also explained in detail. The modelling of the construction sequence and the details of the idealisation of gabion faced walls are also discussed. The developed model is expected to effectively simulate the behaviour of the gabion faced reinforced earth walls as proved in Chapter VI.

# Chapter 5

# EXPERIMENTAL INVESTIGATIONS

## 5.1 GENERAL

The formulation of the finite element prediction tool described in the previous chapter has to be validated through experimental results. For this, experiments were conducted on small scale models of gabion faced reinforced earth walls. While doing so, an attempt was made to explore the possibility of reducing the cost of construction by using quarry dust as a gabion fill material.

The most attractive feature of the gabion walls is their cost effectiveness. Gabion walls can achieve around 30 - 60% savings when compared to RCC walls constructed in similar situations. Even though the structure is a cost effective one, it can be seen that the stone filling used inside gabion boxes increases the cost of construction. In this work, an attempt is made to examine the effects of replacement of the stone filling in the gabion boxes with a mixture of stone and rock waste. The use of rock waste would relieve some of the problems associated with its disposal and it may turn into an inexpensive and advantageous construction product. It can also be noted that there is an added advantage in the use of rock waste from the quarries in the sense that the otherwise colossal cost of the conventional retaining structures is reduced to a very low value. This chapter describes in detail the different experiments carried out for determining the load deformation behaviour of the walls using gabions with different combinations of fill materials as facing.

## 5.2 MODEL STUDIES

In gabion walls, gravity force (self weight) is the predominant stabilising force, which depends on the unit weight of the material ($\gamma_m$) used for construction, which in turn is dependent on the specific gravity (G) of the material by the relation, $\gamma_m = G\ \gamma_w$, where $\gamma_w$ is the unit weight of water. The specific gravity of rock waste is nearly equal to that of stone.

Therefore, gravity force is not affected by the replacement of stone with rock waste. Considering all these points, rock waste was selected as a substitute for stone filling in this work. To represent the rock waste in the model studies, quarry dust, which is one of the easily and cheaply available waste materials, was used. Similarly stone filling was represented by 20mm coarse aggregate filling inside the gabion boxes. Instead of the actual gabion wall with stone filling, the one with a combination of stone filling and quarry dust was considered for the studies. Five different combinations were tried by varying the quantities of quarry dust and stone filling. The experimental studies were carried out on two different model walls constructed at two different sites. The first set of studies was on a 1m high model gabion wall constructed in the field in the premises of College of Engineering, Trivandrum (hereafter referred to as Set I in the text) and the second set on a 60cm high model gabion wall constructed inside a steel tank of size 1m x 1m x 1m in the Geotechnical Engineering laboratory of School of Engineering, CUSAT, Kochi (referred to as Set II in the text hereafter). The model walls were designed according to the physical properties of the materials used for construction like sand (as backfill), coarse aggregate and quarry dust (as gabion fills) and steel mesh (for gabion boxes and reinforcement).

Load tests were conducted on model gabion retaining walls to study the deformation characteristics of gabion faced retaining walls. The purpose of this study was to find out an optimum combination of quarry dust and stone filling, to replace the stone filling in gabion boxes and thus, further reduce the cost of construction of gabion wall. For this, five different combinations of quarry dust and coarse aggregate were used in the gabion fill supporting the model retaining wall. The combinations were varied by percentage weight of the filling materials in gabion boxes. The five different cases were:

i. Coarse aggregate alone
ii. 70% Coarse aggregate + 30% Quarry dust
iii. 50% Coarse aggregate + 50% Quarry dust
iv. 30% Coarse aggregate + 70% Quarry dust
v. Quarry dust alone

## 5. 2. 1 Field model studies – Set I

Field model studies were conducted to study the lateral deformation behaviour for the first set of experiments. The site for Set I experiments was selected where a natural slope was available for retention purpose, inside the premises but away from the active campus of College of Engineering, Trivandrum to avoid disturbance of any kind on the experimental set up. The length of the walls was limited by bays built using bricks. Gabion walls with the different facing materials were constructed in between these bays.

The sand used for backfilling was uniform river sand, with properties: G = 2.72, $D_{10}$ = 0.18mm, $C_u$ = 2.22, $e_{min}$ = 0.56, $e_{max}$ = 0.69. The coarse aggregate used as gabion fill material had the properties: G = 2.83, $D_{10}$ = 18mm, $C_u$ = 1.67. The quarry dust which was also one of the filling materials in gabion boxes, had the properties, G = 2.8, $D_{10}$ = 0.12mm, $C_u$ = 2.89.

### *5.2.1.1 Construction of model gabion wall*

In actual field practice, gabion boxes of various sizes are used for construction such as 1.5m x 1m x 1m, 2m x 1m x 1m and 4m x 1m x 1m. For the reinforcement purpose the base of the gabion boxes are provided with an extension. Generally 0.6 to 0.8 times the height of the wall is taken as the reinforcement extension including the base of the box. The extension and boxes act monolithically. Boxes are provided with a top cover and internal partitions called as diaphragms to prevent bulging of the box. The model gabion wall was constructed over a length of 2m. The height of the wall was fixed as 1m. The wall was constructed at a distance of 2.5m from the natural slope and the space was filled with sand, which acted as a backfill to the wall. Brick bays were constructed on either side to limit the length of the wall. Sixteen numbers of gabion boxes each of size 0.5m x 0.25m x 0.25m were used to retain the backfill. Model gabion box used for the work is shown in Fig. 5.1. Boxes were provided with an extension of 0.55m at the base. Top cover was also provided. Because of the small size of the box, diaphragm walls were avoided.

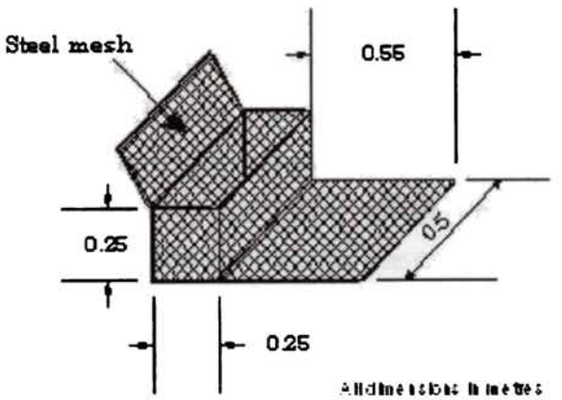


**Fig. 5.1 Dimensions of model gabion box**

**Fig. 5.2 Model gabion box with geotextile lining**

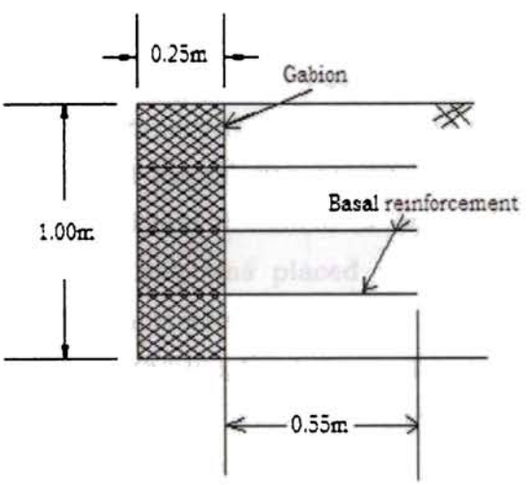


**Fig. 5.3 Cross section of the model wall (Set I)**

**Fig. 5.4 Elevation of the model wall (Set I)**

For the load tests, using coarse aggregate as filling material, the above described model gabion boxes were used as such. But for the quarry dust and other combinations of quarry dust and coarse aggregate as filling material, the inner sides of the gabion boxes were stitched with geotextile Terram 1000. Nylon wires were used for stitching. The geotextile prevents the escape of quarry dust through the mesh openings. The photograph of gabion box used for the combination fillings is shown in Fig. 5.2. Fig. 5.3 shows the cross section of the wall and Fig. 5.4 shows the photograph of elevation of the model gabion wall.

The ground was levelled and 5cm thick layer of sea sand was spread over it. The first layer of four boxes was placed on the levelled ground surface where the wall had to be constructed. The boxes were connected together with steel wires so that they behave as a single unit. The extensions of the boxes were spread over the sand layer. Boxes were filled with filling material corresponding to the cases considered. In the case of combination filling, the quarry dust and coarse aggregate were filled in the boxes after mixing them properly in the required proportions. Filling was done with proper compaction to achieve the required unit weight of 15 $kN/m^3$.

After filling the boxes, the top cover was closed and tightly connected to the sides of the boxes using steel wires. Behind the boxes, geotextile Terram 1000 was placed in order to avoid the entry of granular backfill into the boxes. Then backfilling of sand was done up to the height of the boxes. The backfill sand was compacted in each layer to get an average unit weight of 17.6 $kN/m^3$. Each layer of the fill was compacted to get the same density by controlling the weight of soil and thickness of layer. After levelling the backfill, the next layer of gabion boxes was placed above the first layer and the two layers were stitched with steel wires and the procedure was continued up to the required level. Since the height of the wall was fixed as 1m, four layers of boxes each of height 0.25m were placed to complete the construction. Markings were made on the front of each box of the facing unit for taking measurement due to surcharge loading.

#### *5.2.1.2 Loading set up*

After the construction of wall using gabion boxes loading was done with sand bags. Before placing the sand bags a concrete slab was placed over the retaining wall to enable the surcharge loads to give a uniform pressure as well as to act as a loading platform. Sand bags were placed in layers (Fig. 5. 5). Each layer constituted of 25 bags filled with sand. Each layer provides a surcharge pressure of 2kPa. The load for the first layer of sand bag (2 kPa) and load from the concrete slab (1 kPa) was taken as the seating load and the initial deformations were noted. An aluminium rod was placed above gabion wall,

supported by the brick walls of the bay. This was used as a reference mark to measure the deformations (Fig. 5. 6). In order to measure the lateral deflection the outer edge of the aluminium rod was used as the datum point. A plumb bob was hung down vertical from the outer edge of Aluminium bar. Using a metre scale the initial position of wall and the changed position after loading, were measured. The difference between these values gave the lateral deformation at each point.

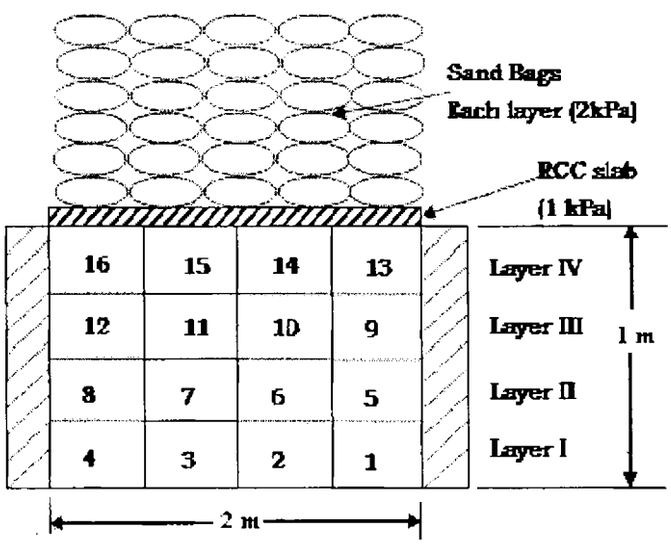


**Fig. 5.5 Schematic sketch of the loading set up**

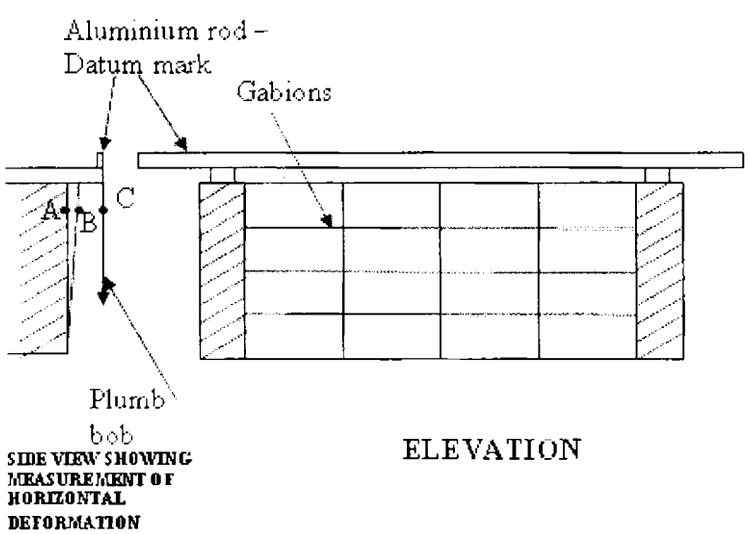


**Fig. 5.6 Deformation measurements (Set I)**

In total, six layers of sand bags were placed one over the other, above the retaining wall. Thus at the end of loading a total pressure of 13 kPa was acting on the wall. After placing each layer of sand bag the loading was kept undisturbed till the deformations stabilized. Before placing the next layer of sand bags, lateral deformations were measured. For Set I experiments, the walls were not loaded to failure due to the practical difficulty of increasing the height of dead load.

## 5. 2. 2 Laboratory model studies – Set II

The Set II experiments consisted of studies on model gabion retaining wall constructed in a steel tank of size 1m x 1m x 1m in the Geotechnical Engineering laboratory of Cochin University of Science and Technology, Kochi. The tests were done using the funding obtained from Kerala State Council for Science, Technology and Environment, Trivandrum. Unlike the Set I experiments, in these experiments, the walls were loaded with strip load using hydraulic jack and the horizontal deflections were measured using dial gauges to get a better control over the loading and deformations.

The sand used for backfilling was uniform river sand, with properties: $G = 2.7$, $D_{10} = 0.2$mm, $C_u = 2.6$, $e_{min} = 0.53$, $e_{max} = 0.71$. The coarse aggregate used as gabion fill material had the properties: $G = 2.87$, $D_{10} = 16$mm, $C_u = 1.313$. The quarry dust which was also one of the filling materials in gabion boxes, had the properties, $G = 2.81$, $D_{10} = 0.16$mm, $C_u = 2.81$.

### *5.2.2.1 Experimental set up*

The height of the wall was fixed as 0.6m and the dimensions of the boxes and basal extension were designed using the physical properties of backfill soil and steel mesh which were obtained from laboratory experiments. Sixteen numbers of gabion boxes each 0.25m long, 0.15m wide and 0.15m high and with basal reinforcement of 0.35m were used to retain the sand backfill inside the tank. The boxes were fabricated by stitching steel mesh panels to get the required shape. Fig. 5.7 shows the complete experimental setup.

**Fig. 5.7 Experimental set up for the model gabion wall**

Four such boxes were stitched one beside the other to form a layer such that they behave as a single unit. Four layers were placed one above the other to form the wall. The boxes were numbered as 1 – 16 continuously as shown in Fig. 5.8.a. The horizontal deformations at the front face of the wall were measured using dial gauges with magnetic base (travel 25mm, least count 0.01mm) at the circled points (eight numbers).

For the load tests using coarse aggregate alone as the filling material, the above described model gabion boxes were used as such. But for the cases where quarry dust is also used as filling material, the inner sides of the gabion boxes were stitched with geotextile Terram 1000. Nylon wires were used for stitching. The geotextile prevents the escape of quarry dust through the mesh openings. The filling material in the boxes was filled at an average unit weight

of 15 kN/m$^3$. In this set of experiments, the combination filling was done in layers. The required proportion of quarry dust was placed as the bottom layer and the coarse aggregate as the top layer, the separation between the two being made using the geotextile material.

The backfill sand was compacted in each layer to get an average unit weight of 16 kN/m$^3$. Each layer of the fill was compacted to get the same density by controlling the weight of soil and thickness of layer. After levelling the backfill, the next layer of gabion boxes was placed above the first layer and they were stitched with nylon wires and the procedure was continued up to the required level. Four layers of boxes each of height 0.15m were placed one above the other to complete the construction. The layers were also interconnected using steel wires such that the entire wall behaves as a single block. Markings with small metal strips were made on the front face of the circled boxes (Fig. 5.8.a) at the centre for taking deformation measurements with dial gauges. Schematic diagram of the test tank with loading setup is shown in Fig. 5.8.

#### *5.2.2.2 Loading set up*

After the construction of the wall using gabion boxes, loading is done using hydraulic jack and lever arrangement. The loading pattern used is of two-point loading acting on a 25mm thick and 0.2m wide strip placed over the sand backfill parallel to the gabion wall. Load was applied using a hydraulic jack, in increments of 3 kN till failure. After applying each increment, the load was kept constant till the deformations stabilized. Prior to next increment lateral deformations were measured using dial gauges.

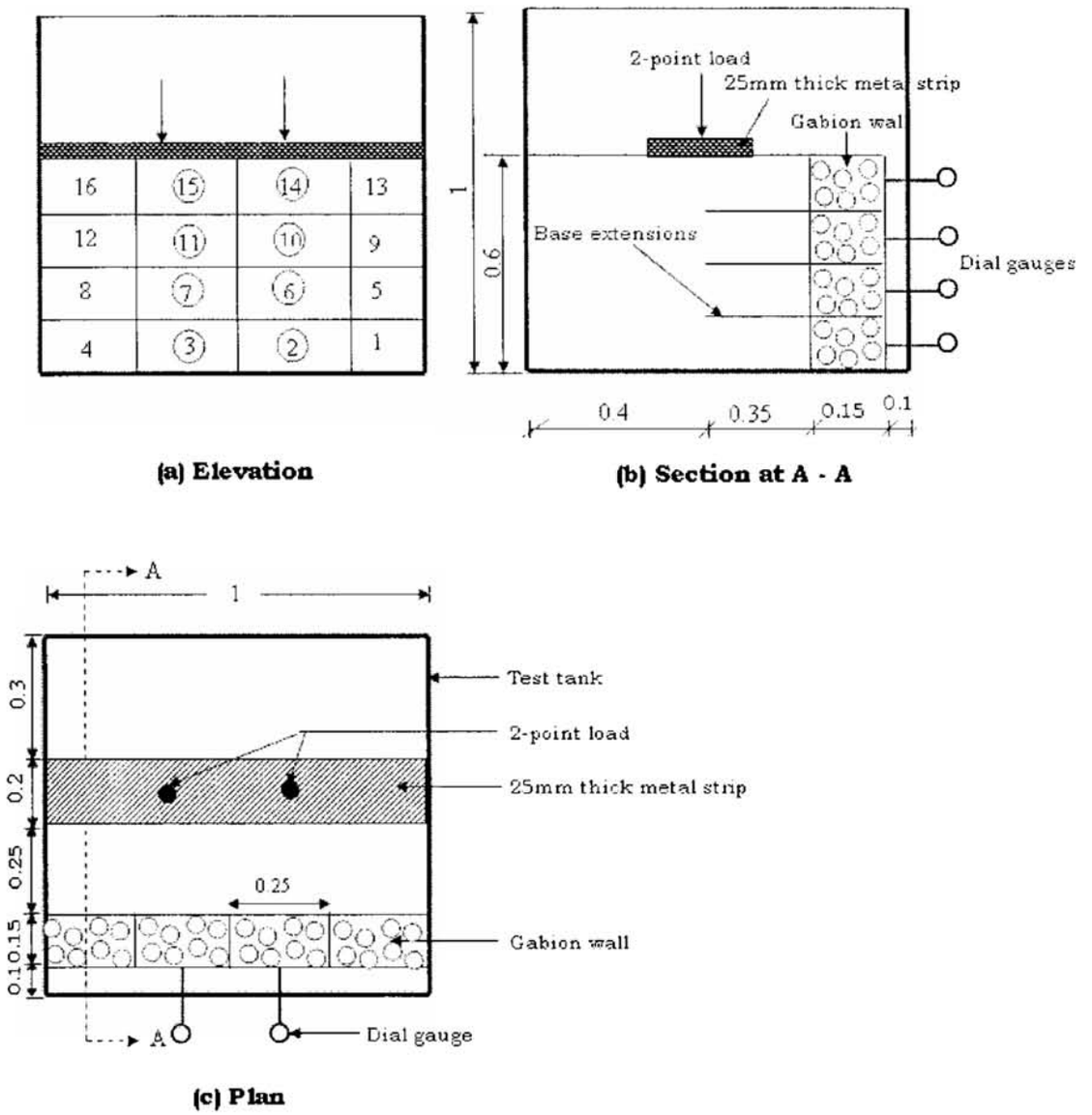


**Fig. 5.8 Schematic diagram of the test tank (Not to scale)**
**(All dimensions in metres)**

## 5.3 RESULTS AND DISCUSSIONS

An account of the results obtained from the experimental studies is presented in this section. Set I experiments were loaded up to 13 kPa which included a seating load of 3 kPa and initial deformations were measured only after stabilisation of the deformations due to the seating load. For the Set II experiments, the wall was kept undisturbed for a day for the stabilisation of

post construction deformations and loading was done on the succeeding day in increments. The load – deformation measurements were noted till failure. The type of loading for the two experiments were also different, viz., surcharge loading was adopted for Set I experiments whereas strip loading was given for Set II experiments. However the results can be used for comparison purposes considering the trends shown by the curves.

### 5.3.1 Load deformation characteristics

The effective replacement of stone filling in gabion boxes by a cheaper material is the focus of the study and is done by comparing the load deformation behaviour of the five different walls constructed with the fill materials mentioned in Section 5.2. Figures 5.9 and 5.10 show the load deformation characteristics for the two sets of experiments in which the deformation is expressed in terms of a dimensionless quantity, top sway factor, $\delta_{st}$ which is defined as $u_t$ / H where H is the wall height and $u_t$ is the top lateral deformation of the wall at the midsection. Although $u_t$ is referred as top lateral deformation, it is measured as the average of the lateral deformations at the centres of gabion boxes numbered as 14 and 15 in Figs. 5.5 and 5.8. From the figures, it can be seen that as the load increases, the lateral deformation also increases, as expected. The quarry dust filled gabion walls show more lateral deformation than that of the coarse aggregate filled gabion walls. The combinations showed intermediate deformations. This may be due to the low stiffness characteristics of quarry dust filled gabions. As a result, as the percentage of quarry dust increased, top lateral deformation also increased. The 50-50 combination shows a top lateral deformation less than that of quarry dust alone and 70% quarry dust and 30% coarse aggregate combination.

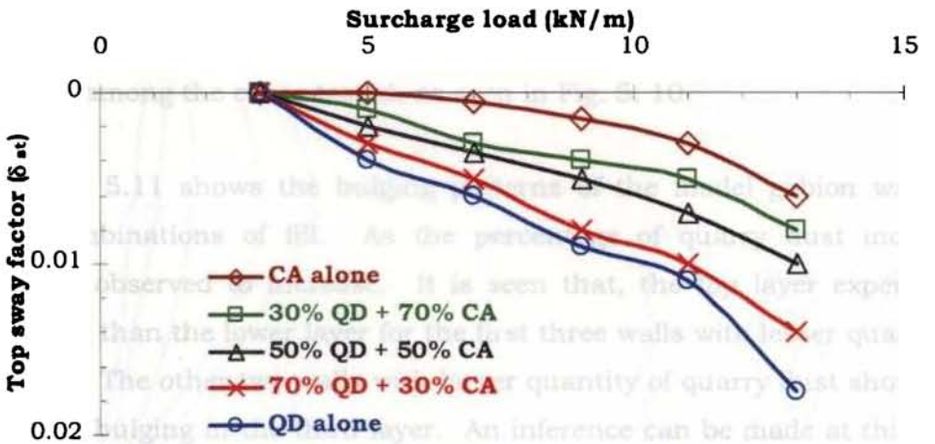


**Fig. 5.9 Load deformation behaviour after seating load (Set I experiments)**

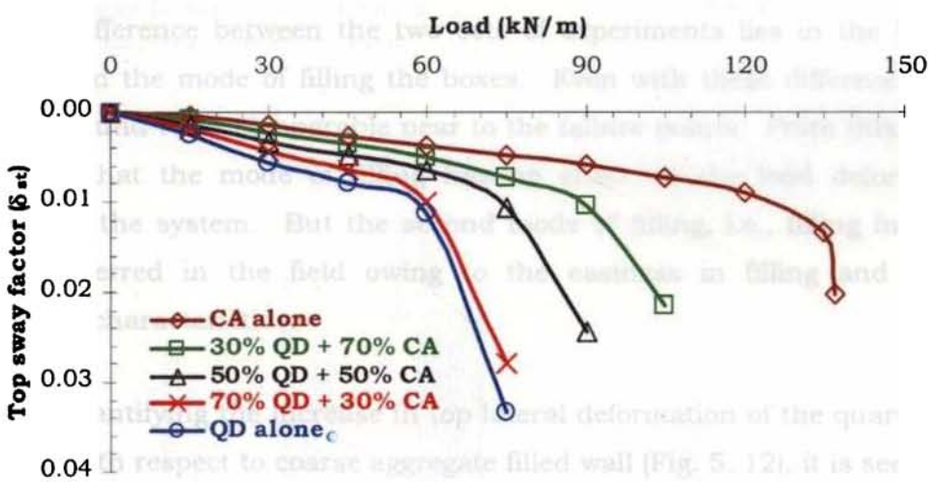


**Fig. 5.10 Load deformation behaviour (Set II experiments)**

## 5.3.2 Bulging patterns

The variation of lateral deformation along the height of the wall which is termed as "bulging pattern", also show the behaviour of retaining walls. The lateral deformations at the mid length of the wall (u) in all the four layers at a specific load value were measured in the experiments to understand the behaviour of the fill materials in the wall facings. The bulging patterns are plotted with the sway factor, $\delta_s = u / H$ along the x-axis and the wall elevation along the y-axis. The bulging patterns are studied for a uniform surcharge load

of 13 kN/m in the case of set I experiments (which is the point where the failure starts) and for set II experiments, a strip load of 60 kN/m, which is the least failure load, among the cases tested, as seen in Fig. 5. 10.

Figure 5.11 shows the bulging patterns of the model gabion walls for different combinations of fill. As the percentage of quarry dust increased bulging was observed to increase. It is seen that, the top layer experienced more bulging than the lower layer for the first three walls with lesser quantity of quarry dust. The other two walls with larger quantity of quarry dust showed an intermediate bulging in the third layer. An inference can be made at this point that the walls with lesser quantity of quarry dust behave in a stiffer manner than the other walls with higher quantities of quarry dust.

The difference between the two sets of experiments lies in the loading difference and the mode of filling the boxes. Even with these differences, the results are found to be comparable near to the failure points. From this, it can be inferred that the mode of filling has no effect on the load deformation behaviour of the system. But the second mode of filling, i.e., filling in layers may be preferred in the field owing to the easiness in filling and higher permeability characteristics.

On quantifying the increase in top lateral deformation of the quarry dust filled walls with respect to coarse aggregate filled wall (Fig. 5. 12), it is seen from both the sets of experiments that filling 30% quarry dust increases the top lateral deformation approximately by 35%. When quarry dust is increased to 50%, almost 70% hike is seen in the deformation value. In general, as the quantity of quarry dust increased, the deformation also increased.

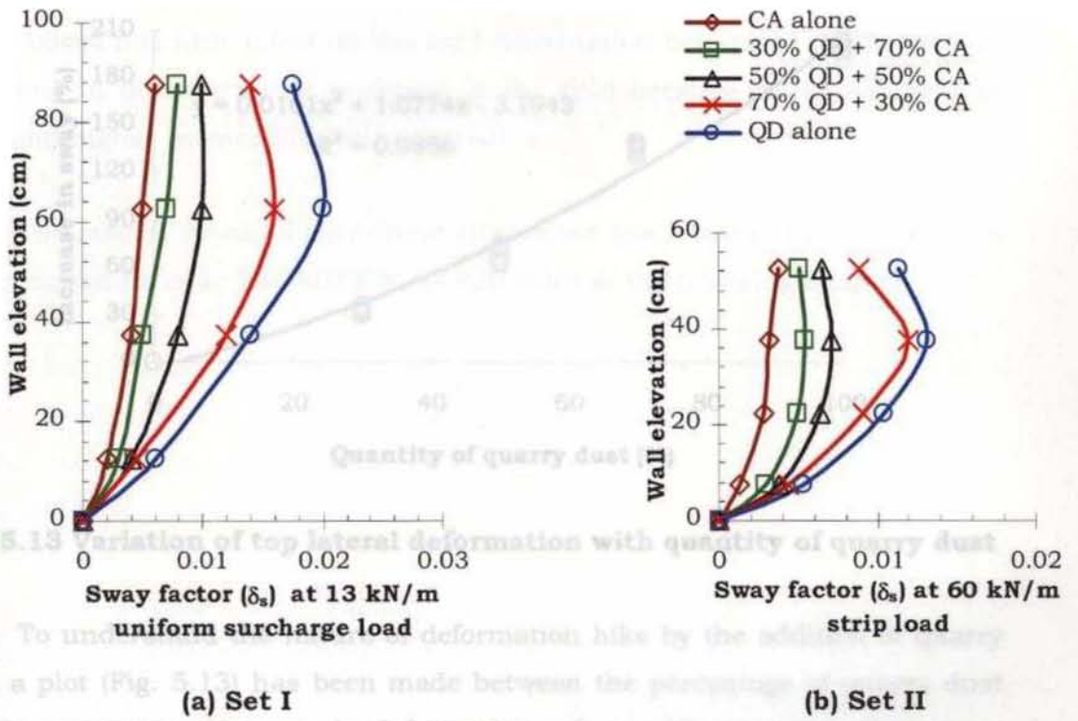


(a) Set I (b) Set II

**Fig. 5.11 Bulging of front face of walls**

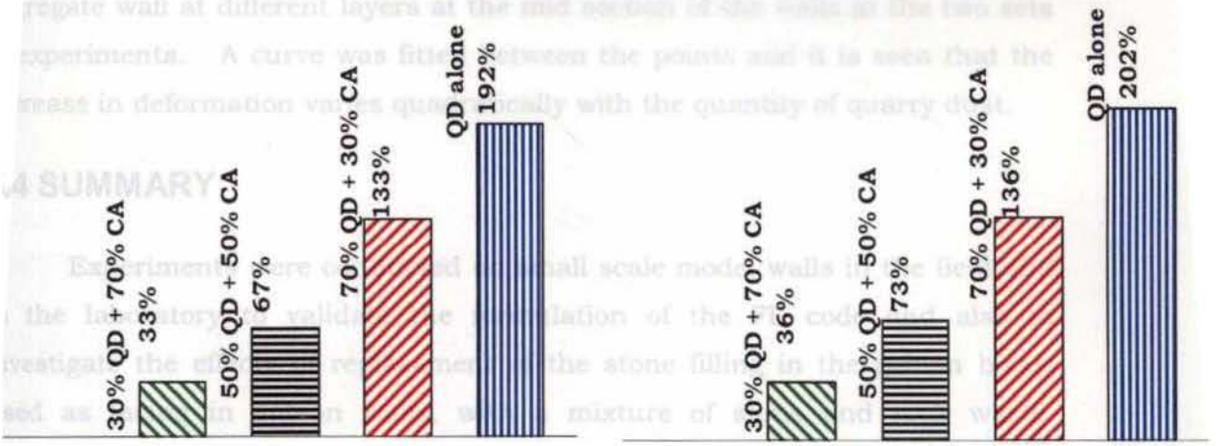


**(a) Set I at 13 kN/m surcharge load** **(b) Set II at 60 kN/m strip load**

**Fig. 5.12 Increase in top sway**

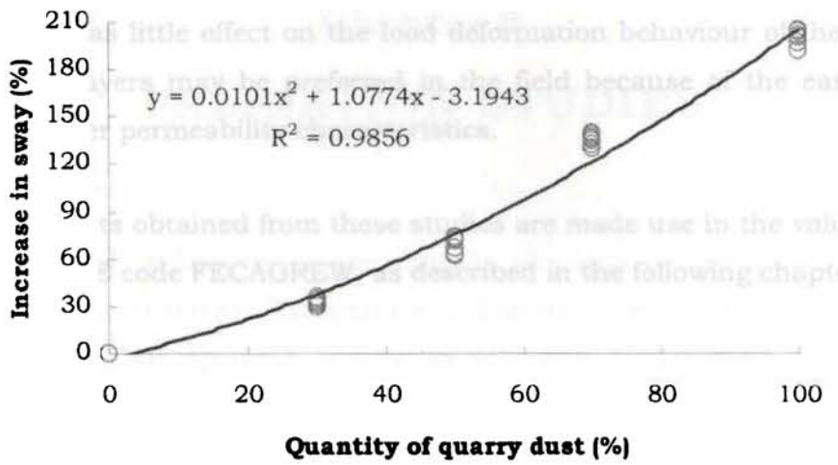


**Fig. 5.13 Variation of top lateral deformation with quantity of quarry dust**

To understand the nature of deformation hike by the addition of quarry dust, a plot (Fig. 5.13) has been made between the percentage of quarry dust and the percentage increase in deformation values with respect to the coarse aggregate wall at different layers at the mid section of the walls in the two sets of experiments. A curve was fitted between the points and it is seen that the increase in deformation varies quadratically with the quantity of quarry dust.

## 5.4 SUMMARY

Experiments were conducted on small scale model walls in the field and in the laboratory to validate the formulation of the FE code and also to investigate the effects of replacement of the stone filling in the gabion boxes used as facing in gabion walls, with a mixture of stone and rock waste. To find an optimum mixture of stone and rock waste to be filled in the gabion boxes, walls were constructed with different combinations of stone and rock waste and were loaded to study the variation in the deformation behaviour of the system. Load deformation curves and bulging patterns were plotted for the different walls and it was seen that the deformations increased with the increase of quarry dust in the facing. Up to 50% replacement of stones with quarry dust, the walls behaved in stiff manner and with further addition of quarry dust the walls became flexible. There is a quadratic increase in the

deformation values with the addition of quarry dust. The mode of filling the gabion boxes has little effect on the load deformation behaviour of the system. But filling in layers may be preferred in the field because of the easiness in filling and higher permeability characteristics.

The results obtained from these studies are made use in the validation of the developed FE code FECAGREW, as described in the following chapter.

# Chapter 6

# VALIDATION STUDIES

## 6.1 GENERAL

In general, validation is the process of checking whether something satisfies a certain criterion. Examples would include: checking if a statement is true (validity), if an appliance works as intended, if a computer system is secure, or if computer data are compliant with an open standard. Validation implies that one is able to testify whether a model or process is correct or compliant with a set of standards or rules.

In the present study, validation indicates checking the accuracy of the prediction tool developed to simulate the behaviour of gabion faced reinforced soil retaining walls. To be exact, it may be noted that, through the validation studies, it should be ensured that the simulation of stresses, strains and displacements should be representative in all respects.

For this, thorough and detailed validation studies were conducted at each phase of the program development. To validate the performance of each element, suitable independent examples are chosen and compared with the available results.

## 6.2 FOUR NODED QUADRILATERAL ELEMENT

This validation study was conducted to check the appropriateness in using the incorporated 2D four noded isoparametric quadrilateral element with regards to linear elastic analysis. For this, a simple case of a cantilever beam with rectangular cross section subjected to an end moment is considered. Here the end moment was replaced by a couple of forces for the purpose of analysis as in Krishnamoorthy (1987). The length of the beam is taken as 200cm, the width 20cm and the depth 30cm. The modulus of elasticity of the

material of the beam is 2 x $10^3$ kN/$cm^2$. The loading on the beam is shown in Fig. 6.1 (a) while the discretisation used for the study is shown in Fig. 6.1 (b).

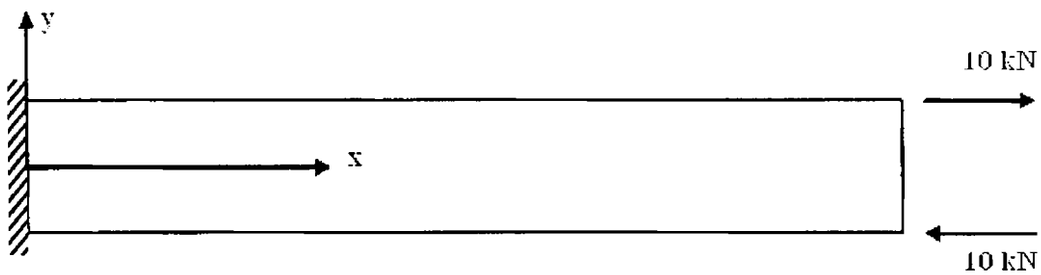


**(a) Cantilever beam**

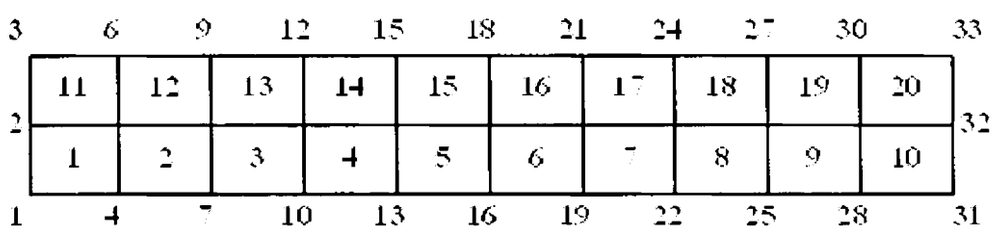


**(b) Discretisation**

**Fig. 6.1 Cantilever beam loaded with couple**

**Table 6.1 Comparison of deflection for cantilever beam**

| Distance from fixed end (cm) | Node numbers | Deflection value (cm) from Krishnamoorthy (1987) | Deflection value (cm) from FECAGREW |
|---|---|---|---|
| 40 | 7, 8, 9 | 0.002182 | 0.002182 |
| 80 | 13, 14, 15 | 0.008727 | 0.008727 |
| 120 | 19, 20, 21 | 0.019636 | 0.019636 |
| 160 | 25, 26, 27 | 0.034909 | 0.034909 |
| 200 | 31, 32, 33 | 0.054346 | 0.054346 |

Linear plane strain elastic analysis was done using FECAGREW and the vertical deflections at the different nodes were noted down. The results presented as Table 6.1 agree quite well with the results from the literature. Hence it may be concluded that the developed code FECAGREW is working

properly and the incorporation of the quadrilateral element has been done accurately.

## 6.3 TWO NODED TRUSS ELEMENT

Linear elastic analysis was conducted to check the accuracy in using the incorporated 2D two noded truss element, in this validation study. For this, a simple case of a two dimensional truss structure shown in Fig. 6.2 (a) was considered. The geometry and loading are taken as symmetrical about the centre line as in Krishnamoorthy (1987). The modulus of elasticity of the material of the truss member is 2 x $10^4$ kN/$cm^2$. The cross sectional area of the truss member is 1 $cm^2$. The discretisation used for the study is shown in Fig. 6.2 (b).

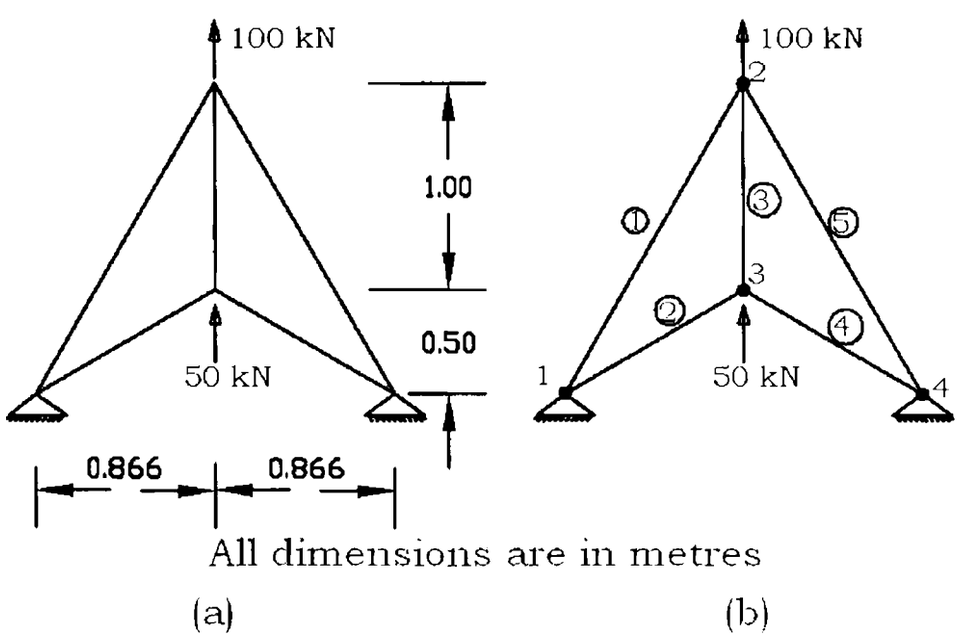


**Fig. 6.2 Plane truss structure**

In this case also, linear plane strain elastic analysis was conducted using FECAGREW and the deflections at the different nodes were noted down. The results are presented in Table 6.2 and they agree quite well with the results from the literature. Axial forces in the truss members were also determined. From the FE analysis using FECAGREW, the axial force in element numbered

as 3 is obtained as 3.724625 kN and the corresponding value obtained from literature (Krishnamoorthy, 1987) is 3.72 kN. Hence, here also, it may be concluded that the incorporation of the truss element in FECAGREW has been done accurately and the elastic analysis is working perfectly for any type of structure.

**Table 6.2 Comparison of deflection for a plane truss structure**

| Node number | Deflection value (cm) from Krishnamoorthy, 1987 | Deflection value (cm) from FECAGREW |
|---|---|---|
| 1 | 0 | 0 |
| 2 | 0.5558 | 0.555834 |
| 3 | 0.5372 | 0.537211 |
| 4 | 0 | 0 |

## 6.4 MODELLING OF NON LINEAR BEHAVIOUR OF SOIL

In order to check the accuracy of formulation of non linear analysis, simulation was done for the experiment results available from literature (Duncan and Chang, 1970). The experiment was based on the behaviour of soil loaded with a strip footing and the vertical displacements at point A (Fig. 6.3) were taken for different loadings till failure.

Analysis was conducted using the hyperbolic parameters and properties of soil as given by Duncan and Chang (1970) in their model tests. The model tests were conducted on a footing resting on a semi - infinite soil mass. Strip footing was of 2.44 in (6.197 cm) wide and 12.44 in (31.149 cm) long. The hyperbolic parameters and the properties of soil used in their investigation are listed in Table 6.3.

**Table 6.3 Input data for soil medium (Duncan & Chang, 1970)**

| Parameters | $\phi$ (degrees) | C (kPa) | K | n | $R_f$ | $\gamma$ (kN/m$^3$) | $\mu$ |
|---|---|---|---|---|---|---|---|
| **Values** | 35.5 | 0 | 300 | 0.55 | 0.83 | 17.49 | 0.35 |

The same parameters were used for conducting the analysis using FECAGREW. The finite element mesh fixed after mesh refinement studies and boundary conditions employed for the analysis is given in Fig. 6.3.

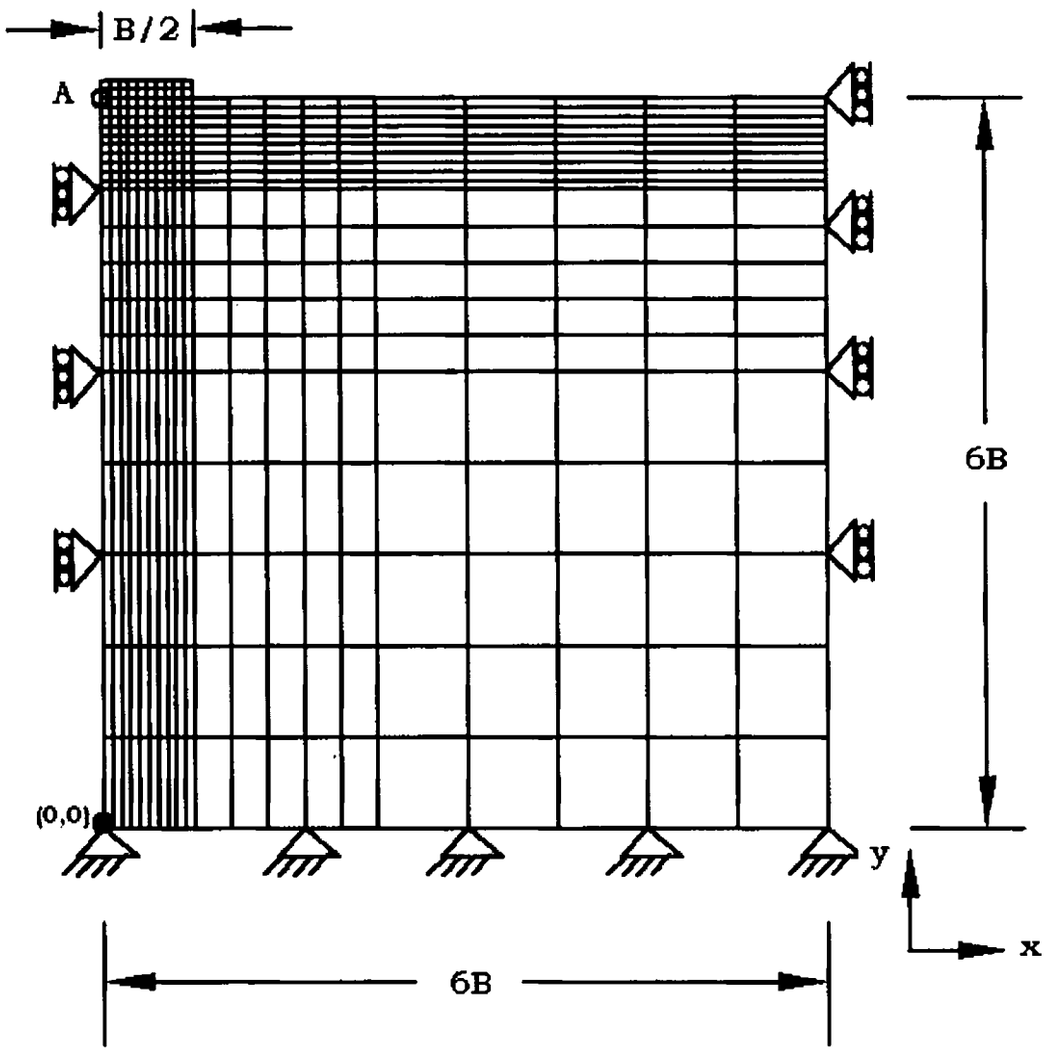


**Fig. 6.3 Discretisation of soil medium**

The mesh consisted of 463 nodes, 400 soil elements and 20 linear quadrilateral elements representing footing. The rigid footing was represented by two rows of quadrilateral elements with very high modulus and subjected to linear analysis only. Since the system under analysis is symmetrical about the centre line only one half portion (right hand side) was considered for the analysis. The vertical displacements at point A (Fig. 6.3) were noted for

different load increments until the system failed. Loads were applied as equivalent concentrated loads at the topmost eleven nodes of the system in increments of 2.5 psi (17.5 kPa) upto 25 psi (175 kPa) to generate an accurate comparison with the result of the model test. The FEM results of FECAGREW were plotted along with the experimental results of Duncan and Chang (1970) for validation purposes and both show very close behaviour (Fig. 6.4). It can be observed from the results that FECAGREW depicts the non linear behaviour of soil with sufficient accuracy.

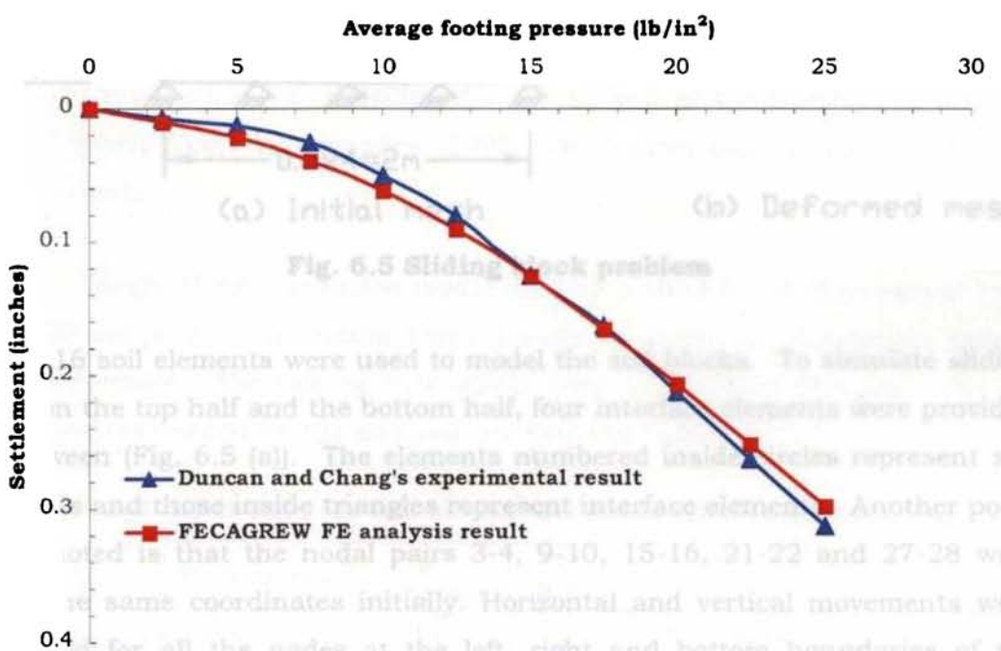


**Fig. 6.4 Validation of non linear analysis of soil medium**

## 6.5 MODELLING OF INTERFACE BEHAVIOUR

The four noded zero thickness line interface element proposed by Goodman et al. (1968) was incorporated in FECAGREW to model the soil – reinforcement interaction and the relative slip between each other. The same element was used to model the interaction between soil and gabion facing also. The problem of sliding blocks (Raghavendra, 1996) which resembles the direct shear test was used to check the sliding behaviour exhibited by these interface elements.

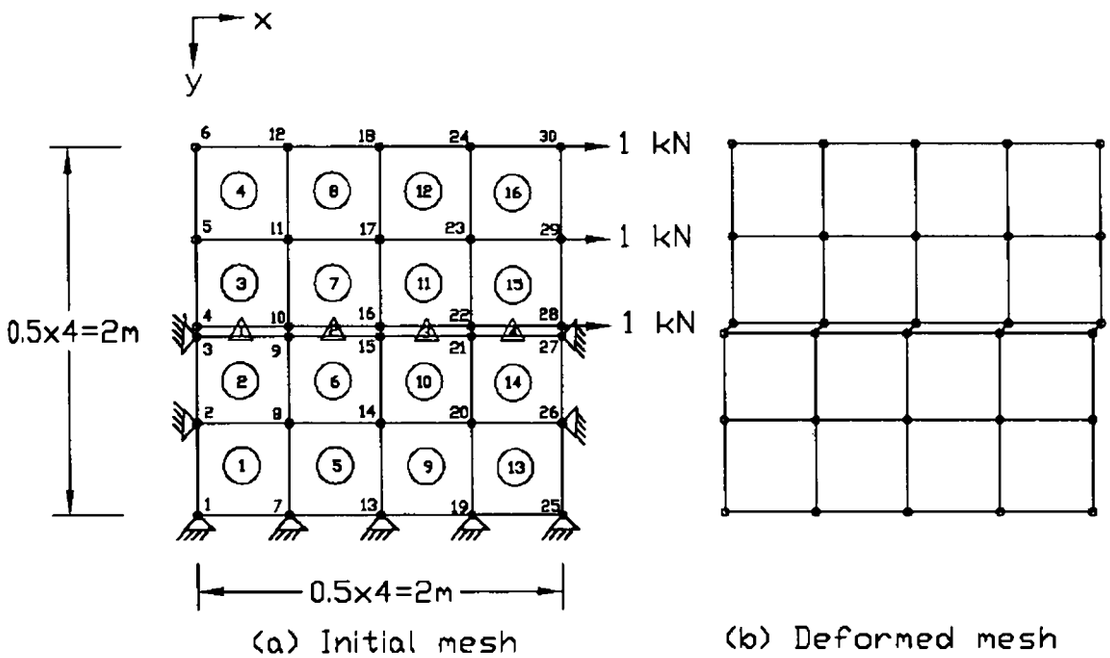


**Fig. 6.5 Sliding block problem**

16 soil elements were used to model the soil blocks. To simulate sliding between the top half and the bottom half, four interface elements were provided in between (Fig. 6.5 (a)). The elements numbered inside circles represent soil elements and those inside triangles represent interface elements. Another point to be noted is that the nodal pairs 3-4, 9-10, 15-16, 21-22 and 27-28 were given the same coordinates initially. Horizontal and vertical movements were restricted for all the nodes at the left, right and bottom boundaries of the bottom half of the system. The movements of all the other nodes were kept free. Unit load was applied to the right nodes of the top half of the system to simulate pulling effect in the horizontal direction. Soil elements and interface elements were given the same parameters listed out in Table 6.4. The interface properties $k_s$ and $k_n$ were given the values 1 x $10^5$ kPa and 2 x $10^8$ kPa respectively.

After FE analysis, it was seen that nodes 4, 10, 16, 22 and 28 exhibited positive non zero u values while the corresponding nodes 3, 9, 15, 21 and 27 of the nodal pairs listed above showed zero u values. This indicates that definitely

sliding occurred between the top and bottom half of the soil elements, which is possible only due to the presence of the interface elements. This proves the effectiveness of the action of the interface elements. From this, it may be concluded that the zero thickness line interface element in FECAGREW is functioning in a proper way.

## 6.6 MODELLING OF REINFORCED SOIL BEHAVIOUR

Next step in the validation studies is checking the effectiveness of soil - reinforcement interface friction. For this, the model study conducted on footing resting on reinforced soil by Singh (1988) was used. The hyperbolic parameters needed for modelling the soil as well as the interface in this study were taken from Raghavendra (1996) who numerically simulated the above model tests.

Singh (1988) conducted model tests on a sand bed of dimensions 390 cm x 390 cm x 210 cm, using three horizontal layers of aluminium strips as reinforcement. The footing dimensions were 15.24 cm x 91.4 cm. The input parameters needed for the analysis are listed in Table 6.4.

**Table 6.4 Input data for reinforced soil foundation (Raghavendra, 1996)**

| | | | | | | | | | |
|---|---|---|---|---|---|---|---|---|---|
| **Soil** | Parameters | $\phi$ (degrees) | C (kPa) | K | n | $R_f$ | $K_{mu}$ | m | $\gamma$ (g/cc) |
| | Values | 42 | 0 | 540 | 0.35 | 0.67 | 489 | 0.1 | 1.73 |
| **Aluminium strips** | Parameters | E ($kg/cm^2$) | A ($cm^2$) | | | | | | |
| | Values | $1.5 \times 10^6$ | 0.054 | | | | | | |
| **Interface** | Parameters | $\delta$ (degrees) | $K^I$ | $n^I$ | $R_f^I$ | | | | |
| | Values | 38 | 124 | 0.54 | 0.56 | | | | |

The finite element mesh fixed after mesh refinement studies and boundary conditions employed for the analysis is given in Fig. 6.6. Vertical spacing of reinforcements = 3.81 cm, number of layers of reinforcement = 3 and the length of reinforcements = 45.72cm.

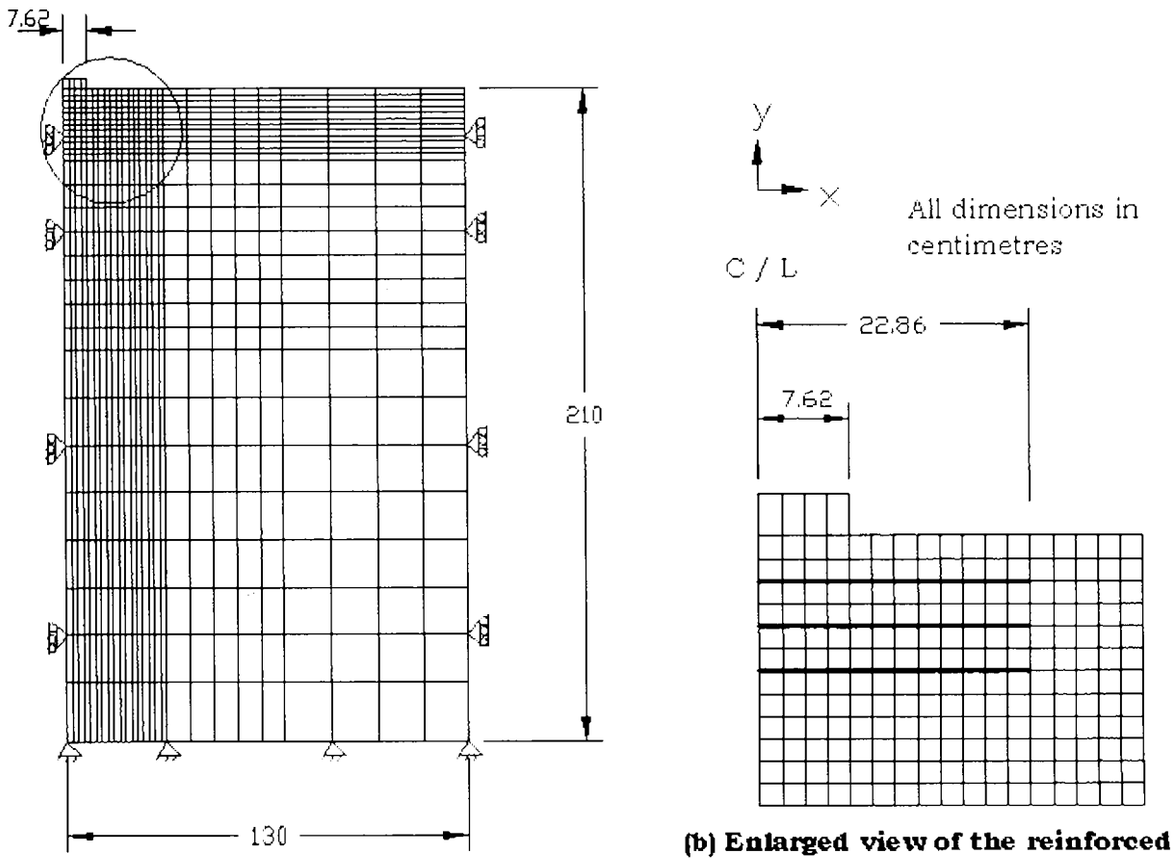


**(a) Discretisation of soil inside tank**

**(b) Enlarged view of the reinforced (circled) portion**

**Fig. 6.6 Discretisation of reinforced soil medium**

The mesh consisted of 899 nodes, 840 soil elements, 4 linear quadrilateral elements representing footing, 36 truss elements and 72 interface elements. The rigid footing is represented by one row of quadrilateral elements with very high modulus and subjected to linear analysis only. Since the system under analysis is symmetrical about the centre line, only one half portion (right hand side) is considered for the analysis. The vertical displacements below the centre of the footing were noted for different load increments until the system failed. Load was applied as a single concentrated load at the top left node of the system in increments of 600 kg (6 kN) till failure. The FEM results of FECAGREW were plotted along with the experimental results of Singh (1988) for validation purposes and both show very close behaviour (Fig. 6.7). This means that modelling of the behaviour of reinforcement as well as the

soil – reinforcement interaction using FECAGREW has been made quite precisely.

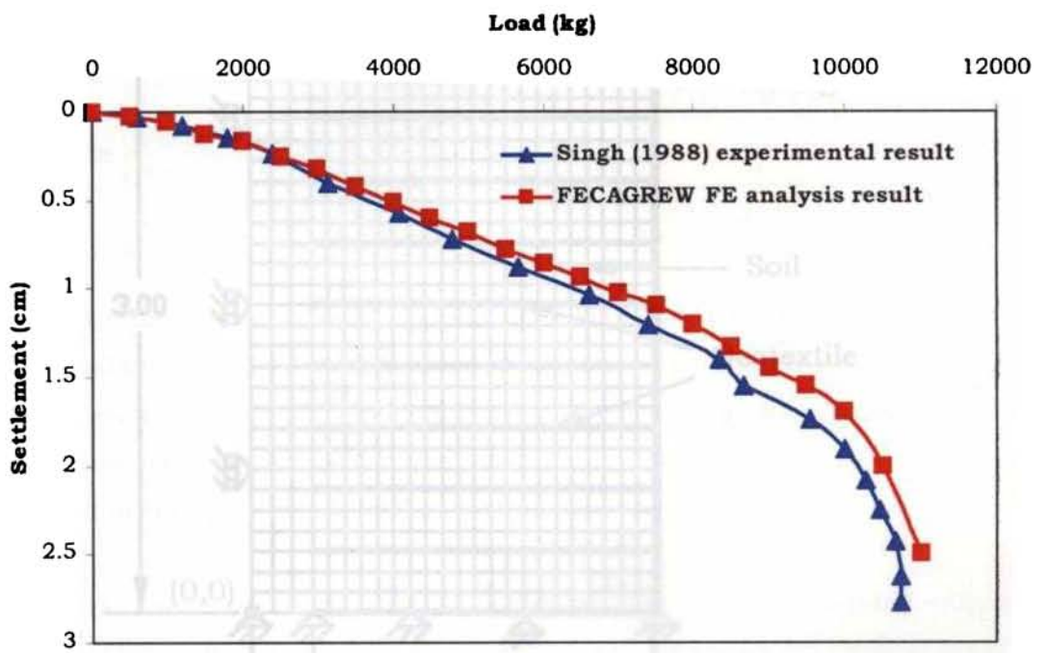


**Fig. 6.7 Validation of reinforced soil behaviour**

## 6.7 MODELLING OF REINFORCED SOIL WALL

The effectiveness of FECAGREW in simulating the non linear behaviour of reinforced soil has been proved in the previous sections. The next step is to check its applicability in the prediction of behaviour of retaining walls which is the major aim of the present work. For this, the modelling of the construction phases described in Section 4.6, should be accurate. To validate this aspect, the FEM results from Helwany et al. (1999) was chosen.

Helwany et al. (1999) used a modified version of DACSAR (Deformation Analysis Considering Stress Anisotropy and Reorientation) to predict the behaviour of geosynthetic reinforced soil retaining walls. The accuracy of this finite element program was verified by comparing the analytical results with the measured results of a 3m high and 1.2m wide test wall. The same results are used here for the validation of the behaviour of reinforced soil walls. The discretisation used for the study is shown in Fig. 6.8.

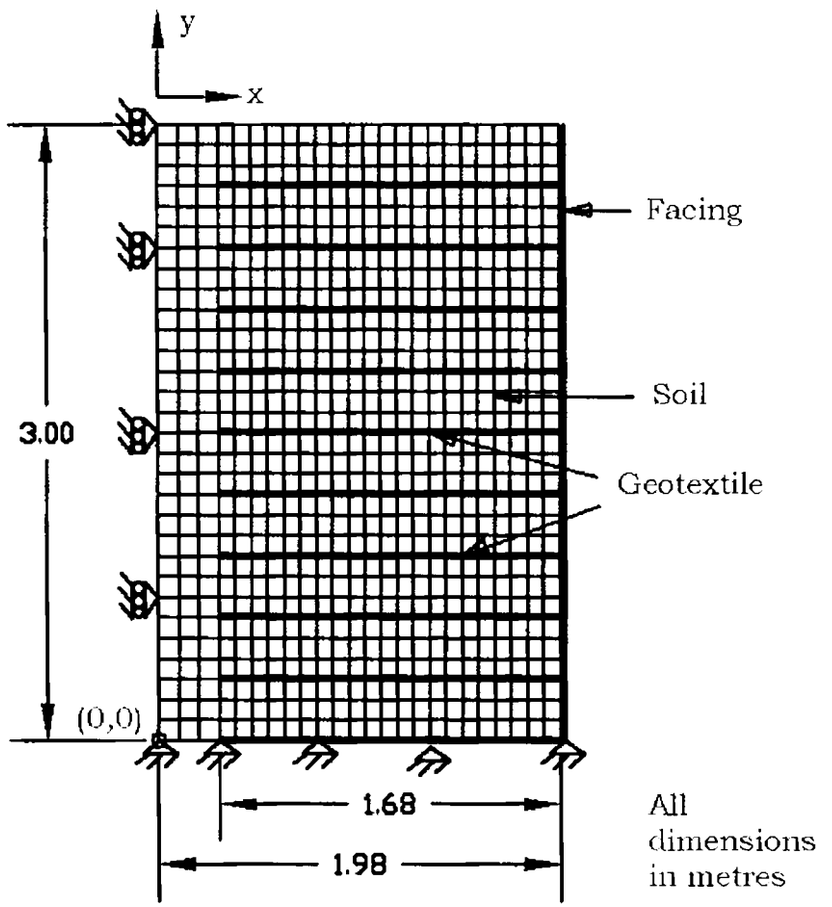


**Fig. 6.8 Discretisation used for validation of reinforced soil wall**

The timber facing was represented by beam elements (incorporated in FECAGREW for the sole purpose of modelling this reinforced soil wall for validation), geotextile reinforcement by truss elements and the soil by plane strain four noded isoparametric quadrilateral elements. The discretised mesh consisted of 775 nodes, 720 soil elements, 210 truss elements and 30 beam elements as given by Helwany et al. (1999). Interface elements were not used as they were not used for modelling in the literature and the purpose of the present study is to reproduce the results obtained by Helwany et al. (1999) using FECAGREW. The construction sequence was simulated by ten construction lifts. The boundary conditions adopted were: all the bottom nodes were completely fixed, top right node was fixed (in order to simulate the field test where fixity was provided at the top) and horizontal motion of all the left

extreme nodes was restricted. The parameters used for modelling the reinforced soil wall are listed out in Table 6.5.

**Table 6.5 Input data for reinforced soil wall**

| | | | | | | | | |
|---|---|---|---|---|---|---|---|---|
| **Soil** | Parameters | $\phi$ (degrees) | C (kPa) | K | n | $R_f$ | $K_{mu}$ | m |
| | Values | 38.4 | 0 | 1116 | 0.66 | 0.87 | 907 | 0 |
| **Geotextile** | Parameters | E (kPa) | A ($m^2$) | | | | | |
| | Values | $5.4 \times 10^3$ | 0.0025 | | | | | |
| **Timber facing** | Parameters | E (kPa) | A ($m^2$) | I ($m^4$) | | | | |
| | Values | $1.4 \times 10^5$ | 0.0025 | $4 \times 10^{-7}$ | | | | |

Surcharge was given as equivalent concentrated loads at the top nodes after simulating all the ten construction phases. The responses of the wall at 105 kPa were considered for comparison purposes. Fig. 6.9 shows the facing deformation of the reinforced soil wall while Fig. 6.10 shows the strains developed in the geotextile at different elevations.

The results obtained from FECAGREW show close agreement with the results of Helwany et al. (1999). From this, it can be stated that FECAGREW is fairly effective in simulating the behaviour of reinforced soil walls and the modelling of the construction phases is accurate.

## 6.8 MODELLING OF GABION FACED REINFORCED SOIL WALL

After successful verification of each component of FECAGREW, it is attempted in this section to compare the load displacement behaviour of a gabion faced retaining wall with the results from actual laboratory experiments. The final step in the development of the FE code was the incorporation of a composite model to represent the behaviour of gabion facing which is detailed in Section 4.5.

Experimental results on such type of walls are very much limited in number in literature as evident from Chapter 2. Hence for validation purposes, test results obtained from the experimental programmes detailed in Section 5.2.2 were used. For modelling purposes, laboratory determination of the hyperbolic constants of soil (as described in Section 4.3.2.1) and interface

(as given in Section 4.4.3.1) as well as the elastic properties of the fill materials were carried out as follows:

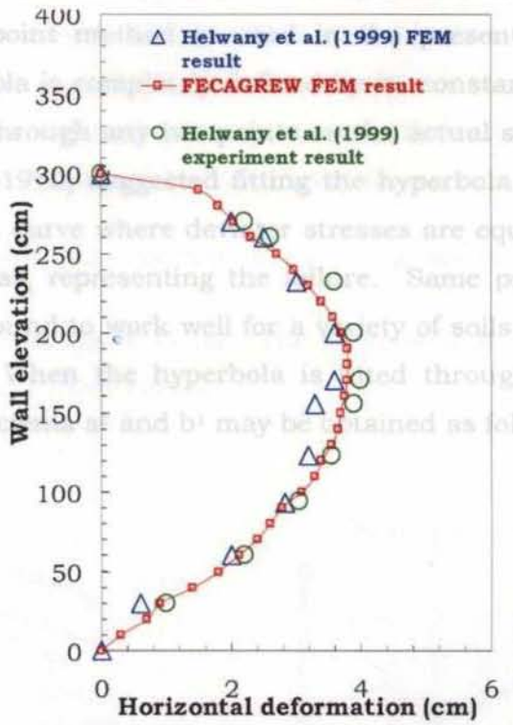


**Fig. 6.9 Validation of reinforced soil wall – Facing deformation**

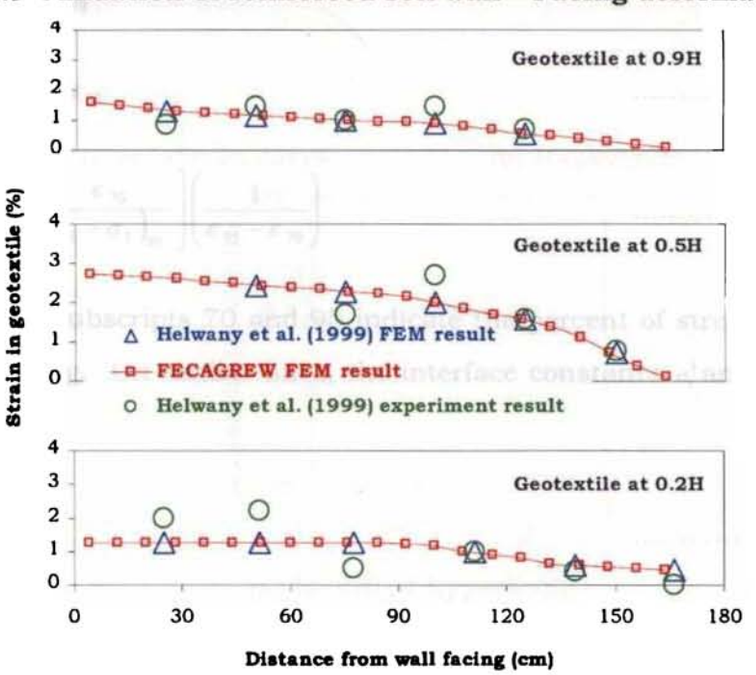


**Fig. 6.10 Validation of reinforced soil wall – Strain in geotextile**

Several methods exist for the evaluation of Kondner's constants $a^1$ and $b^1$ in the hyperbolic formulation of non linear behaviour of soils. Transformed stress – strain curve method (Section 4.3.2.1) is one of them and another method called two point method is used in the present study, due to its simplicity. A hyperbola is completely defined by its constants $a^1$ and $b^1$, if it is constrained to pass through any two points on the actual stress – strain curve. Duncan and Chang (1970) suggested fitting the hyperbola through two points on the stress – strain curve where deviator stresses are equal to 70% and 95% of peak deviator stress, representing the failure. Same procedure is adopted here as it has been found to work well for a variety of soils as cited by Duncan and Chang (1970). When the hyperbola is fitted through 70% and 95% of stress level, the coefficients $a^1$ and $b^1$ may be obtained as follows:

$$\sigma_1 - \sigma_3 = \frac{\varepsilon}{a^1 + b^1 \varepsilon} \qquad \text{..... (6.1)}$$

$$(\sigma_1 - \sigma_3)_{95} = \frac{\varepsilon_{95}}{a^1 + b^1 \varepsilon_{95}} \qquad \text{..... (6.2)}$$

$$(\sigma_1 - \sigma_3)_{70} = \frac{\varepsilon_{70}}{a^1 + b^1 \varepsilon_{70}} \qquad \text{..... (6.3)}$$

$$a^1 = \frac{\varepsilon_{95}}{(\sigma_1 - \sigma_3)_{95}} - b^1 \varepsilon_{95} \qquad \text{..... (6.4)}$$

$$b^1 = \left[ \frac{\varepsilon_{95}}{(\sigma_1 - \sigma_3)_{95}} - \frac{\varepsilon_{70}}{(\sigma_1 - \sigma_3)_{70}} \right] \left( \frac{1}{\varepsilon_{95} - \varepsilon_{70}} \right) \qquad \text{..... (6.5)}$$

in which, subscripts 70 and 95 indicate the percent of stress level used in the curve fitting. On similar lines, the interface constants $a_i^1$ and $b_i^1$ can also be obtained as:

$$a_i^1 = \frac{\Delta_{95}}{\tau_{95}} - b_i^1 \Delta_{95} \qquad \text{..... (6.6)}$$

$$b_i^1 = \left[ \frac{\Delta_{95}}{\tau_{95}} - \frac{\Delta_{70}}{\tau_{70}} \right] \left( \frac{1}{\Delta_{95} - \Delta_{70}} \right) \qquad \text{..... (6.7)}$$

### 6.8.1 Hyperbolic constants for soil

Consolidated drained triaxial tests were conducted on sand specimens prepared at the same density as that of the model tests and the stress – strain curves are shown in Fig. 6.11 (a). Kondner's constants $a^1$ and $b^1$ were calculated using Eqns. 6.4 and 6.5 respectively. The initial modulus, $E_i = 1/a$ and the failure ratio, $R_f$, were also calculated for each curve in Fig. 6.11 (a). Then, $\left(\frac{E_i}{P_{atm}}\right)$ vs. $\left(\frac{\sigma_3}{P_{atm}}\right)$ was plotted to log – log scales and K and n were determined as shown in Fig. 6.11 (b). The value of $R_f$ is taken as the average value obtained from the three curves.

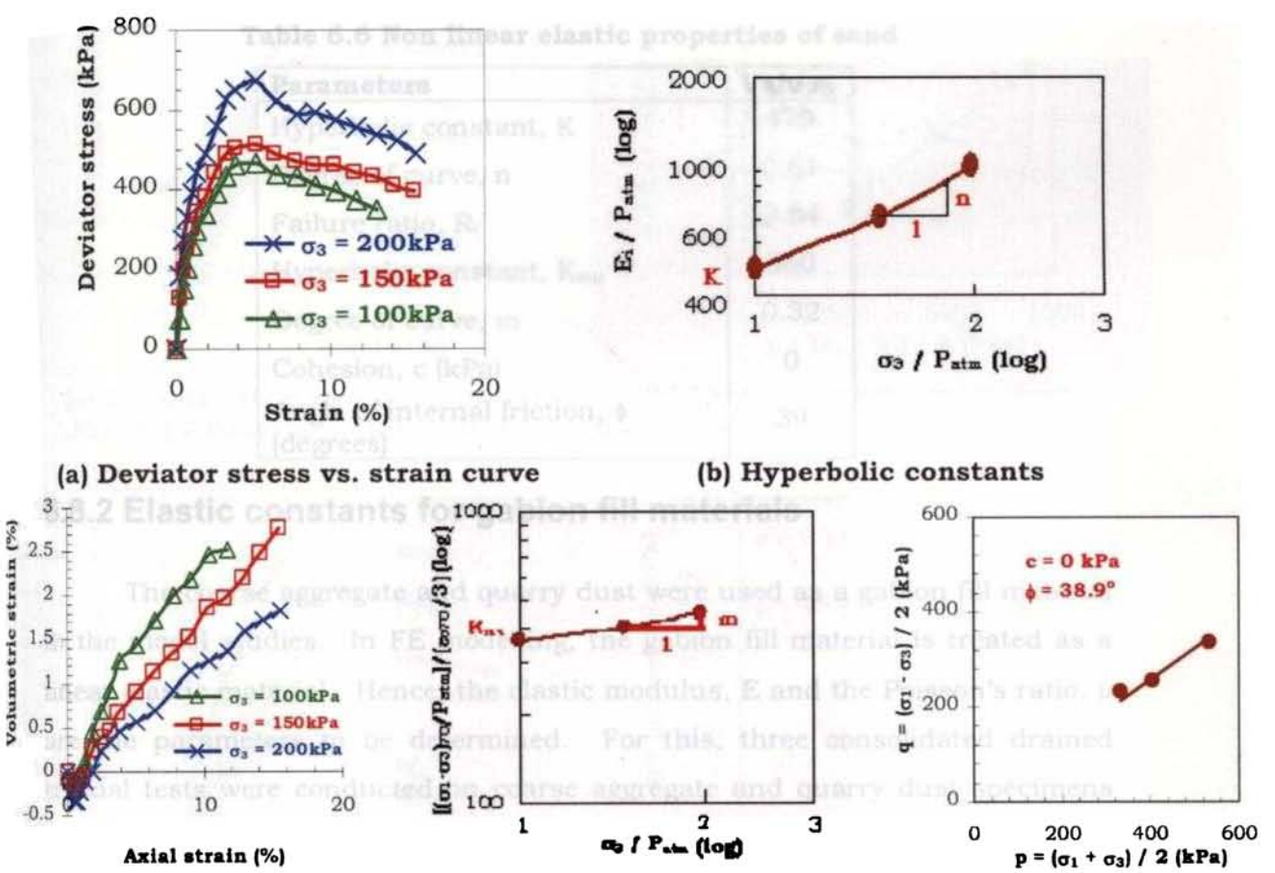


(a) Deviator stress vs. strain curve (b) Hyperbolic constants

(c) Volumetric strain vs. axial strain curve (d) Modified hyperbolic constants (e) Shear strength parameters

**Fig. 6.11 Determination of non linear elastic properties for sand**

In a similar manner, the modified hyperbolic constants $K_{mu}$ and m, for the determination of Poisson's ratio, $\mu$ may be obtained. For this, the volumetric strain vs. axial strain curves for the same triaxial tests are plotted as shown in Fig. 6.11 (c). The deviator stress $(\sigma_1 - \sigma_3)_{70}$ and volumetric strain $(\varepsilon_{v70})$ at 70% stress level were calculated for each curve in Fig. 6.11 (c). Then, $\left(\frac{(\sigma_1 - \sigma_3)_{70}}{\varepsilon_{v70}} \frac{P_{atm}}{3}\right)$ vs. $\left(\frac{\sigma_3}{P_{atm}}\right)$ was plotted to log – log scales and $K_{mu}$ and m were determined as shown in Fig. 6.11 (d). The triaxial tests results were then plotted as p vs. q curve (Fig. 6.11 (e)) to calculate the shear strength parameters c and $\phi$. The values obtained are listed in Table 6.6.

**Table 6.6 Non linear elastic properties of sand**

| Parameters | Values |
|---|---|
| Hyperbolic constant, K | 479 |
| Degree of curve, n | 0.61 |
| Failure ratio, $R_f$ | 0.84 |
| Hyperbolic constant, $K_{mu}$ | 360 |
| Degree of curve, m | 0.32 |
| Cohesion, c (kPa) | 0 |
| Angle of internal friction, $\phi$ (degrees) | 39 |

## 6.8.2 Elastic constants for gabion fill materials

The coarse aggregate and quarry dust were used as a gabion fill material in the model studies. In FE modelling, the gabion fill material is treated as a linear elastic material. Hence, the elastic modulus, E and the Poisson's ratio, $\mu$ are the parameters to be determined. For this, three consolidated drained triaxial tests were conducted on coarse aggregate and quarry dust specimens prepared at the same density as that of the model tests. In the case of coarse aggregate, the tests were conducted on large sized (20 cm dia.) specimens as the average size of the coarse aggregates was 20mm while for the quarry dust the same dimension (7.5 cm dia.) used for testing sand was used. The

stress – strain curves for the coarse aggregate are shown in Fig. 6.12 (a) and that for quarry dust in Fig. 6.13 (a). Kondner's constant $a^1$ was calculated for each curve using Eqn. 6.4 and the initial elastic modulus was taken as $E_i = 1/a^1$. The value of E is taken as the average value of $E_i$ obtained from the three curves. Poisson's ratio was determined from Eqns. 4.17 and 4.18 after obtaining the $\phi$ value from the p vs. q curve (Figs. 6.12 (b) and 6.13 (b)) drawn using the triaxial test results. The properties of coarse aggregate and quarry dust used for validation are tabulated in Table 6.7. The induced cohesion on the fill materials was calculated using Eqns. 4.55 and 4.56.

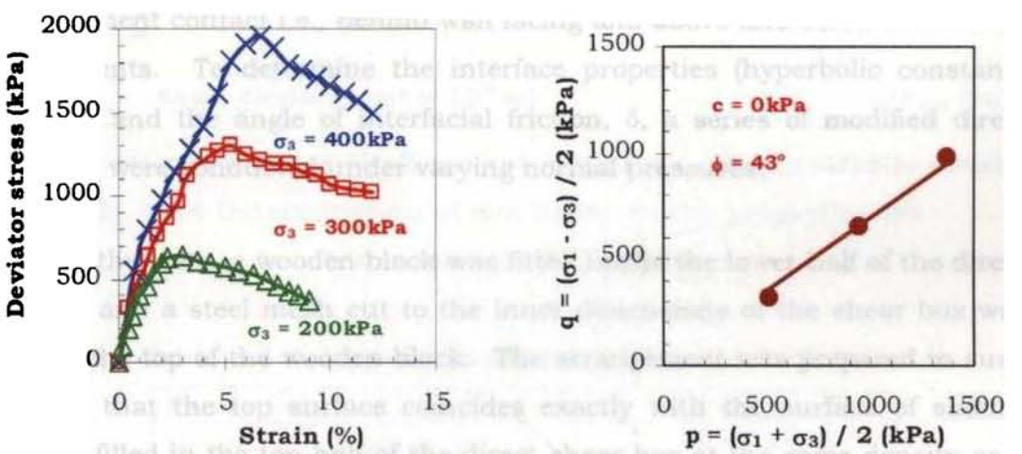


**(a) Deviator stress vs. strain curve** **(b) Shear strength parameters**

**Fig. 6.12 Determination of linear elastic properties for coarse aggregate**

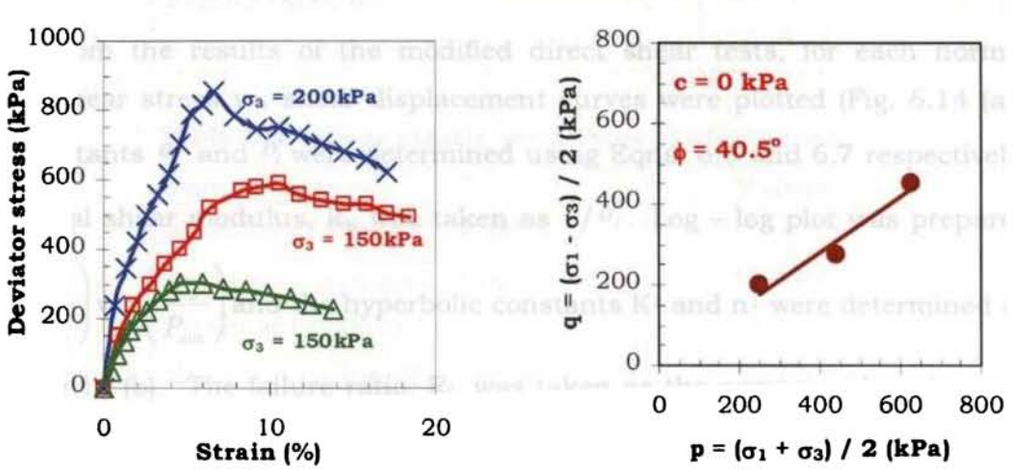


**(a) Deviator stress vs. strain curve** **(b) Shear strength parameters**

**Fig. 6.13 Determination of linear elastic properties for quarry dust**

**Table 6.7 Elastic properties of coarse aggregate and quarry dust**

| Parameters | Coarse aggregate | Quarry dust |
|---|---|---|
| Modulus of elasticity, E (kPa) | 100233 | 32107 |
| Poisson's ratio, $\mu$ | 0.22 | 0.27 |
| Angle of internal friction, $\phi$ (degrees) | 43 | 40.5 |
| Cohesion, C (kPa) | 0 | 0 |
| Induced cohesion (kPa) | 5.72 | 5.4 |

### 6.8.3 Hyperbolic constants for interface

Interface elements were used for modelling regions wherever there is soil - reinforcement contact i.e., behind wall facing and above and below steel mesh reinforcements. To determine the interface properties (hyperbolic constants $K^1$ and $n^1$) and the angle of interfacial friction, $\delta$, a series of modified direct shear tests were conducted under varying normal pressures.

For the tests, a wooden block was fitted inside the lower half of the direct shear box and a steel mesh cut to the inner dimensions of the shear box was pasted at the top of the wooden block. The arrangement was prepared in such a manner that the top surface coincides exactly with the surface of sliding. Sand was filled in the top half of the direct shear box at the same density as it is filled in the model tests.

From the results of the modified direct shear tests, for each normal stress, shear stress vs. shear displacement curves were plotted (Fig. 6.14 (a)). The constants $a_i^1$ and $b_i^1$ were determined using Eqns. 6.6 and 6.7 respectively. The initial shear modulus, $k_{si}$ was taken as $1/a_i^1$. Log – log plot was prepared with $\left(\frac{k_{si}}{\gamma_n}\right)$ vs. $\left(\frac{\sigma_n}{P_{atm}}\right)$ and the hyperbolic constants $K^1$ and $n^1$ were determined as in Fig. 6.14 (b). The failure ratio, $R_f$, was taken as the average value obtained from the four curves. The angle of interfacial friction was obtained using the peak values of shear stresses. The modulus of elasticity of the steel mesh was obtained by conducting tension test using universal testing machine for

geotextile testing (AIMIL Ltd). The properties of the interface and the steel mesh are listed in Tables 6.8 and 6.9 respectively.

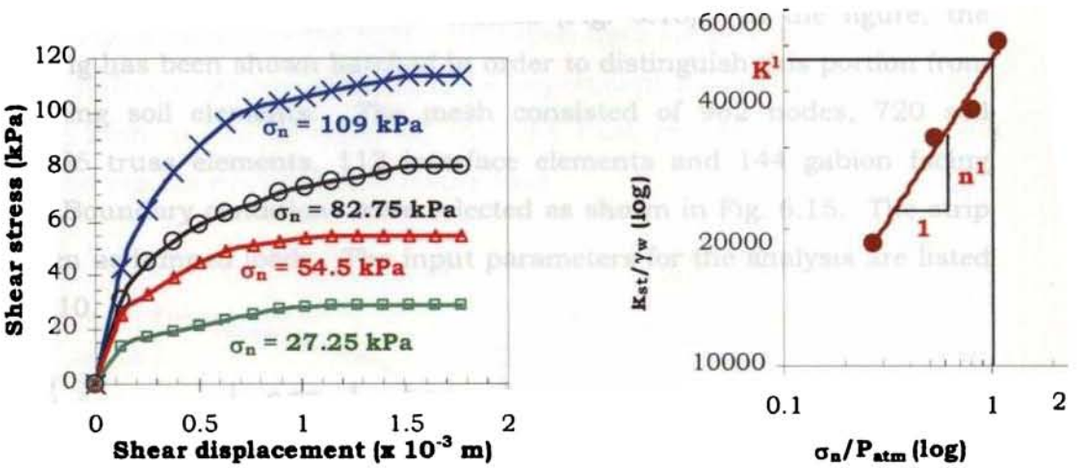


**(a) Shear stress vs. shear displacement curves** **(b) Hyperbolic constants**

**Fig. 6.14 Determination of non linear elastic properties for steel mesh – sand interface**

**Table 6.8 Non linear elastic properties of interface**

| Parameters | Values |
|---|---|
| Hyperbolic constant, $K^1$ | 46338 |
| Degree of curve, $n^1$ | 0.697 |
| Failure ratio, $R_f^1$ | 0.887 |
| Angle of interfacial friction, δ (degrees) | 32.6 |

**Table 6.9 Linear elastic properties of steel mesh**

| Parameters | Values |
|---|---|
| Modulus of elasticity, E (kPa) | $3.33 \times 10^6$ |
| Cross sectional area, A ($m^2$) | 0.0022 |
| Strain at breaking load | 3.2 % |
| Secant modulus, $M_g$ (kN/m) | 22.4 |

### 6.8.4 Finite element modelling

After the determination of the essential properties for FE modelling, mesh was prepared after mesh refinement studies (Fig. 6.15). In the figure, the gabion facing has been shown hatched in order to distinguish this portion from the remaining soil elements. The mesh consisted of 962 nodes, 720 soil elements, 56 truss elements, 112 interface elements and 144 gabion facing elements. Boundary conditions were selected as shown in Fig. 6.15. The strip load is given as lumped loads. The input parameters for the analysis are listed in Table 6.10.

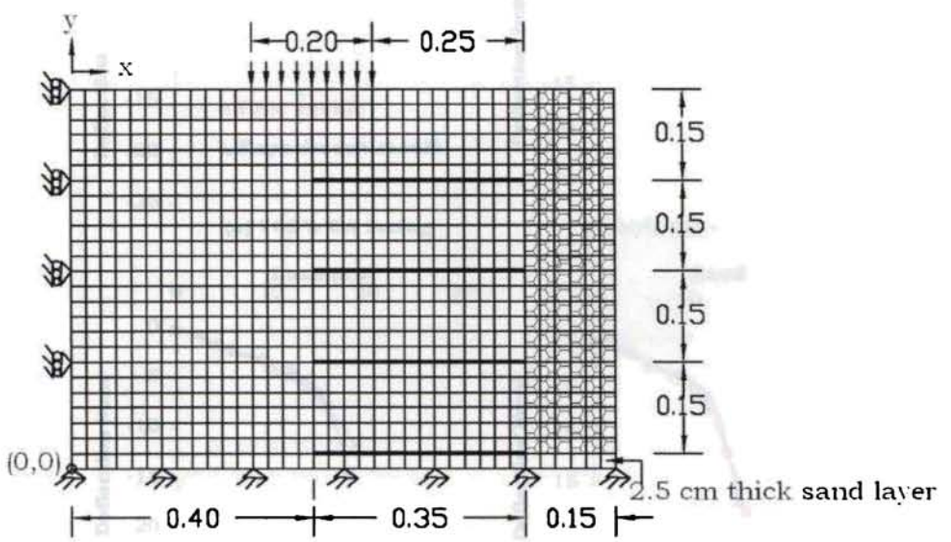


All dimensions in metres

**Fig. 6.15 Discretisation of gabion faced reinforced earth wall**

**Table 6.10 Input data for gabion faced reinforced soil wall**

| | | | | | | | | |
|---|---|---|---|---|---|---|---|---|
| **Soil** | $\phi$ (degrees) | c (kPa) | K | n | $R_f$ | $K_{mu}$ | m | $\gamma$ (kN/m$^3$) |
| | 39 | 0 | 479 | 0.61 | 0.84 | 360 | 0.32 | 16 |
| **Steel mesh** | E (kPa) | A (m$^2$) | | | | | | |
| | 3.33 x 10$^6$ | 0.0022 | | | | | | |
| **Coarse aggregate** | $\phi$ (degrees) | $c_g$ (kPa) | E (kPa) | $\mu$ | | | | |
| | 43 | 5.72 | 100233 | 0.22 | | | | |
| **Quarry dust** | $\phi$ (degrees) | $c_g$ (kPa) | E (kPa) | $\mu$ | | | | |
| | 40.5 | 5.4 | 32107 | 0.27 | | | | |
| **Interface** | $\delta$ (degrees) | $c_a$ (kPa) | $K^1$ | $n^1$ | $R_f$ | | | |
| | 32.6 | 0 | 46338 | 0.697 | 0.887 | | | |

The horizontal deflections of the top point of the facing were noted for different load increments until the system failed. The FEM results of FECAGREW were plotted along with the experimental results for validation purposes. Fig. 6.16 shows the load – deflection data for gabion reinforced soil walls with different facings obtained from experiment as well as FE analysis. Comparing both, it can be observed that the FEM results closely follow the experimental results even upto the failure load.

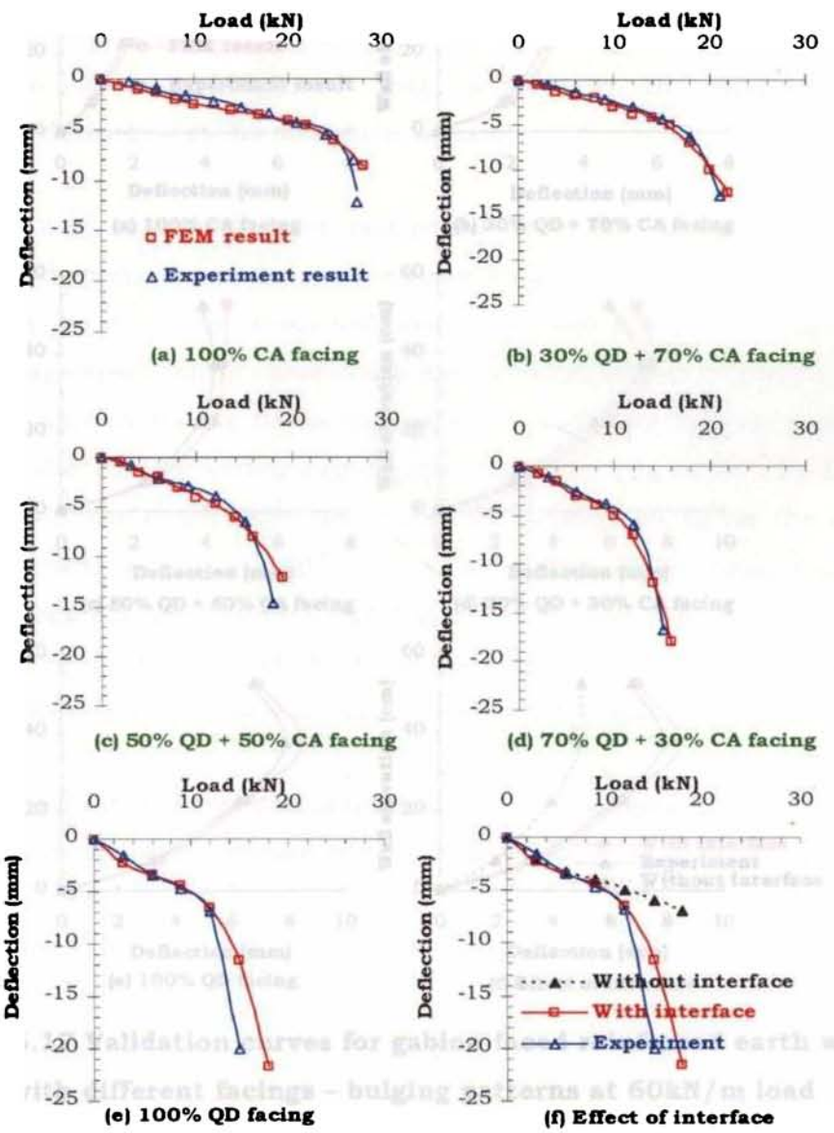


**Fig. 6.16 Validation curves for gabion faced reinforced earth wall with different facings – load deflection curves**

Fig. 6.17 shows the deflections of the front facing of the walls for the different cases studied, obtained from both the experiment and finite element analysis. In the cases, both the curves show a very close comparison in behaviour.

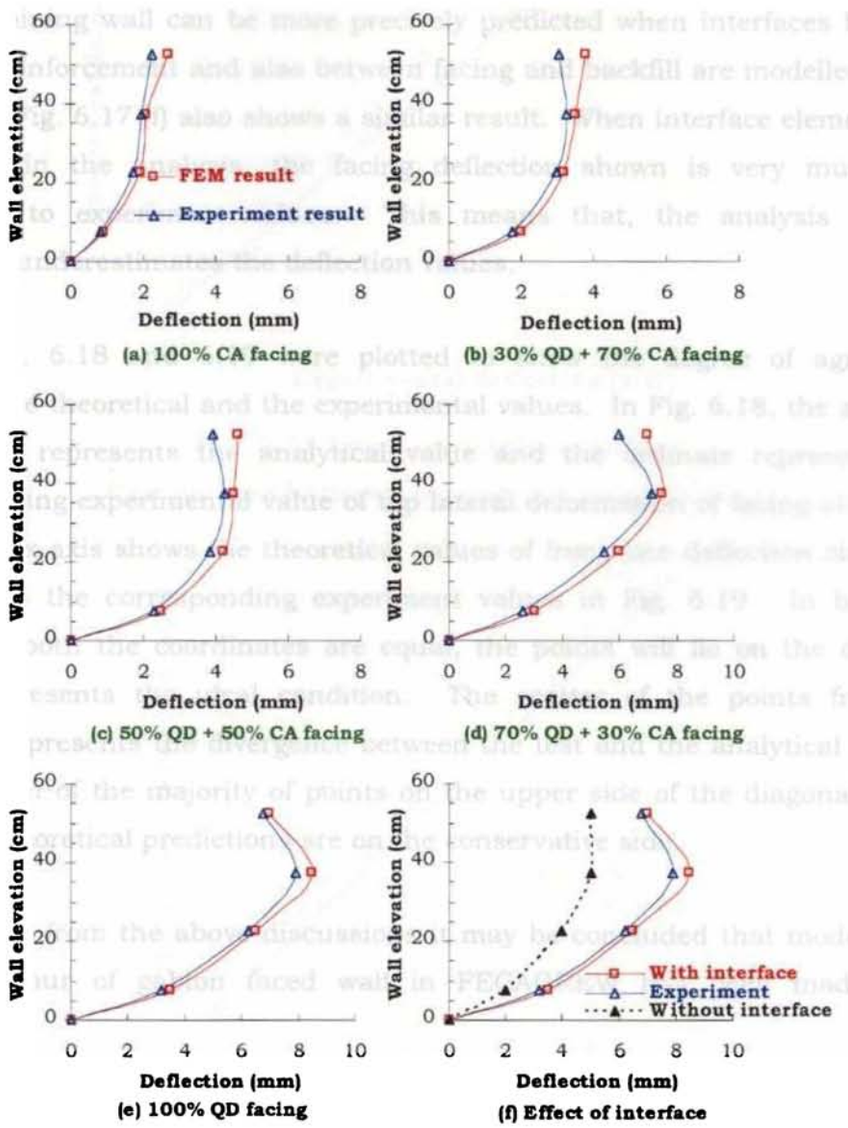


**Fig. 6.17 Validation curves for gabion faced reinforced earth wall with different facings – bulging patterns at 60kN/m load**

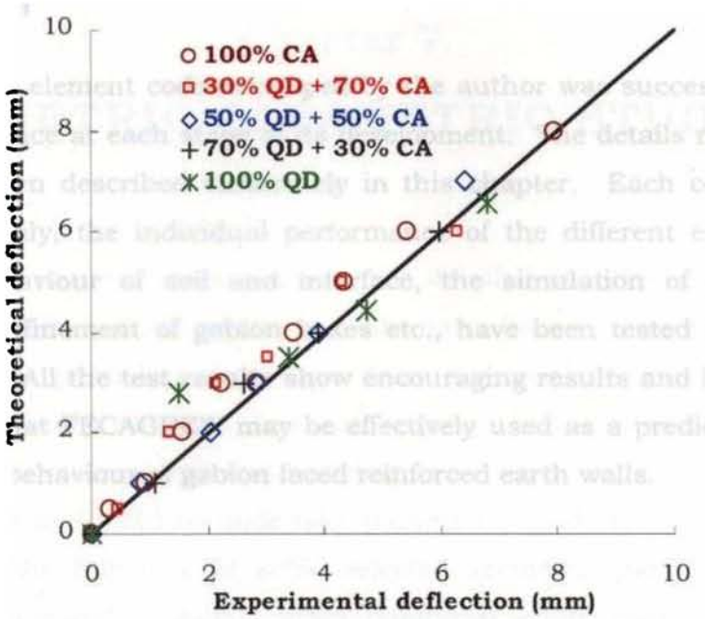


**Fig. 6.18 Load – deflection data:**

**Comparison between theory and experiment**

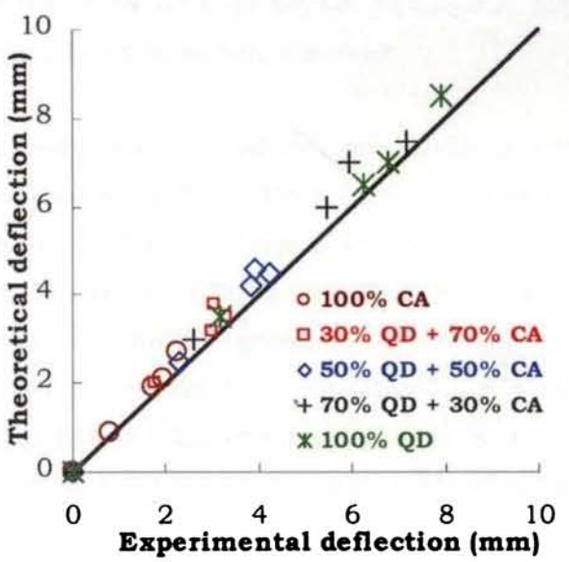


**Fig. 6.19 Facing deflection data:**

**Comparison between theory and experiment**

## 6.9 SUMMARY

The finite element code developed by the author was successfully tested for its performance at each stage of its development. The details regarding the testing have been described elaborately in this chapter. Each component of modelling, namely, the individual performance of the different elements, the non linear behaviour of soil and interface, the simulation of construction phases, the confinement of gabion boxes etc., have been tested step by step systematically. All the test results show encouraging results and hence it may be concluded that FECAGREW may be effectively used as a prediction tool for simulating the behaviour of gabion faced reinforced earth walls.

# Chapter 7

# GEOMETRIC PARAMETRIC STUDIES

## 7.1 GENERAL

The finite element formulation for the detailed analysis of gabion faced reinforced soil walls and the validation of the same based on experimental data as well as prior published data have been discussed in the previous two chapters. The results obtained were encouraging when a small scale model of the gabion faced retaining wall was analysed and compared with the experiment data. This fact motivated to undertake parametric studies, the aim of which was to study the influence of some selected geometric parameters on the deformation behaviour of gabion faced reinforced earth walls at the end of construction stage. Parameters chosen for the study were spacing of reinforcement, length of reinforcement, width of gabion facing and height of wall. For studying the effect of a particular parameter, the same alone was varied, keeping all the other parameters constant.

Conventional wall design procedures are primarily stress based and do not consider deformations separately. Reason for the same being, deformations are relatively insignificant for the typical conditions of wall geometry and loading for which the design procedures were developed. But in circumstances where walls with non - standard geometry or loading cannot be avoided, deformation criteria should be carefully considered. For example, the use of shortened reinforcement layers due to topographic or economic constraints will cause increased deformations which would otherwise become critical, if avoided. Walls with large external loading or sloping backfills, walls where performance criteria requires very small deformations etc., are some other examples where deformations have more or less equal importance to stresses (Chew and Schmertmann, 1990). Hence this work concentrates on deformation studies.

This chapter explains the analyses conducted on gabion faced reinforced soil walls of three different wall heights - 3m, 6m and 9m representing the low, medium and high walls respectively. FE studies were performed by varying the spacing as well as the length of reinforcement and the width of gabion facing. The effect of the position of strip loading on the behaviour of walls was also investigated.

## 7.2 SYSTEM ANALYSED

The system considered for the analyses is described in detail in this section. A gabion faced reinforced earth wall of height, H, is assumed to rest on a soft clay foundation. Most reinforced soil walls analysed to date are built on competent or stiff foundations (Bauer and Brau (1996), Ho and Rowe (1996), Ochiai and Fukuda (1996), Rowe and Ho (1997), Helwany et al. (1999) and so on). In this case, estimation of wall deformation does not need consideration of the external movements of reinforced soil mass, in addition to those resulting from the internal deformation. Consequently, this results in reduced outward lateral deformation at wall face with increasing reinforced soil system stiffness (Ogisako et al., 1988). Where as, a system resting on soft foundation is more liable to external movement due to the movement of foundation soil below and therefore is less stable. Hence, in this study, the gabion wall was assumed to rest on a soft clay foundation.

The reinforcement extending into the soil was assumed to be of same length through out the height of the wall and was taken as equal to H in the basic system chosen for the parametric study. The wall facing at the bottom was assumed to have an embedment of 0.15H into the soft clay. Spacing of reinforcement, h, was taken as 0.08H and width of wall facing as 0.15H, for the basic system, considering the general design practice.

After the convergence studies, the mesh chosen for the analysis consisted of 2290 nodes with two degrees of freedom (u and v) at each node. Horizontal translation was restricted for the nodes on the left and right end

boundaries and all the bottom nodes were completely restrained (Fig. 7.1). The extent of boundary of the system was fixed after studying its effect on the behaviour of the wall. It was found that the response of the wall became insensitive to the location of the boundaries when the front face boundary was located 2H (or more) from the wall face, the back face boundary at 4H (or more) from the wall face and the bottom boundary at H (or more) from the wall base.

The geometry of the model was kept the same for all the parametric studies and only the parameter to be studied was varied accordingly. The FE mesh was fixed such that the same mesh could be used for all the parametric studies performed. The deformation analysis due to self weight of the system was performed which is the most important static load on a retaining wall system. The results were analysed in terms of deformations and lateral pressures.

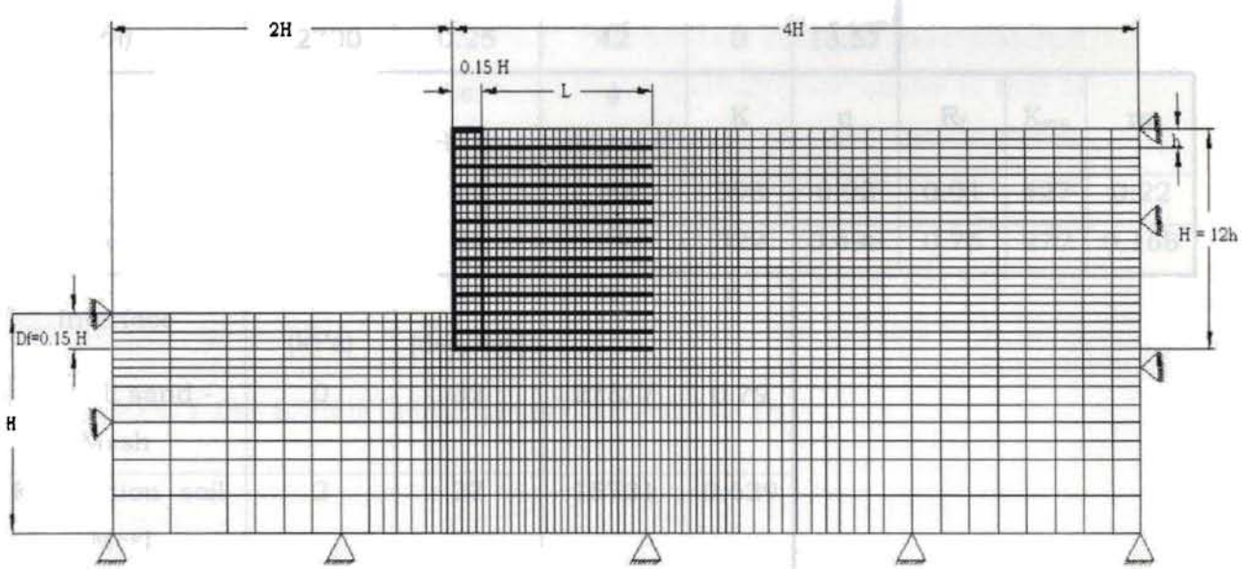


**Fig. 7.1 Finite element mesh used for the parametric studies**

The basal reinforcing mesh of the gabion boxes extending into the soil were modelled using 288 two noded truss elements with axial stiffness only, assuming linear stress strain relationship. The properties of the gabion mesh were determined in the laboratory by conducting tension tests on a sample

specimen of the gabion mesh obtained from Maccaferri Environmental Solutions, Pvt. Ltd., Mumbai, India. The properties are listed in Table 7.1. The gabion wall facing was modelled as a composite material assigning properties obtained from literature (Helwany et al., 1996). 96 four noded isoparametric quadratic elements with linear stress strain relation were used to model the same. Properties used for modelling are tabulated in Table 7.1. The cohesion induced by the gabion facing ($c_i$) was calculated using Eqns. 4.55 and 4.56.

**Table 7.1 Material properties adopted for parametric studies**

| Gabion mesh | E (kPa) | A ($m^2$) | $M_g$ (kN/m) | $\varepsilon_{max}$ (%) |
|---|---|---|---|---|
| | 2235000 | 0.004 | 53 | 10 |

| Gabion facing (after Helwany et al. (1996)) | E (kPa) | $\mu$ | $\phi$ (degrees) | c (kPa) | $c_i$ (kPa) |
|---|---|---|---|---|---|
| | 12700 | 0.25 | 42 | 0 | 13.57 |

| Soil | $\gamma$ ($kN/m^3$) | c (kPa) | $\phi$ (degrees) | K | n | $R_f$ | $K_{mu}$ | m |
|---|---|---|---|---|---|---|---|---|
| Backfill | 18 | 0 | 39 | 998 | 0.92 | 0.91 | 427 | 0.22 |
| Foundation soil | 11 | 5 | 34 | 322 | 0.498 | 0.75 | 272 | 0.168 |

| Interface | $c_a$ (kPa) | $\delta$ (degrees) | $K^1$ | $n^1$ |
|---|---|---|---|---|
| Backfill sand - Mesh | 0 | 32 | 27317 | 0.79 |
| Foundation soil - Mesh | 2 | 27 | 15731 | 0.629 |

The region of analysis included the foundation soil also along with the backfill because the gabion faced retaining walls are usually opted when the ground is soft. The soil material was modelled using 2066 four noded isoparametric quadrilateral elements. The non linear stress – strain behaviour of soil was simulated using Duncan and Chang (1970) hyperbolic model

following Mohr – Coulomb failure criterion. The backfill was assumed to be beach sand and the foundation was assumed to be clayey silt whose properties were determined and are listed in Table 7.1.

In reinforced soil structures, the main criterion adopted in the design is that the desirable failure mode is pullout failure rather than the breaking of reinforcement. This is because the failure due to rupture can reduce the shear strength of the structure to a very low value which may cause catastrophic effects to the structure (Jones, 1985). Hence the failure of reinforcement was not modelled here and it was assumed that the system does not fail by the rupture of reinforcement. The pullout failure of the reinforcement was modelled using four noded zero thickness interface elements at the top and bottom of the reinforcement. 564 interface elements were used in the study. The interface elements were also used behind the vertical face of the gabion wall in contact with the back fill (24 nos.), at the base and in the front face (foundation) in contact with the foundation soil (8 nos.). The interface elements were modelled such that the shear stiffness is governed by a hyperbolic rule similar to that of the soil model and related the interface shear stress and displacement. The properties of the interface elements were determined using large sized direct shear tests on the gabion mesh sample pasted on a wooden block fitted on the lower half of the shear box and the other half of the shear box was filled with the corresponding soil at the required density (as listed in Table 7.1).

## 7.3 EFFECT OF REINFORCEMENT SPACING (h)

It is a common practice in the construction of gabion faced walls to provide the reinforcement at uniform spacing. Considering the economic aspects, varied spacing can be more advantageous than uniform spacing. Hence an attempt is made here to study the influence of spacing of reinforcement on the behaviour of gabion faced reinforced soil walls and to arrive at an optimum value of spacing. For this, different configurations of reinforcement have been chosen as shown in Fig. 7.2. The configurations were fixed such that they are the stable configurations for a particular spacing.

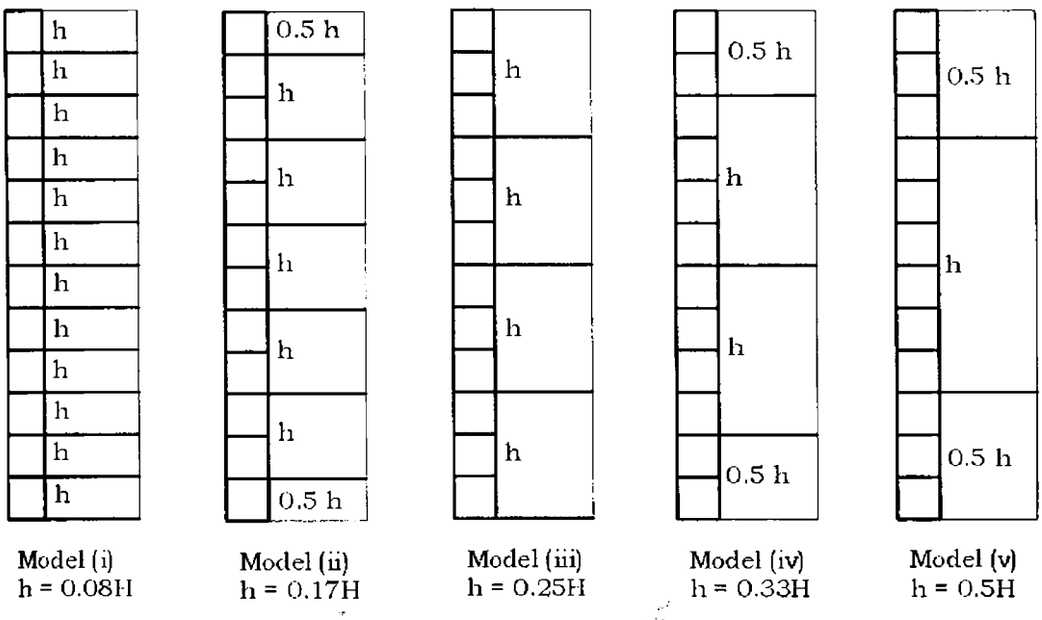


**Fig. 7.2 Reinforcement spacing configurations used in the study**

The horizontal deformations of the facing for all the configurations were noted and plotted as shown in Fig. 7.3. Figure shows the variation of lateral deformation of gabion wall facing for the different models discussed above for H = 6m. The lateral deformation increases as the spacing of the basal reinforcement increases. In all the cases, it is seen that there is not much variation of lateral deformation in the embedded portion of the wall since the outward deformation is restricted by the foundation soil. The shape of the facing deformation changes from a linear form to a bow shaped form as the spacing of basal reinforcement of the reinforced gabion walls decreases and the maximum deformation is as low as 0.0036H. It is also seen that for medium to large spacings, say, h/H = 0.25 to 0.5, the deformation increases almost linearly with height from bottom to top and the maximum deformation at top is nearly 0.012H for h/H = 0.25 and 0.04H for h/H = 0.5.

In the case of unreinforced retaining wall, where the earth pressure increases towards bottom, the wall rotates about the base developing maximum deformation at the top. This rotation is restricted to a certain extent by the lateral ties in the reinforced cases. When closer spacing like 0.08H is used, the

strain is reduced to a very small value of 0.36%. Even if the spacing is reduced beyond a limit, there is not much difference in the reduction of lateral deformation as can be observed from the deformation plots for h/H = 0.08 and h/H = 0.17.

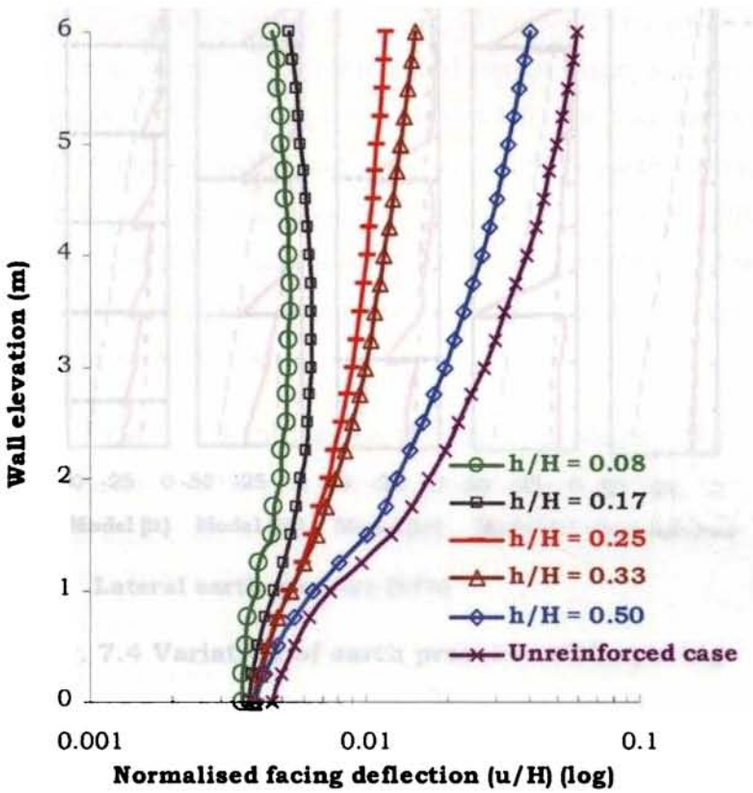


**Fig. 7.3 Facing deflection patterns for different reinforcement spacing configurations**

The behaviour of the gabion faced reinforced soil walls due to the variation in reinforcement spacing have also been analysed in terms of the lateral pressures developed. The variation of earth pressure for the different models were plotted (Fig. 7.4) for H = 6m. In the figure, the large dotted (green) lines represent Rankine's at-rest earth pressure distribution, the small dotted (blue) lines represent Rankine's active earth pressure distribution and the solid (red) lines represent the analytical results for the various models.

The horizontal dashed (black) lines indicate the location of basal reinforcement provided in the gabion boxes in each model.

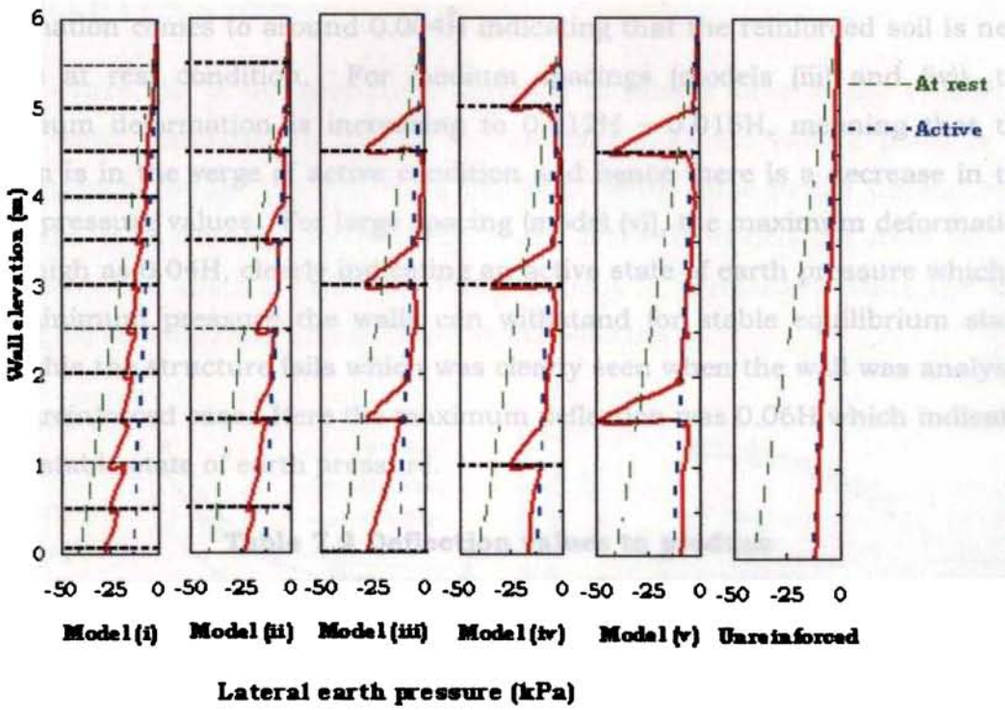


**Fig. 7.4 Variation of earth pressure with spacing**

The earth pressure distribution plots for the different cases analysed show a rise in lateral pressure when compared to the unreinforced case. At the location of reinforcements, a sudden rise of earth pressure can be noted in all the cases, which shows the stress concentration near the reinforcement.

A contradictory result compared to those published for flexible reinforced soil walls (Ogisako et al., 1988) is seen here. Instead of the reduction of earth pressure with decrease in spacing as reported in the literature, here the gabion faced walls being semi rigid walls, an increase in earth pressure is seen with the reduction of spacing. The reason for the same may be explained as follows.

To produce active condition of earth pressure, a retaining wall must rotate laterally away from the soil as per the deflection values listed in Table 7.2. For models (i) and (ii) with smaller spacing, the maximum deformation comes to around 0.004H indicating that the reinforced soil is near to the at rest condition. For medium spacings (models (iii) and (iv)), the maximum deformation is increasing to 0.012H – 0.015H, meaning that the system is in the verge of active condition and hence there is a decrease in the earth pressure values. For large spacing (model (v)), the maximum deformation is as high as 0.04H, clearly indicating an active state of earth pressure which is the minimum pressure the walls can withstand for stable equilibrium state. After this the structure fails which was clearly seen when the wall was analysed for unreinforced case. Here the maximum deflection was 0.06H which indicates an unstable state of earth pressure.

**Table 7.2 Deflection values to produce active earth pressure state (Bowles, 1996)**

| Soil and condition | Maximum deflection values |
|---|---|
| Cohesionless, dense | 0.001H to 0.002H |
| Cohesionless, loose | 0.002H to 0.004H |
| Cohesive, firm | 0.01H to 0.02H |
| Cohesive, soft | 0.02 to 0.05H |

In order to understand the variation of earth pressure with spacing, the earth pressure values for the different cases are to be compared. The total lateral force acting at the back face of the wall seems to be a better parameter for comparison than the lateral earth pressure. Hence for comparison purposes, lateral force was calculated from the earth pressure diagrams using the graphical method (plotting the earth pressure diagrams on graph paper and then calculating the lateral force as the area of the earth pressure diagrams which is obtained by counting the number of cells inscribed by the plots).

The rise in lateral earth pressure in the different cases due to the increase in the reinforcing effect is depicted in Fig. 7.5 (a). The plot was

prepared for L/H = 1.00 and b/H = 0.15. Here the decrease in earth pressure is calculated as:

$$\Delta P = (P_r - P_u) / P_u \times 100\% \qquad \text{.....(7.1)}$$

where, $\Delta P$ is the percentage increase in lateral force of the reinforced cases when compared to that of the unreinforced case (where there is no reinforcement within the fill), $P_u$ is the total lateral force in the unreinforced case and $P_r$ is the total lateral force in the different models got from the FE analysis. The spacing (h) of the reinforcement is normalised using the wall height (H) and the ratio h/H is taken as the abscissa.

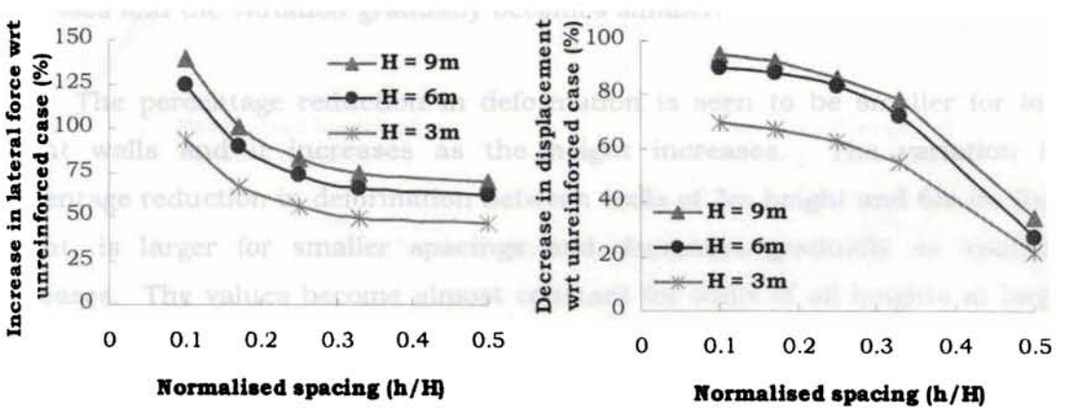


**(a)** **(b)**

**Fig. 7.5 Effect of reinforcement spacing**

The increase in earth pressure when compared to the unreinforced case is maximum for the heavily reinforced case and minimum for the case with minimum reinforcement. This is because, as spacing increases, the walls become unstable and the earth pressure becomes minimum as the system approaches the active condition. But the range of variation is very small unlike the hyperbolic variation exhibited by reinforced soil walls (Ogisako et al., 1988).

The reduction in deformation of reinforced gabion faced walls are plotted against the normalized spacing for the case L/H = 1.00. Here, the percentage reduction in deformation is defined as,

$$\Delta u = (u_u - u_r) / u_u \times 100\% \qquad \text{.....(7.2)}$$

where $u_u$ is the maximum lateral deformation in the unreinforced case and $u_r$ is the maximum lateral deformation in the different reinforced cases. As expected, as the spacing becomes smaller the percentage reduction in deformation increases (Fig. 7.5 (b)).

The plots were prepared for three wall heights and the effect of variation of earth pressure is studied. For walls with low height, the percentage increase in earth pressure is lower when compared to the medium and high walls. It is also seen that as height increases, the percentage rise in earth pressure increases and the variation gradually becomes smaller.

The percentage reduction in deformation is seen to be smaller for low height walls and it increases as the height increases. The variation in percentage reduction in deformation between walls of 3m height and 6m (or 9m) height, is larger for smaller spacings and decreases gradually as spacing increases. The values become almost constant for walls of all heights at large spacings.

From the above discussions, it may be concluded that for any wall height, the ideal spacing of reinforcement may be fixed as, h = 0.1H to 0.2H, as observed from Fig. 7.5 (b). In case of gabion faced walls, the spacing of reinforcement is actually a reflection of the box height as the reinforcement is provided as the basal extensions of the gabion boxes. So if spacings have to be provided at values, smaller than the standard box heights, they should be provided as intermediate ties.

## 7.4 EFFECT OF REINFORCEMENT LENGTH (L)

As per codal provisions, the length of reinforcement should be 0.7H for reinforced soil walls (BS 8006: 1995). To check the applicability of this provision on gabion faced reinforced soil walls, studies were conducted varying the lengths of reinforcement as 0.125H, 0.25H, 0.5H, 0.75H and 1.00H.

Increase in lateral force (with respect to unreinforced case) due to the provision of reinforcement (with different lengths) in the different cases analysed, was plotted for h/H = 0.08 and b/H = 0.15 (Fig. 7.6 (a)). Here the length of reinforcement (L) is normalised using wall height (H) and is taken as the abscissa and percentage increase in lateral force as the ordinate.

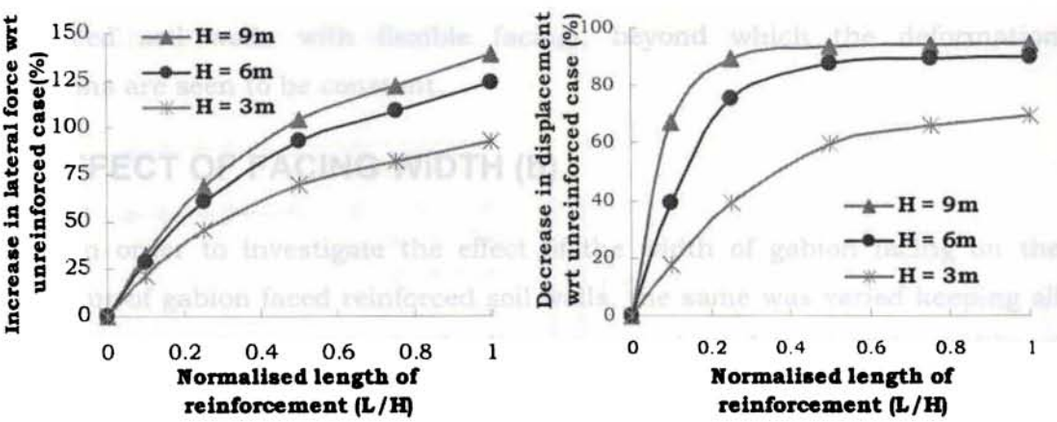


(a) (b)

**Fig. 7.6 Effect of reinforcement length**

As the length of reinforcement increases, percentage increase in lateral force with respect to the unreinforced case increases. In other words, as the quantity of reinforcement increases, the earth pressure exerted on the back face of the wall increases, indicating the transformation of the state of earth pressure from below active condition to near to at – rest condition. i.e., the system changes from an unstable to a stable state which is clearly indicated by the reduction in deflection values with the increase in the quantity of reinforcement.

The variation in length was plotted against the change in deformations with respect to the unreinforced case (Fig. 7.6 (b)). Here also, as expected, as the length of reinforcement increases, the reduction in displacement increases. The variation in the reduction is just marginal for medium and high walls.

As the wall height increases, the percentage increase in lateral force increases, but the variation is very small. The percentage reduction in deformation is lower for low height walls and it increases gradually for walls of larger heights and the variation is nominal for medium and high walls. Moreover, observing from Fig. 7.6 (b), the ideal reinforcement length for gabion faced reinforced soil walls may be fixed as 0.4H – 0.6H (as against 0.7H of reinforced soil walls with flexible facing), beyond which the deformation variations are seen to be constant.

## 7.5 EFFECT OF FACING WIDTH (b)

In order to investigate the effect of the width of gabion facing on the behaviour of gabion faced reinforced soil walls, the same was varied keeping all the other parameters constant. Studies were conducted varying the widths of gabion facing as 0.025H, 0.05H, 0.10H, 0.15H, 0.20H, 0.25H and 0.30H.

The effect of earth pressure on the increase in the width of gabion facing was plotted for h/H = 0.08 and L/H = 1.00. The facing width (b) is normalised using wall height (H). The normalised width of facing is taken as the abscissa, while the lateral force in kN exerted at the back face of the wall and the maximum lateral displacement of the facing in m are taken as the ordinates (Fig. 7.7).

It can be noted that as the facing width increases, there is not much variation in the lateral force exerted at the back face of the wall. This means that the facing rigidity has not much effect on the lateral force developed in the backfill. The variation in facing width has also been plotted against the maximum lateral deflection with respect to the unreinforced case (Fig. 7.7 b). Here it is seen that the increase in facing width decreases the maximum lateral displacement. For very thin facings, the displacements are seen to be maximum. For $b/H \geq 0.1$, the displacement values are almost constant giving a linear horizontal shape to the latter part of the plot.

As the wall height increases, the lateral force and the displacement values also increase (Fig. 7.7). The variation in lateral force is nominal for medium and high walls. In the case of displacements, for thin facings, the variation in displacements with increase in wall height is seen to be large. For thicker facings, the corresponding variations are small. To summarise the study, the facing width may be fixed as 0.1H - 0.15H, beyond which the effect of deformations are seen to be marginal.

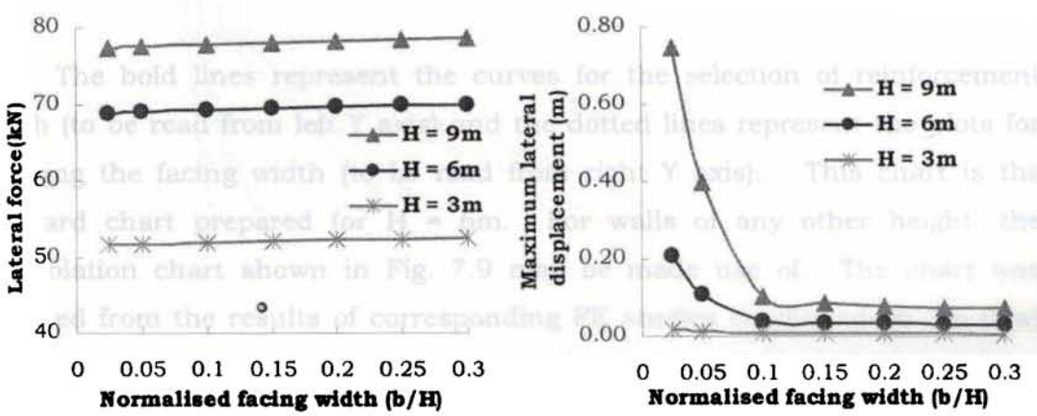


(a) (b)

**Fig. 7.7 Effect of facing width**

## 7.6 SELECTION OF GEOMETRIC PARAMETERS

The present design method for the design of gabion faced reinforced soil walls is based on the assumption that the entire reinforced block acts as a rigid gravity structure and the deformations in the system are not taken into consideration. The design method of gabion faced reinforced soil walls, is a combination method based on the design of conventional gravity retaining structures and reinforced soil walls. As far as the gravity structures are concerned, the assumption may be true since the deformations in the structure are less because of its rigid nature. But the present design method is not a satisfactory method in the case of flexible reinforced soil walls and semi – rigid gabion faced walls, where, the deformations are a main issue. Hence the design method should be modified including the serviceability conditions.

An attempt is made here to prepare a general purpose design chart from which the length and spacing of reinforcement as well as the width of gabion facing can be selected for a maximum deformation of the wall. The design chart (Fig. 7.8) was prepared for maximum lateral deformation ($u_{max}$, on the X axis) in terms of the length of reinforcement (L, on the left Y axis) and width of facing (b, on the right Y axis) for different spacing of reinforcement (h), for a wall height of 6m. All the above parameters were normalised by dividing it by H to make them non – dimensional.

The bold lines represent the curves for the selection of reinforcement length (to be read from left Y axis) and the dotted lines represent the plots for choosing the facing width (to be read from right Y axis). This chart is the standard chart prepared for H = 6m. For walls of any other height, the interpolation chart shown in Fig. 7.9 may be made use of. The chart was prepared from the results of corresponding FE studies conducted on 3m (low) and 9m (high) walls. The same trend as in Fig. 7.8 was obtained for 3m and 9m high walls also but the magnitudes were different. Hence an interpolation chart was prepared with the height of the wall as X axis and magnification factor as Y axis. The magnification factors for L and b ($(L/H)_{rqd\ H}$ / $(L/H)_{H=6m}$ or $(b/H)_{rqd\ H}$ / $(b/H)_{H=6m}$) for different heights were obtained by normalising L and b values with the corresponding values for a 6m wall. A logarithmic curve (Fig. 7.9) could be fitted between the points where the $R^2$ value was obtained as 0.9984 indicating a good fit. The curve was then extrapolated forwards up to 20m height and backwards up to 0.5m height. For selecting the geometric parameters for any wall height, the length and facing width should be obtained from Fig. 7.8 and those values should be multiplied by the magnification factor selected from Fig. 7.9.

This design chart can be used in the preliminary design of gabion faced soil retaining walls to select the length and spacing of reinforcement and the width of gabion facing in order to bring the deformations in the system to a minimum value. The method of using the charts is described in detail in Chapter 9.

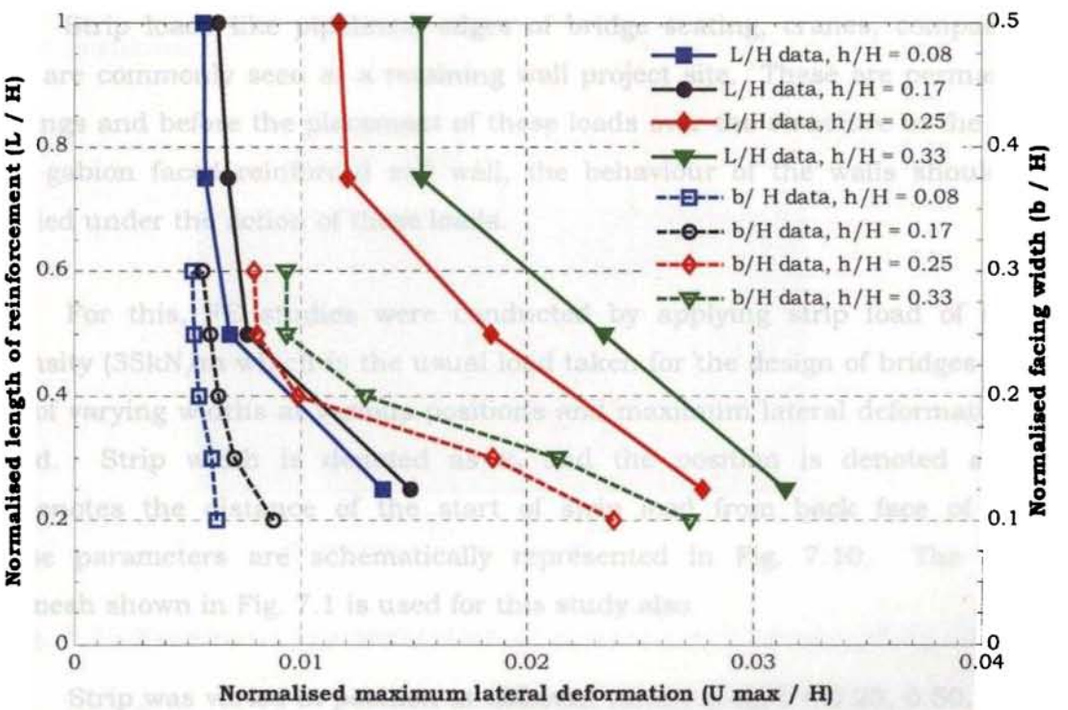


**Fig. 7.8 Design chart for selecting geometric parameters (H = 6m)**

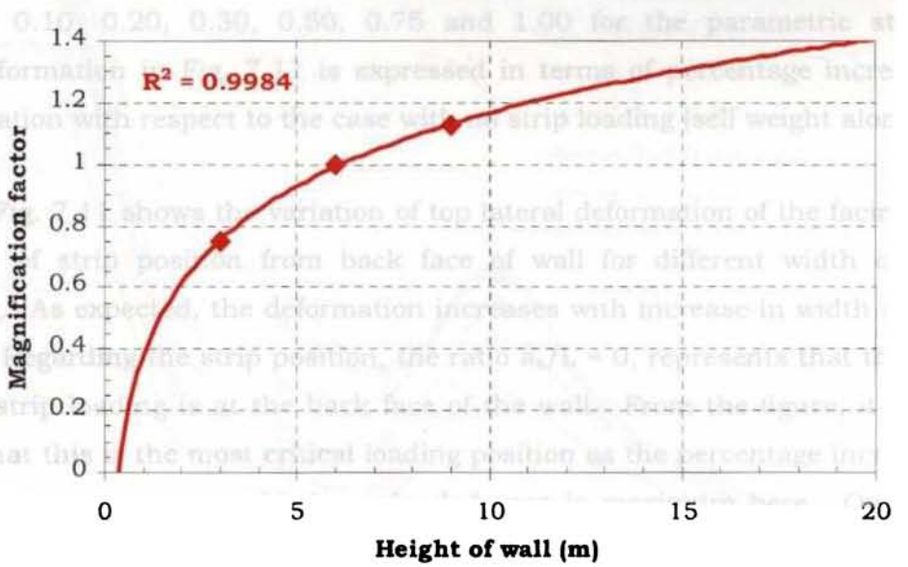


**Fig. 7.9 Interpolation chart for selecting geometric parameters for any height**

## 7.7 EFFECT OF POSITION OF STRIP LOADING

Strip loads like pipelines, edges of bridge seating, cranes, compactors etc., are commonly seen at a retaining wall project site. These are permanent loadings and before the placement of these loads over the structure in the case of a gabion faced reinforced soil wall, the behaviour of the walls should be studied under the action of these loads.

For this, FE studies were conducted by applying strip load of same intensity (35kN/m which is the usual load taken for the design of bridges etc.), but of varying widths at various positions and maximum lateral deformation is noted. Strip width is denoted as $x_s$ and the position is denoted as $a_s$. $a_s$ denotes the distance of the start of strip load from back face of wall. These parameters are schematically represented in Fig. 7.10. The same FE mesh shown in Fig. 7.1 is used for this study also.

Strip was varied in position at different values of $a_s/L$ = 0.25, 0.50, 0.75, 1.00, 1.25, 1.50, 1.75 and 2.00. The strip width was varied at values of $x_s/L$ = 0.10, 0.20, 0.30, 0.50, 0.75 and 1.00 for the parametric studies. The deformation in Fig. 7.11 is expressed in terms of percentage increase in deformation with respect to the case with no strip loading (self weight alone).

Fig. 7.11 shows the variation of top lateral deformation of the facing with change of strip position from back face of wall for different width of strip loading. As expected, the deformation increases with increase in width of strip loads. Regarding the strip position, the ratio $a_s/L = 0$, represents that the start of the strip loading is at the back face of the wall. From the figure, it is very clear that this is the most critical loading position as the percentage increase in deformation with respect to the unloaded case is maximum here. One more critical plane can be identified from the figure where all the curves show a peak. This is at $a_s/L = 1$, where the percentage increase in deformation is found to be more compared to other positions. The best position of strip loading can also be identified from Fig. 7.10 which is $a_s/L > 1.5$. Another suitable position range

may also be located from the figure as $a_s/L$ = 0.5 to 0.75. It is at these two positions where the percentage increase in deformation is lesser compared to other positions.

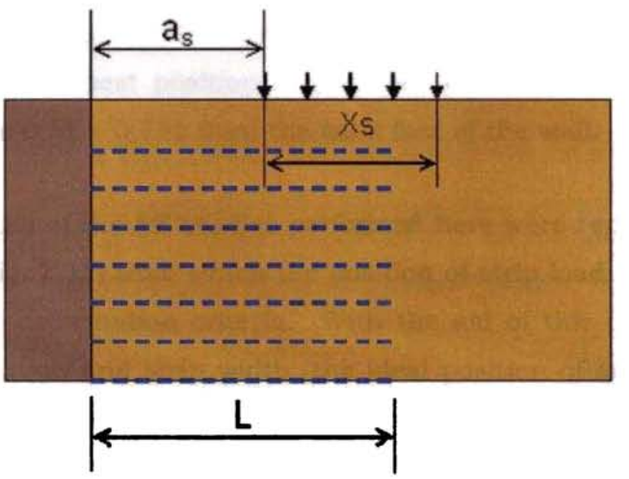


**Fig. 7.10 Schematic representation of parameters of strip loading studies**

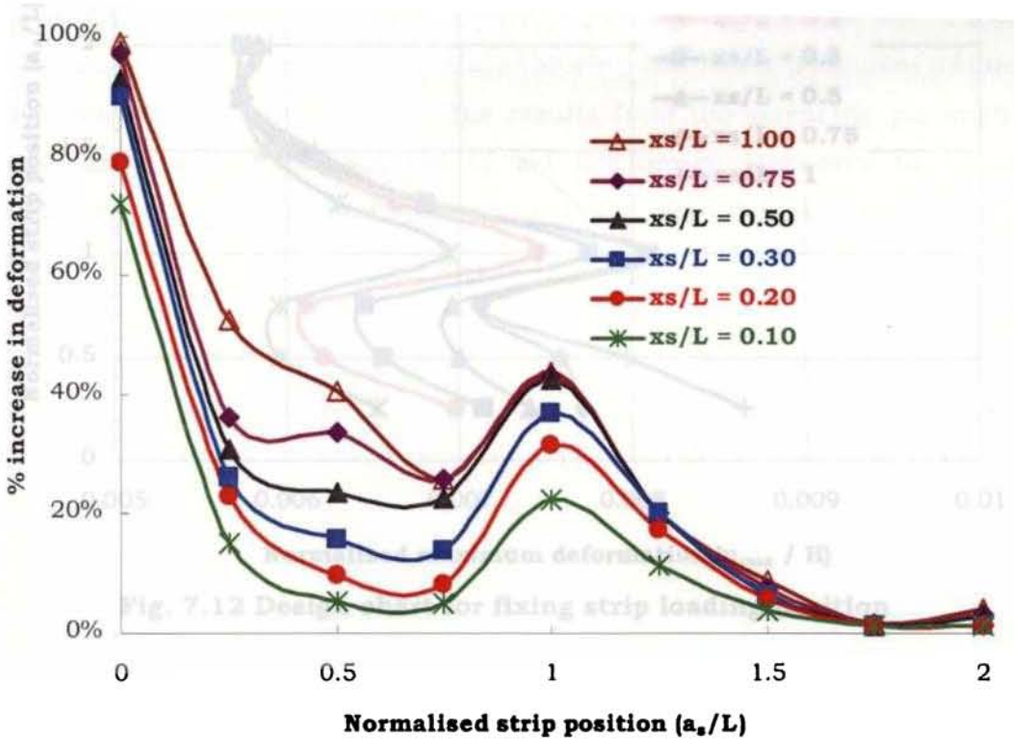


**Fig. 7.11 Effect of strip position on deformation**

Thus the critical planes where the strip loading should not be placed are the beginning and end of the reinforcement lengths. The most ideal position for placing the strip loading is at least 1.5L away from the back face of the wall where L is the length of the reinforcement. i.e., strip should be placed away from the reinforced region. If in any case, the strip has to be placed inside the reinforced area, the best position is the start of the strip loading should be within the range 0.5L – 0.75L from the back face of the wall.

The results of the FE studies performed here were replotted to develop a design chart (Fig. 7.12) from which the position of strip loading may be fixed by considering the deformation criteria. With the aid of this chart, knowing the limiting deformation and strip width, the ideal position of strip loading can be selected, which is described in detail in Chapter 9.

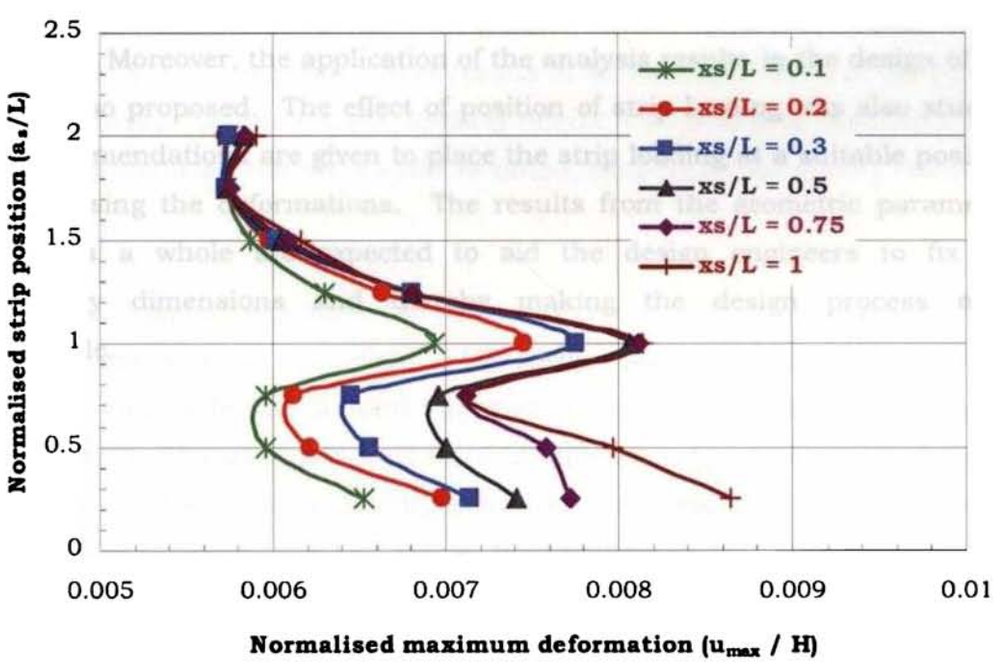


**Fig. 7.12 Design chart for fixing strip loading position**

## 7.8 SUMMARY

Conventional design procedures of retaining walls in general, do not take into account wall deformation which is usually considered as a minor criterion in design. But in the present trend, even standard codes are being amended to accommodate the limit state design where serviceability conditions are also given equal importance, and hence a deformation study is resorted to.

FE analyses of gabion faced reinforced soil retaining walls were carried out for different reinforcement spacings, reinforcement lengths and facing widths on low (3m), medium (6m) and high (9m) walls. The relation between wall heights, spacing of reinforcement and length of reinforcement and the effect of the earth pressure acting on the wall and the facing deformation are discussed in detail in this chapter and optimum values have been suggested in each case. Moreover, the application of the analysis results in the design of the walls is also proposed. The effect of position of strip loading was also studied and recommendations are given to place the strip loading at a suitable position by minimising the deformations. The results from the geometric parametric studies as a whole are expected to aid the design engineers to fix the preliminary dimensions and thereby making the design process more comfortable.

# Chapter 8

# MATERIAL PARAMETRIC STUDIES

## 8.1 GENERAL

The previous chapter presented the results of the parametric studies conducted by varying the geometry and loading of gabion faced reinforced soil retaining walls. These studies are supplemented by varying the material properties of the components like gabion fill, backfill and reinforcement, the results of which are presented in this chapter.

The aim of the material parametric studies is to study the influence of some selected material parameters like gabion fill, backfill and reinforcing mesh on the deformation behaviour of gabion faced reinforced earth walls. For uniformity in the presentation of results in all the cases, most of the studies were conducted for self weight loading only. For studying the effect of a particular parameter, the same alone is varied, keeping all the other parameters constant.

This chapter explains the analyses conducted on a gabion faced reinforced soil wall of 6m height. FE studies were performed for different gabion fill materials like a hard material (rock pieces) and a soft material (in – situ soil). The materials were filled in different proportions, to understand the effect of the gabion fill material on the response of the system. To understand the behaviour of gabion fill – backfill combinations, 11 different rock types and 16 different soil types were used as the gabion fill and backfill respectively, and FE studies were conducted for each of the combinations. To investigate the effect of reinforcement, on the behaviour of gabion faced reinforced soil walls, FE analyses were conducted on a reinforced wall and an unreinforced wall and the results were compared.

## 8.2 EFFECT OF GABION FILL MATERIAL

Reinforced soil walls are flexible in nature while the gabion faced reinforced soil walls exhibit a semi – rigid behaviour, the partial rigidity being imparted by the fill material inside the gabion boxes. So in these walls, the self weight of the fill material is a major stabilising factor. Hence in this work, it was intended to study the influence of the gabion fill material on the behaviour of gabion faced reinforced soil walls. Moreover, at construction sites where the rock pieces are not locally available, the cost of rocks including the transportation cost from distant quarries becomes enormous. So in order to cut down this cost which is a major factor that increases the cost of construction, the suitability of using a locally available cheap material as gabion fill may be thought of. This is another reason which prompted the present study. The results of this study are expected to supplement the experimental studies described in Chapter 5.

For this, different combinations of fill materials were used in the study. The fill materials considered were a hard material and a soft material whose properties were selected arbitrarily (Table 8.1). The hard material was used to simulate the rock properties and the soft material simulated a locally available less stiff material like ordinary soil. The aim of using these two types of fill materials was, when the hard material is used as the fill material, the gabion resembles the stone filled box gabion and in the other case, when a soft material is used as the gabion fill material, the box resembles a soil filled box gabion (Section 3.2.2). In addition to this, filling both the hard and soft materials in different proportions was also studied. A layered system was considered with the soft material in the bottom portion and the hard material in the top portion. Another mode of filling was also studied, by keeping the soft material as a core inside the hard material. Since the hard material resembles the rock pieces with high void ratio, the arrangement of the soft material as layers or as a core does not adversely affect the permeability factor.

**Table 8.1 Properties of gabion fill materials**

| Gabion fill | E (kPa) | $\mu$ | $\phi$ (degrees) | c (kPa) | $c_i$ (kPa) |
|---|---|---|---|---|---|
| Hard material | 100000 | 0.25 | 42 | 0 | 13.57 |
| Soft material | 1000 | 0.35 | 32 | 10 | 10.90 |

The proportions of the gabion fill materials selected for the study were:

- 100% hard material
- 75% hard material + 25% soft material
- 50% hard material + 50% soft material
- 25% hard material + 75% soft material
- 100% soft material

FE studies were conducted for each case and the variations of the horizontal deflection of the top most point of the facing with the applied surcharge pressure were noted. The surcharge was applied as uniform pressure over the backfill which was converted into the lumped load system for the analyses. The results are presented in the form of load vs. top lateral deformation plots for the different cases analysed (Fig. 8.1).

The load deformation plots from the FE studies show the same pattern as obtained from the experimental studies (Section 5.3.1). The 100% hard material takes the maximum load while the 100% soft material fails at a faster rate at low surcharge values. The walls with combination facings show an intermediate behaviour. An interesting feature which can be seen both from the experimental and analytical studies is that the combination fill with 25% soft material behaves very similar to the wall with 100% hard material facing. The 50 – 50 combination filled in layers as well as in core, fails at earlier load stages than the above mentioned two cases followed by the 75% soft – 25% hard material combination. In general, it may be concluded that as the percentage of

soft material increases, the load carrying capacity of the gabion faced reinforced soil walls decreases.

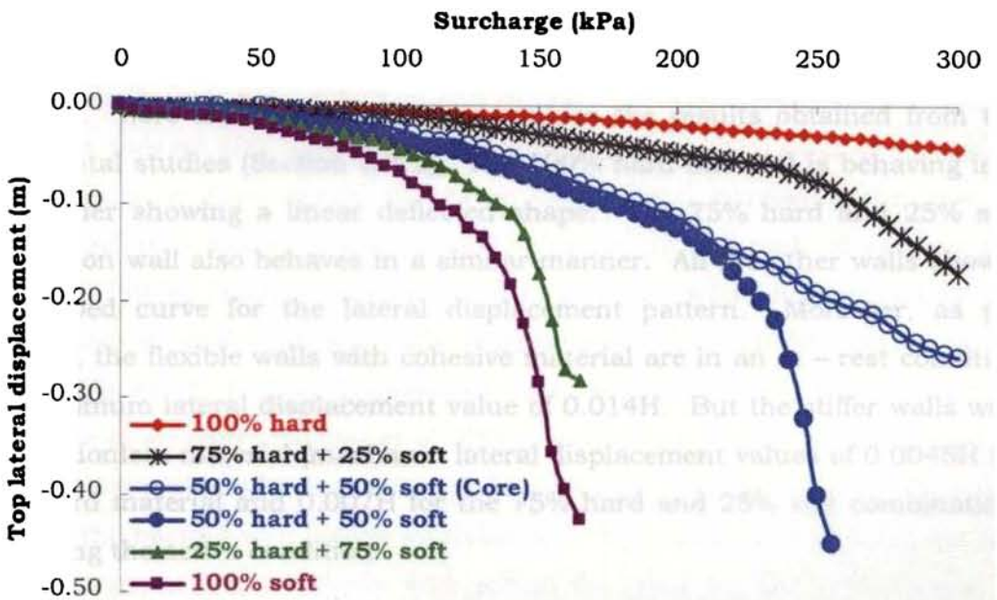


**Fig. 8.1 Load vs. top lateral displacement plots for different gabion fill materials**

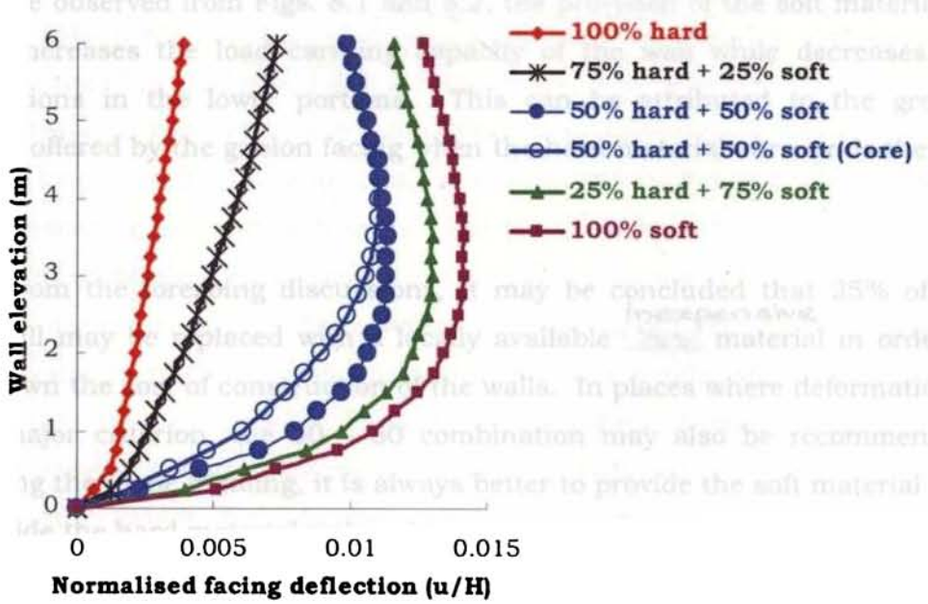


**Fig. 8.2 Facing deflection plots for walls with different gabion fills at 150 kPa surcharge**

To study the deflection behaviour of the front face of the wall, for all the cases of fill materials, the horizontal deformations of all the nodes representing the front face of the wall were noted for 150 kPa surcharge. The incipient failure occurs at this surcharge load in weak walls as can be observed from Fig. 8.1. Fig. 8.2 shows the front face deflections of all the walls considered in the study. Here also the behaviour resembles the results obtained from the experimental studies (Section 5.3.2). The 100% hard material is behaving in a stiff manner showing a linear deflected shape. The 75% hard and 25% soft combination wall also behaves in a similar manner. All the other walls show a bow shaped curve for the lateral displacement pattern. Moreover, as per Table 7.2, the flexible walls with cohesive material are in an at – rest condition with maximum lateral displacement value of 0.014H. But the stiffer walls with the cohesionless material (maximum lateral displacement values of 0.0045H for 100% hard material and 0.007H for the 75% hard and 25% soft combination) are nearing the active condition.

In order to analyse the effect of mode of filling the materials inside the gabions (whether in layers or as a core), 50 – 50 combinations were tried. As can be observed from Figs. 8.1 and 8.2, the provision of the soft material as a core increases the load carrying capacity of the wall while decreases the deformations in the lower portions. This can be attributed to the greater stiffness offered by the gabion facing when the hard material surrounds the soft core.

From the foregoing discussions, it may be concluded that 25% of the gabion fill may be replaced with a locally available inexpensive material in order to bring down the cost of construction of the walls. In places where deformation is not a major criterion, the 50 – 50 combination may also be recommended. Regarding the mode of filling, it is always better to provide the soft material as a core inside the hard material rather than providing the material in layers.

## 8.3 EFFECT OF GABION FILL – BACKFILL COMBINATION

The effects of varying the gabion fill material was presented in detail in the previous section. The backfill material also plays an important role in the behaviour of gabion faced reinforced soil walls. The ideal backfill material is the river sand with very good frictional and drainage characteristics (Jones, 1985). But in the present day conditions, the availability of river sand is becoming scarce, which in turn raises the price factor thus increasing the cost of construction as a whole. Hence researchers are on the path of seeking the suitability of using locally available soil or in-situ soil as backfill material for the construction of reinforced soil walls (Fabian and Fourie (1988), Bolton et al. (1989), Ling et al. (1995), Lesniewska and Porbaha (1998), Helwany et al. (1999), Lee et al. (2001), Mittal et al. (2006) and so on). With the same goal in mind, the present study was conducted on gabion faced reinforced soil walls, replacing the backfill with locally available soil. The study aims to bring out the effects of various backfill types and gabion fill types on the performance of gabion faced reinforced soil walls.

The study was conducted on various cases where eleven different rock types (as gabion fill) and sixteen different soil types (as backfill), with material properties listed in Tables 8.2 & 8.3 respectively, were selected for the present study. Thus, a total of 176 combinations were investigated for a 6m high (medium height) wall. These analyses were repeated for 3m and 9m high walls also representing low and high walls. The values of modulus of elasticity and unit weight of different rock types given (in Table 8.2), are those for intact rock masses. However, gabion fill consists of rock pieces and these will have reduced value of modulus of elasticity and dry unit weight when compared to those of the intact rock mass. Thus the actual values of modulus of elasticity and unit weight of intact rock masses should be reduced to represent the rock pieces in the gabion fill. In the case of dry unit weights, this reduction considered was in accordance with the porosity of the gabion boxes filled with rock pieces as below.

$$\gamma_g = \gamma_{rock}(1-n) \qquad \text{.....(8.1)}$$

where, $\gamma_g$ is the apparent rock density, $\gamma_{rock}$ is the actual value of density obtained from the Table 8.2 and n is the porosity which is taken as 0.3.

**Table 8.2 Properties chosen for gabion fill (Verma, 2000)**

| Rock Type | E (kPa) | μ | ϕ (degrees) | C (kPa) | $C_a$* (kPa) | $C_g$* (kPa) | γ (kN/m3) |
|---|---|---|---|---|---|---|---|
| Basalt | 9.00E+07 | 0.160 | 50.0 | 0 | 16.61 | 16.61 | 27.7 |
| Diabase | 8.00E+07 | 0.180 | 50.0 | 0 | 16.61 | 16.61 | 27.0 |
| Gabbro | 7.50E+07 | 0.135 | 31.0 | 0 | 10.68 | 10.68 | 27.0 |
| Granite | 6.25E+07 | 0.250 | 51.0 | 0 | 17.07 | 17.07 | 26.5 |
| Marble | 6.00E+07 | 0.250 | 37.0 | 0 | 12.12 | 12.12 | 27.5 |
| Gneiss | 5.00E+07 | 0.220 | 35.0 | 0 | 11.61 | 11.61 | 26.0 |
| Quartzite | 4.00E+07 | 0.230 | 35.5 | 0 | 11.74 | 11.74 | 28.2 |
| Hard limestone | 2.00E+07 | 0.200 | 35.0 | 0 | 11.61 | 11.61 | 27.0 |
| Sand stone | 1.00E+07 | 0.125 | 30.0 | 0 | 10.47 | 10.47 | 25.0 |
| Shale | 6.00E+06 | 0.100 | 29.0 | 0 | 10.26 | 10.26 | 24.0 |
| Trachyte | 5.00E+06 | 0.100 | 27.0 | 0 | 9.86 | 9.86 | 23.0 |

*** Calculated using Eqn. 4.55 and 4.56**

For reducing the elastic modulus of rockfill inside gabion boxes, the porosity (n) of gabion boxes and the volume of rock sample used for testing were considered as in Eqn. 8.2.

$$E_g = \frac{E_{rock}\,V_{rock}}{V_g\,(1-n)} \qquad \text{.....(8.2)}$$

where,

$E_g$ = Modulus of elasticity of gabion box

$E_{rock}$ = Modulus of elasticity of rock obtained from testing rock sample

$V_{rock}$ = Volume of rock sample used for testing

$V_g$ = Volume of gabion box and n is the porosity of boxes which is taken as 0.3

The other parameters representing rock in this study like the Poisson's ratio and angle of internal friction were taken as the same for the parent rock and the rock pieces inside gabions as there is no significant change in these values after the disintegration of rock (Verma, 2000).

**Table 8.3 Properties chosen for backfill (Helwany et al., 1999)**

| United Soil classification | Desig-nation | γ (kN/m3) | ϕ (degrees) | C (kPa) | K | n | $R_f$ | $K_{mu}$ | m |
|---|---|---|---|---|---|---|---|---|---|
| GW | GW | 23.6 | 42 | 0 | 600 | 0.4 | 0.7 | 175 | 0.2 |
| GP | GP | 22.8 | 39 | 0 | 450 | 0.4 | 0.7 | 125 | 0.2 |
| SW | SW | 22.1 | 36 | 0 | 300 | 0.4 | 0.7 | 75 | 0.2 |
| SP | SP | 21.3 | 33 | 0 | 200 | 0.4 | 0.7 | 50 | 0.2 |
| SM | SM 1 | 21.3 | 36 | 0 | 600 | 0.25 | 0.7 | 450 | 0 |
| | SM 2 | 20.5 | 34 | 0 | 450 | 0.25 | 0.7 | 350 | 0 |
| | SM 3 | 19.7 | 32 | 0 | 330 | 0.25 | 0.7 | 250 | 0 |
| | SM 4 | 18.9 | 30 | 0 | 150 | 0.25 | 0.7 | 150 | 0 |
| SC | SC 1 | 21.3 | 33 | 24 | 400 | 0.6 | 0.7 | 200 | 0.5 |
| | SC 2 | 20.5 | 33 | 19 | 200 | 0.6 | 0.6 | 100 | 0.5 |
| | SC 3 | 19.7 | 33 | 14 | 150 | 0.6 | 0.7 | 75 | 0.5 |
| | SC 4 | 18.9 | 33 | 10 | 100 | 0.6 | 0.7 | 50 | 0.5 |
| CL | CL 1 | 21.3 | 30 | 19 | 150 | 0.45 | 0.7 | 140 | 0.2 |
| | CL 2 | 20.5 | 30 | 14 | 120 | 0.45 | 0.7 | 110 | 0.2 |
| | CL 3 | 19.7 | 30 | 10 | 90 | 0.45 | 0.7 | 80 | 0.2 |
| | CL 4 | 18.9 | 30 | 5 | 60 | 0.45 | 0.7 | 50 | 0.2 |

It can be seen from Table 8.2 that each rock type is characterised with distinct range of elastic and geotechnical properties. Thus, each of these properties can individually influence the performance of the wall. Hence a dimensionless factor, known as Rock Factor (RF), was introduced by the author for the analysis of the results. RF is an indicator of the stiffness of the rock and includes all the major properties and was defined as:

$$RF = \frac{E}{\gamma D}\frac{\phi^c}{\mu} \qquad \text{.....(8.3)}$$

where,

E = modulus of elasticity of rock mass

$\gamma$ = unit weight of the rock

D = least lateral dimension of the rock pieces filled inside the boxes

$\phi^c$ = angle of friction of the rock in radians

$\mu$ = Poisson's ratio

For the different rock types listed in Table 8.2, the rock factor (RF) values were computed and tabulated in Table 8.4.

**Table 8.4 Rock factor values for different rock types**

| Rock type | Rock Factor (RF) |
|---|---|
| Basalt | 5.91E+07 |
| Diabase | 4.79E+07 |
| Granite | 3.71E+07 |
| Gabbro | 2.80E+07 |
| Marble | 1.88E+07 |
| Gneiss | 1.78E+07 |
| Quartzite | 1.27E+07 |
| Hard limestone | 7.54E+06 |
| Sand stone | 5.59E+06 |
| Shale | 4.22E+06 |
| Trachyte | 3.41E+06 |

FE analyses were conducted for all the 176 combinations of gabion fill and backfill. The response parameters used for the study were the maximum lateral displacements of the wall facing, the maximum axial strain in the reinforcement and the average safety factor (calculated as described below) for the gabion faced soil retaining walls. In each case of analysis, the maximum

horizontal deformation of the wall facing was noted down and converted to normalised value by dividing by wall height, H. Similarly, maximum strain in all the reinforcements were checked and the highest of these values were taken as the maximum axial strain in the reinforcement. This value was seen to occur near the portion where maximum deflection of facing occurred. The average safety factor was calculated by averaging the apparent safety factors of the soil elements located on or near the potential failure plane which passes through the bottom of the retaining wall face and makes an angle of $45^o + \phi^o/2$ with the horizontal. The apparent safety factor is defined as the ratio of the deviatoric stress of a soil element to the deviatoric stress at failure using the Mohr – Coulomb failure criterion (Helwany et al., 1999). The apparent safety factor was found to be minimum along the potential failure plane.

Fig. 8.3 shows the variation of maximum facing deflection ($u_{max}$) with the different rock types for the various types of gravel and sand backfills, silty sand backfills, clayey sand backfills and inorganic clay backfills of low plasticity. Fig. 8.4 shows the maximum strain developed in the reinforcement ($\varepsilon_{rft\ max}$) while Fig. 8.5 shows the average safety factors (ASF) for the corresponding soil types.

On closely analysing the results for maximum wall deflections (Fig. 8.3), it can be seen that gravel and sand backfill exhibit the least deformations, while the clay backfill shows the maximum deformation. Noting the normalised deformation values, it can be seen that the maximum deformation produced by the clay backfill is 0.011H. An interesting thing to be pointed out is that, this value is very much less than 0.05H (Table 7.2), the maximum deflection value for soft cohesive soil to produce an active state of earth pressure. This means that the wall is still in at – rest condition which indicates a stable state. But on noting the values for cohesionless soils, it can be seen that the wall has either approached an active state or is approaching the active state. In this connection, it may be noted that the system analysed is in dry condition and the effect of water on the behaviour of the system was not analysed which is beyond the scope of this work.

For each category of backfill, it can be seen that as the stiffness of backfill increases, the deformation decreases when stronger rocks are used as gabion fill. For weaker rocks, whatever be the stiffness of backfill, the deformation is approaching the same magnitude. Referring to the graphs of maximum strain in reinforcement (Fig. 8.4), it can be seen that the maximum strain exhibited by the reinforcement is 1.05% which is very much less than the permissible strain of gabion mesh which 10%. This means that the reinforcement is safe against breaking failure for any type of backfills or gabion fills. Among the rocks, basalt, diabase, granite and gabbro are igneous in origin. Quartzite, marble and gneiss are metamorphic rocks while trachyte, shale, sandstone and hard lime stone are sedimentary rocks. Observing the graphs, it can be seen that all the igneous rocks are exhibiting a similar behaviour which is indicated by the horizontal line portions of the graphs. The metamorphic rocks show a more or less fair performance when compared to the igneous rocks as indicated by the average safety factor values in Fig. 8.5. While the performance shown by the sedimentary rocks is very poor, when compared to the other two types.

From an overview of these figures, a general statement can be made that as the stiffness of gabion fill and backfill increases, the wall deformation decreases, the strain in reinforcement decreases and the average safety factor increases.

Though the results obtained above are with reference to 6m high wall, the same trend (Fig. 8.3 to 8.5) was shown in the behaviour of for 3m and 9m high walls, but with different magnitudes. Hence, as an extension of these studies, an interpolation chart was prepared with the height of the wall along X axis and the response parameter ratio (RPR) along Y axis. The purpose of this chart is to obtain the behaviour of the system for any height, which can be used further for design purposes. The response parameter ratio is defined as the ratio of the response parameter (like $u_{max}/H$, $\varepsilon_{rfl\ (max)}$ and ASF) for the required height to the response parameter for H = 6m.

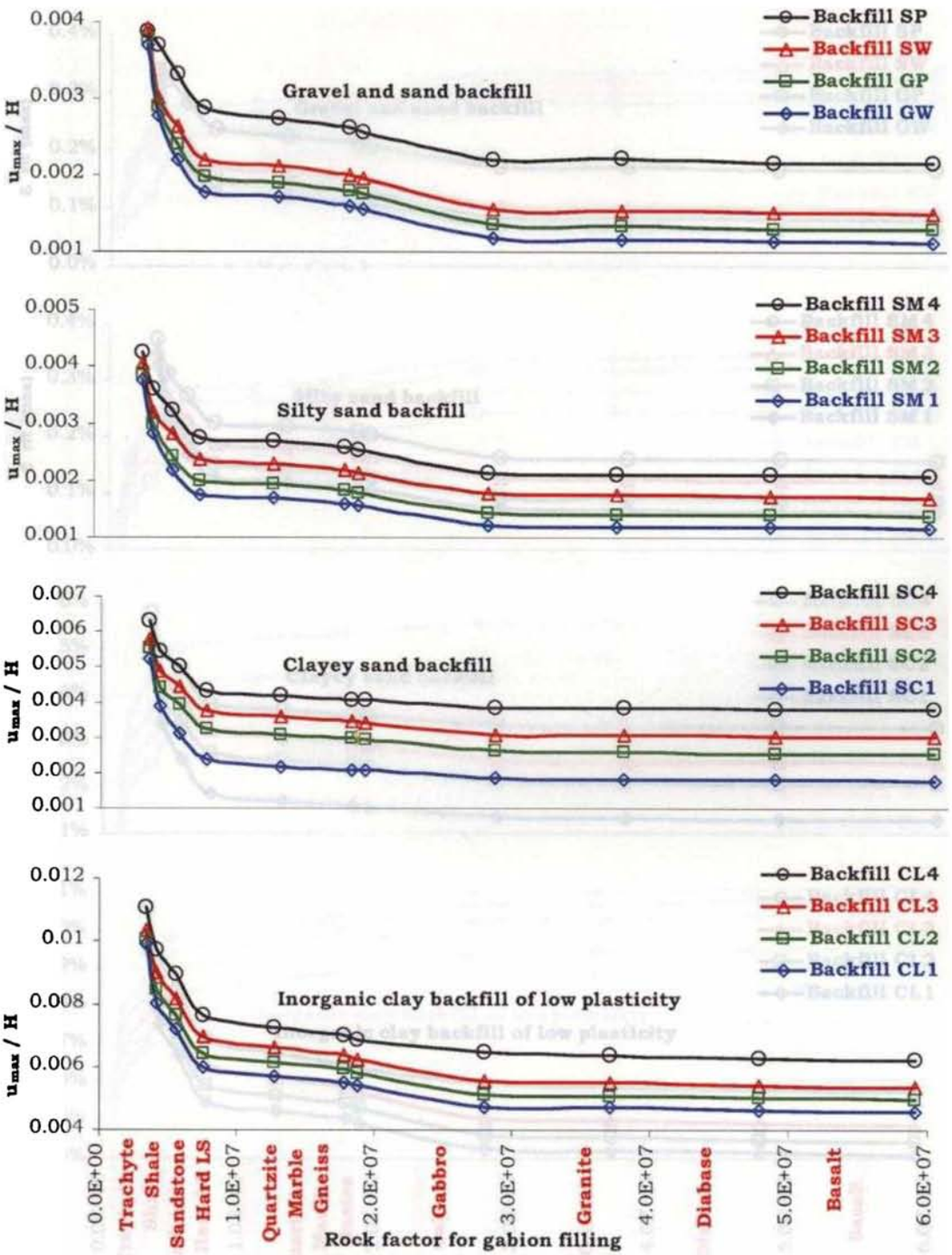


**Fig. 8.3 Variation of maximum wall deflection for different backfills**

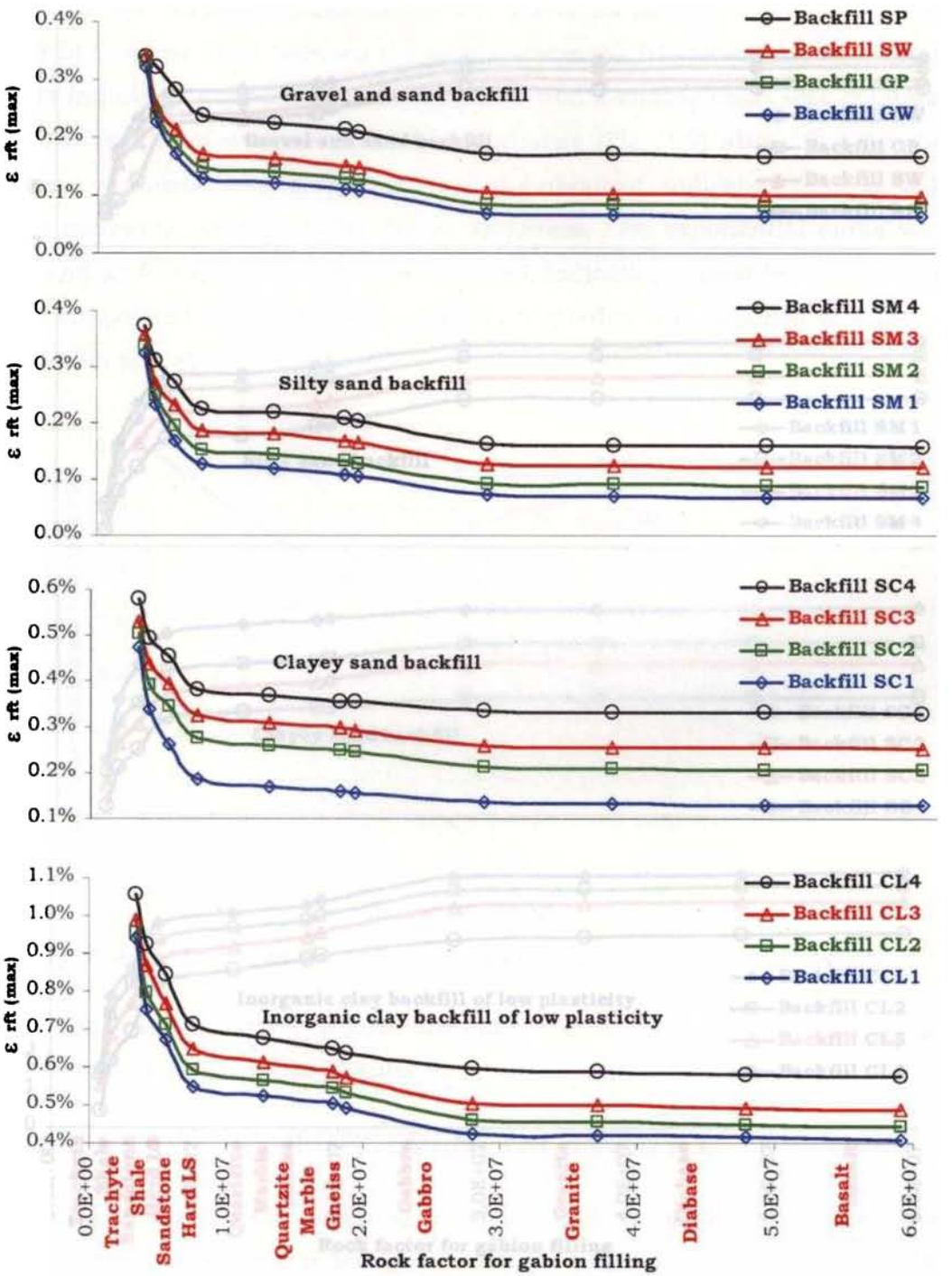


**Fig. 8.4 Variation of maximum strain in reinforcement for different backfills**

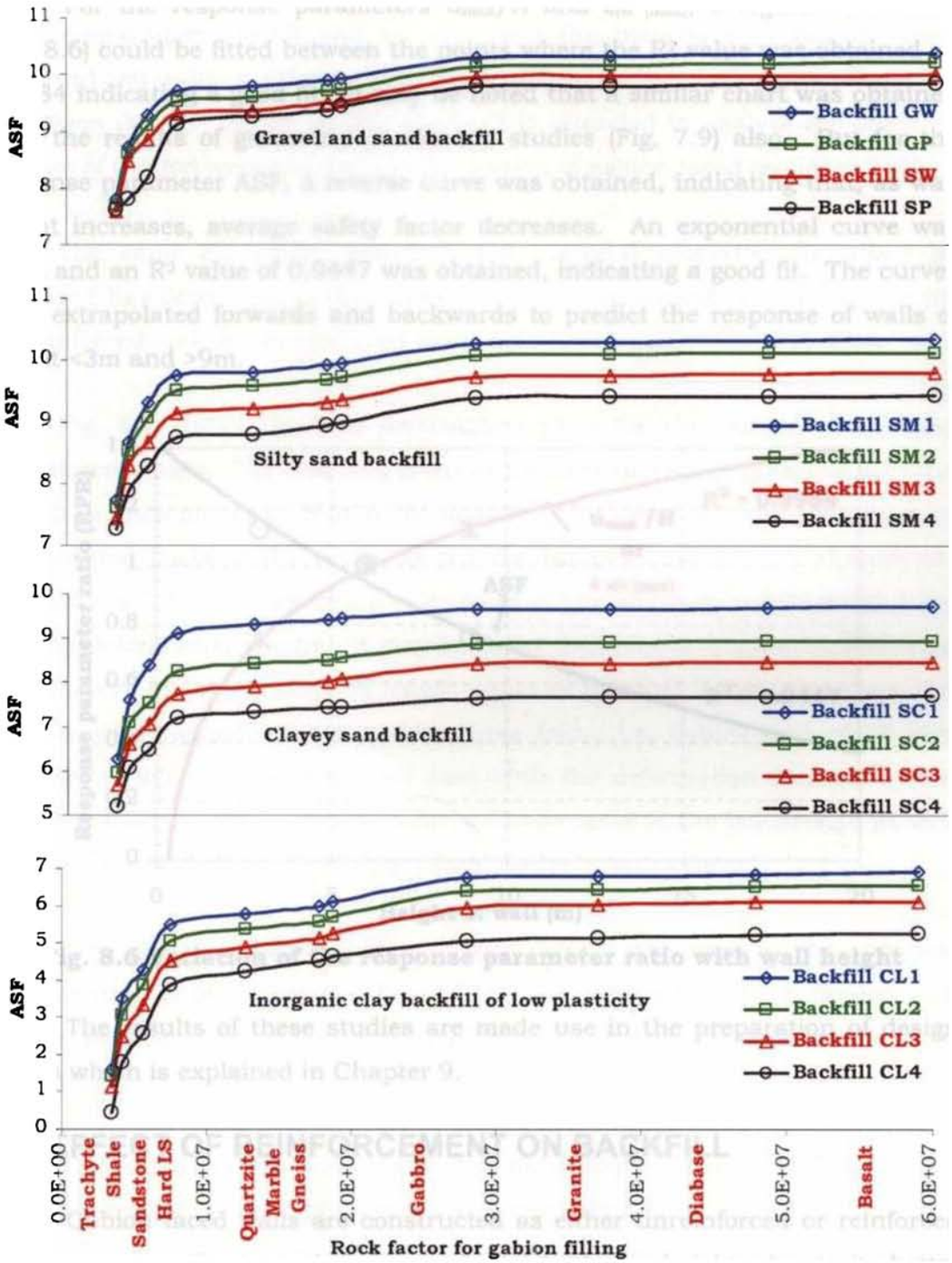


**Fig. 8.5 Variation of average safety factor for different backfills**

For the response parameters $u_{max}/H$ and $\varepsilon_{rft\ (max)}$, a logarithmic curve (Fig. 8.6) could be fitted between the points where the $R^2$ value was obtained as 0.9984 indicating a good fit. It may be noted that a similar chart was obtained from the results of geometric parametric studies (Fig. 7.9) also. But for the response parameter ASF, a reverse curve was obtained, indicating that, as wall height increases, average safety factor decreases. An exponential curve was fitted and an $R^2$ value of 0.9447 was obtained, indicating a good fit. The curves were extrapolated forwards and backwards to predict the response of walls of height <3m and >9m.

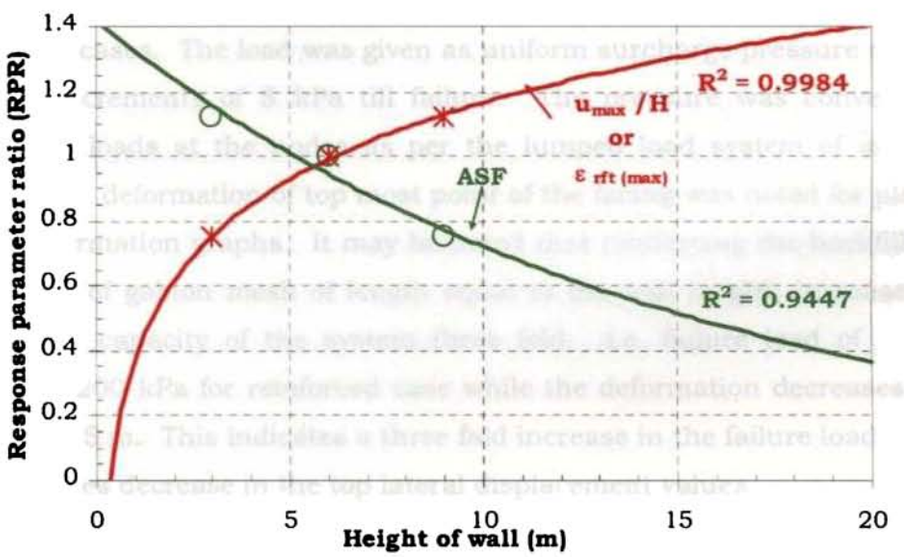


**Fig. 8.6 Variation of the response parameter ratio with wall height**

The results of these studies are made use in the preparation of design charts which is explained in Chapter 9.

## 8.4 EFFECT OF REINFORCEMENT ON BACKFILL

Gabion faced walls are constructed as either unreinforced or reinforced soil type walls. The latter is being preferred for larger heights due to its better performance. But no research works have yet been conducted to understand the effect of reinforcement on gabion faced retaining walls. Numerous studies have been undergone to investigate the reinforcing effect on reinforced soil walls

with flexible facing (Romstad et al. (1976 & 1978), Ogisako et al. (1988), Chew and Schmertmann (1990) and so on). But the behaviour of gabion faced reinforced soil walls is different from them, due to the partial rigidity offered by the gabion facing. Hence, in this study, it is intended to analyse the effect of addition of reinforcement in the backfill portion of gabion faced retaining walls.

The same FE mesh, geometry and material properties described in Chapter 7 has been used in this study also. The same mesh was used both for the reinforced and the unreinforced cases for better comparison of results.

Fig. 8.7 shows the load deformation plots for the reinforced and the unreinforced cases. The load was given as uniform surcharge pressure over the backfill at increments of 5 kPa till failure. The pressure was converted to concentrated loads at the nodes as per the lumped load system of analysis. The horizontal deformation of top most point of the facing was noted for plotting the load deformation graphs. It may be noted that reinforcing the backfill with twelve layers of gabion mesh of length equal to the wall height, increases the load carrying capacity of the system three fold. i.e, failure load of 75 kPa increases to 200 kPa for reinforced case while the deformation decreases from 0.61 m to 0.15 m. This indicates a three fold increase in the failure load as well as a four times decrease in the top lateral displacement values.

Even though a bigger system of wide extents was used for the analysis, the presentation of further results and contour graphs have been limited to a smaller portion (15m long x 6m high) where the reinforcing effect is more pronounced.

Fig. 8.8 shows the difference in the lateral displacement behaviour of the facing in the case of an unreinforced and a reinforced soil gabion faced wall due to self weight loading alone immediately after the construction. In the gabion faced reinforced soil walls, on analysing the magnitudes of displacements, it is seen that, maximum lateral displacement occurs at almost mid wall height. The reinforced case shows an at-rest behaviour with maximum lateral

displacement of 0.004H (as per Table 7.2). In the unreinforced case, the wall shows a linear deflection behaviour and approaches to an active condition even at the stage of self weight loading which is indicated by the maximum lateral displacement value of 0.06H (see Table 7.2).

Vertical soil stress distributions were plotted for both unreinforced and reinforced soil walls at different heights of 0.25H, 0.5H and 0.75H from the base of the wall (Fig. 8.9 (a)). In all the cases, it is seen that the stresses are minimum near the back face of the wall, increasing abruptly and then remaining almost constant throughout the sections. As expected, the stresses are minimum at the top most level considered (0.75H) increasing to a higher value in the bottom levels. The decrease of stresses at the back face of wall at all the sections indicates the sliding of the backfill with respect to the gabion facing, and is particularly true in the case of unreinforced walls.

The plots of stresses at different heights in the unreinforced case (Fig. 8.9 (a)), show a disruption of the smooth pattern at different positions along the sections. This disruption is clearly explained in Fig. 8.9 (b) which shows the vertical stress contours for the unreinforced case. The dotted line shown indicates Rankine's failure plane which is inclined at $45^{o} + \phi/2$ with the horizontal. It is seen that there is a reduction of stresses along the failure plane clearly indicating the impending failure. While scrutinizing the figures of the reinforced case, it is seen that the contours (Fig. 8.9 (c)) and stresses plotted along horizontal sections (Fig. 8.9 (a)) show a smooth pattern. This indicates that the formation of the failure plane has been inhibited by the introduction of reinforcement which redistributes the stresses in the system.

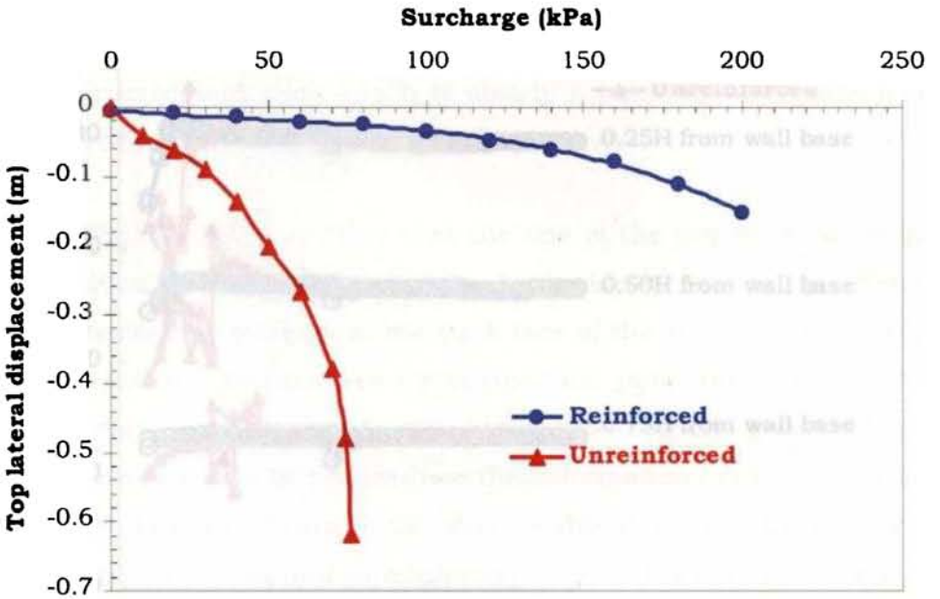


**Fig. 8.7 Load displacement plots**

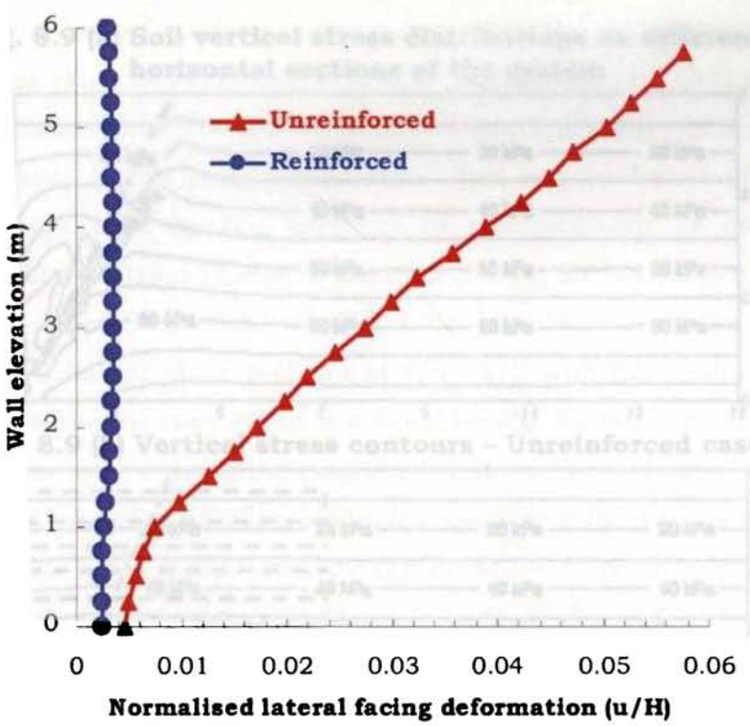


**Fig. 8.8 Lateral displacement of facing at end of construction**

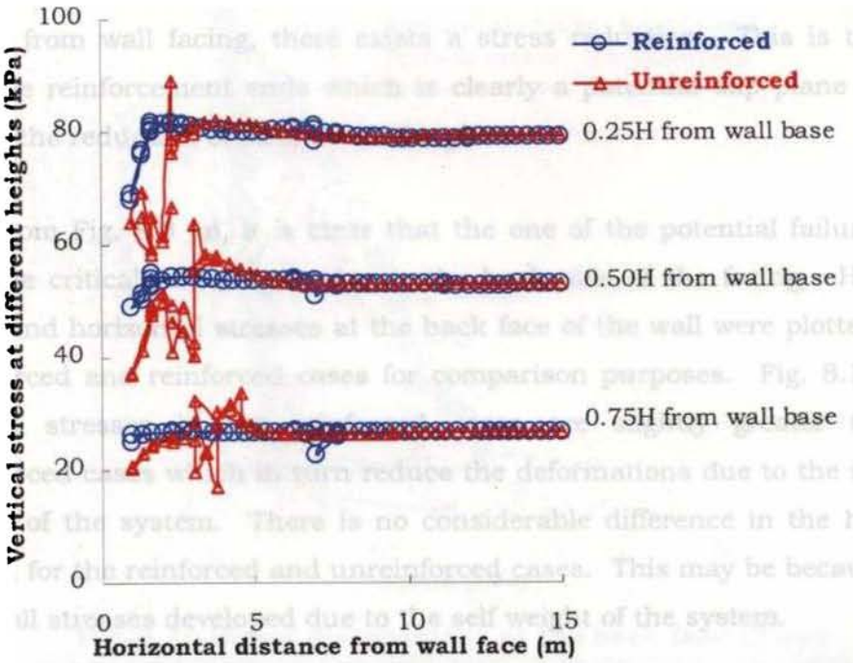


**Fig. 8.9 (a) Soil vertical stress distributions on different horizontal sections of the system**

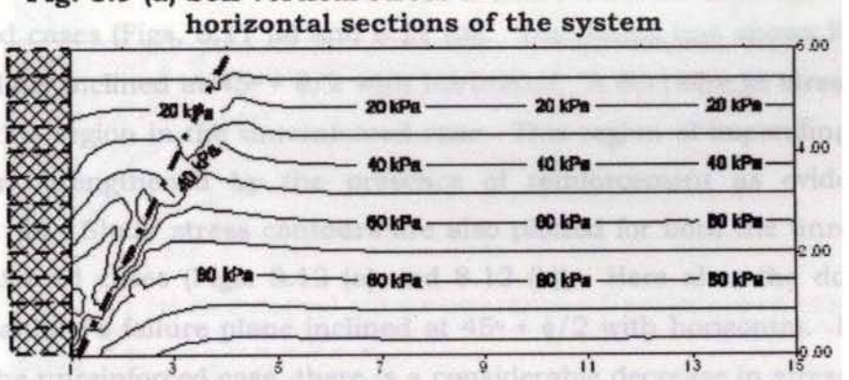


**Fig. 8.9 (b) Vertical stress contours – Unreinforced case**

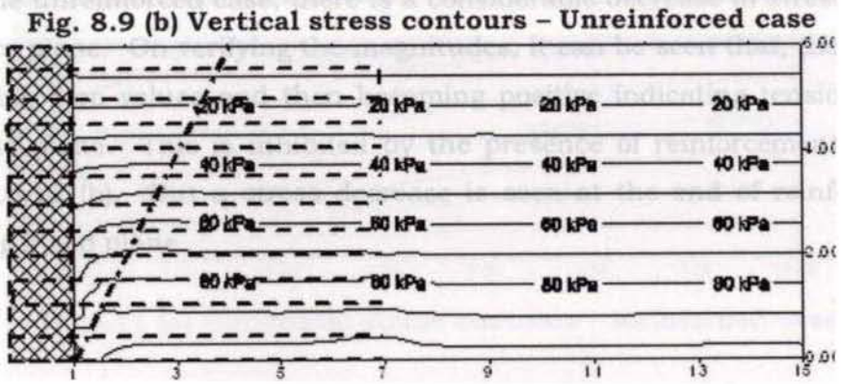


**Fig. 8.9 (c) Vertical stress contours – Reinforced case**

On examining Fig. 8.9 (a) in detail, it is also seen that at 7m horizontal distance from wall facing, there exists a stress reduction. This is the plane where the reinforcement ends which is clearly a potential slip plane and this explains the reduction of stresses in the plane.

From Fig. 8.9 (a), it is clear that the one of the potential failure planes where the critical stresses develop is the back side of the facing. Hence the vertical and horizontal stresses at the back face of the wall were plotted for the unreinforced and reinforced cases for comparison purposes. Fig. 8.10 shows that the stresses in the reinforced cases are slightly greater than the unreinforced cases which in turn reduce the deformations due to the increased stiffness of the system. There is no considerable difference in the horizontal stresses, for the reinforced and unreinforced cases. This may be because of the very small stresses developed due to the self weight of the system.

Horizontal stress contours are plotted for both the unreinforced and reinforced cases (Figs. 8.11 (a) and 8.11 (b)). The dotted line shows Rankine's failure plane inclined at $45^o + \phi/2$ with horizontal. A decrease in stress can be seen in this region in the unreinforced case. This region of impending tension has been strengthened by the presence of reinforcement as evident from Fig. 8.11 (b). Shear stress contours are also plotted for both the unreinforced and reinforced cases (Figs. 8.12 (a) and 8.12 (b)). Here also, the dotted line shows Rankine's failure plane inclined at $45^o + \phi/2$ with horizontal. It is seen that in the unreinforced case, there is a considerable decrease in stresses along the failure plane. On verifying the magnitudes, it can be seen that, the stresses are nearing zero values and then becoming positive indicating tension failure along this plane. This is inhibited by the presence of reinforcement as seen from Fig.8.12 (b). But a stress decrease is seen at the end of reinforcement indicating a slip plane.

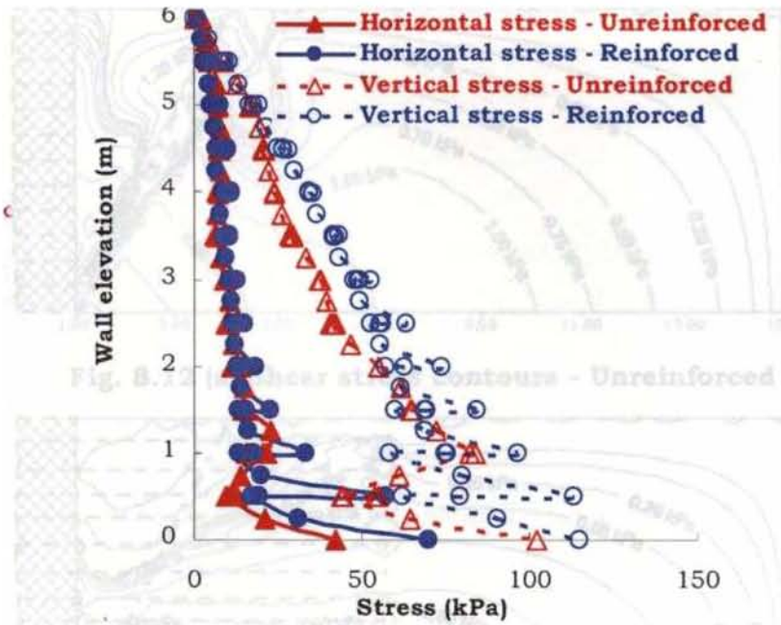


**Fig. 8.10 Stress distributions at the back face of wall**

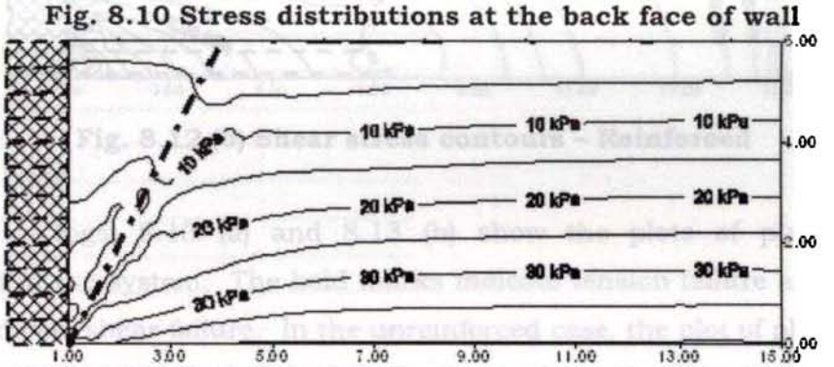


**Fig. 8.11 (a) Horizontal stress contours – Unreinforced case**

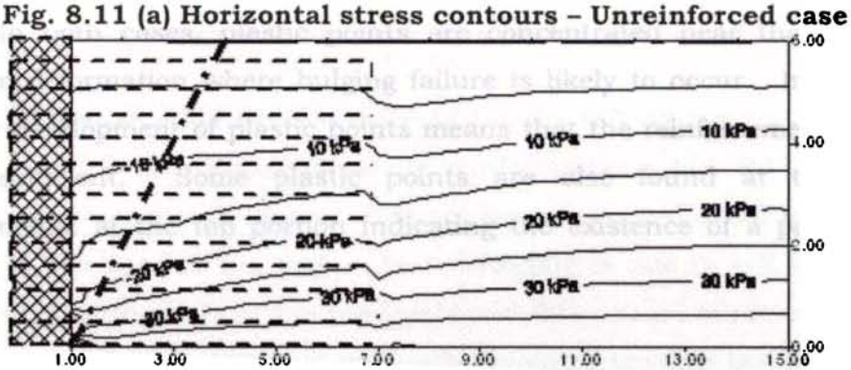


**Fig. 8.11 (b) Horizontal stress contours – Reinforced case**

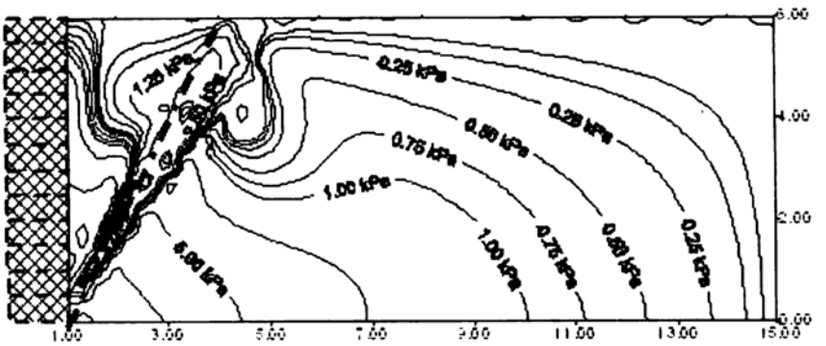


**Fig. 8.12 (a) Shear stress contours – Unreinforced**

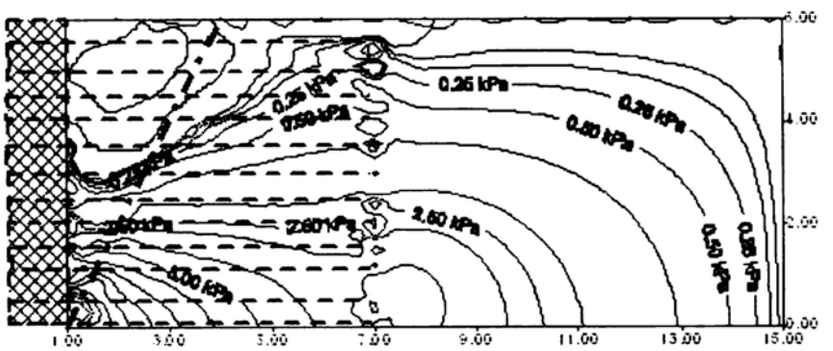


**Fig. 8.12 (b) Shear stress contours – Reinforced**

Figs. 8.13 (a) and 8.13 (b) show the plots of plastic points developed in the system. The bold marks indicate tension failure and the light marks indicate shear failure. In the unreinforced case, the plot of plastic points clearly indicates the Rankine's failure plane where the slipping is likely to occur. In both cases, plastic points are concentrated near the portion of maximum deformation where bulging failure is likely to occur. In reinforced case, the development of plastic points means that the reinforcement provided is not sufficient. Some plastic points are also found at the end of reinforcements at the top portion indicating the existence of a potential slip plane.

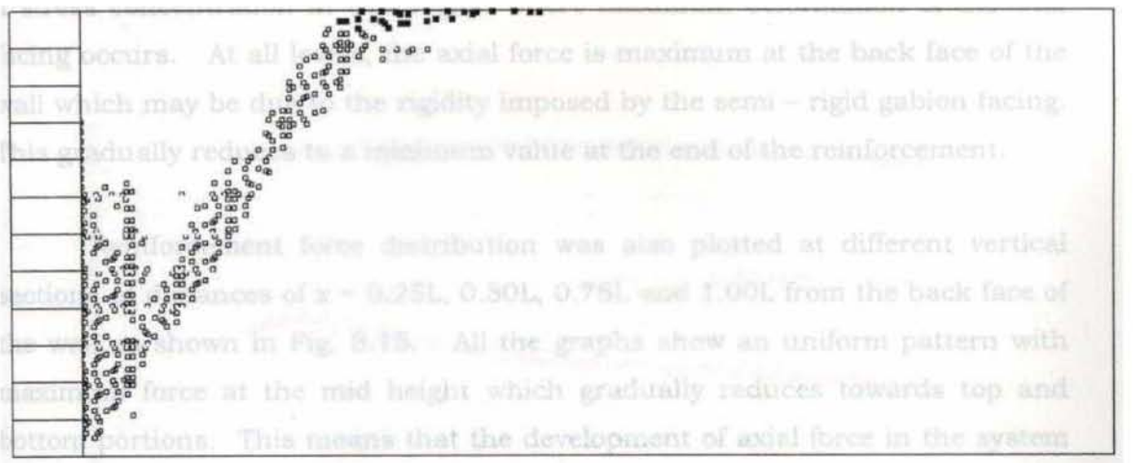

**Fig. 8.13 (a) Plot of plastic points – unreinforced case**

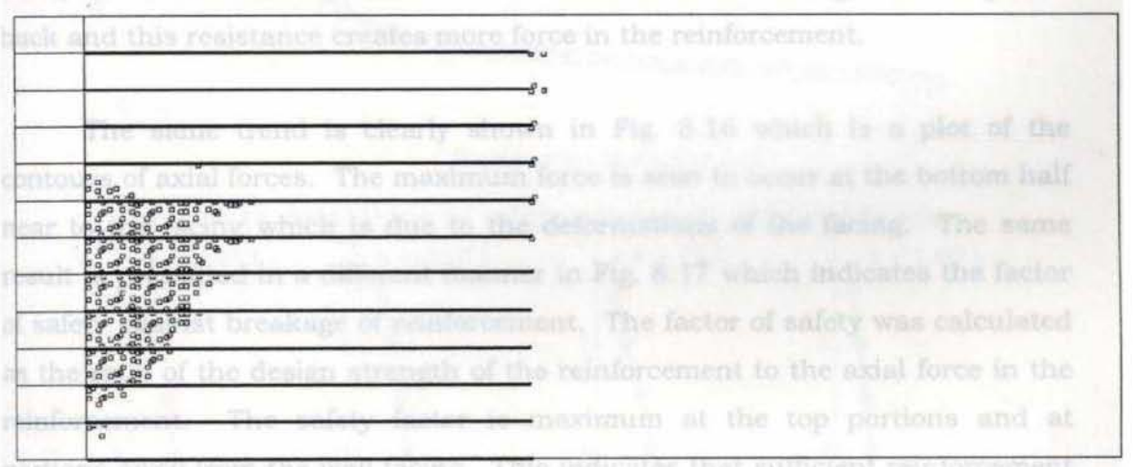

**Fig. 8.13 (b) Plot of plastic points – reinforced case**

After analysing the stresses developed in the soil system, the next step is the analysis of forces developed in the reinforcement. Fig. 8.14 shows the reinforcement force distribution on different heights located at 0.25H, 0.5H and 0.75H from the base of the wall. As the loading is due to self weight only, minimum pressure exists at the top levels and this causes minimum forces at top levels of reinforcement which gradually increases towards bottom, which is clearly seen in Fig. 8.15 also. In Fig. 8.14, the reinforcements at the level y = 0.25H and 0.50H show a rise in the axial forces at the beginning of the reinforcement. This feature is explained by Fig. 8.16, where the contours show

a stress concentration in this region where maximum deformation of the wall facing occurs. At all levels, the axial force is maximum at the back face of the wall which may be due to the rigidity imposed by the semi – rigid gabion facing. This gradually reduces to a minimum value at the end of the reinforcement.

Reinforcement force distribution was also plotted at different vertical sections at distances of x = 0.25L, 0.50L, 0.75L and 1.00L from the back face of the wall as shown in Fig. 8.15. All the graphs show an uniform pattern with maximum force at the mid height which gradually reduces towards top and bottom portions. This means that the development of axial force in the system is clearly governed by the rigidity of the facing. Where facing deformation is more, the reinforcement, which is an extension of the facing, tries to pull it back and this resistance creates more force in the reinforcement.

The same trend is clearly shown in Fig. 8.16 which is a plot of the contours of axial forces. The maximum force is seen to occur at the bottom half near to the facing which is due to the deformations of the facing. The same result is presented in a different manner in Fig. 8.17 which indicates the factor of safety against breakage of reinforcement. The factor of safety was calculated as the ratio of the design strength of the reinforcement to the axial force in the reinforcement. The safety factor is maximum at the top portions and at portions away from the wall facing. This indicates that sufficient reinforcement should be provided near the facing of the wall and at the bottom for minimising the failure risks.

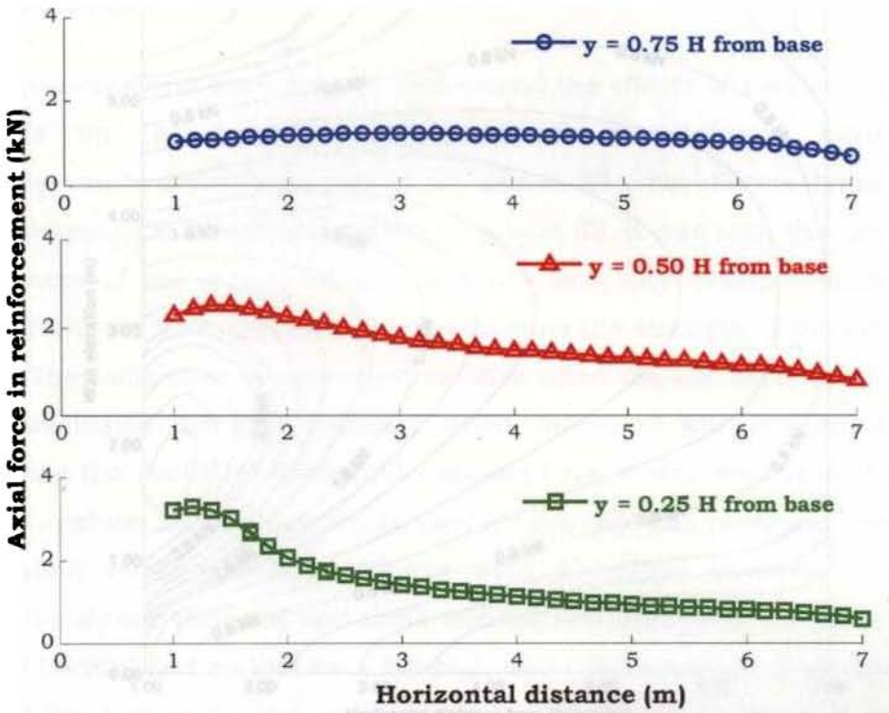


**Fig. 8.14 Axial force in reinforcement at different levels**

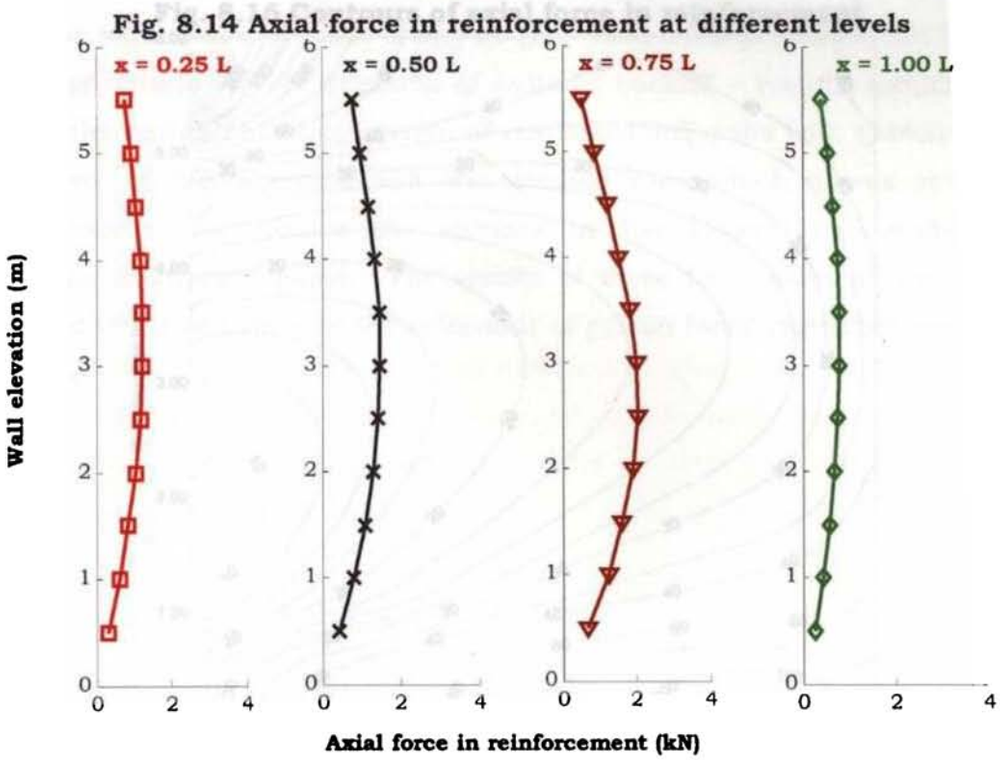


**Fig. 8.15 Axial force in reinforcement on various vertical planes**

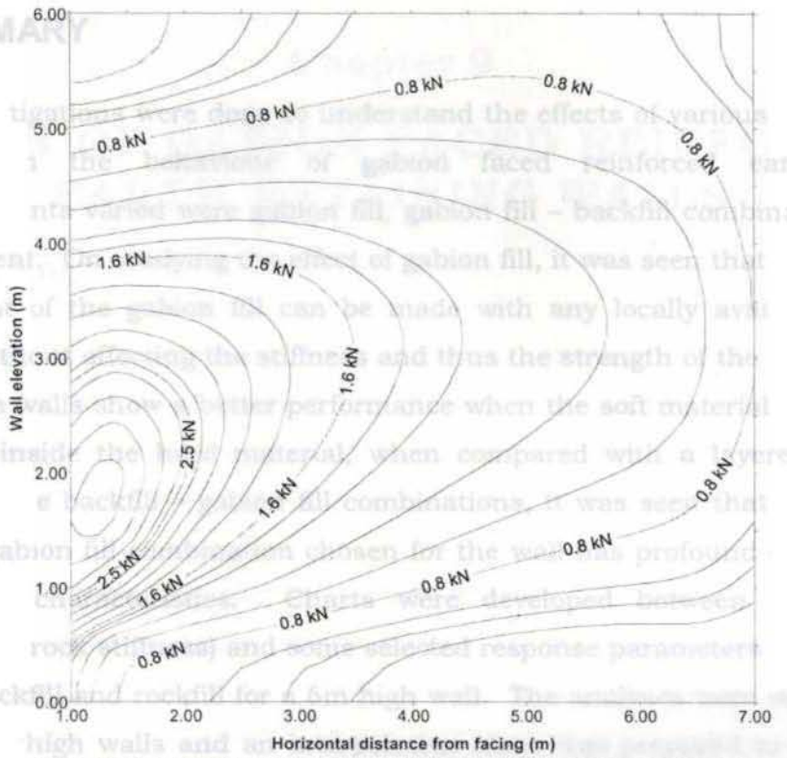


**Fig. 8.16 Contours of axial force in reinforcement**

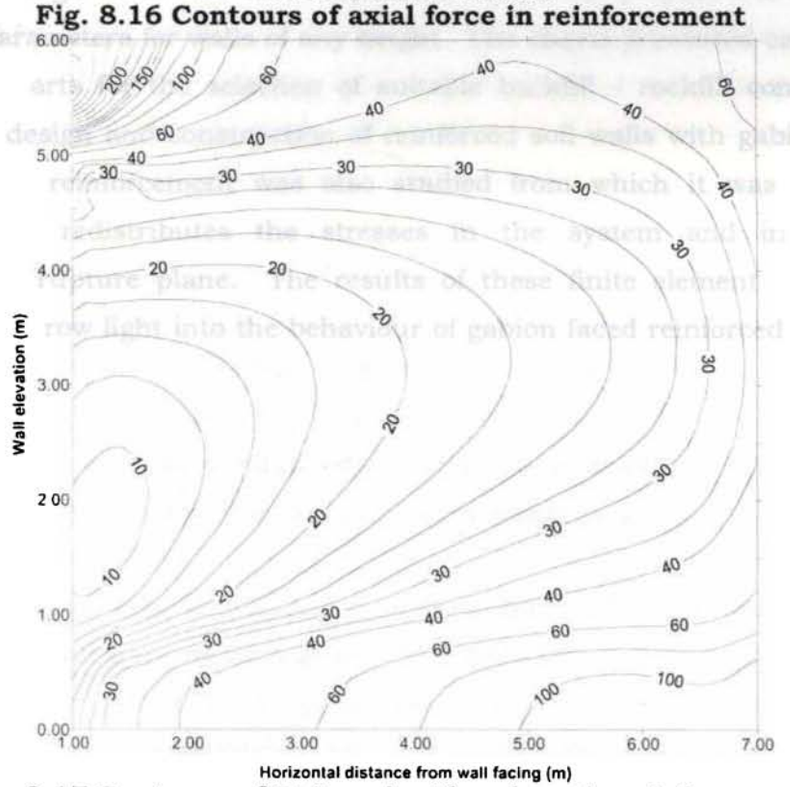


**Fig. 8.17 Contours of FoS against breakage in reinforcement**

## 8.5 SUMMARY

Investigations were done to understand the effects of various component materials on the behaviour of gabion faced reinforced earth walls. The components varied were gabion fill, gabion fill – backfill combinations and reinforcement. On studying the effect of gabion fill, it was seen that nearly 25% replacement of the gabion fill can be made with any locally available cheap material without affecting the stiffness and thus the strength of the system as a whole. The walls show a better performance when the soft material is provided as a core inside the hard material, when compared with a layered system. By varying the backfill – gabion fill combinations, it was seen that the type of backfill – gabion fill combination chosen for the wall has profound effect on its deformation characteristics. Charts were developed between rock factor (indicative of rock stiffness) and some selected response parameters for different types of backfill and rockfill for a 6m high wall. The analyses were repeated for 3m and 9m high walls and an interpolation chart was prepared to derive the response parameters for walls of any height. The charts presented can be used as design charts for the selection of suitable backfill – rockfill combinations during the design and construction of reinforced soil walls with gabion facing. The effect of reinforcement was also studied from which it was seen that reinforcement redistributes the stresses in the system and inhibits the formation of rupture plane. The results of these finite element studies are expected to throw light into the behaviour of gabion faced reinforced earth wall systems.

# Chapter 9

# DESIGN OF GABION FACED REINFORCED EARTH RETAINING WALLS

## 9.1 GENERAL

Design of any structure begins with the selection of trial dimensions. It is then analysed to understand the effect of loads on the behaviour of the structure which yields forces and deformations as results. This information is then compared with criteria for failure conditions to arrive at a safe design.

The gabion faced gravity walls which are more suitable for small heights, follow the conventional design criteria adopted for dry rubble or random rubble masonry walls as per BS 8002 : 1994. This chapter considers the design and analysis of gabion faced reinforced soil walls which are expected to be more economical for larger heights. The modern trend in the design of any structure is the use of the limit state method which always results in a safe and economical design. So this work concentrates on the design of gabion faced reinforced soil walls based on the limit state method.

The conventional practice of design of these walls involves selecting the dimensions of the wall, giving a high factor of safety against different modes of failure which makes the design uneconomical. Moreover, the conventional design involves a trial and error process, which ultimately results in repeated calculations to arrive at a safe design. Here an attempt is made to develop design charts which makes the design process handy and speedy.

The design of gabion faced reinforced soil walls, described herein, is based on the limit state method as per BS 8006: 1995, a detailed description of which is given in Chapter 3. A typical case of gabion faced reinforced earth wall is studied and the conventional design procedure for the same is illustrated initially. This is then followed by the development of design charts using dimensional analysis of the limiting conditions. These charts are expected to

yield a safe, economical and speedy design procedure which overcomes the difficulties mentioned above.

## 9.2 DESIGN PROCEDURE

The following steps are resorted for the design of gabion faced reinforced earth wall.

- Fix the trial dimensions of the wall.
- Determine the forces acting on the wall.
- Check whether the maximum bearing pressure at the base of the wall is within the allowable limit (External stability check).
- Check whether sliding resistance exceeds the active horizontal force by a suitable safety factor (External stability check).
- Check for strength and pullout resistance of the reinforcement layers (Internal stability check).

These steps are repeated iteratively until a suitable design that meets all criteria is achieved.

One metre length of the wall is considered for the analysis. For selecting the overall geometry of the wall, the initial length of reinforcement is taken as 0.7H where H is the height of the wall. The embedment depth ($D_m$) may be fixed as the maximum value obtained from Eqns. 3.5 and 3.6. The width of the gabion facing depends on the dimensions of the gabions; usually available as multiples of 0.5m. For reinforced soil type walls, the facing width is usually kept to a minimum value of 0.5m. The initial sizing of a typical gabion faced reinforced earth wall is shown in Fig. 9.1.

The analysis detailed below accounts for the effects of gabion facing wherever necessary. Surcharge considered is uniformly distributed load only. The effects of vertical strip loading or horizontal shear loading over the reinforced fill are not considered in the analysis.

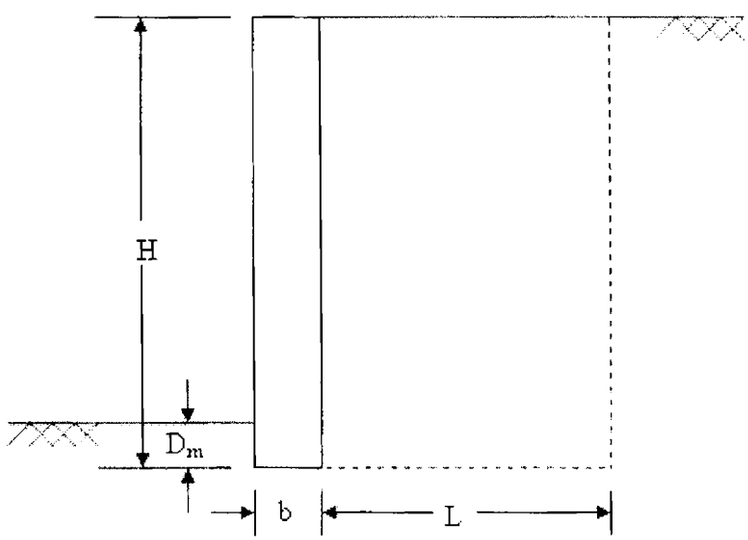


**Fig. 9.1 Initial dimensions of the wall**

### 9.2.1 Forces acting on the wall

The main forces acting on gabion walls are the vertical forces from the weight of the gabions, weight of reinforced soil block, the lateral earth pressure acting on the back face of this soil block and the surcharge over the backfill. These forces are used herein to illustrate the main design principles. If other forces are encountered, such as vehicular loads or seismic loads, they must also be included in the analysis. The soil properties for the reinforced soil block, retained fill and foundation, gabion facing, together with the superimposed loads considered in the stability calculations are shown in Fig. 9.2. In the figure it is assumed that the intensity of surcharge over the backfill and the retained soil is the same. Also the foundation soil and the retained earth are of the same type. The forces acting may be calculated as:

Weight of gabion facing, $W_g$ = $b\,H\,\gamma_g$ ..... (9.1)

Weight of reinforced soil block, $W_s$ = $L\,H\,\gamma_{sl}$ ..... (9.2)

Weight due to surcharge, $W_q$ = $q\,L$ ..... (9.3)

Lateral force due to retaining soil, $P_s$ = $K_{a2}\,\gamma_{s2}\,H^2 / 2$ ..... (9.4)

Lateral force due to surcharge, $P_q$ = $K_{a2}\,q\,H$ ..... (9.5)

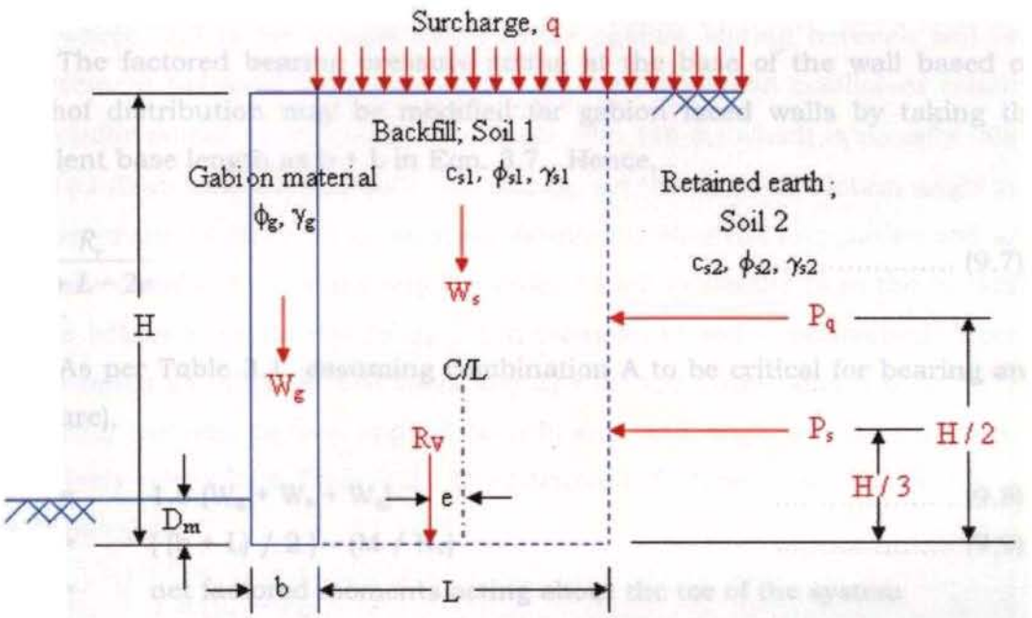


**Fig. 9.2 Material properties and principal forces**

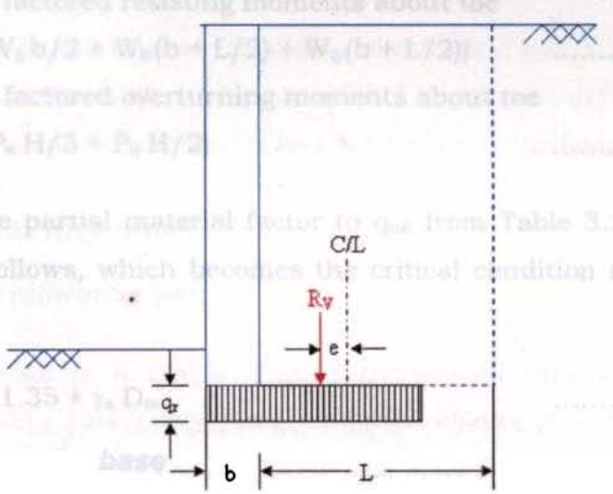


**Fig. 9.3 Pressure distribution along base of wall**

The coefficient of active earth pressure, $K_{a2}$ may be calculated as:

$$K_{a2} = \frac{1 - \sin\phi_{s2}}{1 + \sin\phi_{s2}} \qquad \text{..... (9.6)}$$

## 9.2.2 External stability analysis

### *9.2.2.1 Bearing and tilt failure*

The factored bearing pressure acting at the base of the wall based on Meyerhof distribution may be modified for gabion faced walls by taking the equivalent base length as b + L in Eqn. 3.7. Hence,

$$q_r = \frac{R_v}{b + L - 2e} \qquad \text{..... (9.7)}$$

As per Table 3.1, assuming combination A to be critical for bearing and tilt failure),

$R_v$ = $1.5\ (W_g + W_s + W_q)$ ..... (9.8)

e = $\{ (b + L) / 2 \} - (M / R_v)$ ..... (9.9)

M = net factored moments acting about the toe of the system

M = $M_r - M_o$ ..... (9.10)

$M_r$ = Total factored resisting moments about toe

$M_r$ = $1.5\ (W_g\, b/2 + W_s (b + L/2) + W_q (b + L/2))$ ..... (9.11)

$M_o$ = Total factored overturning moments about toe

$M_o$ = $1.5\ (P_s\, H/3 + P_q\, H/2)$ ..... (9.12)

Applying the partial material factor to $q_{ult}$ from Table 3.2, the Eqn. 3.8 gets modified as follows, which becomes the critical condition for bearing and tilt failure:

$q_r \leq q_{ult} / 1.35 + \gamma_s D_m$ ..... (9.13)

### *9.2.2.2 Sliding along the base*

In the case of gabion faced reinforced soil walls, at the base of the reinforced soil block, the gabion wire mesh comes in contact with the foundation soil. As per Table 3.1, combination B is considered as the worst combination for sliding along the base. Applying appropriate partial material factors from Table 3.2, Eqn. 3.9 for long term stability, where there is reinforcement – to – soil contact at the base of the structure, gets modified as:

$$1.3 R_h \leq R_v \, a \tan\phi_{s2} + \frac{\alpha \, c_{s2} \, L}{1.6} \qquad \text{..... (9.14)}$$

where, 1.3 is the partial safety factor against sliding between soil and reinforcement obtained from Table 3.2, a is the interaction coefficient relating soil - reinforcement interfacial friction angle with tan $\phi_{s2}$ which is usually taken as 2/3 (Gulhati and Dutta, 2005) , $\phi_{s2}$ and $c_{s2}$ are the internal friction angle and cohesion of the retained fill respectively (assuming that the foundation soil and the retained soil are the same and the retained soil is weaker than the backfill), α is the adhesion coefficient relating soil cohesion to soil - reinforcement bond usually taken as unity for stiff clays and 2/3 for soft clays, and, 1.6 and 1 are the partial material factors applied to cohesion and angle of internal friction respectively taken from Table 3.2. The horizontal factored disturbing force, $R_h$, is calculated as:

$$R_h = 1.5 \, (P_s + P_q) \qquad \text{..... (9.15)}$$

$$R_v = W_g + W_s \qquad \text{..... (9.16)}$$

$W_q$ need not be considered for sliding check as it has a partial factor of 0.0 as per Table 3.1 for load combination B. The corresponding partial load factor is unity for the stabilising forces and 1.5 for the disturbing forces.

## 9.2.3 Internal stability analysis

### *9.2.3.1 Rupture of reinforcement*

Load combination A (Table 3.1) is considered critical in this case. Eqn. 3.10 gets modified as follows, neglecting the effects of vertical strip loads and horizontal shear loads on the reinforced soil block.

$$T_j = T_{pj} - T_{cj} \qquad \text{.....(9.17)}$$

Applying partial factors from Tables 3.1 and 3.2, Eqn. 3.11 and Eqn. 3.12 for calculating $T_{pj}$ and $T_{cj}$, become:

$$T_{pj} = \frac{1.5\, K_{a1}\,(\gamma_{s1} h_j + q)\, S_{vj}}{1 - \dfrac{K_{a2}\,(\gamma_{s2} h_j + 3\,q)\left(\dfrac{h_j}{L}\right)^2}{3\,(\gamma_{s1} h_j + q)}} \qquad \text{..... (9.18)}$$

$$T_{cj} = 2\, S_{vj} \frac{c}{1.6} \sqrt{K_a} \qquad \text{..... (9.19)}$$

where, 1.5 is the partial factor applied to loads in combination A (Table 3.1) and 1.6 is the partial material factor applied to cohesion as per Table 3.2. Condition for stability against mesh rupture from Eqn. 3.13 gets modified as:

$$\frac{T_D}{1.1} \geq T_j \qquad \text{..... (9.20)}$$

in which, $T_j$ is the maximum value obtained from Eqn. 9.17. The gabion faced retaining structures are mainly built along highways and beside railway lines and hence the partial factor for economic ramifications of failure is taken as 1.1 here.

In the case of gabion mesh as seen in Chapter 3, the basic material is stainless steel which is heavily galvanised or galvanised plus PVC coated having thickness of approximately 4mm. From Section 3.4.3, it may be seen that, for galvanised steel mesh, $f_m$ may be taken as 1.5 as it is subjected to axial loads only. For galvanised mesh with PVC coating, the partial material factors for gabion mesh reinforcement may be chosen as shown in Table 9.1. Substituting the partial factor values from Table 9.1 in Eqn. 3.2, for PVC coated gabion mesh, $f_m$ may be obtained as 1.5. Hence, it may be inferred that, whatever be the type, the gabion mesh has a partial material factor of 1.5. Hence, in accordance with Eqn. 3.1, design strength of gabion mesh,

$$T_D = T_{ult} \,/\, 1.5 \qquad \text{..... (9.21)}$$

**Table 9.1 Determination of $f_m$ for PVC coated gabion mesh**

| Partial factor | Value chosen | Reason |
|---|---|---|
| $f_{m111}$ | 1.0 | Assuming that the manufacturing of mesh is done according to standards |
| $f_{m112}$ | 1.0 | Assuming that the mesh size is greater than the minimum specified dimension used for determining the base strength |
| $f_{m121}$ | 1.0 | Assuming that large quantities of data for determination of base strength over a long period of time are available |
| $f_{m122}$ | 1.0 | Assuming that the extrapolation of test data can be done over one log cycle of time |
| $f_{m21}$ | 1.5 | Assuming a value grater than unity since, for gabion mesh, minimum steel thickness is less than 4 mm |
| $f_{m22}$ | 1.0 | Since protective layer of PVC coating is provided |

### *9.2.3.2 Loss of adherence of reinforcement*

The perimeter $P_j$ (Eqn. 3.14) of the jth layer of reinforcing elements is modified as follows:

$$P_j \geq \frac{T_j}{\dfrac{(2/3)\tan\phi_{s1}\, L_{ej}\, \gamma_{s1}\, h_j}{1.3\times 1.1} + \dfrac{\alpha\, c\, L_{ej}}{1.6\times 1.3\times 1.1}} \qquad \text{..... (9.22)}$$

where, 1.3 is the partial factor for reinforcement pullout resistance taken from Table 3.2. As per Section 9.2.2.2, $\alpha$ = 1 for stiff clays and 2/3 for soft clays, and 2/3 is the soil – reinforcement interaction factor (a). For gabion faced walls, since the reinforcement is in the form of sheet, perimeter, $P_j$ = 2 m, considering unit length of the wall for analysis. It is also to be noted that load combination B is critical for reinforcement pullout considerations (Table 3.1) and hence the effect of surcharge may be neglected and partial load factor may be taken as unity for self weights.

Thus Eqn. 9.22 becomes:

$$2\,L_{ej} \;\geq\; \frac{T_j}{\dfrac{(2/3)\tan\phi_{s1}\,\gamma_{s1}\,h_j}{1.3\times 1.1} + \dfrac{\alpha\,c}{1.6\times 1.3\times 1.1}} \qquad \text{..... (9.23)}$$

in which, $T_j$ may be calculated from Eqn. 9.17. But Eqn. 9.18 for obtaining $T_{pj}$ gets modified as:

$$T_{pj} \;=\; \frac{K_{a1}\,\gamma_{s1}\,h_j\,S_{vj}}{1 - \dfrac{1.5\,K_{a2}\,\gamma_{s2}\,h_j}{3\,\gamma_{s1}\,h_j}\left(\dfrac{h_j}{L}\right)^2} \qquad \text{..... (9.24)}$$

The modification is due to the load combination B where $f_{fs}$ = 1.0 for the self weights, $f_{fs}$ = 1.5 for earth pressure behind the structure and $f_q$ = 0 (Table 3.1).

### 9.2.4 Serviceability limit state

For gabion mesh, the reinforcement is metallic and hence creep is negligible and consequently, the strain $\varepsilon_j$ in the jth layer of reinforcements may be estimated from Eqn. 3.15. $T_{avj}$ is the average tensile load along the length of the jth layer of reinforcements which may be calculated as $T_j$ from Eqn. 9.17. But Eqn. 9.18 for calculating $T_{pj}$ gets modified as:

$$T_{pj} \;=\; \frac{K_{a1}\,\gamma_{s1}\,h_j\,S_{vj}}{1 - \dfrac{K_{a2}\,\gamma_{s2}\,h_j}{3\,\gamma_{s1}\,h_j}\left(\dfrac{h_j}{L}\right)^2} \qquad \text{..... (9.25)}$$

The modification is because of the reason that the load combination to be considered for serviceability limit state is the Combination C in which $f_{fs}$ = 1 and $f_q$ = 0 as seen from Table 3.1.

## 9.3 DESIGN EXAMPLE

The design and analysis of gabion faced reinforced earth retaining walls explained in Section 9.2 is illustrated with standard numerical values in this section.

### 9.3.1 Data available from site

| | | |
|---|---|---|
| Height of wall, H | = | 5 m |
| Unit weight of material in the gabion box, $\gamma_g$ | = | 20 kN/m$^3$ |
| Unit weight of retained soil, $\gamma_{s2}$ | = | 20 kN/m$^3$ |
| Cohesion of retained soil, $c_{s2}$ | = | 0 kPa |
| Internal friction angle of retained soil, $\phi_{s2}$ | = | 35° |
| Assuming that the retained soil itself is used for backfilling, | | |
| Unit weight of backfill material, $\gamma_{s1}$ | = | 20 kN/m$^3$ |
| Cohesion of backfill material, $c_{s1}$ | = | 0 kPa |
| Internal friction angle of backfill, $\phi_{s1}$ | = | 35° |
| Ultimate bearing capacity of foundation soil, $q_{ult}$ | = | 650 kN/m$^2$ |
| Surcharge, q | = | 10 kN/m$^2$ |
| Ultimate tensile strength of mesh confined in soil, $T_{ult}$ | = | 51 kN/m |
| Allowable strain in mesh, $\varepsilon_{all}$ | = | 10% |
| Stiffness of the mesh, EA | = | 8000 kN |

### 9.3.2 Initial dimensions

From the available data listed above, the initial dimensions of the structure to be designed are fixed as per Section 9.2.

| | | |
|---|---|---|
| Length of reinforcement ($L \approx 0.7H$) | = | 4 m |
| Depth of embedment, $D_m$ | = | Max of. ($H/20$ or $1.35 \times 10^{-3}\ q_{all}$) |
| | ≈ | 0.5 m (taking $q_{all} = q_{ult}/2$) |
| Width of gabion facing, b | = | 0.5 m |

### 9.3.3 Forces acting on the wall

| | | |
|---|---|---|
| Weight of gabion facing, $W_g$ | = | 50 kN/m (from Eqn. 9.1) |
| Weight of reinforced soil block, $W_s$ | = | 400 kN/m (from Eqn. 9.2) |
| Weight due to surcharge, $W_q$ | = | 40 kN/m (from Eqn. 9.3) |

Lateral force due to retaining soil, $P_s$ = 67.75 kN/m (from Eqn. 9.4)

Lateral force due to surcharge, $P_q$ = 13.55 kN/m (from Eqn. 9.5)

## 9.3.4 External stability analysis

### *9.3.4.1 Bearing and tilt failure*

Resultant of all factored vertical loads, $R_v$ = 735 kN/m (from Eqn.9.8)

Total factored resisting moments about toe, $M_r$ = 1668.75 kNm/m (from Eqn. 9.11)

Total factored overturning moments about toe, $M_o$ = 220.2 kNm/m (from Eqn. 9.12)

Net factored moments about toe, M = 1448.57 kNm/m (from Eqn. 9.10)

Eccentricity, e = 0.28 m (from Eqn. 9.9)

Factored bearing pressure at the base of the wall, $q_r$ = 186.47 kPa (from Eqn. 9.7)

On calculating the term, $q_{ult}$ / 1.35 + $\gamma$ $D_m$, the value is obtained as 491.5kPa which is greater than 186.47 kPa, the factored bearing pressure acting at the base of the wall. Hence it can be concluded that the designed structure is safe against tilt and bearing failures.

### *9.3.4.2 Sliding along the base*

Horizontal factored disturbing force, $R_h$ = 121.9 kN/m (from Eqn. 9.15)

Resultant of all factored vertical loads, $R_v$ = 450 kN/m (from Eqn. 9.16)

Factored sliding force (1.3 $R_h$) = 158.5 kN/m

Factored resisting force ($R_v$ a tan $\phi_{s2}$ (taking $c_{s2}$ as zero)) = 210 kN/m (assuming a as 2/3)

Since the factored sliding force is less than the factored resisting force, the structure may be considered safe against sliding failure about its base.

### 9.3.5 Internal stability analysis

Design strength of the gabion wire mesh, $T_D$ = 34 kN/m (from Eqn. 9.21). For internal stability analysis, it is assumed that the spacing between reinforcements ($S_{vj}$), is 0.5m. Assuming that the failure wedge passes through a plane inclined at an angle ($45^o + \phi_{s1}/2$) with the horizontal,

Length of reinforcement in the active zone, $L_{aj}$ = $(H - h_j) \tan (45^o - \phi_{s1}/2)$ ..... (9.26)

Minimum length of reinforcement required for internal stability, $L_{min} = L_{aj} + L_{cj}$ ..... (9.27)

Table 9.2 shows the internal stability calculations against mesh breakage and it can be seen that the tension developed in the reinforcements is less than the factored design strength. Table 9.3 shows the internal stability calculations against mesh pullout and it can be seen that the maximum length of reinforcement required as per internal stability calculations is 2.6m which is very much less than the provided length of 4m. Hence the designed structure may be considered safe against internal failure modes.

**Table 9.2 Internal stability calculations for mesh breakage**

| $h_j$ (m) | $S_{vj}$ (m) | $T_{pj}$ (Eqn. 9.18) (kN/m) | $T_{cj}$ (Eqn. 9.19) (kN/m) | $T_j$ (Eqn. 9.17) (kN/m) | Check (Eqn. 9.20) |
|---|---|---|---|---|---|
| 0.50 | 0.50 | 4.08 | 0 | 4.08 | Safe |
| 1.00 | 0.50 | 6.16 | 0 | 6.16 | Safe |
| 1.50 | 0.50 | 8.29 | 0 | 8.29 | Safe |
| 2.00 | 0.50 | 10.49 | 0 | 10.49 | Safe |
| 2.50 | 0.50 | 12.80 | 0 | 12.80 | Safe |
| 3.00 | 0.50 | 15.22 | 0 | 15.22 | Safe |
| 3.50 | 0.50 | 17.80 | 0 | 17.80 | Safe |
| 4.00 | 0.50 | 20.56 | 0 | 20.56 | Safe |
| 4.50 | 0.50 | 23.56 | 0 | 23.56 | Safe |
| 5.00 | 0.25 | 13.42 | 0 | 13.42 | Safe |

**Table 9.3 Internal stability calculations for mesh pullout**

| $h_j$ (m) | $S_{vj}$ (m) | $T_{pj}$ (Eqn. 9.24) (kN/m) | $T_{cj}$ (Eqn. 9.19) (kN/m) | $T_j$ (Eqn. 9.17) (kN/m) | $L_{aj}$ (Eqn. 9.26) (m) | $L_{ej}$ (Eqn. 9.23) (m) | $L_{min}$ (Eqn. 9.27) (m) |
|---|---|---|---|---|---|---|---|
| 0.50 | 0.50 | 1.36 | 0 | 1.36 | 2.34 | 0.21 | 2.55 |
| 1.00 | 0.50 | 2.73 | 0 | 2.73 | 2.08 | 0.21 | 2.29 |
| 1.50 | 0.50 | 4.14 | 0 | 4.14 | 1.82 | 0.21 | 2.03 |
| 2.00 | 0.50 | 5.61 | 0 | 5.61 | 1.56 | 0.21 | 1.78 |
| 2.50 | 0.50 | 7.15 | 0 | 7.15 | 1.30 | 0.22 | 1.52 |
| 3.00 | 0.50 | 8.80 | 0 | 8.80 | 1.04 | 0.22 | 1.27 |
| 3.50 | 0.50 | 10.58 | 0 | 10.58 | 0.78 | 0.23 | 1.01 |
| 4.00 | 0.50 | 12.54 | 0 | 12.54 | 0.52 | 0.24 | 0.76 |
| 4.50 | 0.50 | 14.72 | 0 | 14.72 | 0.26 | 0.25 | 0.51 |
| 5.00 | 0.25 | 8.59 | 0 | 8.59 | 0.00 | 0.24 | 0.13 |

### 9.3.6 Serviceability limit considerations

The tension and strain in each layer of reinforcement is calculated using Eqn. 9.25 and Eqn. 3.15 respectively and tabulated in Table 9.4. The strain values developed in the reinforcements are below the permissible limit of 10%. Hence the deformations developing within the system are acceptable.

**Table 9.4 Strain in the reinforcements**

| $h_j$ (m) | $T_j$ (Eqn. 9.25) (kN/m) | $\varepsilon_j$ (Eqn. 3.15) % |
|---|---|---|
| 0.50 | 1.36 | 0.068 |
| 1.00 | 2.73 | 0.136 |
| 1.50 | 4.12 | 0.206 |
| 2.00 | 5.55 | 0.277 |
| 2.50 | 7.02 | 0.351 |
| 3.00 | 8.56 | 0.428 |
| 3.50 | 10.19 | 0.509 |
| 4.00 | 11.92 | 0.596 |
| 4.50 | 13.77 | 0.688 |
| 5.00 | 7.89 | 0.394 |

## 9.4 DEVELOPMENT OF DESIGN CHARTS

In the conventional design procedure, if at any stage, the design is found to be unsafe or uneconomical, the entire design procedure has to be reworked, which makes the design process lengthy and cumbersome. Design charts always provide easy and quick methods to arrive at suitable design parameters. For the development of these charts, often it becomes necessary to make suitable assumptions in the design procedure keeping in view that the fundamental principles are followed.

### 9.4.1 Assumptions

In order to simplify the preparation of design charts, certain assumptions were used without causing much variations in the final results.

1. The soil at site is used as the backfill material. Even though the ideal backfill material is a frictional material, the non availability of such type of soil in the near locality may necessitate the use of soil at site itself as a backfill material. Moreover, the design using soils with low frictional resistance will be on the safer side.

2. The retained soil and the foundation soil are the same, which is the condition in most of the cases.

3. The gabion fill and backfill are of the same density and hence the ratio of unit weight of the material in the gabion box ($\gamma_g$) to unit weight of backfill material ($\gamma_s$) is taken as unity. Even though in actual practice this may not be true, the actual ratio between the two will lead only to lesser values of length of reinforcement (L), which means, this assumption provides conservative results.

4. Effect of water table is not considered except in assigning corresponding in situ densities of the soil. Even though there is presence of water table at site, it is a general assumption in the design of gabion faced walls

that due to the highly permeable nature of the gabions there is no pore pressure development in the backfill.

5. Effect of cohesion and inclination of facing are neglected, as they always add on to the stability of a structure which ultimately takes the design to a safer side.

6. Surcharge over the backfill is taken as a uniformly distributed load and the intensity of surcharge over the backfill and the retained soil are assumed to be the same.

## 9.4.2 Selection of variables

Design charts were developed for each mode of failure i.e., external and internal modes of failure as per the limit state method explained in Chapter 3. Different geometric parameters have been considered and non dimensional parameters have been used to derive the charts. In the external mode of failure, bearing and tilt as well as sliding modes of failure were considered. In the internal modes of failure, safety against mesh breakage and mesh pullout was taken into account. For the preparation of design charts, equations for limiting conditions were taken and they were converted into functions of non-dimensional parameters, which serves as variables. Graphs were plotted such that the required length and spacing of reinforcement, for a safe and economical design may be obtained directly from the charts.

## 9.4.3 External stability analysis

### *9.4.3.1 Bearing and tilt failure*

The limiting condition for bearing and tilt failure was obtained from Eqn. 9.13 by neglecting the effect of embedment, which is small when compared to the height of wall. Then the limiting condition becomes:

$$q_r = q_{ult} / 1.35 \qquad \text{..... (9.28)}$$

Substituting the value of $q_r$ from Eqn. 9.7 and on simplification, Eqn. 9.28 comes to the form:

$$1.0125\,(W_g + W_s + W_q)^2$$
$$= q_{ult}\,(W_g\, b/2 + W_s\,(b + L/2) + W_q\,(b + L/2) - P_s\, H/3 - P_q\, H/2) \qquad \text{..... (9.29)}$$

Considering the assumptions cited in Section 9.4.1 and substituting the values from Eqns. 9.1 to 9.5, Eqn. 9.29 may be converted to dimensionless form as:

$$1.0125\,\{(b/H)^2 + (L/H)^2 + (q/\gamma_s H)^2\,(L/H)^2 + 2\,(b/H)\,(L/H) + 2\,(q/\gamma_s H)\,(L/H)^2$$
$$+ 2\,(b/H)\,(L/H)\,(q/\gamma_s H)\} - (q_{ult}/\gamma_s H)\,\{(1/2\,(b/H)^2 + (b/H)\,(L/H) + (1/2\,(L/H)^2$$
$$+ (b/H)\,(L/H)\,(q/\gamma_s H) + 1/2\,(q/\gamma_s H)\,(L/H)^2 - K_a/6 - K_a/2\,(q/\gamma_s H)\} = 0 \qquad \text{..... (9.30)}$$

Putting $q/\gamma_s H$ as surcharge factor, SF, $q_{ult}/\gamma_s H$ as bearing capacity factor, BCF and b/H as facing width factor, FWF and then rewriting in terms of length factor, LF = L/H, Eqn. 9.30 reduces to a quadratic form as:

$$(LF)^2\,\{(1 + SF)\,[1.0125\,(1 + SF) - BCF/2]\}$$
$$+ (LF)\,\{FWF\,(1 + SF)\,[2.025 - BCF]\}$$
$$+ \{FWF^2\,(1.0125 - BCF/2) + (K_a/6)\,BCF\,(1 + 3SF)\} = 0 \qquad \text{..... (9.31)}$$

Solving the quadratic equation, the length of reinforcement which is an indication of the base width of the reinforced structure, may be obtained. This gives a safe design value against bearing and tilt failure. From Eqn. 9.31, it is clear that LF depends on the non dimensional factors $\phi$ (in terms of $K_a$), SF, FWF and BCF.

$$LF = f\,(\phi,\ SF,\ FWF,\ BCF) \qquad \text{..... (9.32)}$$

Using the relation from Eqn. 9.31, graph can be plotted after obtaining different LF values by varying $\phi$, SF and FWF for BCF = 5 and is shown in Fig. 9.4. Similarly, LF values were obtained for other values of BCF like 7.5, 10, 15, 20, 25, 30, 40 and 50.

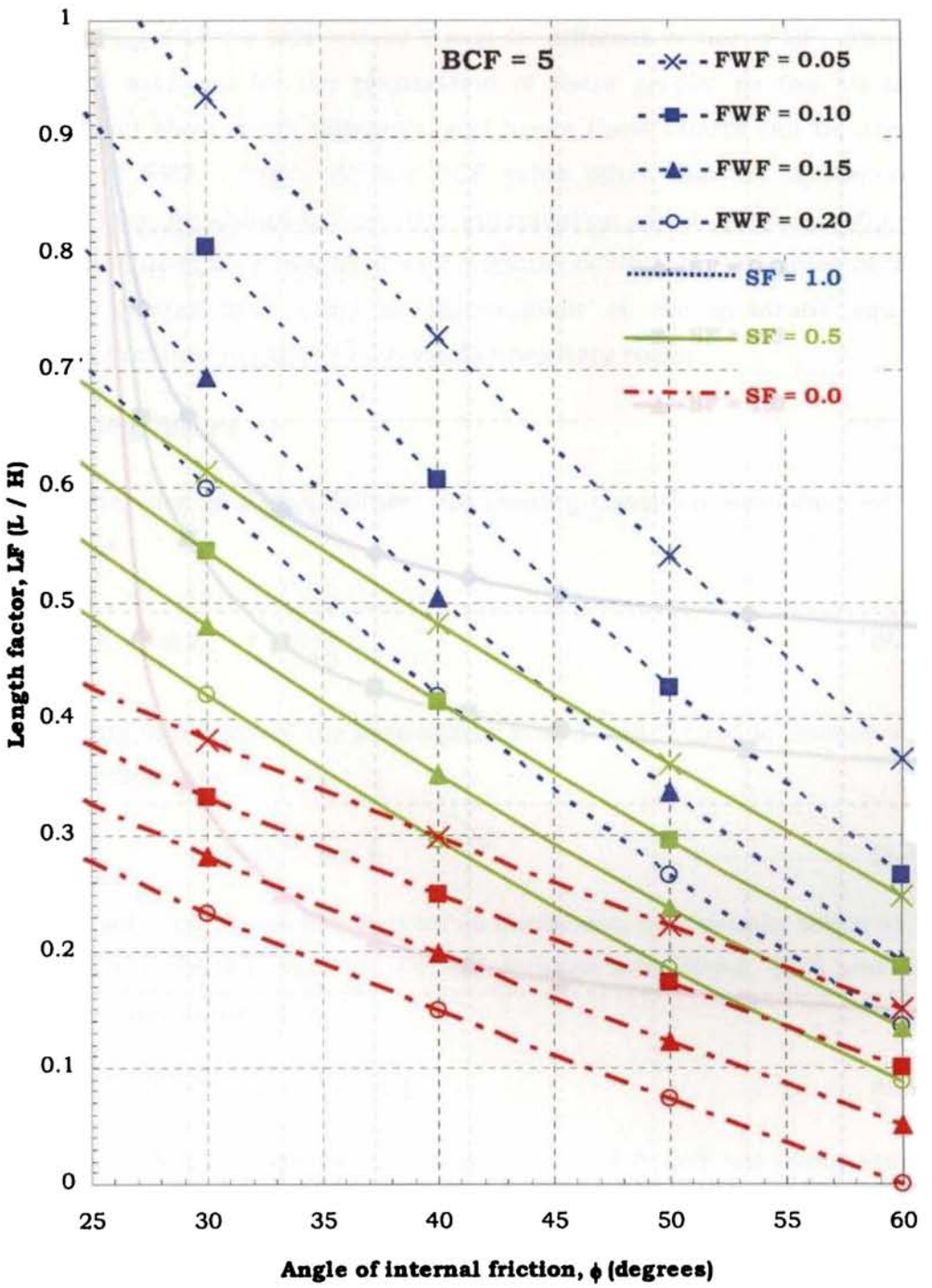


**Fig. 9.4 Design chart from bearing and tilt considerations for BCF = 5**

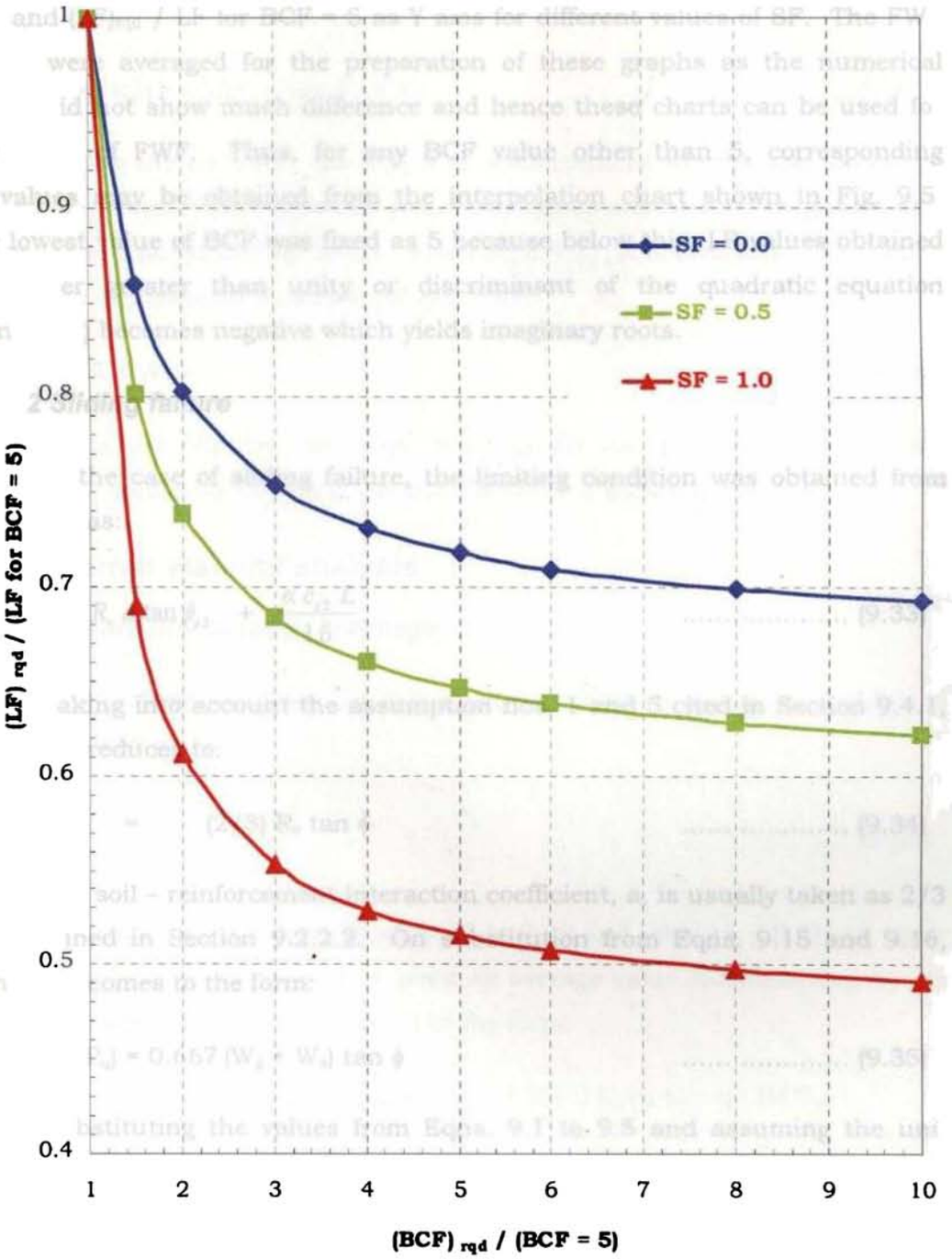


**Fig. 9.5 Design chart from bearing and tilt considerations – Interpolation chart**

Thereafter, charts (Fig. 9.5) were obtained with $(BCF)_{rqd}$ / BCF = 5 as X axis and $(LF)_{rqd}$ / LF for BCF = 5 as Y axis for different values of SF. The FWF values were averaged for the preparation of these graphs as the numerical values did not show much difference and hence these charts can be used for any value of FWF. Thus, for any BCF value other than 5, corresponding LF values may be obtained from the interpolation chart shown in Fig. 9.5. The lowest value of BCF was fixed as 5 because below this, LF values obtained are either greater than unity or discriminant of the quadratic equation (Eqn. 9.31) becomes negative which yields imaginary roots.

### *9.4.3.2 Sliding failure*

In the case of sliding failure, the limiting condition was obtained from Eqn. 9.14 as:

$$1.3\, R_h = R_v\, a \tan\phi_{s2} + \frac{\alpha\, c_{s2}\, L}{1.6} \qquad \text{..... (9.33)}$$

Taking into account the assumption nos. 1 and 5 cited in Section 9.4.1, Eqn. 9.33 reduces to:

$$1.3\, R_h = (2/3)\, R_v \tan\phi \qquad \text{..... (9.34)}$$

The soil – reinforcement interaction coefficient, a, is usually taken as 2/3 as explained in Section 9.2.2.2. On substitution from Eqns. 9.15 and 9.16, Eqn. 9.34 comes to the form:

$$1.95\, (P_s + P_q) = 0.667\, (W_g + W_s) \tan\phi \qquad \text{..... (9.35)}$$

Substituting the values from Eqns. 9.1 to 9.5 and assuming the unit weights to be same for the gabion fill material and backfill, Eqn. 9.35 can be converted to dimensionless form as:

$$2.925\, K_a\, \{ 1/2 + (q/\gamma_s H) \} / \tan\phi = (b/H) + (L/H) \qquad \text{..... (9.36)}$$

Rewriting in terms of length factor, LF = L/H, Eqn. 9.36 reduces to the form:

$$LF = 1.4625\ K_a\ (1 + 2SF)\ /\ \tan\phi - FWF \qquad \text{..... (9.37)}$$

Solving the equation, the length of reinforcement which is an indication of the base width of the reinforced structure, can be obtained. This gives a safe design value against sliding failure. From Eqn. 9.37, it is clear that LF depends on the non dimensional factors $\phi$, SF and FWF.

$$LF = f\ (\phi,\ SF,\ FWF) \qquad \text{..... (9.38)}$$

Using the relation from Eqn. 9.37, graph was plotted after obtaining different LF values by varying $\phi$, SF and FWF and is shown in Fig. 9.6.

## 9.4.4 Internal stability analysis

### *9.4.4.1 Failure due to mesh breakage*

The limiting condition for failure due to mesh breakage was obtained from Eqn. 9.20 as:

$$\frac{T_D}{1.1} = T_j \qquad \text{..... (9.39)}$$

Substituting for $T_j$ from Eqns. 9.17 to 9.19 and taking $L \approx 0.5H$ (in order to simplify the final equation, L is given an average value recommended by the parametric studies), Eqn. 9.39 comes to the form:

$$0.75\ (\gamma_s\ h_j + q)\ H^2\ T_D - K_a\ (\gamma_s\ h_j + 3q)\ h_j^2\ T_D = 1.2375\ K_a\ (\gamma_s\ h_j + q)^2\ H^2\ S_{vj} \qquad \text{..... (9.40)}$$

Dividing through out by $\gamma_s^2 H^5$, Eqn. 9.40 can be converted to dimensionless form as:

$$0.75\ [\ (h_j/H) + (q/\gamma_s H)\ ]\ (T_D/\gamma_s H^2) - K_a\ [\ (h_j/H) + (3q/\gamma_s H)\ ]\ (h_j/H)^2\ (T_D/\gamma_s H^2)$$
$$= 1.2375\ K_a\ [\ (h_j/H) + (q/\gamma_s H)\ ]^2\ (S_{vj}/H) \qquad \text{..... (9.41)}$$

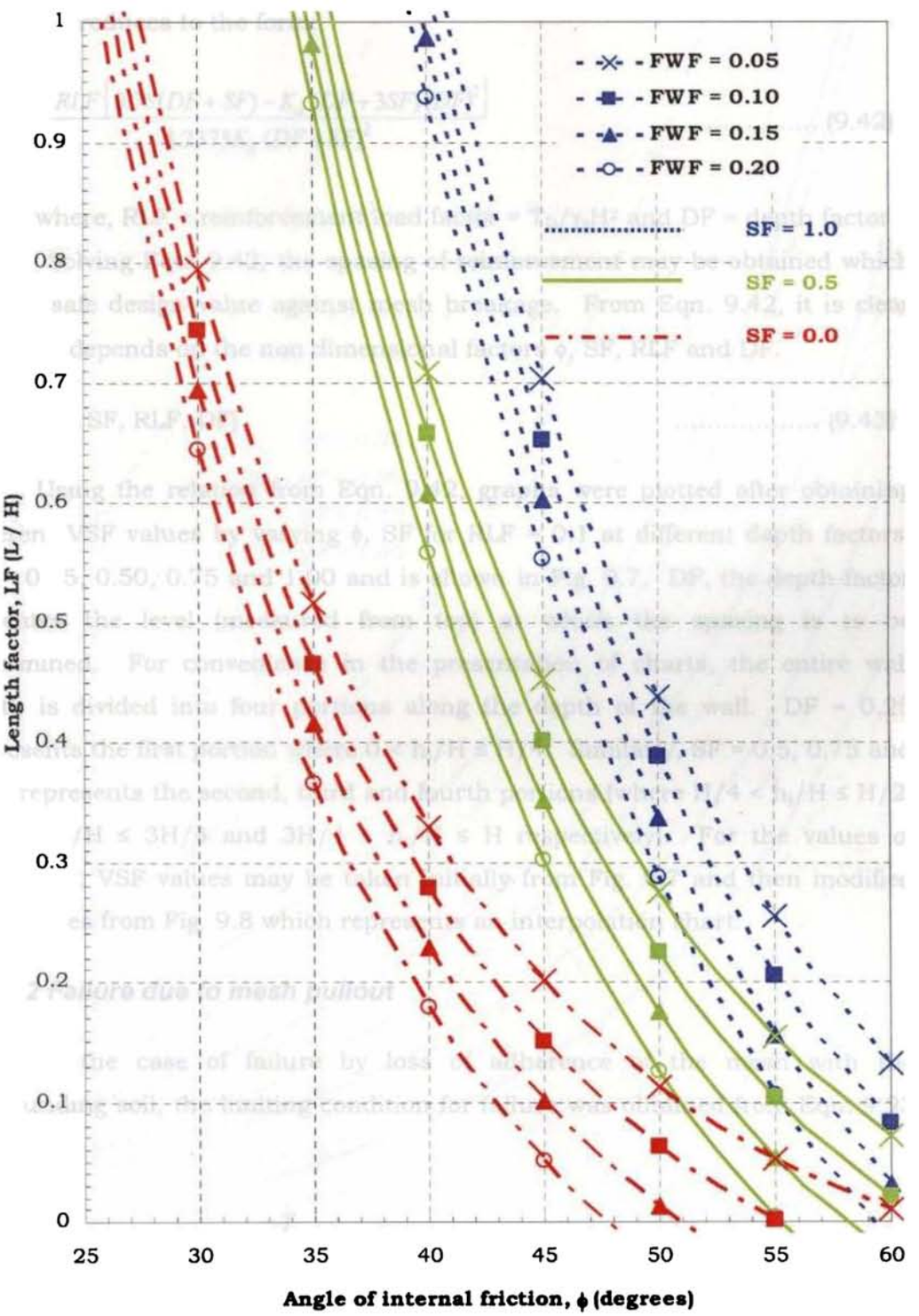


**Fig. 9.6 Design chart from sliding considerations**

Rewriting in terms of the required vertical spacing factor, VSF = $S_{vj}/H$, Eqn. 9.41 reduces to the form:

$$VSF = \frac{RLF\left\{0.75(DF+SF)-K_a\,(DF+3SF)\,(DF)^2\right\}}{1.2375K_a\,(DF+SF)^2} \qquad \text{..... (9.42)}$$

where, RLF = reinforcement load factor = $T_D/\gamma_s H^2$ and DF = depth factor = $h_j/H$. Solving Eqn. 9.42, the spacing of reinforcement may be obtained which gives a safe design value against mesh breakage. From Eqn. 9.42, it is clear that VSF depends on the non dimensional factors $\phi$, SF, RLF and DF.

$$VSF = f\,(\phi,\ SF,\ RLF,\ DF) \qquad \text{..... (9.43)}$$

Using the relation from Eqn. 9.42, graphs were plotted after obtaining different VSF values by varying $\phi$, SF for RLF = 0.1 at different depth factors, DF = 0.25, 0.50, 0.75 and 1.00 and is shown in Fig. 9.7. DF, the depth factor indicates the level (measured from top) at which the spacing is to be determined. For convenience in the presentation of charts, the entire wall depth is divided into four portions along the depth of the wall. DF = 0.25 represents the first portion where $0 < h_j/H \leq H/4$. Similarly, SF = 0.5, 0.75 and 1.00 represents the second, third and fourth portions (where $H/4 < h_j/H \leq H/2$, $H/2 < h_j/H \leq 3H/4$ and $3H/4 < h_j/H \leq H$ respectively). For the values of RLF $\neq$ 0.1, VSF values may be taken initially from Fig. 9.7 and then modified with values from Fig. 9.8 which represents an interpolation chart.

### *9.4.4.2 Failure due to mesh pullout*

In the case of failure by loss of adherence of the mesh with the surrounding soil, the limiting condition for failure was obtained from Eqn. 9.23 as:

$$2\,L_{ej} = \frac{T_j}{\dfrac{(2/3)\tan\phi_{s1}\,\gamma_{s1}\,h_j}{1.3\times1.1} + \dfrac{\alpha\,c}{1.6\times1.3\times1.1_{ii}}} \qquad \text{..... (9.44)}$$

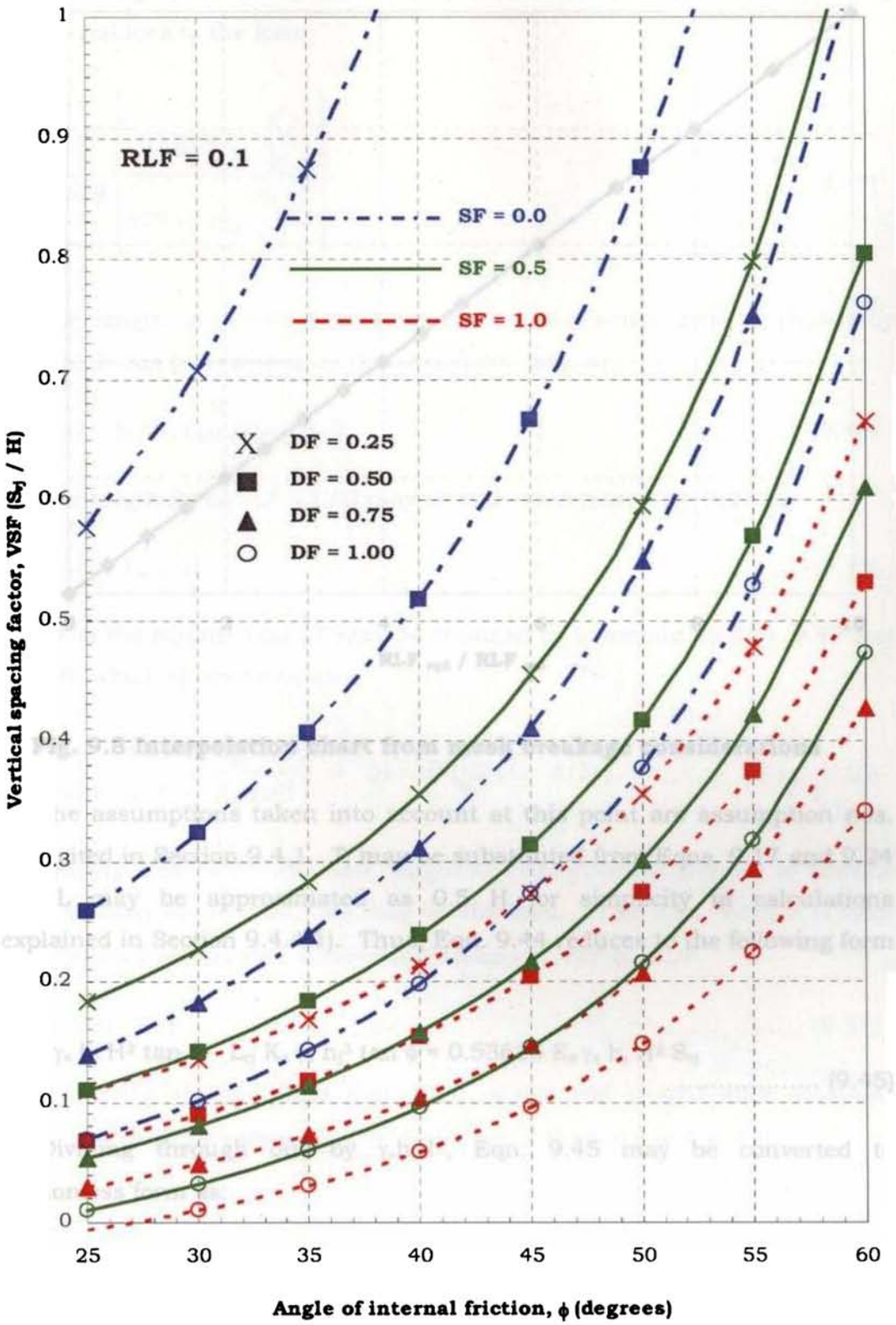


**Fig. 9.7 Design chart from mesh breakage considerations**

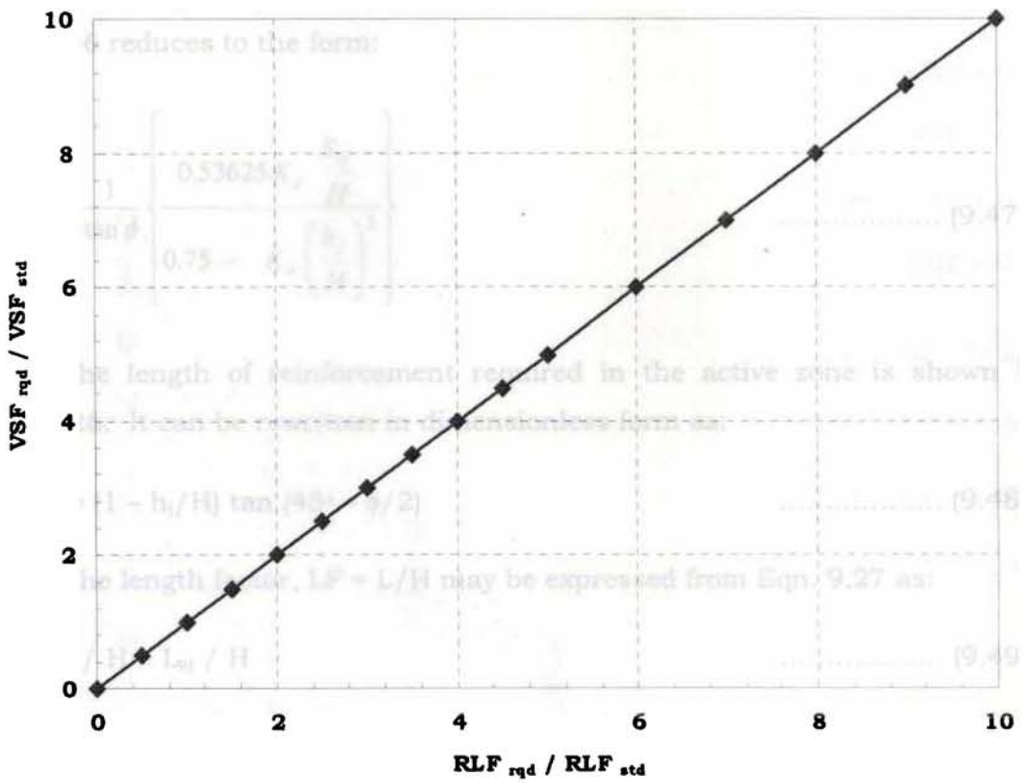


**Fig. 9.8 Interpolation chart from mesh breakage considerations**

The assumptions taken into account at this point are assumption nos. 1 and 4 cited in Section 9.4.1. $T_j$ may be substituted from Eqns. 9.17 and 9.24 where, L may be approximated as 0.5 H for simplicity in calculations (as explained in Section 9.4.4.1). Thus, Eqn. 9.44 reduces to the following form as:

$$0.75\, L_{ej}\, \gamma_s\, h_j\, H^2 \tan\phi - L_{ej}\, K_a\, \gamma_s\, h_j^3 \tan\phi = 0.53625\, K_a\, \gamma_s\, h_j\, H^2\, S_{vj} \qquad \text{..... (9.45)}$$

Dividing through out by $\gamma_s h_j H^4$, Eqn. 9.45 may be converted to dimensionless form as:

$$0.75\, (L_{ej}/H) \tan\phi - K_a\, (h_j/H)^2\, (L_{ej}/H) \tan\phi = 0.53625\, K_a\, (S_{vj}/H) \qquad \text{..... (9.46)}$$

Rewriting in terms of the required embedment length factor, $L_{ej}/H$, Eqn. 9.46 reduces to the form:

$$\frac{L_{ej}}{H} = \frac{1}{\tan\phi}\left\{\frac{0.53625 K_a \frac{S_{vj}}{H}}{0.75 - K_a\left(\frac{h_j}{H}\right)^2}\right\} \qquad \text{..... (9.47)}$$

The length of reinforcement required in the active zone is shown by Eqn. 9.26. It can be rewritten in dimensionless form as:

$$L_{aj} / H = (1 - h_j/H) \tan (45^o - \phi/2) \qquad \text{..... (9.48)}$$

The length factor, LF = L/H may be expressed from Eqn. 9.27 as:

$$LF = L_{ej} / H + L_{aj} / H \qquad \text{..... (9.49)}$$

Thus the equation for LF may be obtained by summing up Eqn. 9.47 and Eqn. 9.48, which is rewritten as:

$$LF = \frac{1}{\tan\phi}\left\{\frac{0.53625 K_a VSF}{0.75 - K_a DF^2}\right\} + \left\{(1 - DF)\tan(45 - \phi/2)\right\} \qquad \text{..... (9.50)}$$

Solving Eqn. 9.50, the safe length of reinforcement needed to provide internal stability to the structure may be obtained. From Eqn. 9.50, it is clear that LF depends on the non dimensional factors $\phi$, VSF and DF.

$$LF = f(\phi, VSF, DF) \qquad \text{..... (9.51)}$$

Using the relation from Eqn. 9.50, graph was plotted after obtaining different LF values by varying $\phi$, VSF and DF and is shown in Fig. 9.9.

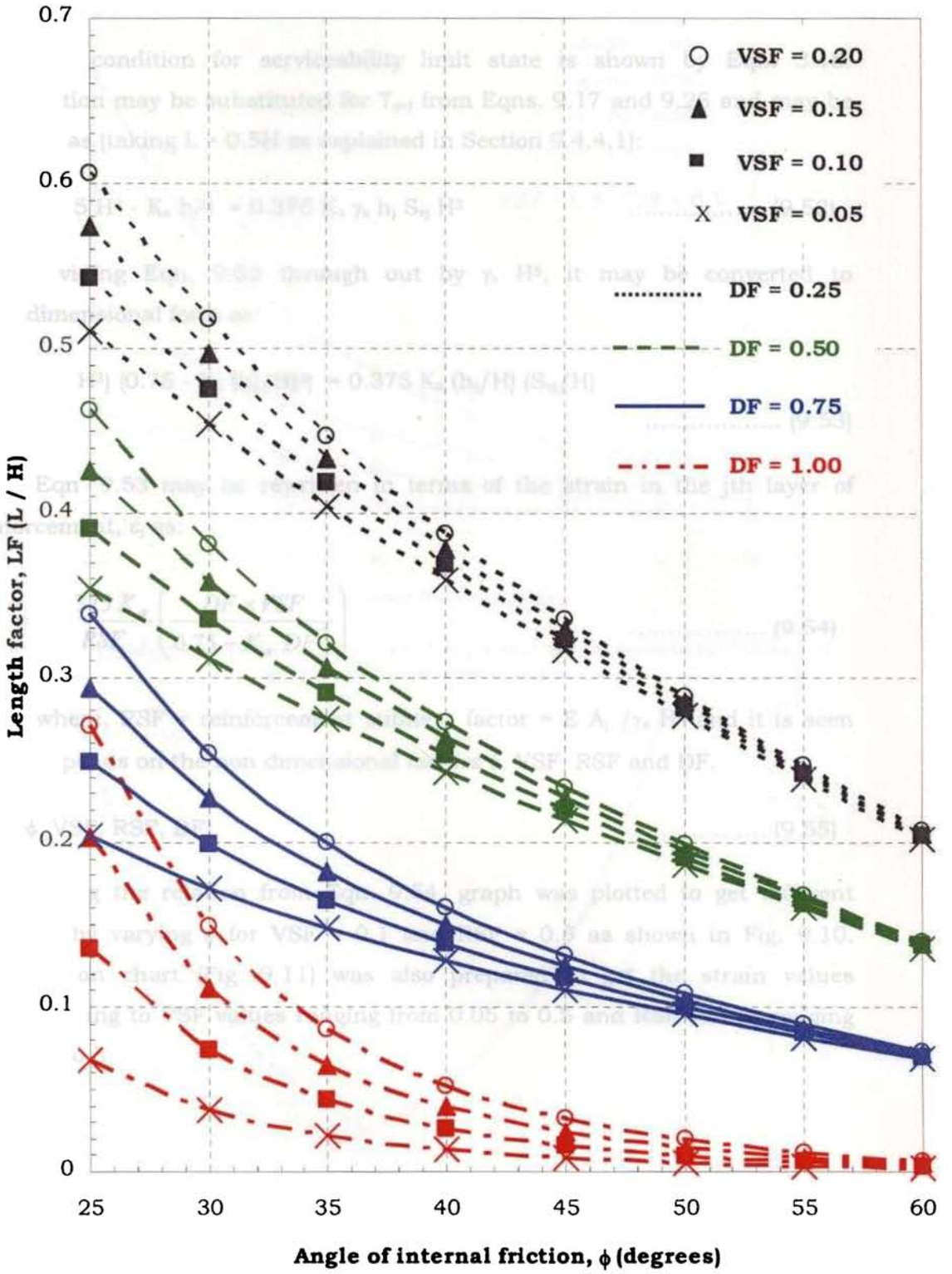


**Fig. 9.9 Design chart from mesh pullout considerations**

### 9.4.5 Serviceability limit state

The condition for serviceability limit state is shown by Eqn. 3.15. The equation may be substituted for $T_{avj}$ from Eqns. 9.17 and 9.25 and may be rewritten as (taking L = 0.5H as explained in Section 9.4.4.1):

$$\varepsilon_j E A_j (0.75 H^2 - K_a h_j^2) = 0.375 K_a \gamma_s h_j S_{vj} H^3 \qquad \text{..... (9.52)}$$

Dividing Eqn. 9.52 through out by $\gamma_s H^5$, it may be converted to non - dimensional form as:

$$\varepsilon_j (E A_j / \gamma_s H^3) \{0.75 - K_a (hj/H)^2\} = 0.375 K_a (h_j/H) (S_{vj}/H) \qquad \text{..... (9.53)}$$

Eqn. 9.53 may be rewritten in terms of the strain in the jth layer of reinforcement, $\varepsilon_j$ as:

$$\varepsilon_j = \frac{0.375 K_a}{RSF} \left( \frac{DF \times VSF}{0.75 - K_a DF^2} \right) \qquad \text{..... (9.54)}$$

where, RSF = reinforcement stiffness factor = $E A_j / \gamma_s H^3$ and it is seen that $\varepsilon_j$ depends on the non dimensional factors $\phi$, VSF, RSF and DF.

$$\varepsilon_j = f (\phi, VSF, RSF, DF) \qquad \text{..... (9.55)}$$

Using the relation from Eqn. 9.54, graph was plotted to get different $\varepsilon_j$ values by varying $\phi$ for VSF = 0.1 and RSF = 0.5 as shown in Fig. 9.10. Interpolation chart (Fig. 9.11) was also prepared to get the strain values corresponding to VSF values ranging from 0.05 to 0.5 and RSF values ranging from 0.5 to 5.

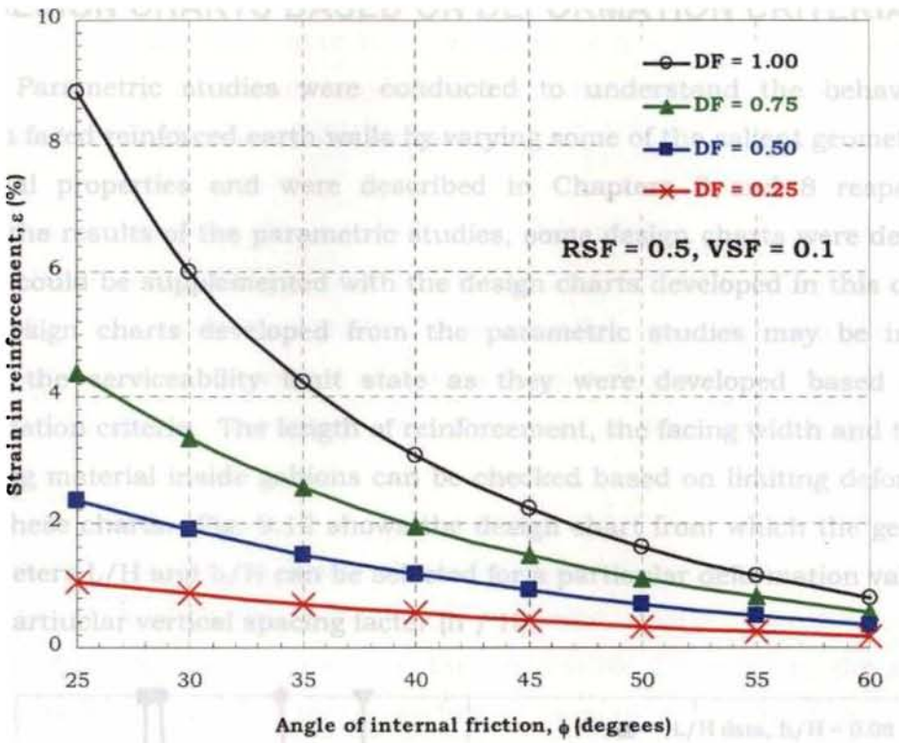


**Fig. 9.10 Design chart from serviceability limit state considerations for RSF = 0.5 and VSF = 0.1**

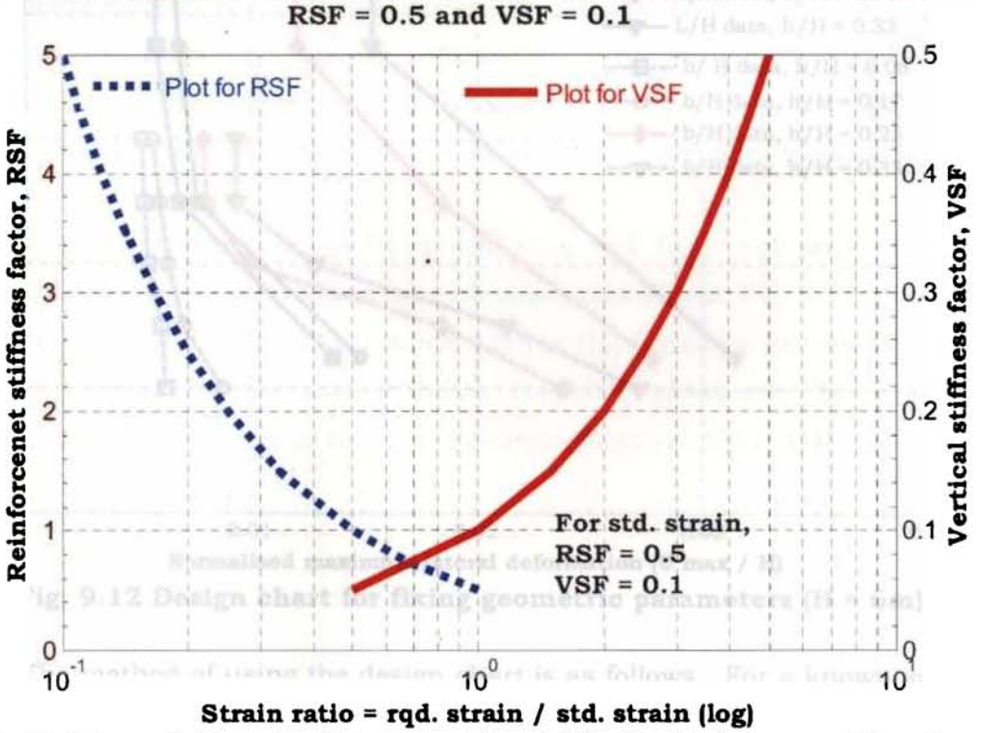


**Fig. 9.11 Interpolation chart from serviceability limit state considerations**

## 9.5 DESIGN CHARTS BASED ON DEFORMATION CRITERIA

Parametric studies were conducted to understand the behaviour of gabion faced reinforced earth walls by varying some of the salient geometric and material properties and were described in Chapters 7 and 8 respectively. From the results of the parametric studies, some design charts were developed which could be supplemented with the design charts developed in this chapter. The design charts developed from the parametric studies may be included under the serviceability limit state as they were developed based on the deformation criteria. The length of reinforcement, the facing width and the type of filling material inside gabions can be checked based on limiting deformation from these charts. Fig. 9.12 shows the design chart from which the geometric parameters L/H and b/H can be selected for a particular deformation value and for a partiuclar vertical spacing factor (h / H).

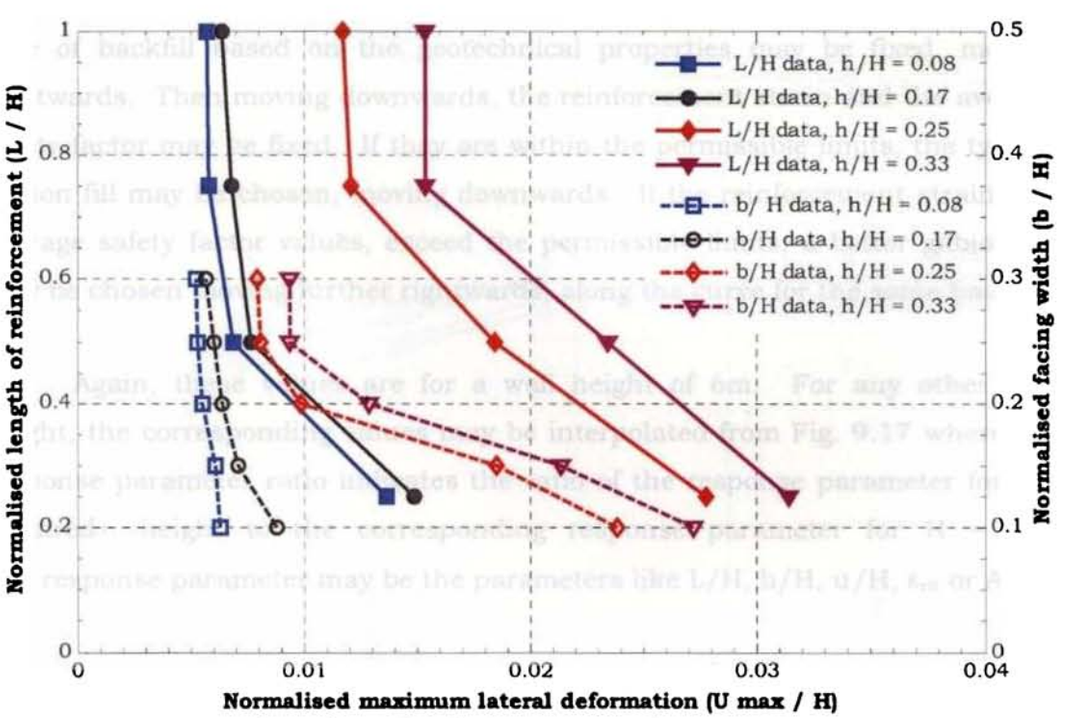


**Fig. 9.12 Design chart for fixing geometric parameters (H = 6m)**

The method of using the design chart is as follows. For a known value of allowable displacement, moving vertically upward, for a particular h/H ratio, the length of reinforcement can be fixed by moving left and then moving

rightwards from the same point, the required width of gabion facing can be chosen. When there are more than one value of h / H for a given allowable displacement, the maximum value should be taken and the corresponding L / H and b/H should be chosen for the design.

The results from the material parametric studies may also be used as design charts for selecting a suitable soil type and rock type as the backfill and gabion fill respectively for a particular deformation after checking the strains developed in the reinforcement and the average safety factor. The results are presented in design chart form from Figs. 9.13 to 9.16 for various types of backfills.

In order to use the design charts for material parameters, depending on the type of backfill, one of the four design charts may be selected. After selecting the design chart, for the permissible deformation, the suitable type of backfill based on the geotechnical properties may be fixed, moving rightwards. Then moving downwards, the reinforcement strain and the average safety factor may be fixed. If they are within the permissible limits, the type of gabion fill may be chosen, moving downwards. If the reinforcement strain and average safety factor values, exceed the permissible limits, a better gabion fill may be chosen moving further rightwards, along the curve for the same backfill.

Again, these values are for a wall height of 6m. For any other wall height, the corresponding values may be interpolated from Fig. 9.17 where the response parameter ratio indicates the ratio of the response parameter for the required height to the corresponding response parameter for H = 6m. The response parameter may be the parameters like L/H, b/H, u/H, $\varepsilon_{rft}$ or ASF.

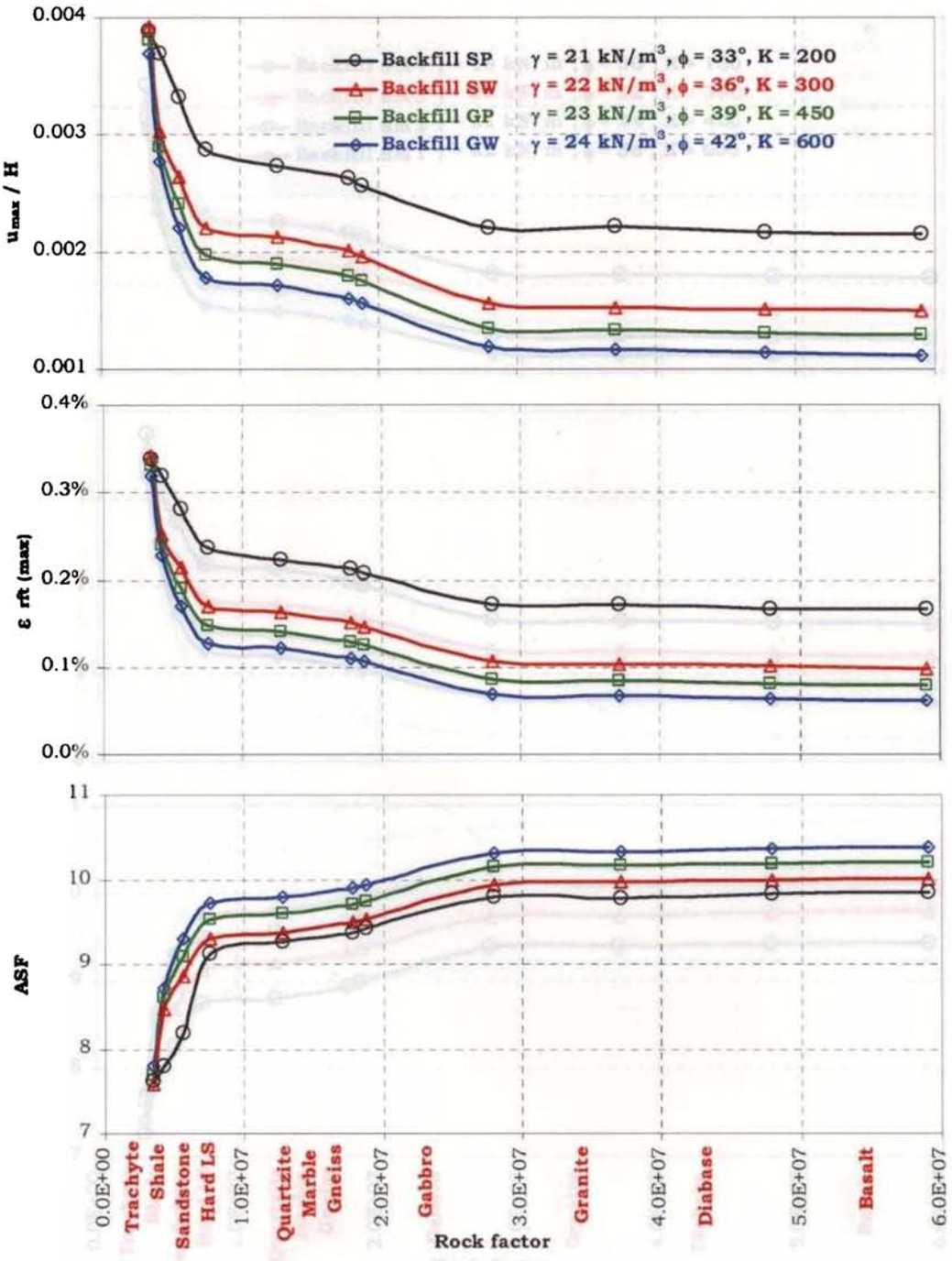


**Fig. 9.13 Design chart for fixing backfill – gabion fill combination (Gravel and sand backfill, H = 6m)**

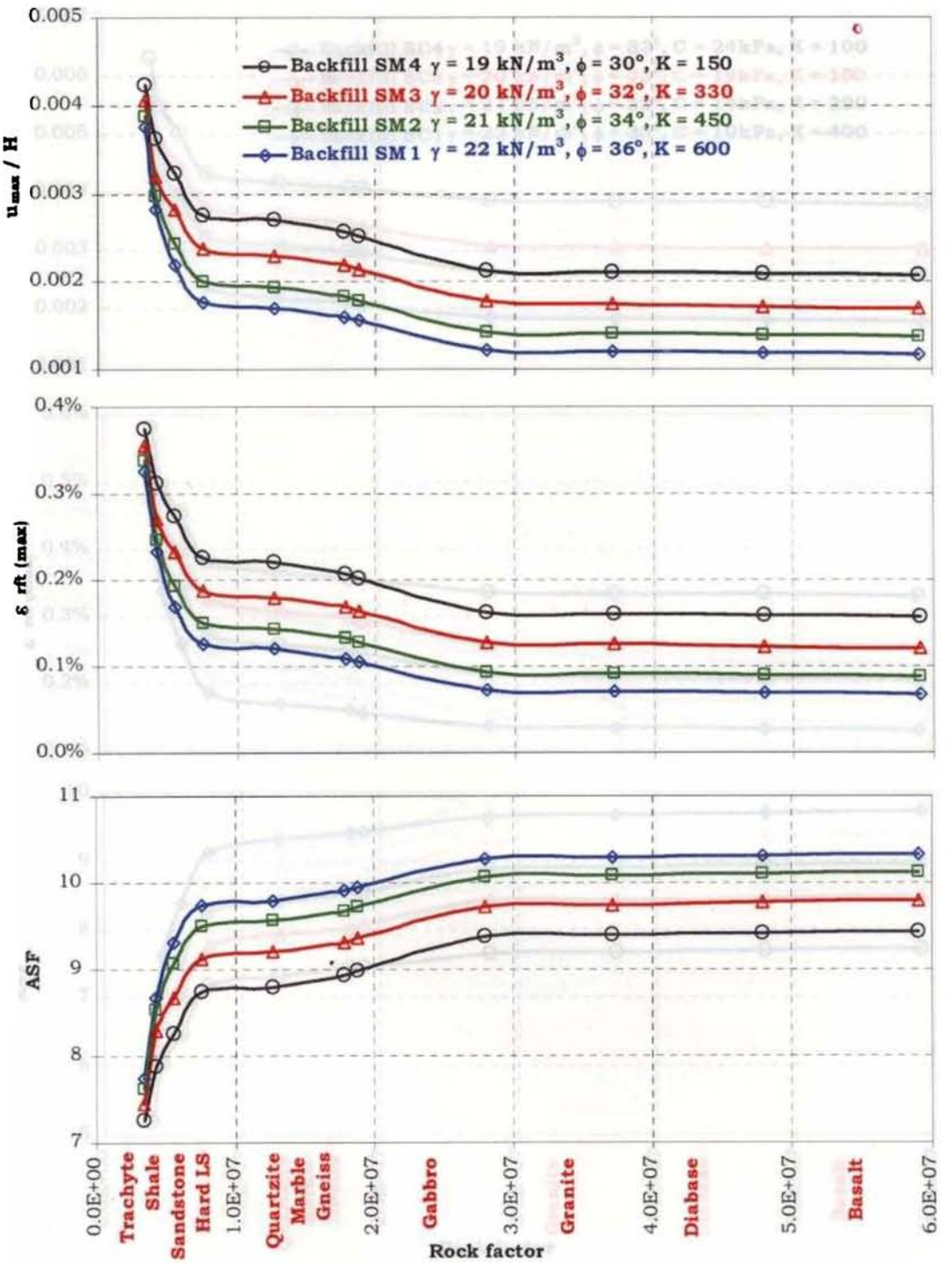


**Fig. 9.14 Design chart for fixing backfill – gabion fill combination (Silty sand backfill, H = 6m)**

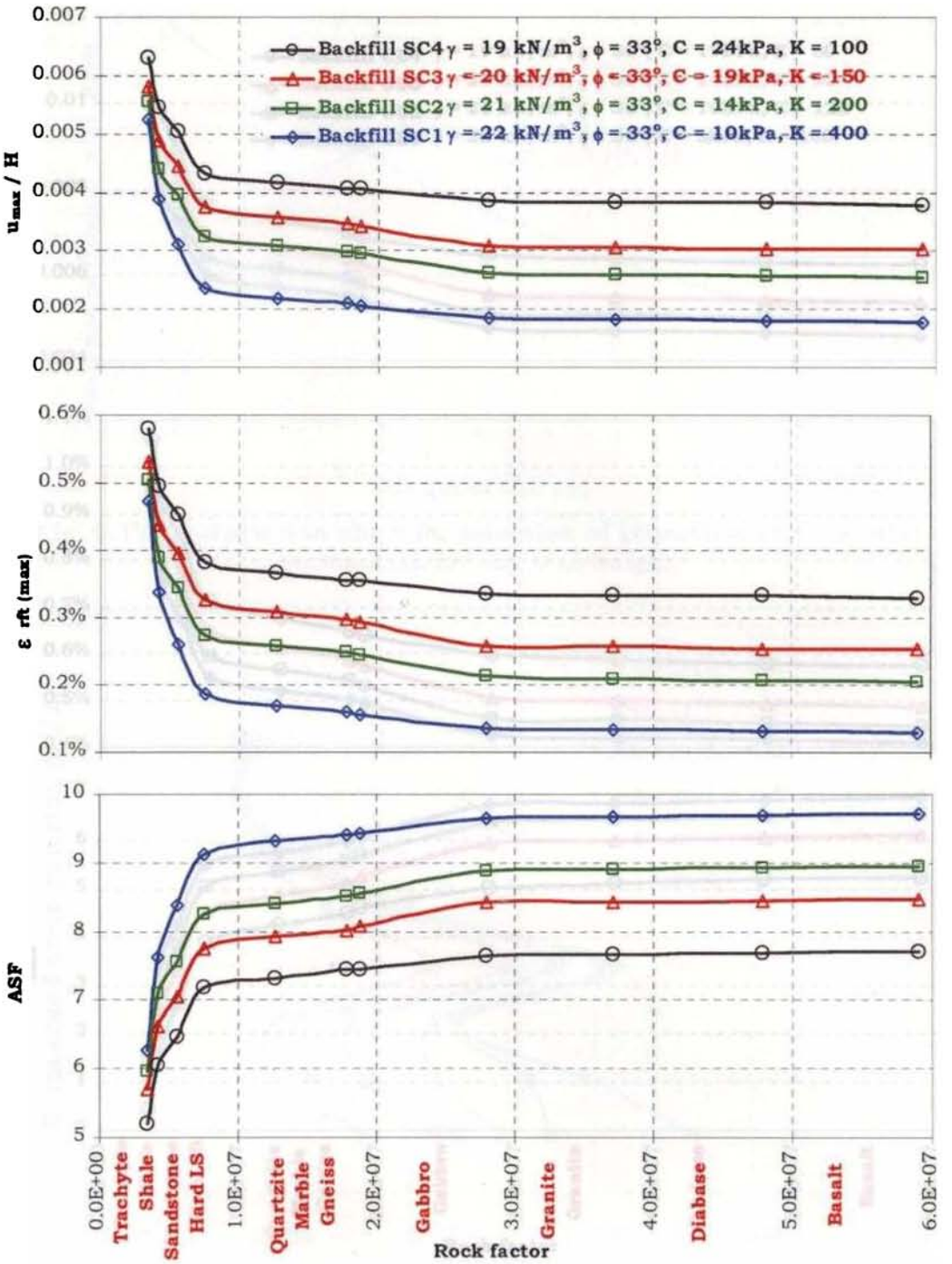


**Fig. 9.15 Design chart for fixing backfill – gabion fill combination (Clayey sand backfill, H = 6m)**

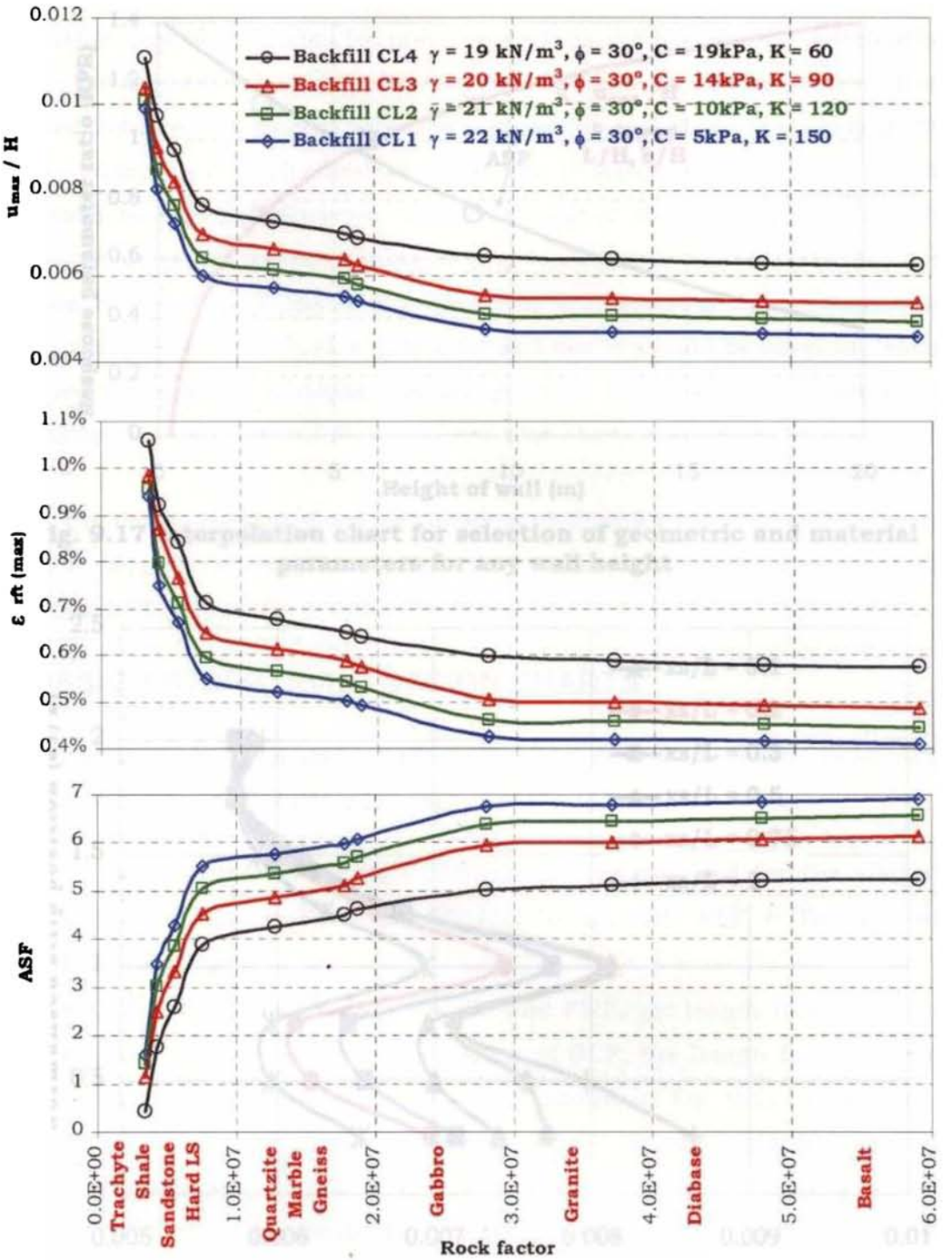


**Fig. 9.16 Design chart for fixing backfill – gabion fill combination (Clay with low plasticity backfill, H = 6m)**

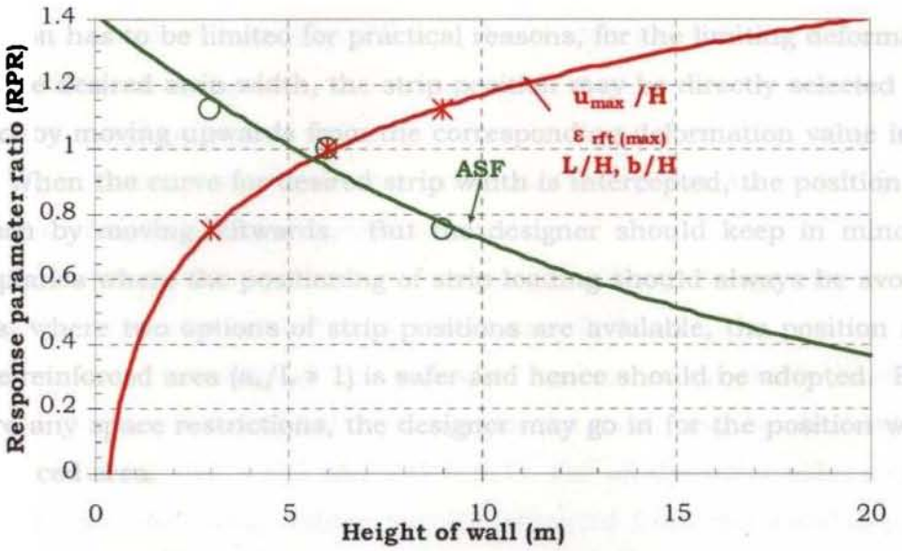


**Fig. 9.17 Interpolation chart for selection of geometric and material parameters for any wall height**

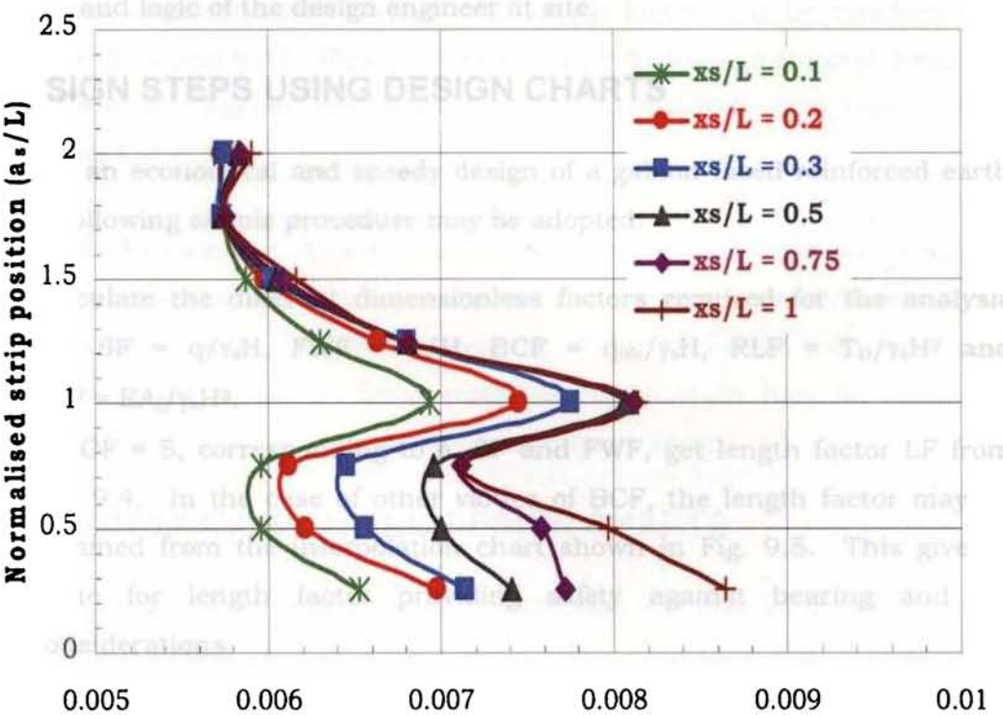


**Fig. 9.18 Design chart for fixing strip loading position**

If a strip load like pipeline, edge of bridge seating, crane, compactor etc., has to be provided over the wall, its position may be fixed using the design

chart in Fig. 9.18. The chart may be used as follows. In places where deformation has to be limited for practical reasons, for the limiting deformation and for the desired strip width, the strip position may be directly selected from the chart by moving upwards from the corresponding deformation value in the X axis. When the curve for desired strip width is intercepted, the position may be chosen by moving leftwards. But the designer should keep in mind the critical planes where the positioning of strip loading should always be avoided. In cases, where two options of strip positions are available, the position away from the reinforced area ($a_s/L > 1$) is safer and hence should be adopted. But if there are any space restrictions, the designer may go in for the position within the reinforced area.

The charts presented are just quick guidelines for material and geometry selection for general conditions. The final decision should depend upon the discretion and logic of the design engineer at site.

## 9.6 DESIGN STEPS USING DESIGN CHARTS

For an economical and speedy design of a gabion faced reinforced earth wall, the following simple procedure may be adopted.

1. Calculate the different dimensionless factors required for the analysis like SF = $q/\gamma_s H$, FWF = $b/H$, BCF = $q_{ult}/\gamma_s H$, RLF = $T_D/\gamma_s H^2$ and RSF = $EA_j/\gamma_s H^3$.
2. If BCF = 5, corresponding to $\phi$, SF and FWF, get length factor LF from Fig. 9.4. In the case of other values of BCF, the length factor may be obtained from the interpolation chart shown in Fig. 9.5. This gives a value for length factor providing safety against bearing and tilt considerations.
3. The safe value for length factor against sliding failure may be obtained from Fig. 9.6 corresponding to $\phi$, SF and FWF.
4. The spacing of reinforcement at salient portions, 0 – H/4, H/4 – H/2, H/2 – 3H/4 and 3H/4 – H represented by DF = 0.25, 0.5, 0.75 and 1.00 respectively may be obtained from Fig. 9.7 as VSF values considering the

mesh rupture criteria for RLF = 0.1. For other values of RLF, the VSF values obtained from Fig. 9.7 may be modified using the interpolation chart shown in Fig. 9.8.

5. Corresponding to the DF and VSF values obtained from Step 4, the length factor value providing adequate safety against mesh pullout failure may be obtained from Fig. 9.9.
6. The length factor required for an economic and safe design may be taken as the maximum value obtained from steps 2, 3 and 5.
7. To ensure the safety of the structure against serviceability limit state considerations, the strain developing in the mesh may be obtained from Fig. 9.10 for RSF = 0.5 and VSF = 0.1. For all the other values of RSF and VSF, the strain values may be obtained from the semilog plot in Fig. 9.11. The strain values thus obtained should not exceed the permissible maximum elongation of the gabion mesh which is 10%.
8. Based on deformation criteria, the length factor may be checked from Figs. 9.12 and 9.17. Figs. 9.13 to 9.17 may be used to suggest a suitable gabion fill – backfill combination. Position of strip loading may be fixed using Fig. 9.18.

In all the cases, in the steps described above, intermediate values may be obtained by interpolation. Thus, assuming the appropriate initial dimensions of the gabion faced walls, length and spacing of reinforcement required for an economical design of gabion faced reinforced earth walls may be arrived at easily by following the eight simple steps mentioned above.

## 9.7 DESIGN EXAMPLE USING DESIGN CHARTS

The design of the wall illustrated in Section 9.3 may be simplified using the above mentioned procedure as follows. The corresponding design charts (mentioned in Section 9.6) required for the design are reproduced for the purpose of illustration.

Step 1: The dimensionless factors required for the problem may be calculated as: SF = 0.1, FWF = 0.1, BCF = 6.5, RLF = 0.068 ≈ 0.1 (taking $T_D = T_{ult}/1.5$) and RSF = 3.2.

Step 2: Bearing considerations: For $\phi = 35^o$, SF = 0, FWF = 0.1, LF = 0.29 (from Fig. 9.19 (a)). For $\phi = 35^o$, SF = 0.5, FWF = 0.1, LF = 0.48 (from Fig. 9.19 (a)). By interpolation, for $\phi = 35^o$, SF = 0.1, FWF = 0.1, LF = 0.336. This is for BCF = 5. But, $BCF_{rqd} = 6.5$. The data for this has to be obtained from Fig. 9.19 (b).

The value of $BCF_{rqd}$ / (BCF = 5) is 1.3. Corresponding to this, for SF = 0.0, the value of $LF_{rqd}$ / (LF for BCF = 5) is 0.9 and for SF = 0.5, it is 0.85. The corresponding value for SF = 0.1 may be interpolated as 0.89. Therefore, LF for BCF = 6.5 is 0.336 x 0.89 = 0.3.

Step 3: Sliding considerations: For $\phi = 35^o$, FWF = 0.1, SF = 0, LF = 0.46 and the corresponding value of LF for SF = 0.5 is 1 (Fig. 9.20). By interpolation, for SF = 0.1, LF = 0.57.

Step 4: Mesh rupture considerations: For this problem, RLF = 0.1 and hence to determine the spacing of reinforcement, Fig. 9.21 may be made use of. Spacing is determined at the four salient depths 0.25H, 0.50H, 0.75H and 1.00H measured from the top.

**Table 9.5 Spacing values at salient depths**

| DF | VSF values | | |
|---|---|---|---|
| | SF = 0 (Fig. 9.7) | SF = 1 (Fig. 9.7) | SF = 0.1 (By interpolation) |
| 0.25 | 0.87 | 0.28 | 0.75 |
| 0.50 | 0.4 | 0.18 | 0.36 |
| 0.75 | 0.24 | 0.12 | 0.22 |
| 1.00 | 0.14 | 0.06 | 0.12 |

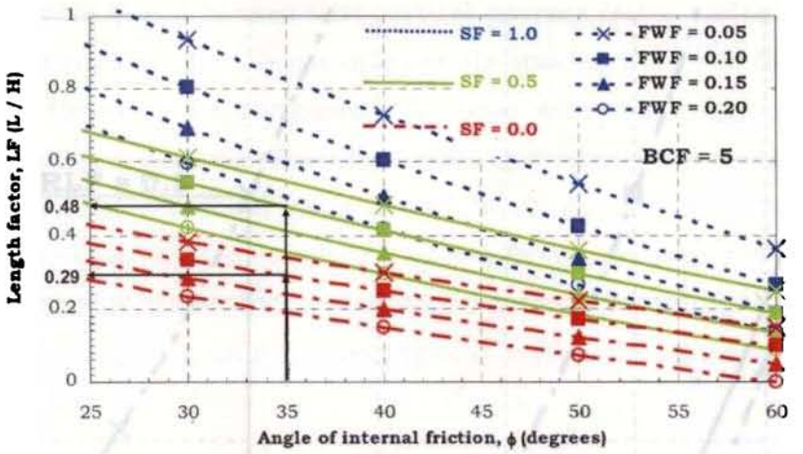


**Fig. 9.19 (a) Illustration of design example: Step 2**

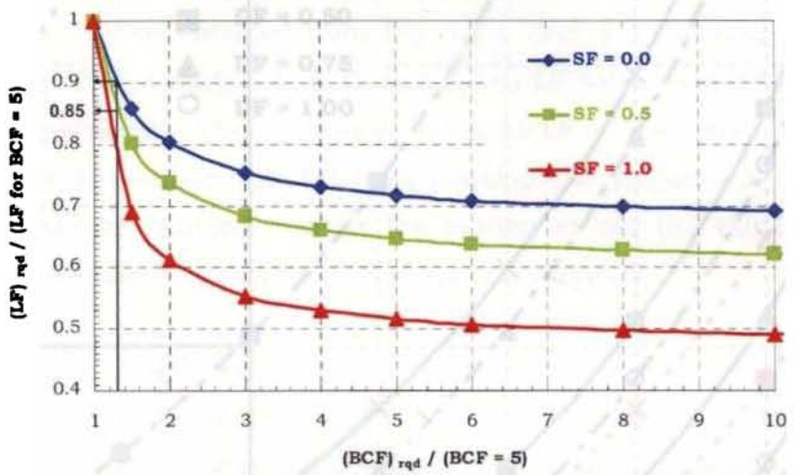


**Fig. 9.19 (b) Illustration of design example: Step 2**

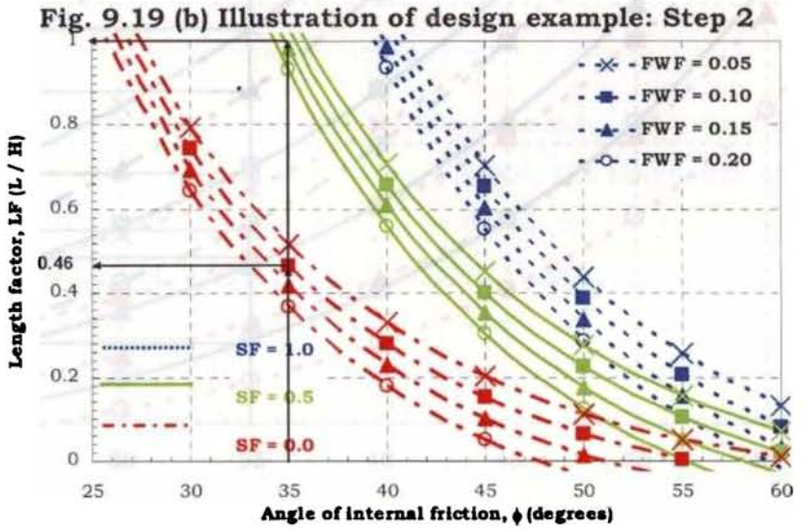


**Fig. 9.20 Illustration of design example: Step 3**

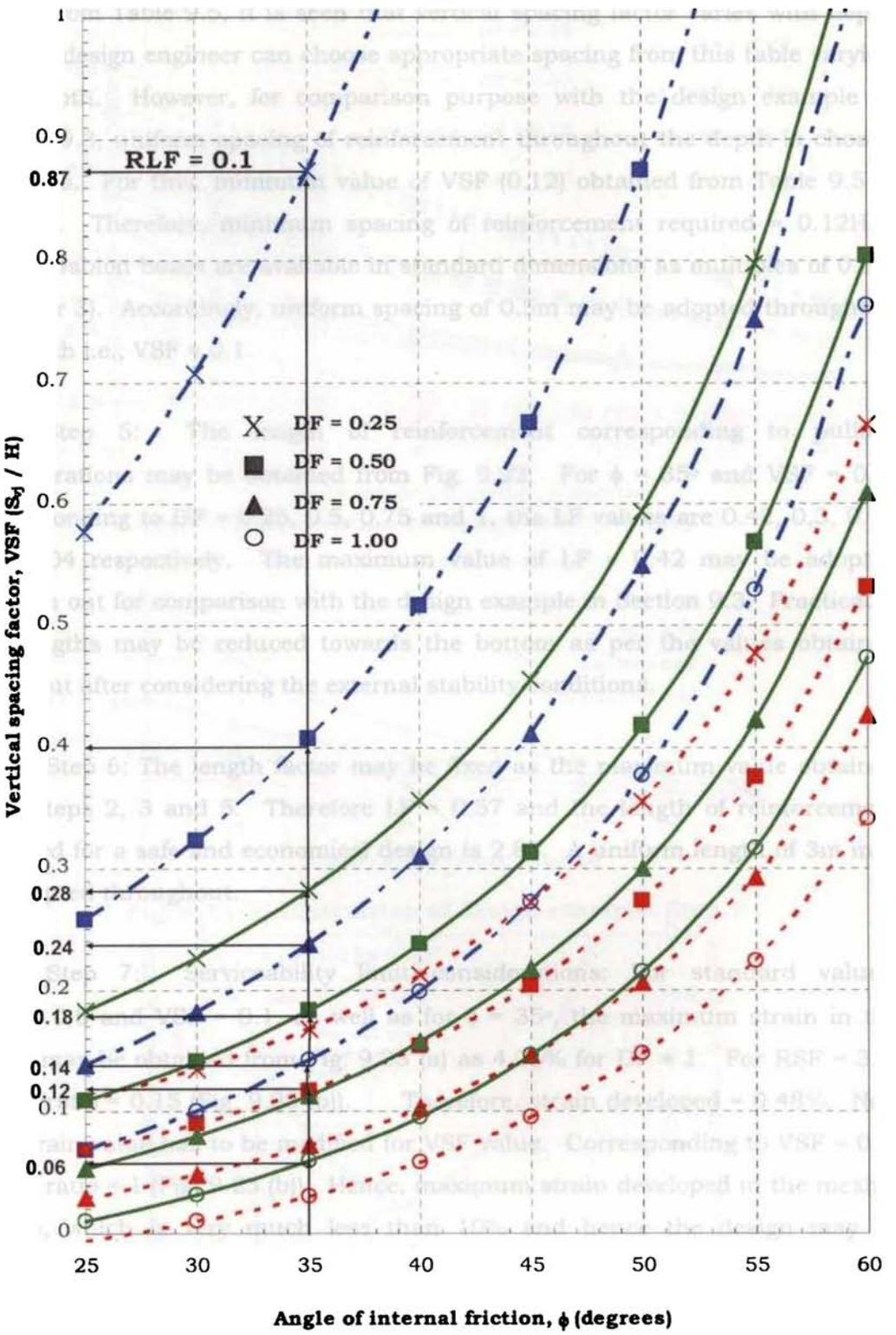


**Fig. 9.21 Illustration of design example: Step 4**

From Table 9.5, it is seen that vertical spacing factor varies with depth and the design engineer can choose appropriate spacing from this table varying with depth. However, for comparison purpose with the design example in Section 9.3, uniform spacing of reinforcement throughout the depth is chosen here also. For this, minimum value of VSF (0.12) obtained from Table 9.5 is adopted. Therefore, minimum spacing of reinforcement required = 0.12H = 0.6m. Gabion boxes are available in standard dimensions as multiples of 0.5m (Chapter 3). Accordingly, uniform spacing of 0.5m may be adopted throughout the depth i.e., VSF = 0.1.

Step 5: The length of reinforcement corresponding to pullout considerations may be obtained from Fig. 9.22. For $\phi$ = 35° and VSF = 0.1, corresponding to DF = 0.25, 0.5, 0.75 and 1, the LF values are 0.42, 0.3, 0.16 and 0.04 respectively. The maximum value of LF = 0.42 may be adopted through out for comparison with the design example in Section 9.3. Practically, the lengths may be reduced towards the bottom as per the values obtained here, but after considering the external stability conditions.

Step 6: The length factor may be fixed as the maximum value obtained from steps 2, 3 and 5. Therefore LF = 0.57 and the length of reinforcement required for a safe and economical design is 2.85. A uniform length of 3m may be adopted throughout.

Step 7: Serviceability limit considerations: For standard values, RSF = 0.5 and VSF = 0.1, as well as for $\phi$ = 35°, the maximum strain in the mesh may be obtained from Fig. 9.23 (a) as 4.25% for DF = 1. For RSF = 3.2, strain ratio = 0.15 (Fig. 9.23 (b)). Therefore, strain developed = 0.48%. Now the strain value has to be modified for VSF value. Corresponding to VSF = 0.1, strain ratio = 1 (Fig. 9.23 (b)). Hence, maximum strain developed in the mesh = 0.48%, which is very much less than 10% and hence the design may be considered as safe.

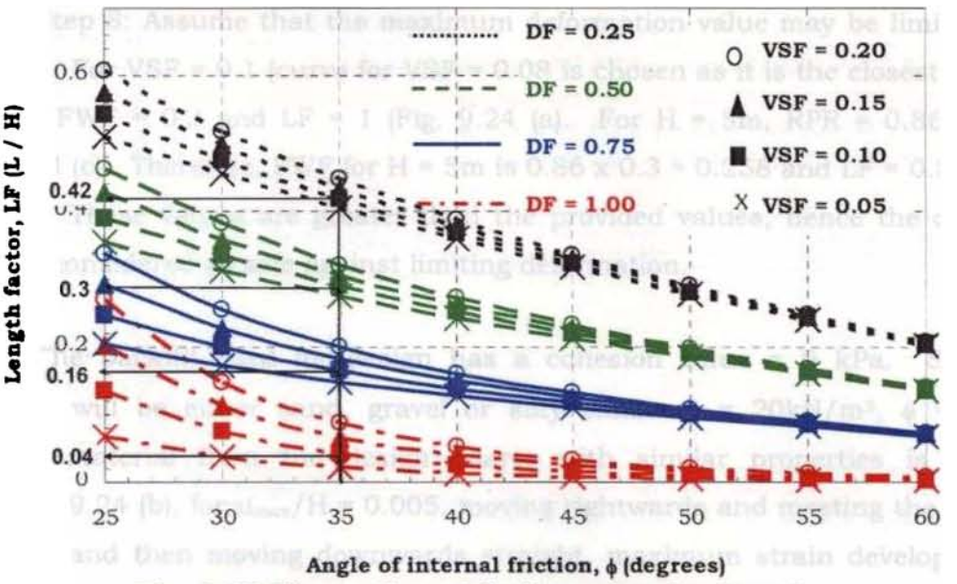


**Fig. 9.22 Illustration of design example: Step 5**

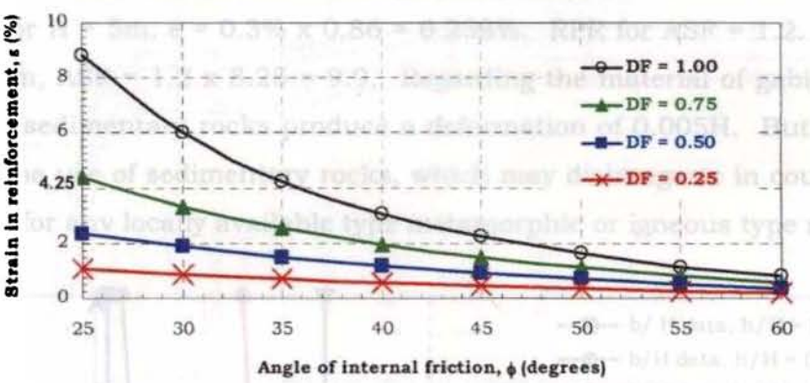


**Fig. 9.23 (a) Illustration of design example: Step 7**

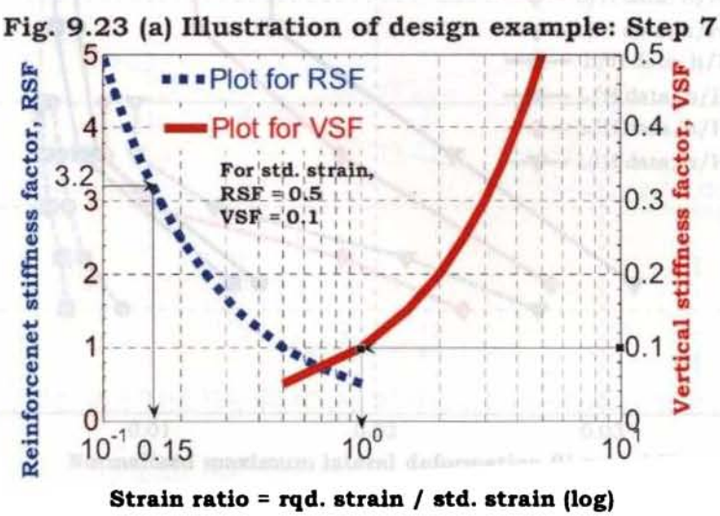


**Fig. 9.23 (b) Illustration of design example: Step 7**

Step 8: Assume that the maximum deformation value may be limited to 0.005H. For VSF = 0.1 (curve for VSF = 0.08 is chosen as it is the closest value to 0.1), FWF = 0.3 and LF = 1 (Fig. 9.24 (a). For H = 5m, RPR = 0.86 from Fig. 9.24 (c). Therefore, FWF for H = 5m is 0.86 x 0.3 = 0.258 and LF = 0.86 x 1 = 0.86. These values are greater than the provided values, hence the design may be considered as safe against limiting deformation.

The backfill used for design has a cohesion value = 0 kPa. So the material will be either sand, gravel or silty sand. $\gamma$ = 20kN/m$^3$, $\phi$ = 35°. Backfill material from the design charts with similar properties is SM3. In Fig. 9.24 (b), for $u_{max}/H$ = 0.005, moving rightwards and meeting the curve for SM3 and then moving downwards straight, maximum strain developed in the reinforcement is 0.3% and average safety factor is 8.25. RPR for $u_{max}/H$ and $e_{rft}$ For H = 5m, e = 0.3% x 0.86 = 0.258%. RPR for ASF = 1.2. Therefore, for H = 5m, ASF = 1.2 x 8.25 = 9.9. Regarding the material of gabion fill, it is seen that sedimentary rocks produce a deformation of 0.005H. But it is better to avoid the use of sedimentary rocks, which may disintegrate in course of time and go in for any locally available type metamorphic or igneous type rocks.

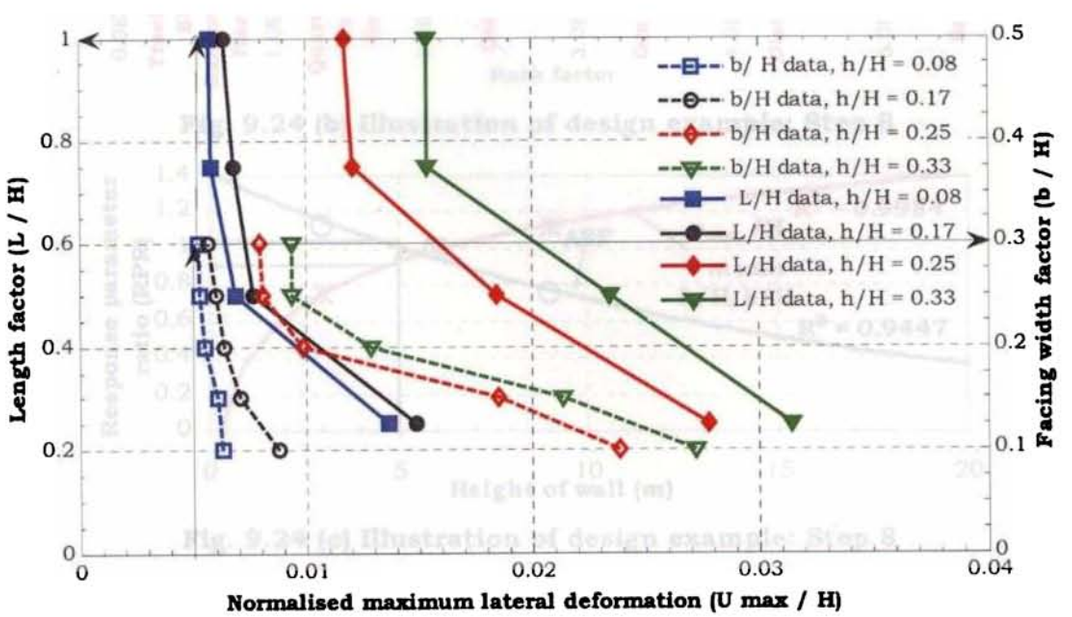


**Fig. 9.24 (a) Illustration of design example: Step 8**

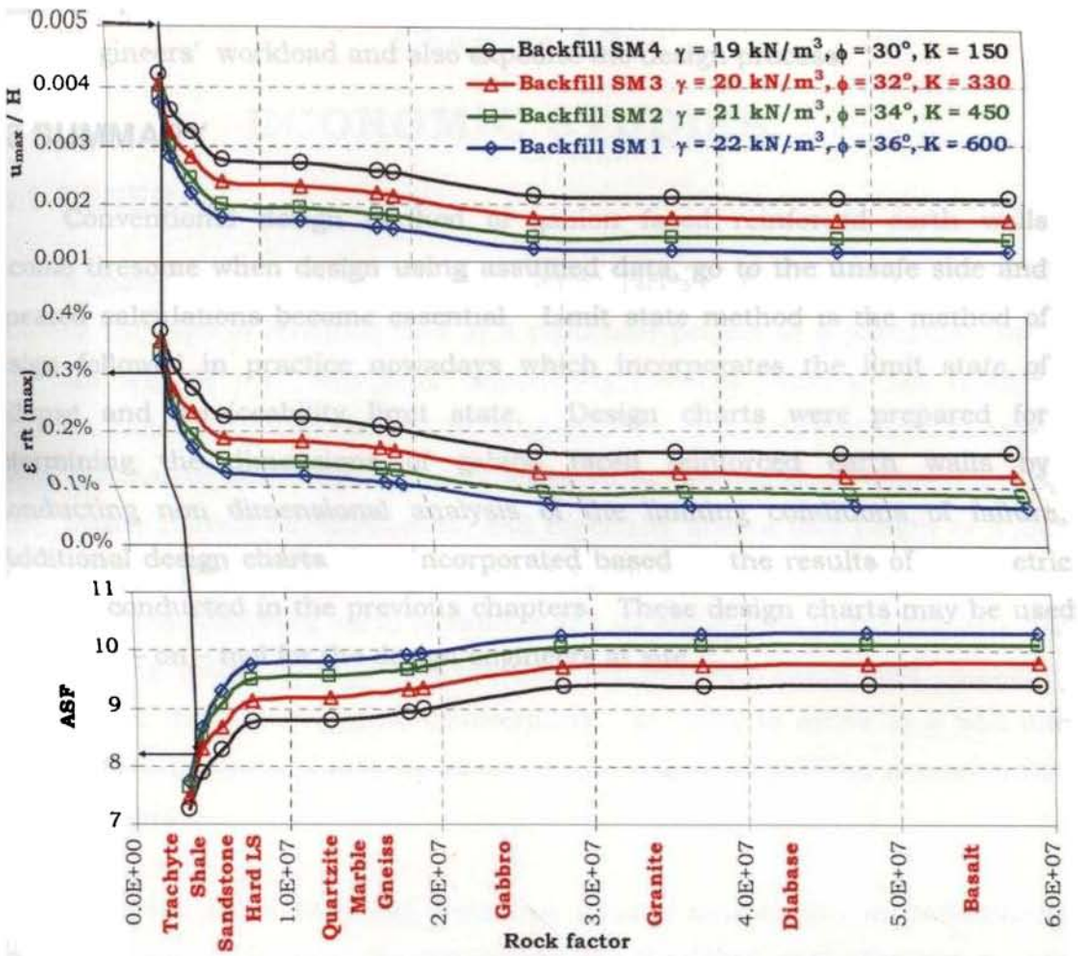


**Fig. 9.24 (b) Illustration of design example: Step 8**

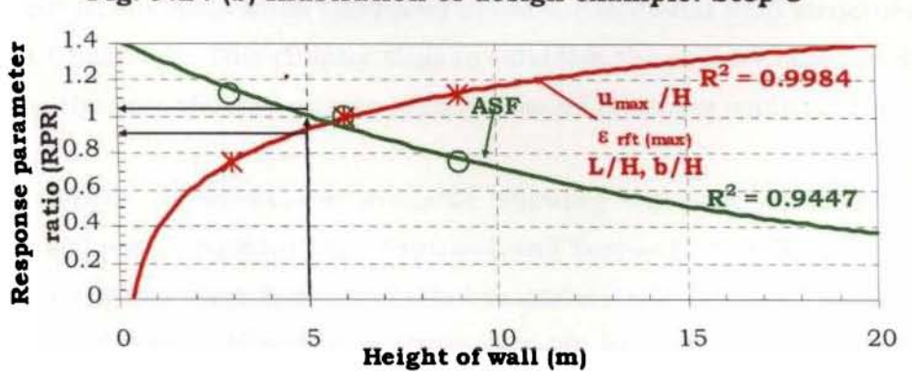


**Fig. 9.24 (c) Illustration of design example: Step 8**

On comparing with the detailed design in Section 9.3, it can be seen that this modified procedure using design charts can be adopted very safely for

design purposes. It is expected that use of the design charts will ease the design engineers' workload and also expedite the design process.

## 9.8 SUMMARY

Conventional design method of gabion faced reinforced earth walls become tiresome when design using assumed data, go to the unsafe side and repeated calculations become essential. Limit state method is the method of design followed in practice nowadays which incorporates the limit state of collapse and serviceability limit state. Design charts were prepared for determining the dimensions of gabion faced reinforced earth walls by conducting non dimensional analysis of the limiting conditions of failure. Additional design charts were incorporated based on the results of parametric studies conducted in the previous chapters. These design charts may be used as hands – on – tool for the design engineers at site.

# Chapter 10

# ECONOMIC STUDIES

## 10.1 GENERAL

A geotechnical design engineer is usually faced with an important task of choosing the type of retaining wall in a particular project at a particular site. This task will be over only after considering carefully, factors like relative economy, factors of safety, feasibility, availability of materials and even relative speed of construction. It is generally accepted in the literature (Ingold, 1982) that, under normal circumstances, and especially after a wall height of about 6 m, conventional RCC walls readily become more uneconomical with the advent of the reinforced earth technique and its application in the construction of retaining walls. This is because they are relatively easier and quicker to build than their conventional counterparts. In order to arrive at a scientific conclusion, however, it may be absolutely necessary to perform a comparative cost analysis.

Gabion faced retaining walls are gaining momentum in construction nowadays due to its inherent advantages like flexibility, cost effectiveness and environment friendliness when compared to the conventional RCC structures as detailed in Chapter 3. This chapter aims to establish the second aspect enlisted above - i.e., the cost effective nature of gabion faced retaining walls.

A number of works are available showing the cost effectiveness of reinforced soil walls (Ingold (1982), Durukan and Tezcan (1992), Koerner (1998) etc.). But no works have been conducted to understand the cost effectiveness of gabion faced walls. Hence an attempt is made here to study the economic aspects of gabion faced retaining walls.

## 10.2 DATA COLLECTION

Soil data from 57 different sites were collected from all over Kerala where retaining walls of different wall heights were constructed. The data are shown in Table 10.1 in the order of heights. At all the 57 sites, RCC walls (for heights ≤ 6m cantilever type and > 6m counterfort type), gabion faced gravity walls and gabion faced reinforced soil walls were designed based on limit state approach with the help of MS Excel worksheets prepared for the design of each type. The dimensions of cantilever walls, counterfort walls and gabion faced retaining walls are tabulated in Tables 10.2, 10.3 and 10.4 respectively. It was assumed that no soil improvement is necessary at the base. Design considerations were based on the requirements of the external and internal stability analyses. In all the cases, whatever be the type of backfill, cohesion of soil was considered to be zero. This is because of the fact that cohesion adds to the stability of the system and hence it is usually neglected for design purposes.

After designing the same, cost estimation of all the 57 x 3 = 171 cases were carried out as per Schedule of rates published by Kerala Public Works Department (Schedule of rates, 2007). Since the rate of gabions and its basal extension was not available in this, they were taken as per the prevailing market rates (provided by Meccaferri Environment Solutions Pvt. Ltd., India). The results of cost estimation are tabulated in Tables 10.5, 10.6 and 10.7. It may be noted that the total cost includes 30% wastage also which is not indicated in the tables.

## Table 10.1: Data collected for economic studies

| Wall no. | Height of wall, H (m) | Angle of internal friction, $\phi$ (degrees) | Density of soil at site, $\gamma$ (kN/m$^3$) | Inclination of sloping backfill, i (degrees) | SBC of soil at site, $q_{all}$ (kPa) | Surcharge q (kPa) |
|---|---|---|---|---|---|---|
| Site 1 | 1 | 28 | 19.5 | 0 | 135 | 10 |
| Site 2 | 1 | 32 | 18 | 10 | 200 | 0 |
| Site 3 | 1 | 34 | 15 | 0 | 150 | 0 |
| Site 4 | 1.5 | 29 | 15 | 0 | 200 | 0 |
| Site 5 | 1.5 | 32 | 17 | 15 | 150 | 0 |
| Site 6 | 1.5 | 37 | 18.85 | 0 | 300 | 10 |
| Site 7 | 2 | 25 | 19 | 0 | 200 | 0 |
| Site 8 | 2 | 33 | 16 | 0 | 150 | 10 |
| Site 9 | 2 | 38 | 15 | 10 | 150 | 0 |
| Site 10 | 2.5 | 27 | 15 | 0 | 150 | 10 |
| Site 11 | 2.5 | 31 | 16.5 | 15 | 200 | 0 |
| Site 12 | 2.5 | 38 | 18 | 0 | 200 | 0 |
| Site 13 | 3 | 30 | 18.5 | 15 | 200 | 0 |
| Site 14 | 3 | 32 | 19.5 | 0 | 135 | 10 |
| Site 15 | 3 | 35 | 19 | 0 | 200 | 0 |
| Site 16 | 3.5 | 26 | 15.5 | 12.5 | 200 | 0 |
| Site 17 | 3.5 | 28 | 17.5 | 0 | 200 | 10 |
| Site 18 | 3.5 | 35 | 16 | 0 | 200 | 0 |
| Site 19 | 4 | 27 | 18.85 | 0 | 250 | 10 |
| Site 20 | 4 | 30 | 16 | 0 | 250 | 0 |
| Site 21 | 4 | 37 | 17 | 10 | 200 | 0 |
| Site 22 | 4.5 | 30 | 18 | 0 | 200 | 0 |
| Site 23 | 4.5 | 32 | 18 | 0 | 200 | 10 |
| Site 24 | 4.5 | 38 | 18 | 15 | 250 | 0 |
| Site 25 | 5 | 28 | 15 | 0 | 150 | 0 |
| Site 26 | 5 | 30 | 17 | 0 | 150 | 7.5 |
| Site 27 | 5 | 30 | 18 | 0 | 150 | 10 |
| Site 28 | 5.5 | 30 | 16 | 0 | 160 | 10 |
| Site 29 | 5.5 | 32 | 19 | 0 | 200 | 0 |
| Site 30 | 5.5 | 38 | 16 | 15 | 160 | 0 |
| Site 31 | 6 | 28 | 18 | 10 | 250 | 0 |
| Site 32 | 6 | 30 | 16 | 0 | 200 | 0 |
| Site 33 | 6 | 37 | 19 | 0 | 200 | 10 |
| Site 34 | 6.5 | 29 | 15 | 15 | 150 | 0 |
| Site 35 | 6.5 | 30 | 16 | 0 | 180 | 0 |
| Site 36 | 6.5 | 38 | 19 | 0 | 200 | 10 |
| Site 37 | 7 | 30 | 16 | 0 | 160 | 0 |
| Site 38 | 7 | 33 | 16 | 0 | 160 | 10 |
| Site 39 | 7 | 38 | 16 | 10 | 200 | 0 |
| Site 40 | 7.5 | 29 | 15 | 0 | 300 | 10 |
| Site 41 | 7.5 | 30 | 16 | 0 | 170 | 0 |
| Site 42 | 7.5 | 38 | 16 | 10 | 170 | 0 |
| Site 43 | 8 | 25 | 15 | 0 | 250 | 0 |
| Site 44 | 8 | 30 | 16 | 0 | 300 | 10 |
| Site 45 | 8 | 37 | 16 | 15 | 300 | 0 |
| Site 46 | 8.5 | 28 | 18 | 10 | 300 | 0 |
| Site 47 | 8.5 | 30 | 15 | 0 | 200 | 0 |
| Site 48 | 8.5 | 34 | 15.85 | 0 | 300 | 12.5 |
| Site 49 | 9 | 31 | 15 | 0 | 300 | 0 |
| Site 50 | 9 | 33 | 18.85 | 0 | 250 | 10 |
| Site 51 | 9 | 38 | 17 | 10 | 300 | 0 |
| Site 52 | 9.5 | 28 | 17.5 | 10 | 280 | 0 |
| Site 53 | 9.5 | 30 | 15 | 0 | 250 | 0 |
| Site 54 | 9.5 | 33 | 17.5 | 0 | 280 | 15 |
| Site 55 | 10 | 30 | 18 | 0 | 300 | 0 |
| Site 56 | 10 | 32 | 16.5 | 0 | 300 | 10 |
| Site 57 | 10 | 40 | 18 | 10 | 250 | 0 |

**Table 10.2 Design details of cantilever type**

| Wall no. | Site data | | | | | | Material properties | | Dimensions | | | | | | |
|---|---|---|---|---|---|---|---|---|---|---|---|---|---|---|---|
| | Height of wall | Angle of internal friction | Unit weight of backfill | Inclination of surcharge | Safe bearing capacity of soil | Surcharge | Characteristic strength of concrete | Yield strength of steel | Stem thickness | | Thickness of base slab | | Width of base slab | | Depth of foundation |
| | H | $\phi$ | $\gamma$ | i | SBC | q | $f_{ck}$ | $f_y$ | Top | Base | Toe | Heel | Toe | Heel | $D_f$ |
| | (m) | (degrees) | (kN/m³) | (degrees) | (kPa) | (kPa) | (N/mm²) | (N/mm²) | (m) | (m) | (m) | (m) | (m) | (m) | (m) |
| Site 1 | 1 | 28 | 19.5 | 0 | 135 | 10 | 15 | 250 | 0.2 | 0.2 | 0.2 | 0.2 | 0.2 | 0.4 | 0.90 |
| Site 2 | 1 | 32 | 18 | 10 | 200 | 0 | 15 | 250 | 0.2 | 0.2 | 0.2 | 0.2 | 0.2 | 0.2 | 1.05 |
| Site 3 | 1 | 34 | 15 | 0 | 150 | 0 | 15 | 250 | 0.2 | 0.2 | 0.2 | 0.2 | 0.2 | 0.2 | 0.80 |
| Site 4 | 1.5 | 29 | 15 | 0 | 200 | 0 | 15 | 250 | 0.2 | 0.2 | 0.2 | 0.2 | 0.4 | 0.5 | 1.61 |
| Site 5 | 1.5 | 32 | 17 | 15 | 150 | 0 | 15 | 250 | 0.2 | 0.2 | 0.2 | 0.2 | 0.4 | 0.5 | 0.83 |
| Site 6 | 1.5 | 37 | 18.85 | 0 | 300 | 10 | 15 | 250 | 0.2 | 0.2 | 0.2 | 0.2 | 0.5 | 0.6 | 0.98 |
| Site 7 | 2 | 25 | 19 | 0 | 200 | 0 | 15 | 250 | 0.2 | 0.2 | 0.2 | 0.2 | 0.5 | 0.6 | 1.73 |
| Site 8 | 2 | 33 | 16 | 0 | 150 | 10 | 15 | 250 | 0.2 | 0.2 | 0.21 | 0.21 | 0.6 | 1 | 0.81 |
| Site 9 | 2 | 38 | 15 | 10 | 150 | 0 | 15 | 250 | 0.2 | 0.2 | 0.2 | 0.2 | 0.5 | 0.6 | 0.57 |
| Site 10 | 2.5 | 27 | 15 | 0 | 150 | 10 | 15 | 250 | 0.2 | 0.2 | 0.26 | 0.26 | 0.7 | 1.4 | 1.41 |
| Site 11 | 2.5 | 31 | 16.5 | 15 | 200 | 0 | 15 | 250 | 0.2 | 0.2 | 0.2 | 0.2 | 0.5 | 1 | 1.24 |
| Site 12 | 2.5 | 38 | 18 | 0 | 200 | 0 | 15 | 250 | 0.2 | 0.2 | 0.2 | 0.2 | 0.5 | 0.8 | 0.63 |
| Site 13 | 3 | 30 | 18.5 | 15 | 200 | 0 | 15 | 250 | 0.2 | 0.2 | 0.24 | 0.24 | 0.6 | 1 | 1.20 |
| Site 14 | 3 | 32 | 19.5 | 0 | 135 | 10 | 15 | 250 | 0.2 | 0.25 | 0.29 | 0.29 | 0.7 | 1.25 | 0.65 |
| Site 15 | 3 | 35 | 19 | 0 | 200 | 0 | 15 | 250 | 0.2 | 0.2 | 0.24 | 0.24 | 0.6 | 1 | 0.77 |
| Site 16 | 3.5 | 26 | 15.5 | 12.5 | 200 | 0 | 15 | 250 | 0.2 | 0.25 | 0.28 | 0.28 | 0.7 | 1.15 | 1.97 |
| Site 17 | 3.5 | 28 | 17.5 | 0 | 200 | 10 | 15 | 250 | 0.2 | 0.3 | 0.35 | 0.33 | 0.9 | 1.6 | 1.49 |
| Site 18 | 3.5 | 35 | 16 | 0 | 200 | 0 | 15 | 250 | 0.2 | 0.2 | 0.28 | 0.28 | 0.7 | 1.2 | 0.92 |
| Site 19 | 4 | 27 | 18.85 | 0 | 250 | 10 | 20 | 415 | 0.2 | 0.3 | 0.45 | 0.37 | 0.9 | 2.2 | 1.87 |
| Site 20 | 4 | 30 | 16 | 0 | 250 | 0 | 15 | 250 | 0.2 | 0.25 | 0.32 | 0.32 | 0.8 | 1.35 | 1.74 |
| Site 21 | 4 | 37 | 17 | 10 | 200 | 0 | 15 | 250 | 0.2 | 0.25 | 0.32 | 0.32 | 0.8 | 1.35 | 0.73 |
| Site 22 | 4.5 | 30 | 18 | 0 | 200 | 0 | 15 | 415 | 0.2 | 0.35 | 0.45 | 0.36 | 0.9 | 1.45 | 1.23 |
| Site 23 | 4.5 | 32 | 18 | 0 | 200 | 10 | 15 | 250 | 0.2 | 0.35 | 0.55 | 0.41 | 1 | 1.65 | 1.05 |
| Site 24 | 4.5 | 38 | 18 | 15 | 250 | 0 | 15 | 415 | 0.2 | 0.3 | 0.4 | 0.36 | 0.9 | 1.5 | 0.79 |
| Site 25 | 5 | 28 | 15 | 0 | 150 | 0 | 20 | 415 | 0.2 | 0.3 | 0.5 | 0.4 | 1 | 1.7 | 1.30 |
| Site 26 | 5 | 30 | 17 | 0 | 150 | 7.5 | 20 | 415 | 0.2 | 0.35 | 0.7 | 0.44 | 1.1 | 1.85 | 0.98 |
| Site 27 | 5 | 30 | 18 | 0 | 150 | 10 | 20 | 415 | 0.2 | 0.4 | 0.75 | 0.45 | 1.1 | 1.9 | 0.93 |
| Site 28 | 5.5 | 30 | 16 | 0 | 160 | 10 | 20 | 415 | 0.2 | 0.4 | 0.85 | 0.55 | 1.2 | 2.2 | 1.11 |
| Site 29 | 5.5 | 32 | 19 | 0 | 200 | 0 | 15 | 250 | 0.2 | 0.4 | 0.55 | 0.44 | 1.1 | 1.8 | 0.99 |
| Site 30 | 5.5 | 38 | 16 | 15 | 160 | 0 | 20 | 415 | 0.2 | 0.3 | 0.55 | 0.44 | 1.1 | 1.8 | 0.57 |
| Site 31 | 6 | 28 | 18 | 10 | 250 | 0 | 15 | 415 | 0.2 | 0.5 | 0.8 | 0.5 | 1.2 | 1.9 | 1.81 |
| Site 32 | 6 | 30 | 16 | 0 | 200 | 0 | 15 | 250 | 0.2 | 0.45 | 0.48 | 0.48 | 1.2 | 1.95 | 1.39 |
| Site 33 | 6 | 37 | 19 | 0 | 200 | 10 | 15 | 415 | 0.2 | 0.45 | 0.65 | 0.48 | 1.2 | 2.05 | 0.65 |

**RCC walls**

| Provision of steel | | | | | | | | | | | |
|---|---|---|---|---|---|---|---|---|---|---|---|
| Steel in stem | | | | Steel in toe slab | | | | Steel in heel slab | | | |
| Main reinforcement | | Distribution reinforcement | | Main reinforcement | | Distribution reinforcement | | Main reinforcement | | Distribution reinforcement | |
| Diameter (mm) | Spacing (mm) | Diameter (mm) | Spacing (mm) | Diameter (mm) | Spacing (mm) | Diameter (mm) | Spacing (mm) | Diameter (mm) | Spacing (mm) | Diameter (mm) | Spacing (mm) |
| 6 | 140 | 8 | 320 | 6 | 210 | 8 | 320 | 8 | 180 | 8 | 320 |
| 6 | 640 | 8 | 320 | 6 | 830 | 8 | 320 | 6 | 3480 | 8 | 320 |
| 6 | 860 | 8 | 320 | 6 | 1030 | 8 | 320 | 6 | 4990 | 8 | 320 |
| 6 | 200 | 8 | 320 | 6 | 350 | 8 | 320 | 6 | 480 | 8 | 320 |
| 6 | 190 | 8 | 320 | 6 | 320 | 8 | 320 | 6 | 560 | 8 | 320 |
| 10 | 250 | 8 | 320 | 10 | 310 | 8 | 320 | 10 | 280 | 8 | 320 |
| 12 | 220 | 8 | 320 | 10 | 320 | 8 | 320 | 10 | 320 | 8 | 320 |
| 12 | 150 | 8 | 320 | 12 | 270 | 8 | 300 | 12 | 150 | 8 | 300 |
| 8 | 210 | 8 | 320 | 8 | 360 | 8 | 320 | 6 | 380 | 8 | 320 |
| 16 | 110 | 8 | 320 | 12 | 200 | 8 | 240 | 16 | 150 | 8 | 240 |
| 16 | 270 | 8 | 320 | 10 | 270 | 8 | 320 | 10 | 200 | 8 | 320 |
| 12 | 200 | 8 | 320 | 8 | 220 | 8 | 320 | 8 | 170 | 8 | 320 |
| 20 | 180 | 8 | 320 | 12 | 230 | 8 | 260 | 12 | 180 | 8 | 260 |
| 20 | 170 | 8 | 280 | 16 | 310 | 8 | 220 | 16 | 150 | 8 | 220 |
| 20 | 250 | 8 | 320 | 10 | 210 | 8 | 260 | 12 | 210 | 8 | 260 |
| 20 | 160 | 8 | 280 | 12 | 180 | 8 | 220 | 12 | 130 | 8 | 220 |
| 20 | 130 | 8 | 260 | 12 | 120 | 8 | 200 | 20 | 160 | 8 | 200 |
| 20 | 170 | 8 | 320 | 12 | 270 | 8 | 220 | 12 | 180 | 8 | 220 |
| 18 | 110 | 8 | 320 | 12 | 200 | 8 | 220 | 18 | 140 | 8 | 220 |
| 18 | 100 | 8 | 280 | 12 | 180 | 8 | 200 | 12 | 110 | 8 | 200 |
| 20 | 160 | 8 | 280 | 12 | 210 | 8 | 200 | 12 | 160 | 8 | 200 |
| 20 | 210 | 8 | 300 | 12 | 230 | 8 | 220 | 12 | 140 | 8 | 220 |
| 20 | 90 | 8 | 240 | 18 | 220 | 8 | 160 | 18 | 110 | 8 | 160 |
| 20 | 230 | 8 | 320 | 16 | 480 | 8 | 220 | 16 | 400 | 8 | 220 |
| 20 | 130 | 8 | 220 | 12 | 200 | 8 | 200 | 12 | 120 | 8 | 200 |
| 20 | 120 | 8 | 300 | 12 | 140 | 8 | 120 | 12 | 70 | 8 | 180 |
| 20 | 130 | 8 | 260 | 16 | 250 | 8 | 120 | 16 | 110 | 8 | 180 |
| 20 | 100 | 8 | 260 | 16 | 220 | 8 | 160 | 20 | 160 | 8 | 160 |
| 20 | 80 | 8 | 220 | 16 | 170 | 8 | 140 | 16 | 100 | 8 | 140 |
| 20 | 130 | 8 | 320 | 16 | 350 | 8 | 180 | 16 | 300 | 8 | 180 |
| 20 | 110 | 8 | 220 | 16 | 210 | 8 | 160 | 16 | 140 | 8 | 160 |
| 20 | 70 | 8 | 200 | 16 | 160 | 8 | 120 | 16 | 90 | 8 | 120 |
| 20 | 150 | 8 | 240 | 12 | 170 | 8 | 160 | 16 | 180 | 8 | 160 |

**Table 10.3 Design details of counterfort t**

| no. | Site data | | | | | | | Material properties | | Dimensions | | | | | | | | |
|---|---|---|---|---|---|---|---|---|---|---|---|---|---|---|---|---|---|---|
| | Height of wall | Angle of internal friction | Unit weight of backfill | Inclination of surcharge | Safe bearing capacity of soil | Surcharge | Length of counterfort (assumed) | Characteristic strength of concrete | Yield strength of steel | Stem thickness | | Thickness of base slab | | Width of base slab | | Counterfort | | Depth of foundation |
| | H | $\phi$ | $\gamma$ | i | SBC | q | L | $f_{ck}$ | $f_y$ | Top | Base | Toe | Heel | Toe | Heel | Projection | Thickness | $D_f$ |
| | (m) | (degrees) | (kN/m³) | (degrees) | (kPa) | (kPa) | (m) | (N/mm²) | (N/mm²) | (m) | (m) | (m) | (m) | (m) | (m) | (m) | (m) | (m) |
| 34 | 6.5 | 29 | 15 | 15 | 150 | 0 | 3 | 20 | 415 | 0.25 | 0.25 | 0.85 | 0.4 | 1 | 2.55 | 0.18 | 0.3 | 1.20 |
| 35 | 6.5 | 30 | 16 | 0 | 180 | 0 | 3 | 15 | 250 | 0.2 | 0.2 | 0.65 | 0.4 | 1 | 2.6 | 0.18 | 0.3 | 1.25 |
| 36 | 6.5 | 38 | 19 | 0 | 200 | 10 | 3 | 20 | 415 | 0.2 | 0.2 | 0.4 | 0.4 | 1.1 | 2.8 | 0.18 | 0.3 | 0.60 |
| 37 | 7 | 30 | 16 | 0 | 160 | 0 | 3 | 25 | 415 | 0.25 | 0.25 | 0.85 | 0.45 | 1.1 | 2.85 | 0.18 | 0.3 | 1.11 |
| 38 | 7 | 33 | 16 | 0 | 160 | 10 | 3 | 20 | 415 | 0.25 | 0.25 | 0.9 | 0.45 | 1.2 | 3.05 | 0.18 | 0.3 | 0.87 |
| 39 | 7 | 38 | 16 | 10 | 200 | 0 | 3 | 20 | 415 | 0.2 | 0.2 | 0.85 | 0.45 | 1.2 | 3.1 | 0.18 | 0.3 | 0.71 |
| 40 | 7.5 | 29 | 15 | 0 | 300 | 10 | 3 | 25 | 250 | 0.2 | 0.2 | 0.75 | 0.45 | 1.2 | 3.4 | 0.18 | 0.3 | 2.41 |
| 41 | 7.5 | 30 | 16 | 0 | 170 | 0 | 3 | 25 | 415 | 0.25 | 0.25 | 0.9 | 0.45 | 1.1 | 3.25 | 0.18 | 0.3 | 1.18 |
| 42 | 7.5 | 38 | 16 | 10 | 170 | 0 | 3 | 20 | 415 | 0.2 | 0.2 | 0.85 | 0.45 | 1.1 | 3.1 | 0.18 | 0.3 | 0.60 |
| 43 | 8 | 25 | 15 | 0 | 250 | 0 | 3 | 20 | 415 | 0.3 | 0.3 | 1.15 | 0.6 | 1.2 | 3.3 | 0.18 | 0.3 | 2.75 |
| 44 | 8 | 30 | 16 | 0 | 300 | 10 | 3 | 20 | 415 | 0.3 | 0.3 | 1.2 | 0.5 | 1.3 | 3.5 | 0.18 | 0.3 | 2.08 |
| 45 | 8 | 37 | 16 | 15 | 300 | 0 | 3 | 20 | 415 | 0.25 | 0.25 | 1 | 0.5 | 1.2 | 3.25 | 0.18 | 0.3 | 1.16 |
| 46 | 8.5 | 28 | 18 | 10 | 300 | 0 | 3 | 20 | 415 | 0.4 | 0.4 | 1.6 | 0.7 | 1.3 | 3.3 | 0.18 | 0.3 | 2.17 |
| 47 | 8.5 | 30 | 15 | 0 | 200 | 0 | 3 | 20 | 415 | 0.3 | 0.3 | 1.15 | 0.55 | 1.3 | 3.4 | 0.18 | 0.3 | 1.48 |
| 48 | 8.5 | 34 | 15.85 | 0 | 300 | 12.5 | 3 | 25 | 415 | 0.25 | 0.25 | 1.25 | 0.55 | 1.4 | 3.85 | 0.18 | 0.3 | 1.51 |
| 49 | 9 | 31 | 15 | 0 | 300 | 0 | 3 | 20 | 415 | 0.3 | 0.3 | 1.25 | 0.55 | 1.4 | 3.6 | 0.18 | 0.3 | 2.05 |
| 50 | 9 | 33 | 18.85 | 0 | 250 | 10 | 3 | 20 | 415 | 0.3 | 0.3 | 1.55 | 0.6 | 1.4 | 3.9 | 0.18 | 0.3 | 1.15 |
| 51 | 9 | 38 | 17 | 10 | 300 | 0 | 3 | 20 | 415 | 0.25 | 0.25 | 1.25 | 0.55 | 1.4 | 3.65 | 0.18 | 0.3 | 1.00 |
| 52 | 9.5 | 28 | 17.5 | 10 | 280 | 0 | 3 | 20 | 415 | 0.45 | 0.45 | 1.85 | 0.7 | 1.4 | 3.95 | 0.18 | 0.3 | 2.09 |
| 53 | 9.5 | 30 | 15 | 0 | 250 | 0 | 3 | 25 | 415 | 0.25 | 0.25 | 1.4 | 0.6 | 1.4 | 3.95 | 0.18 | 0.3 | 1.85 |
| 54 | 9.5 | 33 | 17.5 | 0 | 280 | 15 | 3 | 25 | 415 | 0.3 | 0.3 | 1.75 | 0.6 | 1.6 | 4.2 | 0.18 | 0.3 | 1.39 |
| 55 | 10 | 30 | 18 | 0 | 300 | 0 | 3 | 20 | 415 | 0.45 | 0.45 | 1.8 | 0.75 | 1.5 | 3.95 | 0.18 | 0.3 | 1.85 |
| 56 | 10 | 32 | 16.5 | 0 | 300 | 10 | 3 | 20 | 415 | 0.35 | 0.35 | 1.75 | 0.6 | 1.6 | 4.25 | 0.18 | 0.3 | 1.72 |
| 57 | 10 | 40 | 18 | 10 | 250 | 0 | 3 | 25 | 415 | 0.2 | 0.2 | 1.5 | 0.6 | 1.5 | 4.2 | 0.18 | 0.3 | 0.66 |

**pe RCC walls**

| Provision of steel | | | | | | | | | | | | | | | | | |
|---|---|---|---|---|---|---|---|---|---|---|---|---|---|---|---|---|---|
| Steel in stem | | | | Steel in toe slab | | | | Steel in heel slab | | | | Steel in counterfort | | Steel at connections | | | |
| Main reinforcement | | Distribution reinforcement | | Main reinforcement | | Distribution reinforcement | | Main reinforcement | | Distribution reinforcement | | Main reinforcement | | Counterfort – Stem | | Counterfort – base slab | |
| Dia. | Spacing | Dia. | Spacing | Dia. | Spacing | Dia. | Spacing | Dia. | Spacing | Dia. | Spacing | Dia. | No.s | Dia. | No.s | Dia. | No.s |
| (mm) | (mm) | (mm) | (mm) | (mm) | (mm) | (mm) | (mm) | (mm) | (mm) | (mm) | (mm) | (mm) | - | (mm) | - | (mm) | - |
| 16 | 230 | 6 | 220 | 16 | 200 | 8 | 200 | 12 | 200 | 8 | 200 | 20 | 4 | 8 | 5 | 8 | 5 |
| 16 | 140 | 6 | 180 | 16 | 140 | 8 | 160 | 16 | 190 | 8 | 160 | 20 | 6 | 8 | 7 | 8 | 9 |
| 16 | 270 | 6 | 220 | 16 | 190 | 8 | 200 | 12 | 210 | 8 | 200 | 20 | 3 | 8 | 4 | 8 | 5 |
| 16 | 230 | 6 | 220 | 16 | 220 | 8 | 180 | 16 | 360 | 8 | 120 | 20 | 5 | 8 | 5 | 8 | 6 |
| 16 | 230 | 6 | 220 | 12 | 100 | 8 | 180 | 12 | 250 | 8 | 180 | 20 | 5 | 8 | 5 | 8 | 5 |
| 16 | 290 | 6 | 220 | 16 | 200 | 8 | 180 | 8 | 190 | 8 | 140 | 20 | 4 | 8 | 4 | 8 | 3 |
| 16 | 120 | 6 | 180 | 20 | 140 | 8 | 140 | 16 | 200 | 8 | 140 | 20 | 10 | 8 | 8 | 8 | 10 |
| 16 | 210 | 6 | 220 | 12 | 110 | 8 | 180 | 12 | 200 | 8 | 180 | 20 | 6 | 8 | 5 | 8 | 6 |
| 16 | 300 | 6 | 220 | 16 | 230 | 8 | 180 | 12 | 330 | 8 | 180 | 20 | 4 | 8 | 4 | 8 | 4 |
| 16 | 160 | 6 | 220 | 16 | 160 | 8 | 160 | 16 | 280 | 8 | 160 | 20 | 8 | 8 | 6 | 8 | 8 |
| 16 | 170 | 6 | 220 | 16 | 140 | 8 | 160 | 12 | 190 | 8 | 160 | 20 | 7 | 8 | 6 | 8 | 7 |
| 16 | 250 | 6 | 220 | 12 | 100 | 8 | 160 | 12 | 330 | 8 | 160 | 20 | 5 | 8 | 4 | 8 | 4 |
| 16 | 200 | 6 | 180 | 18 | 140 | 8 | 140 | 12 | 150 | 8 | 140 | 20 | 10 | 8 | 7 | 8 | 9 |
| 16 | 190 | 6 | 220 | 16 | 160 | 8 | 140 | 16 | 360 | 8 | 140 | 20 | 8 | 8 | 5 | 8 | 7 |
| 16 | 200 | 6 | 220 | 16 | 140 | 8 | 140 | 12 | 270 | 8 | 140 | 20 | 7 | 8 | 5 | 8 | 5 |
| 16 | 190 | 6 | 220 | 18 | 170 | 8 | 140 | 12 | 200 | 8 | 140 | 20 | 9 | 8 | 5 | 8 | 7 |
| 16 | 140 | 6 | 220 | 18 | 140 | 8 | 140 | 12 | 180 | 8 | 140 | 20 | 11 | 8 | 6 | 8 | 8 |
| 16 | 220 | 6 | 220 | 18 | 180 | 8 | 140 | 12 | 310 | 8 | 140 | 20 | 7 | 8 | 5 | 8 | 5 |
| 16 | 180 | 6 | 180 | 18 | 130 | 8 | 120 | 12 | 170 | 8 | 120 | 20 | 14 | 8 | 7 | 8 | 9 |
| 16 | 140 | 6 | 220 | 12 | 70 | 8 | 100 | 12 | 190 | 8 | 120 | 20 | 10 | 8 | 6 | 8 | 8 |
| 16 | 150 | 6 | 220 | 16 | 90 | 8 | 120 | 12 | 210 | 8 | 120 | 20 | 12 | 8 | 6 | 8 | 7 |
| 16 | 190 | 6 | 180 | 18 | 120 | 8 | 120 | 12 | 150 | 8 | 120 | 20 | 15 | 8 | 7 | 8 | 10 |
| 16 | 140 | 6 | 120 | 18 | 110 | 8 | 120 | 12 | 190 | 8 | 120 | 20 | 14 | 8 | 6 | 8 | 8 |
| 16 | 210 | 6 | 220 | 16 | 120 | 8 | 120 | 10 | 230 | 8 | 120 | 20 | 10 | 8 | 5 | 8 | 5 |

**Table 10.4 Desig**

| Wall no. | Wall data | | | | In situ soil data | | |
|---|---|---|---|---|---|---|---|
| | Height of wall | Surcharge | Backfill slope angle | Backface slope angle | Angle of internal friction | Unit weight of soil | SBC |
| | H | q | i | α | $\phi_s$ | $\gamma_s$ | |
| | (m) | (kPa) | (degrees) | (degrees) | (degrees) | (kN/m³) | (kPa) |
| Site 1 | 1 | 10 | 0 | -6 | 28 | 19.5 | 135 |
| Site 2 | 1 | 0 | 10 | -6 | 32 | 18 | 200 |
| Site 3 | 1 | 0 | 0 | -6 | 34 | 15 | 150 |
| Site 4 | 1.5 | 0 | 0 | -6 | 29 | 15 | 200 |
| Site 5 | 1.5 | 0 | 15 | -6 | 32 | 17 | 150 |
| Site 6 | 1.5 | 10 | 0 | -6 | 37 | 18.85 | 300 |
| Site 7 | 2 | 0 | 0 | -6 | 25 | 19 | 200 |
| Site 8 | 2 | 10 | 0 | -6 | 33 | 16 | 150 |
| Site 9 | 2 | 0 | 10 | -6 | 38 | 15 | 150 |
| Site 10 | 2.5 | 10 | 0 | -6 | 27 | 15 | 150 |
| Site 11 | 2.5 | 0 | 15 | -6 | 31 | 16.5 | 200 |
| Site 12 | 2.5 | 0 | 0 | -6 | 38 | 18 | 200 |
| Site 13 | 3 | 0 | 15 | -6 | 30 | 18.5 | 200 |
| Site 14 | 3 | 10 | 0 | -6 | 32 | 19.5 | 135 |
| Site 15 | 3 | 0 | 0 | -6 | 35 | 19 | 200 |
| Site 16 | 3.5 | 0 | 12.5 | -6 | 26 | 15.5 | 200 |
| Site 17 | 3.5 | 10 | 0 | -6 | 28 | 17.5 | 200 |
| Site 18 | 3.5 | 0 | 0 | -6 | 35 | 16 | 200 |
| Site 19 | 4 | 10 | 0 | -6 | 27 | 18.85 | 250 |
| Site 20 | 4 | 0 | 0 | -6 | 30 | 16 | 250 |
| Site 21 | 4 | 0 | 10 | -6 | 37 | 17 | 200 |
| Site 22 | 4.5 | 0 | 0 | -6 | 30 | 18 | 200 |
| Site 23 | 4.5 | 10 | 0 | -6 | 32 | 18 | 200 |
| Site 24 | 4.5 | 0 | 15 | -6 | 38 | 18 | 250 |
| Site 25 | 5 | 0 | 0 | -6 | 28 | 15 | 150 |
| Site 26 | 5 | 7.5 | 0 | -6 | 30 | 17 | 150 |
| Site 27 | 5 | 10 | 0 | -6 | 30 | 18 | 150 |
| Site 28 | 5.5 | 10 | 0 | -6 | 30 | 16 | 160 |
| Site 29 | 5.5 | 0 | 0 | -6 | 32 | 19 | 200 |
| Site 30 | 5.5 | 0 | 15 | -6 | 38 | 16 | 160 |
| Site 31 | 6 | 0 | 10 | -6 | 28 | 18 | 250 |
| Site 32 | 6 | 0 | 0 | -6 | 30 | 16 | 200 |

**details of gabion faced retaining walls**

| Backfill soil data | | Gabion data | | Gravity wall dimensions (Unreinforced) | | | Reinforced earth wall dimensions | | | |
|---|---|---|---|---|---|---|---|---|---|---|
| Angle of internal friction | Unit weight of soil | Density | Allowable tensile strength | Top width | Bottom width | Ht of box | Top width | Bottom width | Ht of box | Length of reinforcement |
| $\phi_b$ | $\gamma_b$ | $\gamma_g$ | $T_{all}$ | bt | bb | h | bt | bb | h | L |
| (degrees) | (kN/m³) | (kN/m³) | (kN/m) | (m) | (m) | (m) | (m) | (m) | (m) | (m) |
| 28 | 19.5 | 22 | 30 | 1 | 1.5 | 0.5 | 0.5 | 0.5 | 1 | 0.5 |
| 32 | 18 | 22 | 30 | 0.5 | 0.5 | 0.5 | 0.5 | 0.5 | 1 | 0.5 |
| 34 | 15 | 22 | 30 | 0.5 | 0.5 | 0.5 | 0.5 | 0.5 | 1 | 0.5 |
| 29 | 15 | 22 | 30 | 0.5 | 1 | 0.5 | 0.5 | 0.5 | 0.5 | 1 |
| 32 | 17 | 22 | 30 | 0.5 | 1 | 0.5 | 0.5 | 0.5 | 0.5 | 1 |
| 37 | 18.85 | 22 | 30 | 1 | 1 | 0.5 | 0.5 | 0.5 | 0.5 | 1 |
| 25 | 19 | 22 | 30 | 1 | 1.5 | 0.5 | 0.5 | 0.5 | 1 | 1 |
| 33 | 16 | 22 | 30 | 1 | 1 | 0.5 | 0.5 | 0.5 | 1 | 1 |
| 38 | 15 | 22 | 30 | 0.5 | 1 | 0.5 | 0.5 | 0.5 | 1 | 1 |
| 27 | 15 | 22 | 30 | 1 | 1.5 | 0.5 | 0.5 | 0.5 | 0.5 | 1 |
| 31 | 16.5 | 22 | 30 | 1 | 1.5 | 0.5 | 0.5 | 0.5 | 0.5 | 1 |
| 38 | 18 | 22 | 30 | 1 | 1 | 0.5 | 0.5 | 0.5 | 0.5 | 1 |
| 30 | 18.5 | 22 | 30 | 0.5 | 1.5 | 1 | 0.5 | 0.5 | 1 | 1.5 |
| 32 | 19.5 | 22 | 30 | 1 | 2 | 1 | 0.5 | 0.5 | 1 | 1.5 |
| 35 | 19 | 22 | 30 | 0.5 | 1.5 | 1 | 0.5 | 0.5 | 1 | 1.5 |
| 26 | 15.5 | 22 | 30 | 1 | 1.5 | 0.5 | 0.5 | 0.5 | 0.5 | 1.5 |
| 28 | 17.5 | 22 | 30 | 1 | 2 | 0.5 | 0.5 | 0.5 | 0.5 | 1.5 |
| 35 | 16 | 22 | 30 | 0.5 | 1.5 | 0.5 | 0.5 | 0.5 | 0.5 | 1.5 |
| 27 | 18.85 | 22 | 30 | 1 | 2 | 1 | 0.5 | 0.5 | 1 | 1.5 |
| 30 | 16 | 22 | 30 | 0.5 | 2 | 1 | 0.5 | 0.5 | 1 | 1.5 |
| 37 | 17 | 22 | 30 | 0.5 | 1.5 | 1 | 0.5 | 0.5 | 1 | 1.5 |
| 30 | 18 | 22 | 30 | 1 | 2.5 | 0.5 | 0.5 | 0.5 | 0.5 | 2 |
| 32 | 18 | 22 | 30 | 1 | 2 | 0.5 | 0.5 | 0.5 | 0.5 | 2 |
| 38 | 18 | 22 | 30 | 1 | 2 | 0.5 | 0.5 | 0.5 | 0.5 | 2 |
| 28 | 15 | 22 | 30 | 1 | 2 | 1 | 0.5 | 0.5 | 1 | 2 |
| 30 | 17 | 22 | 30 | 1 | 2.5 | 1 | 0.5 | 0.5 | 1 | 2 |
| 30 | 18 | 22 | 30 | 1.5 | 2.5 | 1 | 0.5 | 0.5 | 1 | 2 |
| 30 | 16 | 22 | 30 | 1.5 | 3 | 0.5 | 0.5 | 0.5 | 0.5 | 2 |
| 32 | 19 | 22 | 30 | 1 | 2.5 | 0.5 | 0.5 | 0.5 | 0.5 | 2 |
| 38 | 16 | 22 | 30 | 0.5 | 2.5 | 0.5 | 0.5 | 0.5 | 0.5 | 2 |
| 28 | 18 | 22 | 30 | 1.5 | 3 | 0.5 | 0.5 | 0.5 | 1 | 2.5 |
| 30 | 16 | 22 | 30 | 1 | 2.5 | 1 | 0.5 | 0.5 | 1 | 2.5 |

**Table 10.4 (Contd.) D**

| Wall no. | Wall data | | | | In situ soil data | | |
|---|---|---|---|---|---|---|---|
| | Height of wall | Surcharge | Backfill slope angle | Backface slope angle | Angle of internal friction | Unit weight of soil | SBC |
| | H | q | i | α | $\phi_s$ | $\gamma_s$ | |
| | (m) | (kPa) | (degrees) | (degrees) | (degrees) | (kN/m³) | (kPa) |
| Site 33 | 6 | 10 | 0 | -6 | 37 | 19 | 200 |
| Site 34 | 6.5 | 0 | 15 | -6 | 29 | 15 | 150 |
| Site 35 | 6.5 | 0 | 0 | -6 | 30 | 16 | 180 |
| Site 36 | 6.5 | 10 | 0 | -6 | 38 | 19 | 200 |
| Site 37 | 7 | 0 | 0 | -6 | 30 | 16 | 160 |
| Site 38 | 7 | 10 | 0 | -6 | 33 | 16 | 160 |
| Site 39 | 7 | 0 | 10 | -6 | 38 | 16 | 200 |
| Site 40 | 7.5 | 10 | 0 | -6 | 29 | 15 | 300 |
| Site 41 | 7.5 | 0 | 0 | -6 | 30 | 16 | 170 |
| Site 42 | 7.5 | 0 | 10 | -6 | 38 | 16 | 170 |
| Site 43 | 8 | 0 | 0 | -6 | 25 | 15 | 250 |
| Site 44 | 8 | 10 | 0 | -6 | 30 | 16 | 300 |
| Site 45 | 8 | 0 | 15 | -6 | 37 | 16 | 300 |
| Site 46 | 8.5 | 0 | 10 | -6 | 28 | 18 | 300 |
| Site 47 | 8.5 | 0 | 0 | -6 | 30 | 15 | 200 |
| Site 48 | 8.5 | 12.5 | 0 | -6 | 34 | 15.85 | 300 |
| Site 49 | 9 | 0 | 0 | -6 | 31 | 15 | 300 |
| Site 50 | 9 | 10 | 0 | -6 | 33 | 18.85 | 250 |
| Site 51 | 9 | 0 | 10 | -6 | 38 | 17 | 300 |
| Site 52 | 9.5 | 0 | 10 | -6 | 28 | 17.5 | 280 |
| Site 53 | 9.5 | 0 | 0 | -6 | 30 | 15 | 250 |
| Site 54 | 9.5 | 15 | 0 | -6 | 33 | 17.5 | 280 |
| Site 55 | 10 | 0 | 0 | -6 | 30 | 18 | 300 |
| Site 56 | 10 | 10 | 0 | -6 | 32 | 16.5 | 300 |
| Site 57 | 10 | 0 | 10 | -6 | 40 | 18 | 250 |

**sign details of gabion faced retaining walls**

| Backfill soil data | | Gabion data | | Gravity wall dimensions (Unreinforced) | | | Reinforced earth wall dimensions | | | |
|---|---|---|---|---|---|---|---|---|---|---|
| ngle of internal friction | Unit weight of soil | Density | Allowable tensile strength | Top width | Bottom width | Ht of box | Top width | Bottom width | Ht of box | Length of reinforcement |
| $\phi_b$ | $\gamma_b$ | $\gamma_g$ | $T_{all}$ | bt | bb | h | bt | bb | h | L |
| (degrees) | (kN/m³) | (kN/m³) | (kN/m) | (m) | (m) | (m) | (m) | (m) | (m) | (m) |
| 37 | 19 | 22 | 30 | 1 | 2.5 | 1 | 0.5 | 0.5 | 1 | 2.5 |
| 29 | 15 | 22 | 30 | 1 | 3 | 0.5 | 0.5 | 0.5 | 0.5 | 2.5 |
| 30 | 16 | 22 | 30 | 1 | 3.5 | 0.5 | 0.5 | 0.5 | 0.5 | 2.5 |
| 38 | 19 | 22 | 30 | 1 | 3 | 0.5 | 0.5 | 0.5 | 0.5 | 2.5 |
| 30 | 16 | 22 | 30 | 1 | 4 | 1 | 0.5 | 0.5 | 1 | 2.5 |
| 33 | 16 | 22 | 30 | 1 | 4 | 1 | 0.5 | 0.5 | 1 | 2.5 |
| 38 | 16 | 22 | 30 | 1 | 3 | 1 | 0.5 | 0.5 | 1 | 2.5 |
| 29 | 15 | 22 | 30 | 1 | 4 | 0.5 | 0.5 | 0.5 | 0.5 | 3 |
| 30 | 16 | 22 | 30 | 1 | 4 | 0.5 | 0.5 | 0.5 | 0.5 | 3 |
| 38 | 16 | 22 | 30 | 1 | 3.5 | 0.5 | 0.5 | 0.5 | 0.5 | 3 |
| 25 | 15 | 22 | 30 | 1 | 4.5 | 1 | 0.5 | 0.5 | 1 | 3 |
| 30 | 16 | 22 | 30 | 1 | 4 | 1 | 0.5 | 0.5 | 1 | 3 |
| 37 | 16 | 22 | 30 | 1 | 4 | 1 | 0.5 | 0.5 | 1 | 3 |
| 28 | 18 | 22 | 30 | 1.5 | 4.5 | 0.5 | 0.5 | 0.5 | 0.5 | 3.5 |
| 30 | 15 | 22 | 30 | 1 | 4.5 | 0.5 | 0.5 | 0.5 | 0.5 | 3.5 |
| 34 | 15.85 | 22 | 30 | 1 | 4.5 | 0.5 | 0.5 | 0.5 | 0.5 | 3 |
| 31 | 15 | 22 | 30 | 1.5 | 4.5 | 1 | 0.5 | 0.5 | 1 | 3.5 |
| 33 | 18.85 | 22 | 30 | 1.5 | 5 | 1 | 0.5 | 0.5 | 1 | 3.5 |
| 38 | 17 | 22 | 30 | 1 | 4 | 1 | 0.5 | 0.5 | 1 | 3.5 |
| 28 | 17.5 | 22 | 30 | 1.5 | 4.5 | 0.5 | 0.5 | 0.5 | 0.5 | 3.5 |
| 30 | 15 | 22 | 30 | 1.5 | 4.5 | 0.5 | 0.5 | 0.5 | 0.5 | 3.5 |
| 33 | 17.5 | 22 | 30 | 1.5 | 5 | 0.5 | 0.5 | 0.5 | 0.5 | 3.5 |
| 30 | 18 | 22 | 30 | 1.5 | 5 | 1 | 0.5 | 0.5 | 1 | 4 |
| 32 | 16.5 | 22 | 30 | 1.5 | 5 | 1 | 0.5 | 0.5 | 1 | 4 |
| 40 | 18 | 22 | 30 | 1.5 | 4.5 | 1 | 0.5 | 0.5 | 1 | 4 |

## Table 10.5 Estimation of RCC walls

| Wall no. | Height of wall (m) | Clearing grass | Earthwork excavation | Concrete | Steel | Sand | Labour | Total cost |
|---|---|---|---|---|---|---|---|---|
| | | Rs.200 /- per 100 m² | Rs.800/- per 10m³ | Rs.3636/- per m³ | Rs.34/- per kg | Rs.1500/- per m³ | Rs.50/- per m³ | Rs. per m³ |
| Site 1 | 1 | 3.6 | 172.8 | 1219 | 325.26 | 600 | 20 | 3042.858 |
| Site 2 | 1 | 3.2 | 153.6 | 1081.68 | 293.09 | 300 | 10 | 2394.041 |
| Site 3 | 1 | 3.2 | 153.6 | 1081.68 | 287.81 | 300 | 10 | 2387.177 |
| Site 4 | 1.5 | 4.2 | 285.6 | 1536.16 | 442.83 | 1125 | 37.5 | 4460.677 |
| Site 5 | 1.5 | 4.2 | 285.6 | 1536.16 | 460.94 | 1125 | 37.5 | 4484.22 |
| Site 6 | 1.5 | 4.6 | 312.8 | 1681.16 | 566.04 | 1350 | 45 | 5147.48 |
| Site 7 | 2 | 4.6 | 404.8 | 2145.2 | 1011.91 | 1800 | 60 | 7054.463 |
| Site 8 | 2 | 5.6 | 495.04 | 2347.82 | 1017.21 | 3000 | 100 | 9055.371 |
| Site 9 | 2 | 4.6 | 404.8 | 2145.2 | 715.12 | 1800 | 60 | 6668.636 |
| Site 10 | 2.5 | 6.6 | 728.64 | 2637.77 | 1141.37 | 5250 | 175 | 12921.194 |
| Site 11 | 2.5 | 5.4 | 583.2 | 2699.68 | 1258.87 | 3750 | 125 | 10948.795 |
| Site 12 | 2.5 | 5 | 540 | 2554.24 | 1462.35 | 3000 | 100 | 9960.067 |
| Site 13 | 3 | 5.6 | 725.76 | 3097.79 | 1926.19 | 4500 | 150 | 13526.942 |
| Site 14 | 3 | 6.4 | 842.24 | 3219.51 | 1922.18 | 5625 | 187.5 | 15343.679 |
| Site 15 | 3 | 5.6 | 725.76 | 3097.79 | 1646.66 | 4500 | 150 | 13163.553 |
| Site 16 | 3.5 | 6.2 | 937.44 | 3546.76 | 2091.21 | 6037.5 | 201.25 | 16666.468 |
| Site 17 | 3.5 | 7.6 | 1164.32 | 3752.05 | 2226.9 | 8400 | 280 | 20580.131 |
| Site 18 | 3.5 | 6.2 | 937.44 | 3828.61 | 2346.07 | 6300 | 210 | 17716.816 |
| Site 19 | 4 | 8.8 | 1538.24 | 4126.36 | 2507.68 | 13200 | 440 | 28367.404 |
| Site 20 | 4 | 6.8 | 1175.04 | 4092.09 | 2751.74 | 8100 | 270 | 21314.371 |
| Site 21 | 4 | 6.8 | 1175.04 | 4092.09 | 2432.39 | 8100 | 270 | 20899.216 |
| Site 22 | 4.5 | 7.4 | 1438.56 | 7055.5 | 4561.3 | 9787.5 | 326.25 | 30129.463 |
| Site 23 | 4.5 | 8 | 1571.2 | 6808.11 | 4682.62 | 11137.5 | 371.25 | 31952.284 |
| Site 24 | 4.5 | 7.4 | 1438.56 | 6300.99 | 4714 | 10125 | 337.5 | 29800.485 |
| Site 25 | 5 | 8 | 1728 | 8599.04 | 8504.81 | 12750 | 425 | 41619.305 |
| Site 26 | 5 | 8.6 | 1871.36 | 9326.14 | 9993.39 | 13875 | 462.5 | 46198.087 |
| Site 27 | 5 | 8.8 | 1918.4 | 9271.5 | 9991.63 | 14250 | 475 | 46689.929 |
| Site 28 | 5.5 | 9.6 | 2323.2 | 10234.84 | 12451.42 | 18150 | 605 | 56906.278 |
| Site 29 | 5.5 | 8.6 | 2043.36 | 11726.1 | 13767.48 | 14850 | 495 | 55757.702 |
| Site 30 | 5.5 | 8.4 | 1995.84 | 10886.18 | 9233.42 | 14850 | 495 | 48709.492 |
| Site 31 | 6 | 9.2 | 2392 | 16907.4 | 12661.97 | 17100 | 570 | 64532.741 |
| Site 32 | 6 | 9.2 | 2384.64 | 13656.82 | 16796.25 | 17550 | 585 | 66276.483 |
| Site 33 | 6 | 9.4 | 2436.48 | 15707.52 | 10045.57 | 18450 | 615 | 61443.161 |
| Site 34 | 6.5 | 9.6 | 2649.6 | 15174.85 | 8623.57 | 24862.5 | 828.75 | 67793.531 |
| Site 35 | 6.5 | 9.6 | 2649.6 | 14447.65 | 12209.45 | 25350 | 845 | 72164.69 |
| Site 36 | 6.5 | 10.2 | 2815.2 | 16011.13 | 7851.84 | 27300 | 910 | 71367.881 |
| Site 37 | 7 | 10.4 | 3099.2 | 19481.89 | 9752.16 | 29925 | 997.5 | 82245.995 |
| Site 38 | 7 | 11 | 3278 | 20590.87 | 9872.22 | 32025 | 1067.5 | 86897.967 |
| Site 39 | 7 | 11 | 3278 | 18372.71 | 9364.26 | 32550 | 1085 | 84059.261 |
| Site 40 | 7.5 | 11.6 | 3688.8 | 19498.05 | 15650.16 | 38250 | 1275 | 101885.693 |
| Site 41 | 7.5 | 11.2 | 3561.6 | 19525.32 | 11078.49 | 36562.5 | 1218.75 | 93545.218 |
| Site 42 | 7.5 | 10.8 | 3434.4 | 18725.4 | 8908.7 | 34875 | 1162.5 | 87251.84 |
| Site 43 | 8 | 11.6 | 3990.4 | 25895.79 | 15629.92 | 39600 | 1320 | 112382.023 |
| Site 44 | 8 | 12.2 | 4148 | 25895.79 | 15221.57 | 42000 | 1400 | 115280.828 |
| Site 45 | 8 | 11.4 | 3876 | 25823.27 | 13078.37 | 39000 | 1300 | 108015.752 |
| Site 46 | 8.5 | 12 | 4416 | 30316 | 15860.26 | 42075 | 1402.5 | 122306.288 |
| Site 47 | 8.5 | 12 | 4344 | 31702.98 | 16408.34 | 43350 | 1445 | 126441.016 |

## Table 10.5 (Contd.) Estimation of RCC walls

| Wall no. | Height of wall (m) | Clearing grass | Earthwork excavation | Concrete | Steel | Sand | Labour | Total cost |
|---|---|---|---|---|---|---|---|---|
| | | Rs.200 /- per 100 m² | Rs.800/- per 10m³ | Rs.3636/- per m³ | Rs.34/- per kg | Rs.1500/- per m³ | Rs.50/- per m³ | Rs. per m³ |
| Site 48 | 8.5 | 13 | 4706 | 30048.2 | 15339.33 | 49087.5 | 1636.25 | 131079.364 |
| Site 49 | 9 | 12.6 | 4813.2 | 30055.48 | 20480.35 | 48600 | 1620 | 137256.119 |
| Site 50 | 9 | 13.2 | 5068.8 | 30436.96 | 20655.32 | 52650 | 1755 | 143753.064 |
| Site 51 | 9 | 12.6 | 4813.2 | 27055.48 | 22529.18 | 49275 | 1642.5 | 136926.348 |
| Site 52 | 9.5 | 13.6 | 5548.8 | 28729.96 | 26745.18 | 56287.5 | 1876.25 | 154961.677 |
| Site 53 | 9.5 | 13.2 | 5332.8 | 28416.9 | 24798.1 | 56287.5 | 1876.25 | 151742.175 |
| Site 54 | 9.5 | 14.2 | 5736.8 | 29643.81 | 25241.79 | 59850 | 1995 | 159226.08 |
| Site 55 | 10 | 13.8 | 5934 | 30777.94 | 21530.38 | 59250 | 1975 | 155325.456 |
| Site 56 | 10 | 14.4 | 6105.6 | 30814.6 | 22229.87 | 63750 | 2125 | 162551.311 |
| Site 57 | 10 | 13.8 | 5851.2 | 31014.8 | 23897.24 | 63000 | 2100 | 163640.152 |

## Table 10.6 Estimation of gabion faced gravity walls

| Wall no. | Height of wall (m) | Clearing grass | Earthwork excavation | Gabions | Stones | Labour | Geotextile | Total cost |
|---|---|---|---|---|---|---|---|---|
| | | Rs. 200/- per 100 m² | Rs.800/- per 10m³ | Rs.975/- per m³ | Rs.400/- per m³ | Rs.150/- per m³ | Rs.50/- per m² | Rs. per m³ |
| Site 1 | 1 | 4.00 | 160 | 1218.75 | 500 | 187.5 | 50 | 2756.33 |
| Site 2 | 1 | 2.00 | 80 | 637.5 | 200 | 75 | 50 | 1357.85 |
| Site 3 | 1 | 2.00 | 80 | 637.5 | 200 | 75 | 50 | 1357.85 |
| Site 4 | 1.5 | 3.00 | 180 | 1434.38 | 450 | 168.75 | 75 | 3004.46 |
| Site 5 | 1.5 | 3.00 | 180 | 1434.38 | 450 | 168.75 | 75 | 3004.46 |
| Site 6 | 1.5 | 3.00 | 180 | 1912.5 | 600 | 225 | 75 | 3894.15 |
| Site 7 | 2 | 4.00 | 320 | 3187.5 | 1000 | 375 | 100 | 6482.45 |
| Site 8 | 2 | 3.00 | 240 | 2550 | 800 | 300 | 100 | 5190.9 |
| Site 9 | 2 | 3.00 | 240 | 1912.5 | 600 | 225 | 100 | 4004.65 |
| Site 10 | 2.5 | 4.00 | 400 | 3984.38 | 1250 | 468.75 | 125 | 8101.76 |
| Site 11 | 2.5 | 4.00 | 400 | 3984.38 | 1250 | 468.75 | 125 | 8101.76 |
| Site 12 | 2.5 | 3.00 | 300 | 3187.5 | 1000 | 375 | 125 | 6487.65 |
| Site 13 | 3 | 4.00 | 480 | 3825 | 1200 | 450 | 150 | 7941.7 |
| Site 14 | 3 | 5.00 | 600 | 5737.5 | 1800 | 675 | 150 | 11657.8 |
| Site 15 | 3 | 4.00 | 480 | 3825 | 1200 | 450 | 150 | 7941.7 |
| Site 16 | 3.5 | 4.00 | 560 | 5578.13 | 1750 | 656.25 | 175 | 11340.4 |
| Site 17 | 3.5 | 5.00 | 700 | 6693.75 | 2100 | 787.5 | 175 | 13599.6 |
| Site 18 | 3.5 | 4.00 | 560 | 4462.5 | 1400 | 525 | 175 | 9264.45 |
| Site 19 | 4 | 5.00 | 800 | 7650 | 2400 | 900 | 200 | 15541.5 |
| Site 20 | 4 | 5.00 | 800 | 6375 | 2000 | 750 | 200 | 13169 |
| Site 21 | 4 | 4.00 | 640 | 5100 | 1600 | 600 | 200 | 10587.2 |
| Site 22 | 4.5 | 6.00 | 1080 | 10040.6 | 3150 | 1181.25 | 225 | 20387.7 |

**Table 10.6 (Contd.) Estimation of gabion faced gravity walls**

| Wall no. | Height of wall (m) | Clearing grass | Earthwork excavation | Gabions | Stones | Labour | Geotextile | Total cost |
|---|---|---|---|---|---|---|---|---|
| | | Rs. 200/- per 100 m² | Rs.800/- per 10m³ | Rs.975/- per m³ | Rs.400/- per m³ | Rs.150/- per m³ | Rs.50/- per m² | Rs. per m³ |
| Site 23 | 4.5 | 5.00 | 900 | 8606.25 | 2700 | 1012.5 | 225 | 17483.4 |
| Site 24 | 4.5 | 5.00 | 900 | 8606.25 | 2700 | 1012.5 | 225 | 17483.4 |
| Site 25 | 5 | 5.00 | 1000 | 9562.5 | 3000 | 1125 | 250 | 19425.3 |
| Site 26 | 5 | 6.00 | 1200 | 11156.3 | 3500 | 1312.5 | 250 | 22652.2 |
| Site 27 | 5 | 6.00 | 1200 | 12750 | 4000 | 1500 | 250 | 25617.8 |
| Site 28 | 5.5 | 7.00 | 1540 | 15778.1 | 4950 | 1856.25 | 275 | 31728.3 |
| Site 29 | 5.5 | 6.00 | 1320 | 12271.9 | 3850 | 1443.75 | 275 | 24916.6 |
| Site 30 | 5.5 | 6.00 | 1320 | 10518.8 | 3300 | 1237.5 | 275 | 21654.4 |
| Site 31 | 6 | 7.00 | 1680 | 17212.5 | 5400 | 2025 | 300 | 34611.9 |
| Site 32 | 6 | 6.00 | 1440 | 13387.5 | 4200 | 1575 | 300 | 27181.1 |
| Site 33 | 6 | 6.00 | 1440 | 13387.5 | 4200 | 1575 | 300 | 27181.1 |
| Site 34 | 6.5 | 7.00 | 1820 | 16575 | 5200 | 1950 | 325 | 33640.1 |
| Site 35 | 6.5 | 8.00 | 2080 | 18646.9 | 5850 | 2193.75 | 325 | 37834.7 |
| Site 36 | 6.5 | 7.00 | 1820 | 16575 | 5200 | 1950 | 325 | 33640.1 |
| Site 37 | 7 | 9.00 | 2520 | 22312.5 | 7000 | 2625 | 350 | 45261.5 |
| Site 38 | 7 | 9.00 | 2520 | 22312.5 | 7000 | 2625 | 350 | 45261.5 |
| Site 39 | 7 | 7.00 | 1960 | 17850 | 5600 | 2100 | 350 | 36227.1 |
| Site 40 | 7.5 | 9.00 | 2700 | 23906.3 | 7500 | 2812.5 | 375 | 48493.6 |
| Site 41 | 7.5 | 9.00 | 2700 | 23906.3 | 7500 | 2812.5 | 375 | 48493.6 |
| Site 42 | 7.5 | 8.00 | 2400 | 21515.6 | 6750 | 2531.25 | 375 | 43653.8 |
| Site 43 | 8 | 10.00 | 3200 | 28050 | 8800 | 3300 | 400 | 56888 |
| Site 44 | 8 | 9.00 | 2880 | 25500 | 8000 | 3000 | 400 | 51725.7 |
| Site 45 | 8 | 9.00 | 2880 | 25500 | 8000 | 3000 | 400 | 51725.7 |
| Site 46 | 8.5 | 10.00 | 3400 | 32512.5 | 10200 | 3825 | 425 | 65484.3 |
| Site 47 | 8.5 | 10.00 | 3400 | 29803.1 | 9350 | 3506.25 | 425 | 60442.7 |
| Site 48 | 8.5 | 10.00 | 3400 | 29803.1 | 9350 | 3506.25 | 425 | 60442.7 |
| Site 49 | 9 | 10.00 | 3600 | 34425 | 10800 | 4050 | 450 | 69335.5 |
| Site 50 | 9 | 11.00 | 3960 | 37293.8 | 11700 | 4387.5 | 450 | 75142.9 |
| Site 51 | 9 | 9.00 | 3240 | 28687.5 | 9000 | 3375 | 450 | 58190 |
| Site 52 | 9.5 | 10.00 | 3800 | 36337.5 | 11400 | 4275 | 475 | 73186.8 |
| Site 53 | 9.5 | 10.00 | 3800 | 36337.5 | 11400 | 4275 | 475 | 73186.8 |
| Site 54 | 9.5 | 11.00 | 4180 | 39365.6 | 12350 | 4631.25 | 475 | 79316.7 |
| Site 55 | 10 | 11.00 | 4400 | 41437.5 | 13000 | 4875 | 500 | 83490.6 |
| Site 56 | 10 | 11.00 | 4400 | 41437.5 | 13000 | 4875 | 500 | 83490.6 |
| Site 57 | 10 | 10.00 | 4000 | 38250 | 12000 | 4500 | 500 | 77038 |

**Table 10.7 Estimation of gabion faced reinforced soil walls**

| Wall no. | Height of wall (m) | Clearing grass | Earthwork excavation | Gabions | Stones | Labour | Geotextile | Basal reinforcement | Total cost |
|---|---|---|---|---|---|---|---|---|---|
| | | Rs. 200/- per 100 $m^2$ | Rs.800/- per $10m^3$ | Rs.1500/- per $m^3$ | Rs.400/- per $m^3$ | Rs.150/- per $m^3$ | Rs.50/- per $m^2$ | Rs.150/- per $m^2$ | Rs. per $m^3$ |
| Site 1 | 1 | 3.00 | 120 | 750 | 200 | 225 | 50 | 75 | 1849.9 |
| Site 2 | 1 | 3.00 | 120 | 750 | 200 | 225 | 50 | 75 | 1849.9 |
| Site 3 | 1 | 3.00 | 120 | 750 | 200 | 225 | 50 | 75 | 1849.9 |
| Site 4 | 1.5 | 4.00 | 240 | 1125 | 300 | 360 | 75 | 300 | 3125.2 |
| Site 5 | 1.5 | 4.00 | 240 | 1125 | 300 | 360 | 75 | 300 | 3125.2 |
| Site 6 | 1.5 | 4.00 | 240 | 1125 | 300 | 360 | 75 | 300 | 3125.2 |
| Site 7 | 2 | 4.00 | 320 | 1500 | 400 | 540 | 100 | 300 | 4113.2 |
| Site 8 | 2 | 4.00 | 320 | 1500 | 400 | 510 | 100 | 225 | 3976.7 |
| Site 9 | 2 | 4.00 | 320 | 1500 | 400 | 450 | 100 | 225 | 3898.7 |
| Site 10 | 2.5 | 4.25 | 425 | 1875 | 500 | 796.875 | 125 | 375 | 5331.46 |
| Site 11 | 2.5 | 4.00 | 400 | 1875 | 500 | 703.125 | 125 | 375 | 5176.76 |
| Site 12 | 2.5 | 4.00 | 400 | 1875 | 500 | 562.5 | 125 | 375 | 4993.95 |
| Site 13 | 3 | 5.00 | 600 | 2250 | 600 | 1125 | 150 | 525 | 6831.5 |
| Site 14 | 3 | 5.00 | 600 | 2250 | 600 | 1125 | 150 | 450 | 6734 |
| Site 15 | 3 | 5.00 | 600 | 2250 | 600 | 1125 | 150 | 450 | 6734 |
| Site 16 | 3.5 | 5.55 | 777 | 2625 | 700 | 1456.88 | 175 | 675 | 8338.75 |
| Site 17 | 3.5 | 5.20 | 728 | 2625 | 700 | 1365 | 175 | 600 | 8057.66 |
| Site 18 | 3.5 | 5.00 | 700 | 2625 | 700 | 1312.5 | 175 | 525 | 7855.25 |
| Site 19 | 4 | 5.00 | 800 | 3000 | 800 | 1500 | 200 | 750 | 9171.5 |
| Site 20 | 4 | 5.00 | 800 | 3000 | 800 | 1500 | 200 | 675 | 9074 |
| Site 21 | 4 | 5.00 | 800 | 3000 | 800 | 1500 | 200 | 675 | 9074 |
| Site 22 | 4.5 | 6.00 | 1080 | 3375 | 900 | 1856.25 | 225 | 900 | 10844.9 |
| Site 23 | 4.5 | 6.00 | 1080 | 3375 | 900 | 2008.13 | 225 | 900 | 11042.4 |
| Site 24 | 4.5 | 6.00 | 1080 | 3375 | 900 | 1687.5 | 225 | 900 | 10625.6 |
| Site 25 | 5 | 6.50 | 1300 | 3750 | 1000 | 2437.5 | 250 | 1050 | 12732.2 |
| Site 26 | 5 | 7.50 | 1500 | 3750 | 1000 | 2812.5 | 250 | 975 | 13383.5 |
| Site 27 | 5 | 8.00 | 1600 | 3750 | 1000 | 3000 | 250 | 975 | 13757.9 |
| Site 28 | 5.5 | 8.15 | 1793 | 4125 | 1100 | 3361.88 | 275 | 1200 | 15421.9 |
| Site 29 | 5.5 | 6.50 | 1430 | 4125 | 1100 | 2681.25 | 275 | 1200 | 14063.1 |
| Site 30 | 5.5 | 6.00 | 1320 | 4125 | 1100 | 2454.38 | 275 | 1200 | 13624.5 |
| Site 31 | 6 | 8.20 | 1968 | 4500 | 1200 | 3690 | 300 | 1500 | 17116.1 |
| Site 32 | 6 | 7.00 | 1680 | 4500 | 1200 | 3150 | 300 | 1425 | 15940.6 |
| Site 33 | 6 | 7.00 | 1680 | 4500 | 1200 | 3150 | 300 | 1350 | 15843.1 |
| Site 34 | 6.5 | 10.75 | 2795 | 4875 | 1300 | 5240.63 | 325 | 1725 | 21152.8 |
| Site 35 | 6.5 | 8.15 | 2119 | 4875 | 1300 | 3973.13 | 325 | 1500 | 18330.4 |
| Site 36 | 6.5 | 7.50 | 1950 | 4875 | 1300 | 3656.25 | 325 | 1575 | 17795.4 |
| Site 37 | 7 | 10.80 | 3024 | 5250 | 1400 | 5670 | 350 | 1725 | 22658.7 |
| Site 38 | 7 | 11.50 | 3220 | 5250 | 1400 | 6037.5 | 350 | 1725 | 23392.2 |

**Table 10.7 (Contd.) Estimation of gabion faced reinforced soil walls**

| Wall no. | Height of wall (m) | Clearing grass | Earthwork excavation | Gabions | Stones | Labour | Geotextile | Basal reinforcement | Total cost |
|---|---|---|---|---|---|---|---|---|---|
| | | Rs. 200/- per 100 m² | Rs.800/- per 10m³ | Rs.1500/- per m³ | Rs.400/- per m³ | Rs.150/- per m³ | Rs.50/- per m² | Rs.150/- per m² | Rs. per m³ |
| Site 39 | 7 | 7.30 | 2044 | 5250 | 1400 | 3832.5 | 350 | 1800 | 19088.9 |
| Site 40 | 7.5 | 10.00 | 3000 | 5625 | 1500 | 5625 | 375 | 2025 | 23608 |
| Site 41 | 7.5 | 11.50 | 3450 | 5625 | 1500 | 6468.75 | 375 | 1950 | 25194.3 |
| Site 42 | 7.5 | 10.00 | 3000 | 5625 | 1500 | 5625 | 375 | 1950 | 23510.5 |
| Site 43 | 8 | 11.40 | 3648 | 6000 | 1600 | 6840 | 400 | 2400 | 27169.2 |
| Site 44 | 8 | 9.80 | 3136 | 6000 | 1600 | 5880 | 400 | 2475 | 25351 |
| Site 45 | 8 | 8.20 | 2624 | 6000 | 1600 | 4920 | 400 | 2400 | 23337.9 |
| Site 46 | 8.5 | 11.20 | 3808 | 6375 | 1700 | 7140 | 425 | 2700 | 28807 |
| Site 47 | 8.5 | 12.05 | 4097 | 6375 | 1700 | 7681.88 | 425 | 2550 | 29693.2 |
| Site 48 | 8.5 | 9.50 | 3230 | 6375 | 1700 | 6056.25 | 425 | 2475 | 26352 |
| Site 49 | 9 | 10.00 | 3600 | 6750 | 1800 | 6750 | 450 | 3150 | 29263 |
| Site 50 | 9 | 12.70 | 4572 | 6750 | 1800 | 8572.5 | 450 | 3075 | 32801.9 |
| Site 51 | 9 | 9.10 | 3276 | 6750 | 1800 | 6142.5 | 450 | 3075 | 27953.4 |
| Site 52 | 9.5 | 13.35 | 5073 | 7125 | 1900 | 9511.88 | 475 | 3600 | 36007.7 |
| Site 53 | 9.5 | 11.45 | 4351 | 7125 | 1900 | 8158.13 | 475 | 3525 | 33209.2 |
| Site 54 | 9.5 | 12.40 | 4712 | 7125 | 1900 | 8835 | 475 | 3525 | 34559.7 |
| Site 55 | 10 | 12.00 | 4800 | 7500 | 2000 | 9000 | 500 | 3975 | 36123.1 |
| Site 56 | 10 | 12.00 | 4800 | 7500 | 2000 | 9000 | 500 | 3975 | 36123.1 |
| Site 57 | 10 | 12.00 | 4800 | 7500 | 2000 | 9000 | 500 | 3900 | 36025.6 |

## 10.3 COST PREDICTION MODELS

After fixing the wall geometry and estimation of the walls as shown in the previous section, the cost of the walls in rupees per metre length was plotted against the height in metres. A curve of best fit was fitted between the data and a power curve was obtained. $R^2$ values of nearly 0.98 were obtained for all the cases which indicate the best fit nature of the curves (Fig. 10.1). From the equations of the curves, the cost prediction models were obtained as:

- For RCC walls, $C = 2062.8\ H^{1.8885}$
- For gabion faced gravity walls, $C = 1531.6\ H^{1.69}$
- For gabion faced reinforced soil walls, $C = 1662\ H^{1.3051}$

where, C = cost per metre length of the wall in Indian Rupees, H = height of wall in metres. From these prediction models, the cost of walls can be approximately obtained without doing the complete estimation.

The same result is presented in another form in Fig. 10.2 to study the variation of the cost with wall height. It is seen that for small wall heights, the variation of cost is not prominent for the different types. This means that the economy is not a major aspect for low height walls while selecting the type of walls at a site. A geotechnical engineer has to go for the feasibily, availability of materials etc., for the selection of wall type. But as the height of walls increases, the difference in cost increases and the economy becomes a crucial factor

The RCC walls are costlier than the gabion faced walls because of the immense cost involved in the steel and concrete components. The cost of concrete includes the rates of shuttering, placing and curing of concrete as well as those of materials. The cost of steel includes the placing and tieing of steel bars apart from the material cost. As the height increases, it is seen that the RCC walls are costlier and the gabion faced soil retaining walls are the cheapest.

The results are presented in the form of savings in cost also (Fig. 10.3) where, the savings are calculated as:

$$S = (C_r - C_g) / C_g \times 100\%$$

where, S is the percentage savings in cost, $C_r$ is the cost per metre length of RCC walls in Indian Rupees and $C_g$ is the cost per metre length of gabion walls in Indian Rupees.

From Fig. 10.3, it is seen that the range of savings varies from 30% - 70% for gabion faced reinforced soil walls and from 30% - 50% for gabion faced gravity type retaining walls. For low height walls the percentage savings is smaller and as the height increases the percentage savings in cost also increases.

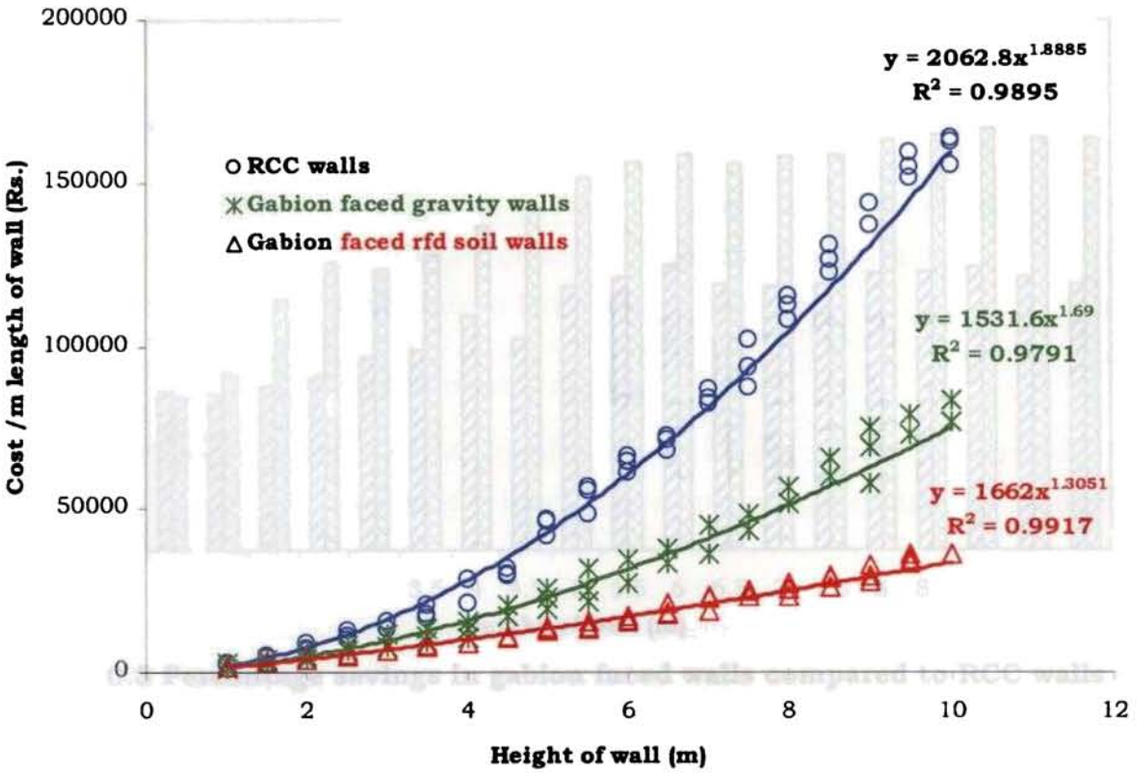


**Fig. 10.1 Variation of cost of retaining walls with height**

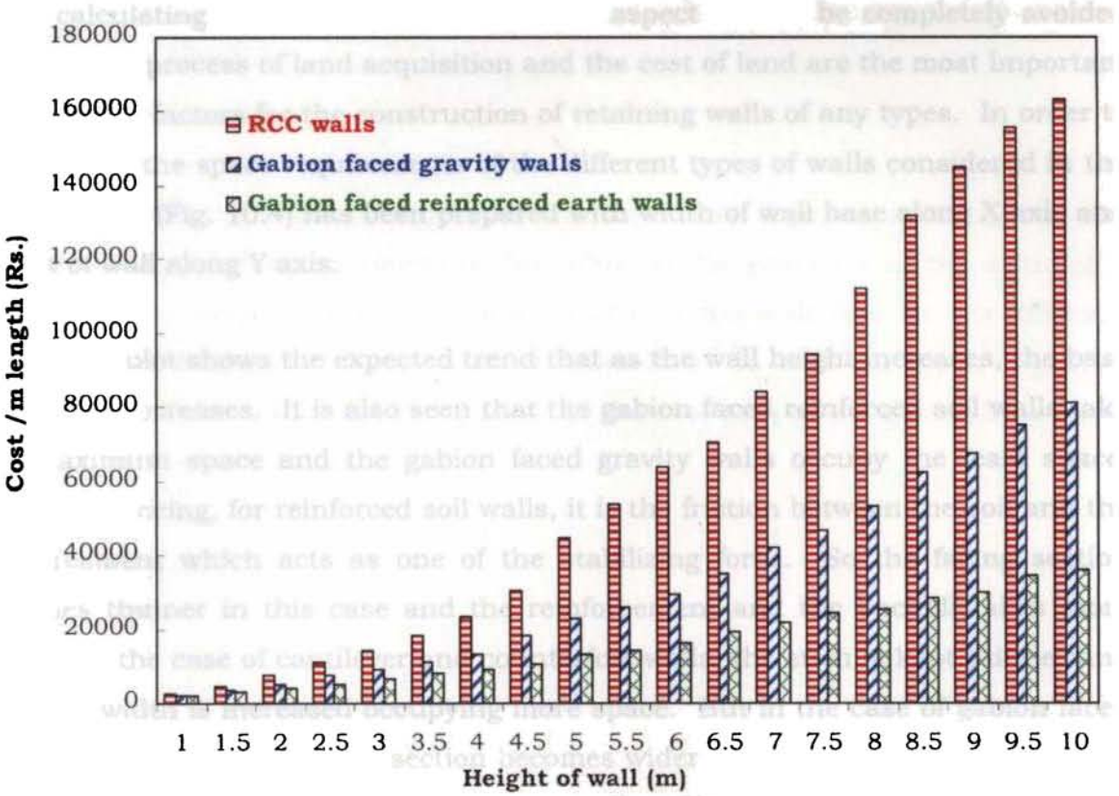


**Fig. 10.2 Cost variation of retaining walls**

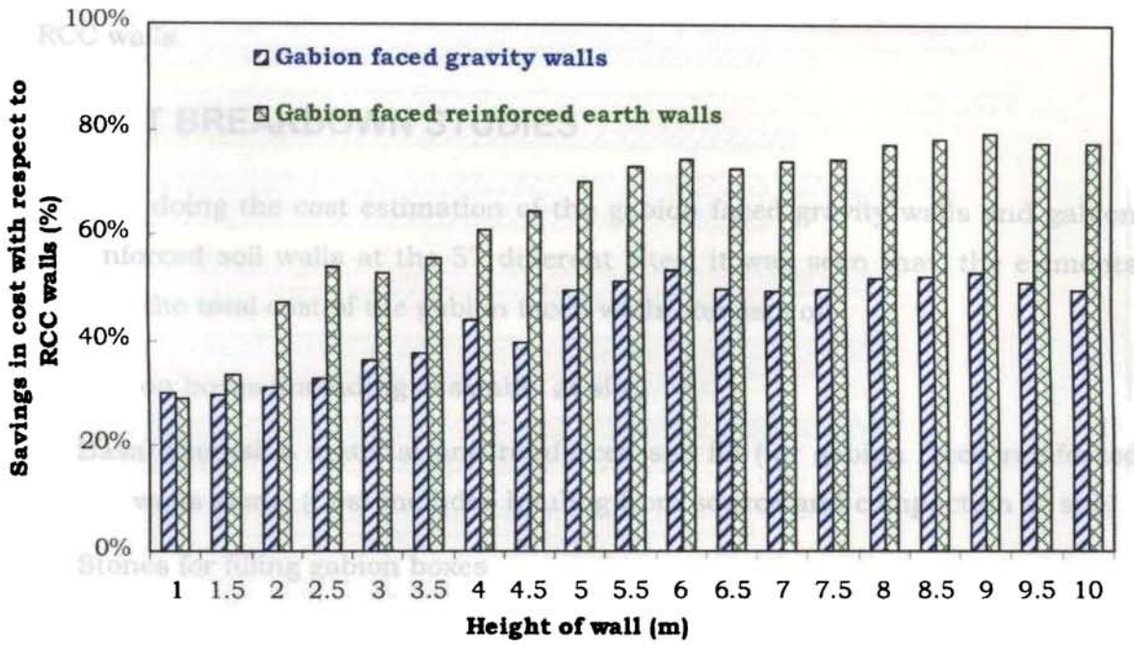


**Fig. 10.3 Percentage savings in gabion faced walls compared to RCC walls**

The space required for construction is yet another important factor which controls the economy of construction. This aspect is not considered in the study while calculating the cost of walls. But this aspect cannot be completely avoided because the process of land acquisition and the cost of land are the most important and primary factors for the construction of retaining walls of any types. In order to understand the space requirements of the different types of walls considered in the study, a plot (Fig. 10.4) has been prepared with width of wall base along X axis and height of wall along Y axis.

The plot shows the expected trend that as the wall height increases, the base width also increases. It is also seen that the gabion faced reinforced soil walls take the maximum space and the gabion faced gravity walls occupy the least space. The reason being, for reinforced soil walls, it is the friction between the soil and the reinforcement which acts as one of the stabilizing force. So the facing section becomes thinner in this case and the reinforcement and the backfill takes more space. In the case of cantilever and counterfort walls, the stem is kept thinner and the base width is increased occupying more space. But in the case of gabion faced gravity walls, the entire cross section becomes wider as the height of wall increases as in the case of random rubble masonry walls. Since the entire width increases

rather than the base width alone, the total width required is less when compared to the RCC walls.

## 10.4 COST BREAKDOWN STUDIES

After doing the cost estimation of the gabion faced gravity walls and gabion faced reinforced soil walls at the 57 different sites, it was seen that, the elements comprising the total cost of the gabion faced walls consists of:-

- Gabion boxes (including assembly at site)
- Basal extension material and reinforced soil fill (for gabion faced reinforced soil walls alone) (Cost includes hauling from source and compaction at site)
- Stones for filling gabion boxes
- Geotextile provided as a filter at the back of wall
- Site clearance and earthwork excavation at site
- Laboratory and in – situ testing of soil
- Transportation of materials
- Labour charges
- Overhead and Profit

For retaining walls of any type, the total cost depends not only on the relative costs of individual elements, but also on the geometry of the structure. The values are calculated for per square metre of the wall face for the different walls and are averaged and presented in Table 10.8. In both the types of gabion faced walls, it is seen that the major share of the cost goes to the gabion boxes and the minor share is for the geotextile.

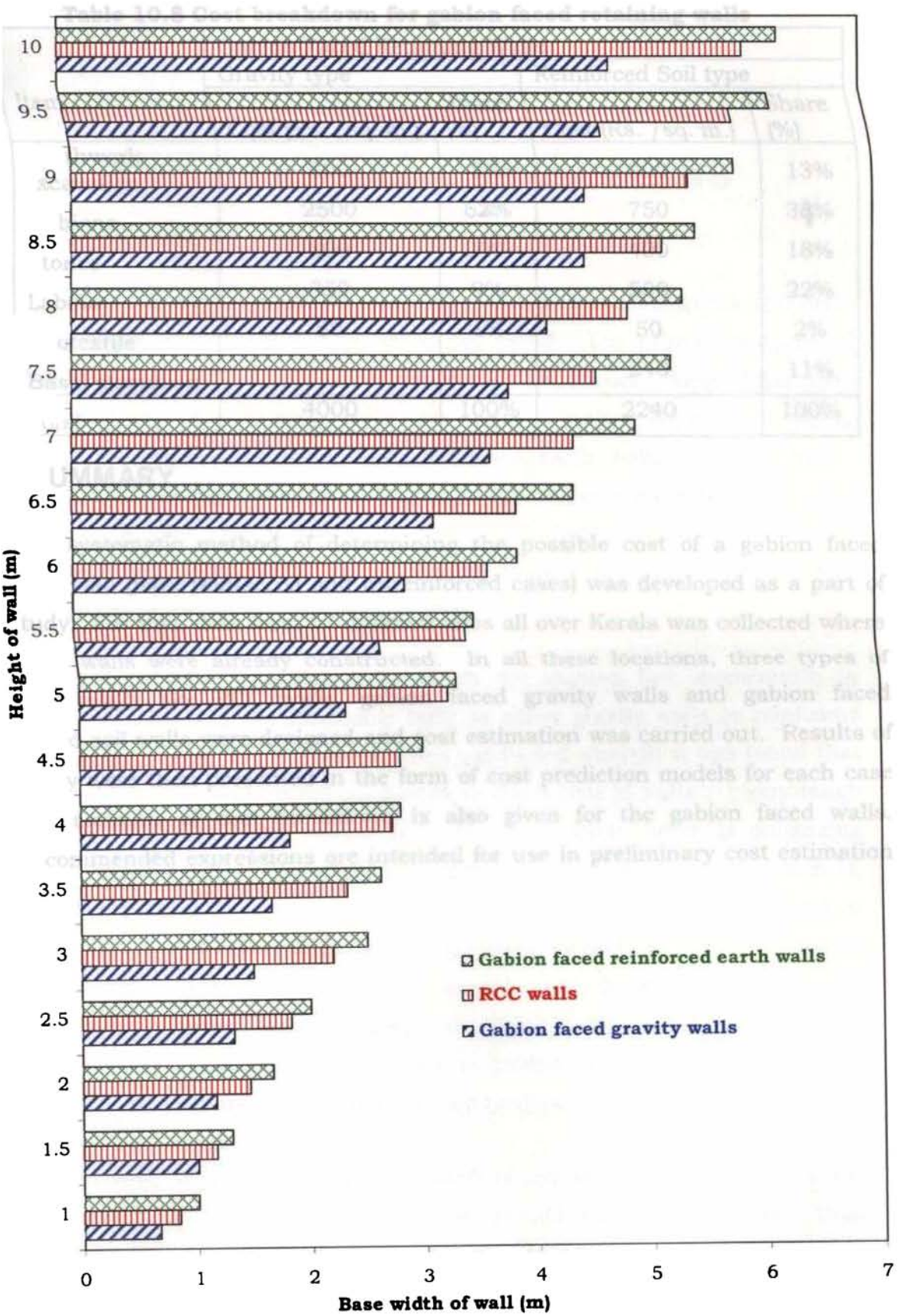


**Fig. 10.4 Space requirements of retaining walls**

**Table 10.8 Cost breakdown for gabion faced retaining walls**

| Item | Gabion Faced Retaining Walls | | | |
|---|---|---|---|---|
| | Gravity type | | Reinforced Soil type | |
| | Cost (Rs. /sq. m.) | Share (%) | Cost (Rs. /sq. m.) | Share (%) |
| Earthwork excavation | 300 | 8% | 300 | 13% |
| Gabions | 2500 | 62% | 750 | 34% |
| Stones | 800 | 20% | 400 | 18% |
| Labour | 350 | 9% | 500 | 22% |
| Geotextile | 50 | 1% | 50 | 2% |
| Basal extension | | | 240 | 11% |
| Total | 4000 | 100% | 2240 | 100% |

## 10.5 SUMMARY

A systematic method of determining the possible cost of a gabion faced retaining wall (both reinforced and unreinforced cases) was developed as a part of the study. For this, data from 57 different sites all over Kerala was collected where retaining walls were already constructed. In all these locations, three types of retaining walls like RCC walls, gabion faced gravity walls and gabion faced reinforced soil walls were designed and cost estimation was carried out. Results of the study were then presented in the form of cost prediction models for each case and an estimate of cost breakdown is also given for the gabion faced walls. The recommended expressions are intended for use in preliminary cost estimation purposes.

# Chapter 11

# SUMMARY AND CONCLUSIONS

## 11.1 SUMMARY

Retaining walls, one of the most important geotechnical structures, finds application in every nook and corner of the world. The primary purpose of these structures, is to provide lateral support for soil or rock. Some of the more common types of retaining walls are gravity walls, counterfort walls, cantilevered walls, and mechanically stabilised earth walls. Among these, mechanically stabilised earth retaining walls have become more popular in the past two decades and it relies on the friction between soil and external intrusions made into the soil to resist the lateral earth pressure. They are also called as reinforced earth walls or reinforced soil walls.

Gabion faced retaining walls which are gaining fast momemtum in construction recently are commonly built as either gravity walls or reinforced earth walls. A vast literature survey was conducted wherein it was found that the number of research works conducted on these type of walls is very much limited in number. This means that the construction boom is enhancing without understanding the actual behaviour of these retaining walls which is, of course, leading to catastrophic situations. These walls being semi-rigid in nature behaves differently from the rigid gravity walls and the flexible reinforced earth walls. Thus there arises an urgent need to study in detail the performance of gabion faced retaining walls which has been taken as the topic of the present thesis work. This study is limited to gabion faced reinforced earth walls as they are more suited to larger heights.

In order to understand the behaviour of any system with respect to any point in it, numerical analysis has been proved to be a better tool than experimental methods by many researchers. Among the different numerical methods, finite element method stands in the forefront due to its versatility in modelling different applications and complex behaviours. Hence in this study,

finite element method was used as a prediction tool to simulate the behaviour of gabion faced reinforced soil walls.

A vast literature survey was conducted, where in, it was observed that, there exists a gap in literature which deals with gabion faced retaining walls. Further, the literature studies were extended to understand how the experimental investigations, analytical studies as well as numerical modelling could be conducted on retaining walls in general and how they could be applied to simulate the behaviour of gabion faced walls. Published literature on gabion faced walls was seen to be very few in number and hence all the available literature and design manuals of manufacturers were compiled and presented. Limit state method for design and analysis of reinforced soil walls as per BS 8006 : 1995 was also studied in detail as a part of literature study, so as to apply it to the design of gabion faced reinforced soil walls.

A finite element code named as FECAGREW (Finite Element Code for the Analysis of Gabion faced Retaining Walls) was developed by the author in C programming language as the first phase of the study. Plane strain condition was used for the analysis. Isoparametric quadrilateral (four noded 2D) elements were used to model the soil medium and the gabion facing. The reinforcing mesh was modelled using truss elements (two noded 2D) and the soil – mesh interaction using zero thickness (four noded 2D) line interface elements. The non linear behaviour of soil was modelled using hyperbolic stress - strain relation and the failure was modelled using Mohr - Coulomb failure criterion. The gabion facing was treated to behave linearly but simulation of failure was made using Mohr - Coulomb failure criterion. The confinement of gabion mesh was modelled as apparent cohesion induced into the gabion fill material. Construction phases were also modelled to simulate the constructional behaviour of the walls.

The developed FE code was validated at each stage using published data from literature and the final validation was done using experimental studies on gabion faced reinforced soil walls constructed in the laboratory. Related experiments for determining the essential parameters for modelling were also

conducted in the laboratory. The experimental model studies were then extended to check the viability of using an alternate cheap material like rock waste in place of the costly rock boulders inside gabion boxes. For this two sets of similar experiments were conducted on walls of different dimensions, one inside the laboratory and the other in the field.

FECAGREW was then used to conduct parametric studies on a gabion faced reinforced soil wall resting on a soft foundation by varying some of the salient geometric and material parameters. The goemetric paramters varied were spacing of reinforcement, length of reinforcement, width of gabion facing and height of gabion wall. The effects of gabion fill, gabion fill - backfill combination and the effect of reinforcement were studied in the material paramteric studies.

Design charts were developed for gabion faced reinforced soil walls to fix the dimensions of the structure without the usual tedious and repeated calculations. For this dimensional analysis of salient parameters in the limiting failure conditions as per BS 8006 : 1995 were carried out. The results of the studies were expressed as a set of dimensionless parameters. Graphs were then plotted using these to derive the necessary independent parameters for each failure condition. These graphs can be used as handy design charts for the design of gabion faced retaining walls. Additional design charts were then developed from the material and geometric parametric studies as a supplement to these charts. A design example was also worked out to illustrate the use of the design charts.

Economic studies were also conducted to prove the cost effectiveness of gabion faced walls by collecting field data from 57 different sites all over Kerala and cost prediction models were proposed for different types of retaining walls.

The design charts developed as well as conclusions drawn from the studies are expected to aid the design engineers at site and complement the construction works going on through out the world.

## 11.2 CONCLUSIONS

The major conclusions drawn from the present studies may be goruped into four parts as:

i. General
ii. Conclusions based on geometric parametric studies
iii. Conclusions based on material parametric studies
iv. Conclusions based on economic studies

### 11.2.1 General

- A two dimensional non linear FE code is developed with the acronym FECAGREW which can be used as a good prediction tool for the behaviour of gabion faced retaining walls, as established by the validation through experiments.
- The experimental studies show that there can be 25% replacement of rock pieces inside the gabions by a cheap and loacally available material like rock waste without much altering the stability of the structure. In cases where deformation can be allowed to a certain extent, even a 50 – 50 combination of rock pieces and rock dust may be used.
- Design charts were developed as design aids for the gabion faced reinforced soil walls based on the limit state method of design as per BS 8006: 1995.

### 11.2.2 Based on geometric parametric studies

- For any wall height, the ideal spacing of reinforcement may be fixed as, h = 0.1H to 0.2H. (In case of gabion faced walls, the spacing of reinforcement is actually a reflection of the box height as the reinforcement is provided as the basal extensions of the gabion boxes. So if spacings have to be provided at values, smaller than the standard box heights, they should be provided as intermediate ties).
- The ideal reinforcement length for gabion faced reinforced soil walls may be fixed as 0.4H – 0.6H (as agianst 0.7H of reinforced soil walls with

flexible facing), beyond which the deformation variations are seen to be constant.

- The facing width of gabion faced reinforced soil walls may be fixed as 0.1H - 0.15H, beyond which the effect of deformations and pressure are seen to be marginal. The facing width has negligible effect on the lateral forces developed in the backfill.
- The critical planes where the strip loading should not be placed are the beginning and end of the reinforcement lengths. The most ideal position for placing the strip loading is at least 1.5L away from the back face of the wall where L is the length of the reinforcement. If in any case, the strip has to be placed inside the reinforced area, the best position is that the start of the strip loading should be in the portion 0.5L – 0.75L within the reinforced region.

### 11.2.3 Based on material parametric studies

- 25% of the gabion fill may be replaced with a locally available inexpensive material in order to bring down the cost of construction of the walls.
- In places where deformation is not a major criterion, the 50 – 50 combination may also be recommended.
- Regarding the mode of filling, it is always better to provide the soft material as a core inside the middle portion of the hard material rather than providing the material in layers.
- As stiffness of gabion fill and backfill increases, wall deformation decreases, reinforcement strain decreases and average safety factor increases.
- When used as gabion fill material, all the types of igneous rocks exhibit similar behaviour with the best performance. The metamorphic rocks show a more or less fair performance when compared to the igneous rocks while the performace shown by the sedimentary rocks is very poor when compared to the other two types. Hence, igneous rocks may be

considered as most suitable for gabion fills. Metamorphic rocks if locally available can also be adopted, but sedimentary rocks may be discarded

- Maximum strain exhibited by the reinforcement is only 1.05%, which is very much less than the permissible strain of gabion mesh which is 10%. This means that the reinforcement is safe against breaking failure for all the types of backfills and gabion fills.
- Addition of reinforcement of length equal to wall height and spacing equal to box height, shows a three fold increase in the failure load as well as four times decrease in the deformations with respect to the unreinforced case.
- On analysing the deformation behaviour of the reinforced and the unrienforced medium height walls, it was seen that the reinforced case shows earth pressure nearing an at-rest condition while the earth pressure in the case of an unreinforced wall exceeds the active condition even at the stage of self weight loading.
- The introduction of reinforcement inhibits the formation of the failure plane in gabion faced walls by redistributing the stresses in the system.
- The safety factor for reinforcement was seen to be maximum at the top portions and at portions away from the wall facing. This indicates that sufficient reinforcement should be provided near the facing of the wall and at the bottom for minimising the failure risks.

### 11.2.4 Based on economic studies

- Cost prediction models were developed for different types of retaining walls based on the data collected from 57 different sites all over Kerala, which could be directly used for the estimation of cost of retaining walls.
- 30 – 50% savings could be obtained by going in for gabion faced gravity walls while the percentage goes up to 60 – 70% for gabion faced reinforced soil walls.

- Space requirements are minimum for gabion faced gravity walls and maximum for gabion faced reinforced soil walls among the wall types considered in the study.
- From the cost breakdown studies, it is seen that the maximum share goes to the cost of gabions.

The use of gabion faced reinforced earth retaining walls is growing at an enormous rate. This growth is justified on the basis of excellent performance – to – date, superb aesthetics, relative ease - of - construction and overall low cost. It is felt that these walls are completely justified in their growth at present rates, and when augmented by the results of the present studies will be the choice of all wall systems in the future. The present studies throw more light on the behaviour of gabion faced reinforced soil walls, which will increase the level of confidence in the practising engineers.

## 11.3 SCOPE FOR FUTURE WORK

In the present study, the behaviour of gabion faced MSE walls were examined under the action of static loads only. Gabion walls are flexible structures, which move away from the soil sufficiently to minimize the soil pressures under disturbing forces such as earthquake force. As a result they can be used effectively in regions prone to earthquake forces. Hence, the performance of these walls under the action of dynamic forces needs to be examined. Thus the study can be extended to problems involving forces that are dynamic in nature, like the earthquake forces.

Similarly, the backfill soil considered was non – cohesive and of dry nature. Since the cohesionless fill materials are becoming expensive, other alternatives like cohesive fills are being adopted. Hence future studies may be carried out on the effect of cohesive backfills on the behaviour of gabion faced reinforced soil walls by modelling the permeability and consolidation behaviour of these soils. Also, for almost all practical cases, the effect of ground water is an important parameter. Thus this aspect can also be examined in future works.

# REFERENCES


1. Addenbrooke, T. I., Potts, D. M. and Dabee, B. (2000): Displacement flexibility number for multipropped retaining wall design, ASCE Journal of Geotechnical and Geoenvironmental Engineering Division, Vol. 126, No. 8, August, 2000, pp. 718 – 726.

2. Alfaro, M. C., Hayashi, S., Miura, N. and Bergado, D. T. (1997): Deformation of reinforced soil wall embankment system on soft clay foundation, Soils and Foundations, Vol. 37, No. 4, December, 1997, pp. 33 - 46.

3. Arab, R., Villard, P. and Gourc, J. P. (1998): Large deformation FEM analysis of a reinforced earth structure, Geosynthetics International, Vol. 2, pp. 597 – 604.

4. Bang, S. and Hwang, S. I. (1986): Transition of active lateral earth pressures behind retaining walls, Computers and Geotechnics, Vol. 2, Issue 4, pp. 219 - 238.

5. Basudhar, P. K., Vashistha, A., Deb, K. and Dey, A. (2008): Cost optimization of reinforced earth walls, Geotechnical and Geological Engineering, Vol.26, No.1, February 2008, pp. 1 - 12.

6. Bathe, K. J. (1996): Finite element procedures, Prentice Hall of India Limited, New Delhi, India.

7. Bathurst, R. J. and Karpurapu, R. G. (1993): Large-scale triaxial compression testing of geocell-reinforced granular soils, Geotechnical Testing Journal, Vol. 16, No. 3, pp. 296 – 303.

8. Bathurst, R. J. and Simac, M. R. (1993): Two computer programs for the design and analysis of geosynthetic reinforced soil retaining walls, Geotextiles and Geomembranes, Vol. 12 (5), pp. 381- 396.

9. Bathurst, R. J., Allen, T. M. and Walters, D. L. (2005): Reinforcement loads in geosynthetic walls and the case for a new working stress design method, Geotextiles and Geomembranes, Vol. 23 (4) , August 2005, pp. 287-322.

10. Bauer, A. and Brau, G. (1996): Back analyses of a steep slope reinforced with non wovens, Geosynthetics: Applications, Design and Construction, Balkema, Rotterdam, pp. 225 – 228.

11. Bauer, G.E. (1988): Stability considerations of reinforced earth structures, First Indian Geotextiles Conference on Reinforced Soil and Geotextiles, Bombay, India, pp. B.15 – B.22.

12. Bauer, G.E. and Halim, A. O. A. E. (1989): The deformation and stress responses and stability analysis of reinforced soil structures, Computer and Physical Modelling in Geotechnical Engineering, Balkema, Rotterdam, pp. 13 – 24.

13. Beena, K. S. (1993): Studies on the settlement of reinforced sand on foundations, Ph.D. thesis, Department of Civil Engineering, Indian Institute of Technology, Madras, Chennai, India.

14. Bentler, J. G. and Labuz, J. F. (2006): Performance of a cantilever retaining wall, ASCE Journal of Geotechnical and Geoenvironmental Engineering Division, Vol. 132, No. 8, August, 2006, pp. 1062 – 1070.

15. Bergado, D. T., Chai, J. C. and Miura, N. (1995): FE analysis of grid reinforced embankment system on soft Bangkok clay, Computers and Geotechnics, Vol. 17, pp. 447 – 471.

16. Bergado, D. T., Teerawattanasuk, Youwai, S. and Voottipruex, P. (2000 A): Finite element modeling of hexagonal wire reinforced embankment on soft clay, Canadian Geotechnical Journal, Vol. 37, pp. 1209 – 1226.

17. Bergado, D. T., Voottipruex, P., Modmoltin, C. and Khwanpruk, S. (2000 B): Behaviour of full scale test wall reinforced with hexagonal wire mesh, Ground Improvement, Vol. 4, pp. 47 – 58.

18. Bergado, D. T., Teerawattanasuk, C., Wongsawanon, T., and Voottipruex, P. (2001): Interaction between hexagonal wire mesh reinforcement and silty sand backfill, Geotechnical Testing Journal, GTJODJ, Vol. 24, No. 1, March 2001, pp. 23 – 38.

19. Bolton, M. D., Britto, A. M., Powrie, W. and White, T. P. (1989): Finite element analysis of a centrifuge model of a retaining wall embedded in a heavily overconsolidated clay, Computers and Geotechnics, Vol. 7, pp. 289 - 318.

20. Bowles, J. E. (1996): Foundation Analysis and Design, Fifth Edition, McGraw Hill Inc., New York.

21. Briaud, J. L., Nicholson, P. and Lee, J. (2000): Behavior of full - scale VERT wall in sand, ASCE Journal of Geotechnical and Geoenvironmental Engineering Division, Vol. 126, No. 9, September, 2000, pp. 808 – 818.

22. BS 1052 (1980): Specification for mild steel wire for general engineering purposes, British Standards Institute, U. K.

23. BS 4102 (1998): Specification for steel wire for general fencing purposes, British Standards Institute, U. K.

24. BS 443 (1982): Specification for testing zinc coatings on steel wire and for quality requirements, British Standards Institute, U. K.

25. BS 729 (1995): Quality requirements for welding - Fusion welding of metallic materials - Standard quality requirements, British Standards Institute, U. K.

26. BS 8002 (1994): Code of practice for earth retaining structures, British Standards Institute, U. K.

27. BS 8006 (1995): Code of Practice for strengthened/reinforced soils and other fills, British Standards Institute, U. K.

28. BS EN ISO 3834 (2005): Quality requirements for fusion welding of metallic materials - Standard quality requirements, British Standards Institute, U. K.

29. Chang, M. F. (1997): Lateral earth pressures behind retaining walls, Canadian Geotechnical Journal, Vol. 34, pp. 498 – 509.

30. Chen, H. T., Hung, W. Y., Chang, C. C., Chen, Y. J. and Lee, C. J. (2007): Centrifuge modeling test of a geotextile-reinforced wall with a very wet clayey backfill, Geotextiles and Geomembranes, Vol. 25, pp. 346–359.

31. Chen, R. H. and Chiu, Y. M. (2008): Model tests of geocell retaining structures, Geotextiles and Geomembranes, Vol. 26, pp. 56 – 70.

32. Chen, T. J. and Fang, Y. S. (2002): A new facility for measurement of earth pressure at rest, Technical Note, Geotechnical Engineering, Journal of South East Asian Society, Vol. 33, No. 3, December 2002, pp. 153 - 159.

33. Chew, S. H. and Schmertmann, G. R. (1990): Reinforced soil deformations by finite element method, Performance of Reinforced Soil Structures, British Geotechnical Society, pp. 35 – 40.

34. Collin, J. G. (2001): Lessons learned from a segmental retaining wall failure, Geotextiles and Geomembranes, Vol. 19, pp. 445 – 454.

35. Cook, R. D., Malkus, D. S., Plesha, M. E. and Witt, R. J. (2001): Concepts and applications of finite element analysis, Fourth Edition, John Wiley and Sons, New York.

36. Day, P. W. (1994): Factors affecting the movement of retaining structures, XIII International Conference on Soil Mechanics and Foundation Engineering, New Delhi, India, Vol. V, pp. 109 - 114.

37. Desai, C. S. (1974): Numerical design – analysis of piles in sand, ASCE Journal of the Geotechnical Engineering Division, Vol. 100, No. GT6, June, pp. 613 - 635.

38. Desai, C. S. and Abel, J. F. (1987): Introduction to the finite element method for engineering analysis, CBS publishers, New Delhi, India.

39. Desai, C. S. and Sargand, S. (1984): Hybrid FE procedure for soil structure interaction, ASCE Journal of Geotechnical Engineering Division, Vol. 110, No. 4, April 1984, pp. 473 – 486.

40. Desai, C. S., Phan, H. V. and Perumpral, T. V. (1982): Mechanics of 3D soil structure interaction, ASCE Journal of the Engineering Mechanics Division, Vol. 108, No. EM5, October 1982, pp. 731 – 747.

41. Duncan, J. M. and Chang, C.Y. (1970): Nonlinear analysis of stress and strain in soil, ASCE Journal of Soil Mechanics and Foundations Division, Vol. 96, pp. 1629 - 1653.

42. Duncan, J. M., Byrne, P. M., Wong, K. S. and Mabry, P. (1980): Strength, stress – strain and bulk modulus parameters for finite element analyses of stresses and movements in soil masses, Report No. UCB/GT/80-01.

43. Durukan, Z. and Tezcan, S. S. (1992): Cost analysis of reinforced soil walls, Geotextiles and Geomembranes, Vol. 11, pp. 29 – 43.

44. Fabian, K. J. and Fourie, A. B. (1988): Clay – geotextile interaction in large retaining wall models, Geotextiles and Geomembranes, Vol. 7, pp. 179 – 201.

45. Fang, Y. S., Ho, Y. C. and Chen, T. J. (2002): Passive earth pressure with critical state concept, ASCE Journal of Geotechnical and Geoenvironmental Engineering Division, Vol. 128, No. 8, August, 2002, pp. 651 - 659.

46. Fannin, R. J. and Hermann, S. (1990): Performance data for a sloped reinforced soil wall, Canadian Geotechnical Journal, Vol. 27, pp. 676 – 686.

47. Fantini, P. and Roberti, R. (1996): Highway Frejus Torino: A case history of a green reclamation around a highway viaduct with geogrid reinforced walls, Geosynthetics: Applications, Design and Construction, Balkema, Rotterdam, pp. 387 – 392.

48. Ferriolo F., Vicari, M., Kulkarni, T. P. and Gharpure, A. D. (1997): Landslide road protection and river training works with gabion structures, Proceedings of Geosynthetics Asia '97, Bangalore, India, pp. II.13 – II.20.

49. Filz, G. M. and Duncan, J. M. (1997): Vertical shear loads on nonmoving walls I: Theory, ASCE Journal of Geotechnical and Geoenvironmental Engineering Division, Vol. 123, No. 9, September, 1997, pp. 856 – 862.

50. Filz, G. M., Duncan, J. M. and Ebeling, R. M. (1997): Vertical shear loads on nonmoving walls II: Applications, ASCE Journal of Geotechnical and Geoenvironmental Engineering Division, Vol. 123, No. 9, September, 1997, pp. 863 – 873.

51. Fishman, K. L., Desai, C. S. and Sogge, R. L. (1993): Field behaviour of instrumented geogrid soil reinforced wall, ASCE Journal of Geotechnical Engineering Division, Vol. 119, No. 8, August, 1993, pp. 1293 – 1307.

52. Frankowska, K. K. (2005): A case study of a geosynthetic reinforced wall with wrap-around facing, Geotextiles and Geomembranes, Vol. 23 [1], February 2005, pp. 107-115.

53. Fukuoka, M., Imamura, Y. and Nishimura, J. (1986): Fabric faced retaining wall with multiple anchors, Geotextiles and Geomembranes, Vol. 4, pp. 207 – 221.

54. Garg, K. G. (1997): Stabilisation of slopes in Garhwal Himalaya, Proceedings of Geosynthetics Asia '97, Bangalore, India, pp. A.27 – A.34.

55. Garg, K. G. (1998): Retaining wall with reinforced backfill – A case study, Geotextiles and Geomembranes, Vol.16, pp. 135 – 149.

56. Garga, V. K. and O'Shaughnessy, V. (2002): Tire - reinforced earth fill. Part 1: Contribution of a test fill, performance and retaining wall design, Canadian Geotechnical Journal, Vol. 37, No.1, pp.75 - 96.

57. Ghaboussi, J. Wilson, E. L. and Isenberg, J. (1973): Finite element for rock joints and interfaces, ASCE Journal of Soil Mechanics and Foundations Division, Vol. 99, No. SM10, September 1973, pp. 833 - 848.

58. Goodman, R. E., Taylor, R. L. and Brekke, T. L. (1968): A model for the mechanics of jointed rock, ASCE Journal of the Soil Mechanics and Foundations Division, Vol. 94, No. SM3, May, 1968, pp. 637 – 659.

59. Greco, V. R. (2001): Active earth thrust on cantilever walls with short heel, Technical Note, Canadian Geotechnical Journal, Vol. 38, pp. 401 – 409.

60. Gulhati, S. K. and Dutta, M. (2005): Geotechnical Engineering, Tata Mc Graw Hill Publishing Co. Ltd., New Delhi, India.

61. Hanna, A. and Khoury, I. A. (2005): Passive earth pressure of overconsolidated cohesionless backfill, ASCE Journal of Geotechnical and Geoenvironmental Engineering Division, Vol. 131, No. 8, August, 2005, pp. 978 – 986.

62. Harr, M. E. (1966): Foundations of Theoretical Soil Mechanics, International Student Edition, Mc Graw Hill Book Comapny, New York, U. S. A.

63. Hatami, K., Bathurst, R. J. and Di Pietro, P. (2001): Static response of reinforced soil retaining walls with nonuniform reinforcement, International Journal of Geomechanics, Vol. 1, Issue 4, pp. 477 - 506.

64. Hazarika, H. and Matsuzawa, H. (1996): Wall displacement modes dependent active earth pressure analyses using smeared shear band method with two bands, Computers and Geotechnics, Vol. 19, pp. 193 - 219.

65. Hegazy, Y. A. (2002): Facing connection strength of a geosynthetic mechanically stabilized earth wall, 4th International Conference on Ground Improvement Techniques, Kuala Lumpur, Malaysia, pp. 415 - 420.

66. Helwany, S. M. B., Tatsuoka, F., Tateyama and Kojima, M. (1996): Effects of facing rigidity on the performance of geosynthetic reinforced soil retaining wall, Soils and Foundations, Vol. 36, No. 1, pp. 27 - 38.

67. Helwany, S. M. B., Wu, J. T. H. and Kitsabunnarat, A. (2007): Simulating the behavior of GRS bridge abutments, ASCE Journal of Geotechnical and Geoenvironmental Engineering Division, Vol. 133, No. 10, October, 2007, pp. 1229 - 1240.

68. Helwany, S. M. B., Reardon, G. and Wu, J. T. H. (1999): Effects of backfill on the performance of GRS retaining walls, Geotextiles and Geomembranes, Vol. 17 [1], pp. 1 – 16.

69. Henkel, D. J., and Gilbert, G. C. (1952): The effect of rubber membranes on the measured triaxial compression strength of clay samples, Geotechnique, Vol. 3, pp. 20 - 29.

70. Ho, S. K. and Rowe, R. K. (1996): Effect of wall geometry on the behaviour of reinforced soil walls, Geotextiles and Geomembranes, Vol. 14 (10), pp. 521- 541.

71. Horiya, S., Izhisaki, H. and Takano, Y. (1988): Hi – Tex wall method, Proceedings of First Indian Geotextiles Conference on Reinforced Soil and Geotextiles, Bombay, India, pp. D. 21 – D. 26.

72. Horvath, J. S. (2003): Controlled yielding using geofoam compressible inclusions: The new frontier in earth – retaining structures, International e-Conference on Modern Trends in Foundation Engineering - Geotechnical Challenges And Solutions, Indian Institute of Technology, Madras, September 8 - 12, 2003, http://www.ecfg.iitm.ac.in.

73. Ingold, T. S. (1982): Reinforced earth, Thomas Telford Ltd., London, U. K.

74. Isabel, M., Pinto, M. and Cousens, T. W. (1996): Geotextile reinforced brick faced retaining walls, Geotextiles and Geomembranes, Vol. 14, pp. 449 – 464.

75. Iyer, T. S. R., Girish, M. S. and Anish Kumar, K. (2001): Model retaining walls using bamboo grids with coir interface, IGC 2001- The New Millennium Conference, Indore (M.P.), India, pp. 280 - 283.

76. Jalla, R. (1999): Design of multiple level retaining walls, ASCE Journal of Architectural Engineering, Vol. 5, Issue 3, September, 1999, pp. 82 - 88.

77. Janbu, N. (1963): Soil compressibility as determined by oedometer and triaxial tests, Proceedings of European Conference on Soil Mechanics and Foundation Engineering, Wiesbadeu, Vol. 1, pp. 19 – 25.

78. Jayasree, P. K. (1996): Finite element analysis of layered soil systems, M. Tech. Thesis, Department of Civil Engineering, College of Engineering, Trivandrum, India.

79. Jones, C. J. F. P. (1985): Earth Reinforcement and Soil Structures, Butterworths Advanced Series in Geotechnical Engineering, London, U. K.

80. Karpurapu, R. and Bathurst, J. (1992): Numerical Investigation of Controlled Yielding of Soil-Retaining Wall Structures, Geotextiles and Geomembranes, Vol. 11, pp. 115 – 131.

81. Karpurapu, R. and Bathurst, J. (1994): Finite element analysis of geosynthetic reinforced soil retaining walls, XIII International Conference on Soil Mechanics and Foundation Engineering, New Delhi, India, Vol. IV, pp. 1381 – 1384.

82. Karpurapu, R. and Bathurst, R. J. (1995): Behaviour of geosynthetic reinforced soil retaining walls using the finite element method, Computers and Geotechnics, Vol. 17 (3), pp. 279.

83. Kim, J. S. and Barker, R. M. (2002): Effect of live load surcharge on retaining walls and abutments, ASCE Journal of Geotechnical and Geoenvironmental Engineering Division, Vol. 128, No.10, October 2002, pp. 803 - 813.

84. Kobayashi, M. and Porbaha, A. (1997): Poorly draining geotextile reinforced retaining walls – A numerical study, Geosynthetics Asia 1997, Bangalore, India, pp. II.21 – II.28.

85. Koerner, J., Soong, T. Y. and Koerner, R.M. (1998): Earth retaining wall costs in the USA, Geosynthetic Institute, Folsom, Pennsylvania.

86. Koerner, K. M. and Soong, T. Y. (2001): Geosythetic reinforced segmental retaining walls, Geotextiles and Geomembranes, Vol. 19 [6], 2001, pp. 359 - 386.

87. Koerner, R. M. (1998): Designing with goesynthetics, Fourth edition, Prentice Hall, Eaglewood Cliffs, N.J., U. S. A.

88. Kondner, R. L. (1963): Hyperbolic stress – strain response: Cohesive soils, ASCE Journal of Soil Mechanics and Foundations Division, Vol. 89, No. SM1, pp. 115 - 143.

89. Krishnamoorthy, C. S. (1987): Finite element analysis – Theory and programming, Tata Mc Graw Hill Book Co., New Delhi, India.

90. Larkin, T.J. and Williams, P. W. M. (1994): Simplified computer modelling of lateral earth pressure, XIII International Conference on Soil Mechanics and Foundation Engineering, New Delhi, India, Vol. IV, pp. 1423 – 1428.

91. Lee, J. H., Salgado, R., Bernal, A. and Lovell, C.W. (1999): Shredded tires and rubber - sand as lightweight backfill, ASCE Journal of Geotechnical and Geoenvironmental Engineering Division, Vol. 125, No. 2, February, 1999, pp. 132 - 141.

92. Lee, K., Cho, J., Salgado, R. and Lee, I. (2001): Retaining wall model test with waste foundry sand mixture backfill, Geotechnical Testing Journal, Vol. 24, No. 4, December 2001, pp. 401– 408.

93. Lee, K. L., Adams, B.D. and Vagneron, J. M. J. (1983): Reinforced earth retaining walls, ASCE Journal of the Soil Mechanics and Foundation Division, Vol. 99, No. SM10, pp. 745 – 764.

94. Leshchinsky, D., Hu, Y. and Han, J. (2004): Limited reinforced space in segmental retaining walls, Geotextiles and Geomembranes, Vol. 22, pp. 543 – 553.

95. Leshchinsky, D. and Perry, E. B. (1988): Geotextile- reinforced walls subjected to uniform surcharge loads, First Indian Geotextile Conference on Reinforced Soil and Geotextiles, Bombay, India, pp. B. 23 – B. 30.

96. Lesniewska, D. and Porbaha, A. (1998): Numerical simulation of scaled retaining walls by rigid – plastic approach, Computers and Geotechnics, Vol. 23, Issues 1 - 2, July 1998, pp. 113 – 129.

97. Ling, H. I., Tatsuoka, F. and Tateyama, M. (1995): Simulating performance of GRS – RW by finite element procedure, ASCE Journal of Geotechnical Engineering Division, Vol. 121, No. 4, April, 1995, pp. 330 – 340.

98. Long, M. (2001): Database for retaining wall and ground movements due to deep excavations, ASCE Journal of Geotechnical and Geoenvironmental Engineering Division, Vol. 127, No. 3, March, 2001, pp. 203 – 224.

99. Ma, C. C. and Wu, J. T. H. (2004): Field performance of an independent full-height facing reinforced soil wall, ASCE Journal of Performance of Constructed facilities, Vol. 18, Issue 3, August, 2004, pp. 165 – 172.

100. Maccaferri Environmental Solutions Private Ltd., Design manual, Mumbai, 2002.

101. Madhavi Latha, G. (2000): Investigations on the behaviour of geocell supported embankments, Ph.D. thesis, Department of Civil Engineering, Indian Institute of Technology, Madras, Chennai, India.

102. Madhavi Latha, G., Dash, S.K., Rajagopal, K. and Krishnaswamy, N.R. (2001): Finite element analysis of strip footing on geocell reinforced sand beds, Indian Geotechnical Journal, Vol. 31, No.(4), pp.454 – pp. 478.

103. Madhavi Latha, G. and Murthy, V.S. (2007): Effects of reinforcement form on the behaviour of geosynthetic reinforced sand, Geotextiles and Geomembranes, Vol. 25, pp. 23 - 32.

104. Madhavi Latha, G., Rajagopal, K. and Krishnaswamy, N.R. (2006): Experimental and theoretical investigations on geocell-supported embankments, International Journal of Geomechanics, Vol. 6, No. 1, pp. 30 - 35.

105. Mannsbart, G. and Kropik, C. (1996): Non-woven geotextiles used for temporary reinforcement of a retaining structure under a railroad track, Geosynthetics: Application, Design and Construction, Balkema, Rotterdam, 1996, pp. 121 - 124.

106. Matsuzawa, H. and Hazarika, H. (1996): Analyses of active earth pressure against rigid retaining walls subjected to different modes of movement, Soils and Foundations, Vol. 36, No. 3, September 1996, pp. 51 - 65.

107. Mittal, S. Garg, K. G. and Saran, S. (2006): Analysis and design of retaining wall having reinforced cohesive frictional backfill, Geotechnical and Geological Engineering, Vol. 24, pp. 499 – 522.

108. Miura, N., Sakai, A., Taesiri, Y., Yamanouchi, T. and Yasuhara, K. (1990): Polymer grid reinforced pavement on soft clay grounds, Geotextiles and Geomembranes, Vol. 9, 1990, pp. 99 – 123.

109. Motta, E. (1996): Earth pressure on reinforced earth walls under general loading, Soils and Foundations, Vol. 36, No. 4, December 1996, pp. 113 – 117.

110. Naylor, D. J. (1978): A study of reinforced earth walls allowing strip slips, Proceedings of Symposium on Earth Reinforcements, A. S. C. E. annual convention, Pittsburg, Pennsylvania, April 1978, pp. 618 – 643.

111. Ochiai, Y. and Fukuda, N. (1996): Experimental study on geotextile reinforced soil walls with different facings, Geosynthetics: Application, Design and Construction, Balkema, Rotterdam, 1996, pp.113 - 118.

112. Ogisako, E. Ochiai, H., Hayashi, S. and Sakai, A. (1988): FEM analysis of polymer grid reinforced – soil retaining walls and its application to the design method,

International Geotechnical Symposium on Theory and Practice of Earth Reinforcement, Fukuoka, Japan, October 1988, pp. 559 – 564.

113. Palmeira, E. M. and Lanz, D. (1994): Stresses and deformations in geotextile reinforced model walls, Geotextiles and Geomembranes, Vol. 13 (5), pp. 331- 348.

114. Park, T. and Tan, S. A. (2005): Enhanced performance of reinforced soil walls by the inclusion of short fiber, Geotextiles and Geomembranes, Vol. 23 [4], August 2005, pp. 348 – 361.

115. Porbaha, A. and Goodings, D. J. (1996): Centrifuge modeling of geotextile - reinforced cohesive soil retaining walls, ASCE Journal of Geotechnical Engineering Division, Vol. 122, No. 10, October, 1996, pp. 840 – 848.

116. Porbaha, A. and Goodings, D. J. (1997): Laboratory investigation of non uniformly reinforced soil retaining structures, Geotechnical Testing Journal, GTJODJ, Vol. 20, No. 3, September 1997, pp. 289 - 295.

117. Porbaha, A., Zhao, A., Kobayashi, M. and Kishida, T. (2000): Upper bound estimate of scaled reinforced soil retaining walls, Geotextiles and Geomembranes, Vol. 18, pp. 403 – 413.

118. Potts, D. M. and Zdravkovic, L. (1999 A): Finite element analysis in Geotechnical Engineering: Theory, Thomas Telford Publishing, London, U. K.

119. Potts, D. M. and Zdravkovic, L. (1999 B): Finite element analysis in Geotechnical Engineering: Application, Thomas Telford Publishing, London, U. K.

120. Raghavendra, H. B. (1996): Some studies on the analysis of reinforced soil beds, Ph.D. thesis, Department of Civil Engineering, Indian Institute of Science, Bangalore, India.

121. Rajagopal, K., Krishnaswamy, N.R., and Madhavi Latha, G. (2001): Finite element analysis of embankments supported on geocell layer using composite model, Proceedings of 10th International Conference on Computer Methods and Advances in Geomechanics, January 2001, Arizona, USA.

122. Rao, G. V., Kate, J. M. and Saxena, A. (1988): Model studies of reinforced earth wall, First Indian Geotextile Conference on Reinforced Soil and Geotextiles, Bombay, India, pp. A. 35 – A. 40.

123. Rao, P. J. and Singh, J. P. (1988): Retaining wall alternatives – Techno economics, Proceedings of First Indian Geotextiles Conference on Reinforced Soil and Geotextiles, Bombay, India, pp. D. 15 – D. 19.

124. Rimoldi, P., Riccutti, A. and Majumdar, R. (1997): Designing geogrid reinforced soil walls and slope systems, Geosynthetics Asia 1997, Bangalore, India, pp. 12 – 33.

125. Romstad, K. M., Al – Yassin, Z., Herrmann, L. R. and Shen, C. K. (1978): Stability analysis of reinforced earth retaining structures, Proceedings of Symposium on Earth Reinforcements, A. S. C. E. annual convention, Pittsburg, Pennsylvania, April 1978, pp. 685 – 713.

126. Romstad, K. M., Herrmann, L. R. and Shen, C. K. (1976): Integrated study of reinforced earth – I: Theoretical formulation, ASCE Journal of Geotechnical Engineering Division, Vol. 102, No. GT 5, May 1976, pp. 457 - 471.

127. Rowe, R. K. and Ho, S. K. (1997): Continuous panel reinforced soil wall on rigid foundation, ASCE Journal of Geotechnical and Geoenvironmental Engineering Division, Vol. 123 (10), pp. 912 - 920.

128. Rowe R. K. and Skinner, G. D. (2001): Numerical analysis of geosynthetic reinforced retaining wall constructed on a layered soil foundation, Geotextiles and Geomembranes, Vol. 19, pp. 387 – 412.

129. Saran, S. and Talwar, D.V. (1983): Analysis and design of retaining walls and reinforced earth backfills, Journal of the Institution of Engineers, Vol. 64, pp. 7 - 14.

130. Sawicki, A. and Lesniewska, D. (1987): Failure modes and bearing capacity of reinforced soil retaining walls, Geotextiles and Geomembranes, Vol. 5, pp. 29 – 44.

131. Schedule of rates, Kerala Public Works Department, Government of Kerala, 2007.

132. Sharma, K. G. and Desai, C. S. (1992): Analysis and implementation of thin layer interfaces and joints, ASCE Journal of Engineering Mechanics Division, Vol. 118, No.12, December 1992, pp. 2442 – 2462.

133. Shen, C. K., Romstad, K. M. and Herrmann, L. R. (1976): Integrated study of reinforced earth - II: Behaviour and design, ASCE Journal of Geotechnical Engineering Division, Vol. 102, No. GT 6, June 1976, pp. 577 - 590.

134. Shinde, A. L. and Mandal, J. N. (2007): Behavior of reinforced soil retaining wall with limited fill zone, Geotechnical and Geological Engineering, Vol. 25, pp. 657 - 672.

135. Simac, M. R., Bathurst, R. J. and Fennessey, T. W. (1997 A): Design of gabion – geosynthetic retaining walls on the Tellico plains to Robbinsville highway, Geosynthetics '97 Conference, California, USA, pp. 105 – 118.

136. Simac, M. R., Bathurst, R. J. and Fennessey, T. W. (1997 B): Case study of a hybrid gabion basket geosynthetic reinforced soil wall, Ground Improvement, Vol. 1, pp. 9 – 17.

137. Singh, D. N. and Basudhar, P. K. (1993): Determination of the optimal lower-bound-bearing capacity of reinforced soil-retaining walls by using finite elements and non-linear programming, Geotextiles and Geomembranes, Vol. 12, pp. 665 – 686.

138. Singh, H. R. (1988): Bearing capacity of reinforced soil beds, Ph.D. thesis, Department of Civil Engineering, Indian Institute of Science, Bangalore, India.

139. Skinner, D. G. and Rowe, R. K. (2005): Design and behaviour of a geosynthetic reinforced retaining wall and bridge abutment on a yielding foundation, Geotextiles and Geomembranes, Vol. 23 [3], June 2005, pp. 234 - 260.

140. Soong, T. Y. and Koerner, R. M. (1997): On the required connection strength of geosynthetically reinforced walls, Geotextiles and Geomembranes, Vol. 15, pp. 377 – 393.

141. Srbulov, M. (2001): Analyses of stability of geogrid reinforced steep slopes and retaining walls, Computers and Geotechnics, Vol. 28, Issue 4, June 2001, pp. 255-268.

142. Sreekantiah, H. R. (2001): Finite element analysis of reinforced soil retaining wall, IGC 2001 – The New Millennium Conference, Indore (M. P.), India, pp. 417 – 420.

143. Sreekantiah, H. R. and Sowmya, N. J. (2001): Prediction of deformation behaviour of reinforced soil retaining walls, International Conference on Civil Engineering, Bangalore, July, 2001, pp. 961 – 968.

144. Tweedie J. J., Humphrey, D. N. and Sandford, T. C. (1998): Tire shreds as lightweight retaining wall backfill: Active conditions, ASCE Journal of Geotechnical and Geoenvironmental Engineering Division, Vol. 124, No. 11, November, 1998, pp. 1061 – 1070.

145. Tyagi, V.K. and Mandal, J.N. (2001): Techno - commercial optimization of backfill for soil reinforced structures, IGC 2001, The New Millennium Conference, Indore (M.P.), India, pp. 247 - 250.

146. Verma, B. P. (2000): Rock mechanics for engineers, Third edition, Khanna Publishers, New Delhi, India.

147. Vidal, H. (1969): The principle of reinforced earth, Highway Research Record, No. 282, Washington D. C., U. S. A.

148. Villemus, B., Morel, J.C., and Boutin C. (2007): Experimental assessment of dry stone retaining wall stability on a rigid foundation, Engineering Structures, Vol. 29, pp. 2124 – 2132.

149. Wang, C. D. (2007): Lateral force induced by rectangular surcharge loads on a cross-anisotropic backfill, ASCE Journal of Geotechnical and Geoenvironmental Engineering Division, Vol. 133, No. 10, October, 2007, pp. 1259 – 1276.

150. Wiseman, G. and Shani, A. (1994): Geomesh reinforced soil walls – description and testing, XIII International Conference on Soil Mechanics and Foundation Engineering, New Delhi, India, Vol. IV, pp. 1797 – 1802.

151. Won, M. S. and Kim, Y. S. (2007): Internal deformation behavior of geosynthetic-reinforced soil walls, Geotextiles and Geomembranes 25, pp. 10 – 22

152. Yoo C. (2004): Performance of a 6-year-old geosynthetic reinforced segmental retaining wall, Geotextiles and Geomembranes, Vol. 22, pp. 377 – 397.

153. Yoo, C. and Jung, H. S. (2004): Measured behavior of a geosynthetic-reinforced segmental retaining wall in a tiered configuration, Geotextiles and Geomembranes, Vol. 22, pp. 359 – 376.

154. Yoo, C. and Lee, K. M. (2003): Instrumentation of anchored segmental retaining wall, Geotechnical Testing Journal, Vol. 26, No. 4, pp. 1 – 8.

155. Zienkiewicz, O. C. and Taylor, R. L. (1989): Finite element method, Fourth edition, Mc Graw Hill Book Co., Singapore.

# BIBLIOGRAPHY


1. Babu, G. L. S. (2006): An introduction to soil reinforcement and geosynthetics, Universities Press (India) Pvt. Ltd., Hyderabad, India.

2. Baker, R. and Klein, Y. (2004 A): An integrated limiting equilibrium approach for design of reinforced soil retaining structures: Part I—formulation, Geotextiles and Geomembranes, Vol. 22, pp. 119 – 150.

3. Baker, R. and Klein, Y. (2004 B): An integrated limiting equilibrium approach for design of reinforced soil retaining structures: Part II—design examples, Geotextiles and Geomembranes, Vol. 22, pp. 151 – 177.

4. Baker, R. and Klein, Y. (2004 C): An integrated limiting equilibrium approach for design of reinforced soil retaining structures: Part III—optimal design, Geotextiles and Geomembranes, Vol. 22, pp. 455 – 479.

5. Basma, A. A., Barakat, S. A. And Omar, M. T. (2003): Reliability based risk index for the design of reinforced earth structures, Geotechnical and Geological Engineering, Vol. 21, pp. 225 – 242.

6. Bentler, J. G. and Labuz, J. F. (2006): Performance of a Cantilever Retaining Wall, ASCE Journal of Geotechnical and Geoenvironmental Engineering Division, Vol. 132, No. 8, August, 2006, pp. 1062 – 1070.

7. Briaud, J. L., Nicholson, P. and Lee, J. (2000): Behavior of full - scale VERT wall in sand, ASCE Journal of Geotechnical and Geoenvironmental Engineering Division, Vol. 126, No. 9, September, 2000, pp. 808 – 818.

8. Chang, J. C. and Forsyth, R. A. (1977): Finite element analysis of reinforced earth wall, ASCE Journal of Geotechnical Engineering Division, Vol. 103, No. GT 7, July, 1977, pp. 711 - 724.

9. Chen, T. J. and Fang, Y. S. (2002): A new facility for measurement of earth pressure at rest, Technical Note, Geotechnical Engineering, Journal of South East Asian Society, Vol. 33, No. 3, December 2002, pp. 153 - 159.

10. Fang, Y. S., Ho, Y. C. and Chen, T. J. (2002): Passive earth pressure with critical state concept, ASCE Journal of Geotechnical and Geoenvironmental Engineering Division, Vol. 128, No. 8, August, 2002, pp. 651 - 659.

11. Fannin, R. J. and Hermann, S. (1990): Performance data for a sloped reinforced soil wall, Canadian Geotechnical Journal, Vol. 27, pp. 676 – 686.

12. Fukuoka, M., Imamura, Y. and Nishimura, J. (1986): Fabric faced retaining wall with multiple anchors, Geotextiles and Geomembranes, Vol. 4, pp. 207 – 221.

13. Gotteland, Ph., Gourc, J.P., Jommi, C. and Nova, R. (1996): Finite difference analysis of geosynthetic reinforced earth walls, Geosynthetics: Applications, Design and Construction, Balkema, Rottedam, pp. 503 - 510.

14. Han, J. and Gabr, M. A. (2002): Numerical analysis of geosynthetic - reinforced and pile - supported earth platforms over soft soil, ASCE Journal of Geotechnical and Geoenvironmental Engineering Division, Vol. 128, No. 1, January, 2002, pp. 44 – 53.

15. Hanna, A. and Khoury, I. A. (2005): Passive earth pressure of overconsolidated cohesionless backfill, ASCE Journal of Geotechnical and Geoenvironmental Engineering Division, Vol. 131, No. 8, August, 2005, pp. 978 – 986.

16. Hazarika, H., Okuzono, S., Matsu, Y. and Takada, K. (2002): Evaluation of lightweight materials as geo – inclusion in reducing earth pressure on retaining wall, 4th International Conference on Ground Improvement Techniques, Kuala Lumpur, Malaysia, pp. 399 – 403.

17. Henkel, D.J., and Gilbert, G.C. (1952): The effect of rubber membranes on the measured triaxial compression strength of clay samples, Geotechnique, Vol. 3, pp. 20 – 29.

18. Herrmann, L. R. and Al – Yassin, Z. (1978): Numerical analysis of reinforced soil systems, Proceedings of symposium on earth reinforcements, A. S. C. E. annual convention, Pittsburg, Pennsylvania, April 1978, pp. 428 – 457.

19. Hoeg, K. and Murarka, R. P. (1974): Probabilistic analysis and design of a retaining wall, ASCE Journal of the Geotechnical Engineering Division, Vol. 100, No. GT3, March 1974, pp. 349 – 366.

20. Horiya, S., Izhisaki, H. and Takano, Y. (1988): Hi – Tex wall method, Proceedings of First Indian Geotextiles Conference on Reinforced Soil and Geotextiles, Bombay, India, pp. D. 21 – D. 26.

21. Huang, C. C., Menq, F. Y. and Chou, Y. C. (1999): "The effect of the bending rigidity of a wall on lateral pressure distribution", Canadian Geotechnical Journal, Vol. 36, No. 61 pp. 1039 - 1055.

22. Huang, T. K. (1997): "Mechanical behavior of interconnected concrete - block retaining wall", ASCE Journal of Geotechnical and Geoenvironmental Engineering Division, Vol. 123, No. 3, March, 1997, pp. 197 - 203.

23. Isabel, M., Pinto, M. and Cousens, T. W. (1996): Geotextile reinforced brick faced retaining walls, Geotextiles and Geomembranes, Vol. 14, pp. 449 – 464.

24. Jayalekshmi, S. (2003): Studies on geosynthetic reinforced retaining walls, Ph. D. Thesis, Indian Institute of Technology, Madras, India.

25. Lee, S. H., Kim, S. I., Lee, J. H. and Chang, B. S. (2004): Two-parameter beam-column model and back analysis for flexible earth retaining walls, Computers and Geotechnics, Vol. 31, pp. 457 – 472.

26. Likar, J. and Vukadian, V. (2003): Time - dependent back analyses of a multi anchored pile retaining wall, Technical Note, ASCE Journal of Geotechnical and Geoenvironmental Engineering Division, Vol. 129, No. 1, January, 2003, pp. 91 - 95.

27. Madhav, M.R. and Rao, N.S.K. (1969): Earth pressure under seismic conditions, Soils and Foundations, Vol. 9, No. 4., Japan.

28. Nakai, T. (1985): Finite element computations for active and passive earth pressure problems of retaining wall, Soils and Foundations, Vol. 25, No. 3, September 1985, pp. 98 – 112.

29. Nimmesgern, M. (1996): The consideration of the deformations in the design of reinforced retaining walls, Geosynthetics: Application, Design and Construction, Balkema, Rotterdam, 1996, pp.171 – 173.

30. Palmeira, E. M. and Lanz, D. (1994): Stresses and deformations in geotextile reinforced model walls, Geotextiles and Geomembranes, Vol. 13 (5), pp. 331- 348.

31. Patel, N. M. and Chandrasekharam, Y. (1992): FEM studies on geosynthetic reinforced soil structures, Indian Geotechnical Conference, Calcutta, India, December 1992, pp. 247 – 250.

32. Porbaha, A. and Goodings, D. J. (1996): Centrifuge modeling of geotextile - reinforced cohesive soil retaining walls, ASCE Journal of Geotechnical Engineering Division, Vol. 122, No. 10, October, 1996, pp. 840 – 848.

33. Porbaha, A. and Goodings, D. J. (1997): Laboratory investigation of non uniformly reinforced soil retaining structures, Geotechnical Testing Journal, GTJODJ, Vol. 20, No. 3, September 1997, pp. 289 - 295.

34. Powrie, W. (1996): Limit equilibrium analysis of embedded retaining walls, Geotechnique, Vol. 46, No. 4, pp. 709 – 723.

35. Rao, G. V. (2007): Geosynthetics – An Introduction, Sai Master Geoenvironmental Services Pvt. Ltd., New Delhi, India.

36. Rao, G. V., Kate, J. M. and Saxena, A. (1988): Model studies of reinforced earth wall, First Indian Geotextile Conference on Reinforced Soil and Geotextiles, Bombay, India, pp. A. 35 – A. 40.

37. Rudra Pratap (2007): Getting started with MATLAB 7– A quick Introduction for Scientists and Engineers', Oxford University Press, New York.

38. Sarba, A. and Erbatur, F. (1996): Optimization and sensitivity of retaining structures, ASCE Journal of Geotechnical Engineering Division, Vol. 122, No. 8, August, 1996, pp. 649 – 656.

39. Savicki, A. (1999): Creep of geosynthetic reinforced soil retaining walls, Geotextiles and Geomembranes, Vol. 17, pp. 51 - 65.

40. Sheahan, T. C. and Ho, C. L. (2003): Simplified trial wedge method for soil nailed analysis, ASCE Journal of Geotechnical and Geoenvironmental Engineering Division, Vol. 129, No. 2, February, 2003, pp. 117 - 124.

41. Tatlisoz, N., Edil, T. B. and Benson, C. H. (1998): Interaction between reinforcing geosynthetics and soil - tire chip mixtures, ASCE Journal of Geotechnical and Geoenvironmental Engineering Division, Vol. 124, No. 11, November, 1998, pp. 1109 – 1119.

42. Tatsuoka, F., Tateyama, M. and Koseki, J. (1996): Performance of soil retaining walls for railway embankments, Special issue of Soils and Foundations, January 1996, pp. 311 - 324.

43. Tweedie J. J., Humphrey, D. N. and Sandford, T. C. (1998): Tire shreds as lightweight retaining wall backfill: Active conditions, ASCE Journal of Geotechnical and Geoenvironmental Engineering Division, Vol. 124, No. 11, November, 1998, pp. 1061 – 1070.

44. Vaziri, H. H. (1996): Numerical study of parameters influencing the response of flexible retaining walls, Canadian Geotechnical Journal, Vol. 33, pp. 290 – 308.

45. Villemus, B., Morel, J.C., and Boutin C. (2007): Experimental assessment of dry stone retaining wall stability on a rigid foundation, Engineering Structures, Vol. 29, pp. 2124 – 2132.

46. Wiseman, G. and Shani, A. (1994): Geomesh reinforced soil walls – description and testing, XIII International Conference on Soil Mechanics and Foundation Engineering, New Delhi, India, Vol. IV, pp. 1797 – 1802.

# PUBLICATIONS BASED ON THE RESEARCH WORK


1) Jayasree P. K. , Dr. K. S. Beena, Leena G. (2004): Study on quarry dust filled gabion retaining walls, First CUSAT National Conference on Recent Advances in Civil Engineering, RACE 2004, March 25 – 27, 2004, pp. 327 – 335.
2) Dr. K. S. Beena, Jayasree P. K., Leena G. (2004): Studies on cost reduction of gabion retaining walls, International Conference on Geosynthetics and Geoenvironmental Engineering, ICCGE 2004, IIT Bombay, December 14 – 16, 2004, pp. 355 – 360.
3) Jayasree P. K., Dr. K. S. Beena (2005): Gabion retaining walls – the ecofriendly walls, PRITHVI 2005 – Global Eco Meet, Swadeshi Science Congress, Trivandrum, Kerala, February 19 – 25, 2005.
4) Jayasree P. K., K. S. Beena, Indu B. & Sachin P. (2005): Design charts for the environment friendly Gabion Retaining Walls, Geotechnics In Environmental Protection GEN-2005, Allahabad, April 9 – 10, 2005, pp. III 12 – III 15.
5) Indu B., Jayasree P. K. And Beena K. S. (2005): Parametric studies on gabion retaining walls, National Conference On Technological Trends, 2005, College of Engineering, Trivandrum, November 25 – 26, 2005, pp. 77 – 81. (This Paper Received The Best Paper Award For The Conference).
6) Beena K. S. and Jayasree P. K. (2007): Reuse of rock waste filling in gabion retaining walls, Engineering Structures (Under Review).
7) Beena K. S. and Jayasree P. K. (2008): Geometric parametric studies on gabion faced reinforced soil walls, Canadian Geotechnical Journal (Under Review).
8) Beena K. S. and Jayasree P. K. (2008): Material parametric studies on gabion faced reinforced soil walls, Journal of Geotechnical and Geological Engineering (Under Review).
9) Beena K. S. and Jayasree P. K. (2008): Design aids for gabion faced reinforced soil walls, Geotechnique (Under Review).